FROM INTRACELLULAR SIGNALING CASCADES TO BEHAVIOR: TOWARDS A BETTER UNDERSTANDING OF OXYTOCIN'S MOLECULAR EFFECTS

DISSERTATION ZUR ERLANGUNG DES

DOKTORGRADES DER NATURWISSENSCHAFTEN (DR. RER. NAT.)

DER FAKULTÄT FÜR BIOLOGIE UND VORKLINISCHE MEDIZIN

DER UNIVERSITÄT REGENSBURG

vorgelegt von **Julia Winter**

aus Pfarrkirchen

im Jahr 2019

Das Promotionsgesuch wurde eingereicht am: 18.10.2019

Die Arbeit wurde angeleitet von: Dr. rer. nat. Benjamin Jurek

Unterschrift:

Dissertation

Durchgeführt am Institut für Zoologie der Universität Regensburg

Am Lehrstuhl für Tierphysiologie und Neurobiologie

unter Anleitung von

Dr. rer. nat. Benjamin Jurek

Table of Contents

Table of Contents

Summary

Summary

The neuropeptide oxytocin (OT) plays a prominent role in the regulation of a variety of behavioral processes like maternal behavior, anxiety-, and stress-related behaviors as well as social behaviors. Due to the well-known link to psychiatric disorders associated with anxiety, fear, and socio-emotional dysfunctions, OT is considered a viable treatment option for these diseases (Neumann and Slattery, 2016). Despite the profound knowledge from various rodent (Blume et al., 2008; Jurek et al., 2015; Jurek et al., 2012) and human studies (MacDonald and Feifel, 2014; Meyer-Lindenberg et al., 2011) on the beneficial effects of acute or short-term OT applications, the impact of extended treatment duration on the behavioral outcomes and OT receptor (OTR) signaling cascades remains rather sparsely investigated (Neumann and Slattery, 2016).

Thus, the thesis presented here aimed to unravel the molecular mechanisms and the behavioral effects that are caused by chronic OT. *Intracerebroventricular* infusions of a high dose of OT (10 ng/h) *via* osmotic minipumps for 14 days led to increased anxiety-related behavior in male rats, whereas a lower dose (1 ng/h) had no effect. Additionally, a strong sexual dimorphism was observable. Female rats showed increased anxiety levels induced by the low dose of chronic OT and a trend in the higher dose, suggesting a higher sensitivity of females to OT.

On a molecular level, I identified a sex-specific signaling cascade mediating the observed chronic OT-induced anxiogenic phenotype. Chronic OT stimulated mitogen-activated protein kinase (MAPK) signaling *via* phosphorylation of the kinases mitogen-activated protein kinase kinase (MEK1/2) and the extracellular signal-regulated kinase 1/2 (ERK1/2), and recruited further downstream the transcription factor myocyte enhancer factor 2 (MEF2). In more detail, dephosphorylation of the isoform MEF2A at the amino acid residue serine 408, a transcriptional inhibitory phosphorylation site, appeared to be the main player in chronic OT-induced anxiogenesis in male rats. Subsequent analysis of several stress-, anxiety-, and neuroplasticity-related MEF2-target genes revealed an involvement of the corticotropin releasing factor receptor 2 α (CRFR2α). In comparison to the CRFR1, CRFR2 has overall anxiolytic properties, brain region- and stress-dependent anxiogenic effects have been previously observed, though (Dedic et al., 2018; Deussing and Chen, 2018 and references therein). I confirmed the anxiolytic properties of CRFR2 activity in the paraventricular nucleus (PVN) of the hypothalamus of male rats in an agonist/antagonist experiment under mild stress conditions. The close link between stress and the OT system

(Winter and Jurek, 2019 and references therein) was confirmed in my study, as the anxiogenic effect of chronic OT depended on a mild stressor 24 h prior to behavioral testing. The *Crfr2* mRNA undergoes several alternative splicing events, resulting in two different isoforms in rodents (CRFR2α, CRFR2β) and an additional one in humans (CRFR2γ). I found changes in the expression of the brain-specific CRFR2α in male rats after chronic OT treatment. Not only was the expression of CRFR2α altered, but also an additional alternative splicing event of *Crfr2α* mRNA towards a shorter soluble isoform, sCRFR2α (Chen et al., 2005; Evans and Seasholtz, 2009) could be linked to chronic OT infusions. I detected a shift from membrane-associated mCRFR2α expression towards cytoplasmic distribution and extracellular release of the soluble sCRFR2α caused by chronic OT. Manipulation of either mCRFR2α or sCRFR2α expression conferred anxiogenic properties to the splice variant sCRFR2α.

Knockdown studies *in vitro* linked both the expression and alternative splicing of the CRFR2α to MEF2A activity. However, in females no activation of MEF2 and downstream of CRFR2α, and alternative splicing could be detected. Signaling *via* alternative MAPK targets is conceivable and deserves further investigation.

Furthermore, with OT-induced changes in neuronal morphology shown in previous studies (Lestanova et al., 2016a; Meyer et al., 2018) as well as in this thesis, OT caused significant neurite retraction, and the behavioral consequences due to chronic administration of OT, treatment duration and dosage have to be considered carefully in a clinical context.

The establishment of a new OTR knockout cell line by means of CRISPR-Cas9 enables further comparative signaling as well as morphological analysis. Here, the impairment of MAPK signaling and neurite retraction could be linked to the loss of the OTR.

Overall, the presented data elucidate the differential behavioral as well as molecular consequences of acute versus chronic OT applications in rodents. It provides a general strategy for the analysis of neuropeptide effects both *in vitro* and *in vivo* and challenges the beneficial effects of OT and its status as a potential treatment option for psychiatric disorders. Treatment dosage, duration as well as the gender of the patients have to be taken into account. However, the newly discovered connection between anxiety and the soluble splice variant sCRFR2α might lead to new anamnesis and treatment approaches for anxiety disorders.

Zusammenfassung

Zusammenfassung

Das Neuropeptid Oxytocin (OT) spielt eine zentrale Rolle bei der Regulierung verschiedener Verhaltensabläufe. Sowohl mütterliches Verhalten, Reaktionen in Stresssituation als auch Sozialverhalten werden maßgeblich von OT beeinflusst (Jurek and Neumann, 2018). Daher rückte OT ebenfalls in den Fokus der Wissenschaft als ein mögliches Medikament für die Behandlung von psychischen Erkrankungen, wie Angststörungen (Neumann and Slattery, 2016). Der zugrundeliegende Wirkmechanismus von OT ist bereits gut erforscht. Zahlreiche Studien in Mäusen, Ratten (Blume et al., 2008; Jurek et al., 2015; Jurek et al., 2012), sowie in Menschen (MacDonald and Feifel, 2014; Meyer-Lindenberg et al., 2011) konnten bereits positive Verhaltenseffekte von OT zeigen. Die Aktivierung verschiedener Signalkaskaden, allen voran der *mitogen-activated protein kinase* (MAPK) Signalweg, konnten mit OT bereits in Zusammenhang gebracht werden. Allerdings haben sich bis jetzt nur wenige Studien mit den Langzeiteffekten einer OT-Behandlung auseinandergesetzt. Das ist insbesondere von großer Bedeutung im Hinblick auf die potentielle Behandlung von autistischen Kindern mit OT (Neumann and Slattery, 2016).

Ziel der vorliegenden Arbeit war es, die Effekte einer chronischen OT-Behandlung sowohl auf molekularer Ebene als auch im Hinblick auf Verhaltensänderungen zu untersuchen. Männlichen und weiblichen Ratten wurden osmotische Minipumpen implantiert, welche über einen Zeitraum von 14 Tagen kontinuierlich zwei verschiedene Dosen (1 ng pro Stunde und 10 ng pro Stunde) OT in den Lateralventrikel abgaben. In beiden Geschlechtern konnte ich anschließend erhöhtes Angstverhalten in verschiedenen Verhaltenstests feststellen. Weibchen schienen sensitiver bereits auf die niedrigere Dosis (1 ng/h) zu reagieren, wohingegen in Männchen nur eine hohe Dosis OT (10ng pro Stunde) zu vermehrter Angst führte. Die nachfolgende molekulare Analyse der aktivierten Signalkaskaden zeigte auch hier geschlechtsspezifische Unterschiede. Die starke angstfördernde Wirkung, die die hohe Dosis in Männchen hervorgerufen hat, basiert auf einer Aktivierung des MAPK Signalwegs durch die Phosphorylierung der Kinasen MEK1/2 und nachfolgend ERK1/2. Dies wurde auch bereits in Zusammenhang mit akuter OT Gabe gezeigt (Blume et al., 2008; Jurek et al., 2015; Jurek et al., 2012). Weiterführende molekularbiologische Untersuchungen zeigten dann allerdings gravierende Unterschiede zwischen einer akuten und einer chronischen Gabe von OT auf. Chronische OT-Behandlung führte zur Aktivierung des Transkriptionsfaktors *myocyte enhancer factor* 2 (MEF2). Dieser verfügt über verschiedene Isoformen (MEF2A, B, C und D) und kann an

vielfältigen Aminosäuren phosphoryliert werden, was unterschiedliche Effekte auf die Transkription der Zielgene hat. Je nach Phosphorylierungsstelle kann die Transkription entweder aktiviert oder inhibiert werden. Insbesondere ein reduzierter Phosphorylierungsgrad von MEF2A an der Aminosäure Serin 408 scheint an der Verhaltensänderung durch hochdosiertes chronisches OT beteiligt zu sein. Phosphorylierung an dieser Stelle führt in der Regel zur Inhibierung nachfolgender Transkription. In diesem Fall wird durch verminderte Phosphorylierung die Expression und das alternative Spleißen der *corticotropin releasing factor receptor* 2 α (*Crfr2α*) mRNA verstärkt. Je nachdem in welcher Gehirnregion dieser Rezeptor aktiviert wird und abhängig von der Stresssituation, hat er angstlösende oder angstfördernde Eigenschaften. Durch gezielte Aktivierung und Blockierung konnte ich eine angstlösende Funktion dieses Rezeptors im Paraventrikulären Nukleus (PVN) des Hypothalamus von männlichen Ratten feststellen. Dabei waren die Ratten leichten, kurzfristigen Stressbedingungen ausgesetzt.
Wie bereits erwähnt, ist auch das alternative Spleißen dieses Rezeptors von chronischem OT betroffen. Dies hat zur Folge, dass mehr von einer löslichen, kleineren Spleißvariante (sCRFR2α) produziert wird, welche nicht nur im PVN, sondern auch in der zerebrospinalen Flüssigkeit nachgewiesen werden konnte. Bis jetzt war die Funktion dieser Spleißvariante weitgehend unbekannt. Durch gezielte Manipulation auf mRNA Ebene konnte ich jedoch ihre angstfördernden Eigenschaften nachweisen. Außerdem konnte ich durch weiterführende *in vitro* Studien die vermehrte Expression von sCRFR2α und die veränderte Aktivität von MEF2A direkt in Zusammenhang stellen und einen Einfluss von OT auf die Morphologie von Neuronen feststellen.
Die Signalkaskade von OT über MAPK Aktivierung, reduzierte MEF2A Aktivität und anschließendes alternatives Spleißen konnte jedoch nur in männlichen Ratten nachgewiesen werden, was eine geschlechtsspezifische Regulierung nahelegt. Im Hinblick auf OT als mögliches Medikament für psychische Erkrankungen ist es unbedingt nötig, den genauen Mechanismus auch in Weibchen zu untersuchen, um optimierte Behandlungspläne für weibliche und männliche Patienten zu erstellen.
Um weitere molekularbiologische Untersuchungen der Signalkaskaden zu erleichtern, wurde eine OTR Knockout Zelllinie generiert. Erste Analysen zeigten bereits verminderte Aktivität des MAPK Signalweges, als auch Verlust der charakteristischen Änderungen der Morphologie, die Stimulationen mit OT normalerweise auslösen.
Zusammengefasst trägt die hier vorgelegte Arbeit zu einem besseren Verständnis sowohl der molekularen Signalwege als auch der Veränderungen auf Verhaltensebene bei, welche von chronischer OT-Behandlung hervorgerufen werden. Es zeigten sich gravierende Unterschiede im Vergleich zu akuter OT Behandlung, die für die weitere Entwicklung von

OT als Medikament für psychische Erkrankungen berücksichtigt werden müssen. Die hier aufgezeigte Herangehensweise zur Analyse von chronischen Effekten kann verallgemeinert auch als Basis für Studien an anderen Neuropeptiden herangezogen werden.

Abbreviations

acOT	acute OT
ACTH	adrenocorticotropic hormone
ANOVA	analysis of variance
ASD	autism spectrum disorder
ASO	antisense oligonucleotides
ASV	antisauvagine-30
AVP	arginine-vasopressin
BNST	bed nucleus of the stria terminalis
bp	base pairs
BRET	bioluminescence resonance energy transfer
BSA	bovine serum albumin
CA	closed arm
CaMK	Ca^{2+}/Calmodulin activated kinase
cAMP	cyclic adenosine monophosphate
Cas	CRISPR-associated
cDNA	complementary DNA
cFOS	cellular- Finkel-Biskis-Jinkins murine osteosarcoma virus homologue
cOT	chronic OT
CREB	cAMP response element-binding protein
CRF	corticotropin releasing factor
CRF-BP	corticotropin releasing factor binding protein
CRFR1/2	corticotropin releasing factor receptor 1/2
CRISPR	clustered regularly interspaced short palindromic repeats
crRNA	CRISPR-RNA
CRTC	CREB transcriptional co-activator
CSF	cerebrospinal fluid
DAG	1,2-diacylglycerol
DB	dark box
dbcAMP	dibutyryl-cAMP
ddH_2O	double-distilled H_2O
DMEM/F-12	Dulbecco's modified eagle medium F-12

DSB	double-strand break
ECD	extracellular domain
ECL	extracellular loop
EDTA	ethylenediaminetetraacetic acid
e.g.	*exempli gratia*
EGFR	epidermal growth factor receptor
EPM	elevated plus maze
ERK1/2	extracellular signal-regulated kinase 1/2
ERK5	extracellular signal-regulated kinase 5
FACS	fluorescence-activated cell sorting
FBS	fetal bovine serum
GABA	γ-aminobutyric acid
GC	glucocorticoid
GDP	guanosine diphosphate
GFP	green fluorescent protein
GPCR	G protein-coupled receptor
GR	glucocorticoid receptor
GRK	G protein-coupled receptor kinases
GTP	guanosine triphosphate
HEPES	4-(2-hydroxyethyl)-1-piperazineethanesulfonic acid
HPA	hypothalamic-pituitary-adrenal
i.c.v.	intracerebroventricular
In/Del	insertion/deletion
i.e.	*id est*
IP3	inositol 1,4,5,-triphosphate
IZ	inner zone
JNK	c-Jun-N-terminal kinase
kb	kilobase
KD	knockdown
KO	knockout
LB	light box
LDB	light-dark box
LDCV	large-dense core vesicles
MADS	MCMI, Agamous, Deficiens and Serum response factor
MAP	microtubule-associated proteins
MAPK	mitogen-activated protein kinase

mCRFR2α	membrane-bound CRFR2α
MEF2	myocyte enhancer factor 2
MEK1/2	mitogen-activated protein kinase kinase
MMEJ	microhomology-mediated end joining
mRNA	messenger RNA
MSK	mitogen and stress activated kinase
MβCD	methyl-ß-cyclodextrin
NHEJ	non-homologous end joining
NLS	nuclear localization sequence
NMD	nonsense-mediated decay
NMDAR	N-methyl-D-aspartate receptors
OA	open arm
OFT	open field test
OT	oxytocin
OTR	oxytocin receptor
OtrIN	Otr interneurons
p	phospho
p38	protein 38 kDa
PAM	protospacer adjacent motif
Pax	paired box
PBS	phosphate-buffered saline
PCR	polymerase chain reaction
PFA	para-formaldehyde
PI3K	phosphatidylinositol-4,5-bisphosphate 3-kinase
PIP_2	phosphatidylinositol 4,5-biphosphate
PKA	protein kinase A
PKC	protein kinase C
PLC	phospholipase C
PPT	polypyrimidine tract
PTC	premature termination codon
PVN	paraventricular nucleus of the hypothalamus
Rab4/5	Ras-related in brain 4/5
Ras	rat sarcoma
RNP	ribonucleoprotein
rpm	revolutions per minute
RSK	ribosomal protein S6 kinase

RT	room temperature
RT-PCR	reverse transcription PCR
S	serine
SCP	stresscopin
scr	scrambled
sCRFR2α	soluble CRFR2α
SEM	standard error of the mean
siRNA	small interfering RNA
SNARE	soluble N-ethylmaleimide-sensitive factor attachment receptor
snRNP	small nuclear RNP
ssDNA	single-stranded DNA
TALEN	transcription activator-like effector nuclease
TBS	tris(hydroxymethyl)aminoethane-buffered saline
TBST	TBS supplemented with 0.1 % Tween-20
TGOT	Thr^4, Gly^7-OT
Th	tyrosine hydroxylase
Thr	threonine
TMD	transmembrane domain/helix
TMH	transmembrane helix
tracrRNA	trans activating CRISPR-RNA
TRPV2	transient receptor potential vanilloid type-2 Ca^{2+}
TSB	target site blocker
UCN	urocortin
VEH	vehicle
VGCC	voltage-gated Ca^{2+} channels
ZFN	zink finger nuclease

Introduction

Introduction

1. Anxiety

“What is an emotion?” This fundamental question was already asked by William James 135 years ago (James, 1884); however, there are no scientific concepts that directly match the totality of all facets of emotions. This variety requires various models to approach the complexity and the components of emotions. From an ethological perspective, anxiety is a highly adaptive and complex response. Only appropriate conditions and correct stimuli guarantee the desired intensity and persistence of the behavior in various vertebrate species. Anxiety-related behaviors require time and effort for the successful reaction to the plethora of threats living organisms have to face. Dysregulations in intensity, persistence, or response to an incorrect stimulus are some of the sources for insufficiency in anxiety systems (Blanchard et al., 2008).

In humans, the Diagnostic and Statistical Manual of Mental Disorders (DSM V, American Psychiatric Association, 2013) defines 12 subtypes of anxiety disorders, namely separation anxiety disorder, selective mutism, specific phobia, social anxiety disorder (social phobia), panic disorder, panic attack specifier, agoraphobia, generalized anxiety disorder, substance/medication-induced anxiety disorder, anxiety disorder due to another medical condition, other specified anxiety disorder, and unspecified anxiety disorder. Despite the high prevalence and burden of anxiety disorders (Wittchen et al., 2011), treatment remains relatively elusive. Research on the molecular and neurocircuit background of anxiety disorders has progressed substantially, nevertheless no mechanistically new treatment options have been brought to the market within the last two decades. Standard first-line treatments are selective serotonin-reuptake inhibitors and serotonin-norepinephrine reuptake inhibitors. Second line and other treatments include tricyclic antidepressants, like Clomipramine, monoamine oxidase inhibitors, benzodiazepines, and anticonvulsants (Hoffman and Mathew, 2008; Murrough et al., 2015). Other viable candidates for the medication of anxiety disorder that emerged are neuropeptides, like the corticotropin releasing factor (CRF, Baldwin et al., 1991; Dunn and File, 1987; Holsboer, 1999; Holsboer and Ising, 2008), the neuropeptide Y (Heilig, 2004; Sorensen et al., 2004) or the endocannabinoid system. Here, several new “druggable” targets are investigated for the alleviation of anxiety disorders. For review see (Patel et al., 2017). The neuropeptide oxytocin (OT) is well known for its anxiolytic, antistress, reproductive, and prosocial effect.

The impact on anxiety and the treatment of anxiety disorders will be discussed in more detail in the following chapters (see 2. The oxytocin system, Neumann and Slattery, 2016).

1.1. Animal models to study anxiety

To fully understand the fundamentals of anxiety from neural circuits to molecular signaling, appropriate animal models are indispensable. In this context, rodents like mice or rats have proven to be suitable model organisms (reviewed in Calhoon and Tye, 2015). Classical assessment of anxiety-related behavior includes approach-avoidance assays, like the elevated plus maze (EPM; Pellow et al., 1985; Pellow and File, 1986), the open field test (OFT; Hall and Ballachey, 1932) or the light-dark box (LDB; Ambrogi Lorenzini et al., 1984). These tests are based on the conflict between the innate drive of the animals to explore new contexts and the impulse to avoid bright, open and exposed areas. Other approaches to measure anxiety-related behavior are active-avoidance tests like the shock probe burying and the marble burying test. Hyponeophagia, measuring the amount and latency of food intake in a novel environment, can be addressed by the novelty-suppressed feeding test (Deacon, 2011). Concluding, social behaviors are assessed by social tests like ultrasonic vocalization and social interaction (for detailed review see Blanchard et al., 2008).
In this study, anxiety and the effects of OT and manipulation of the CRFR2α on anxiety were assessed by EPM, LDB, and OFT. To investigate the social component of the treatments, social preference (Lukas et al., 2011) was additionally measured.

1.2. Molecular underpinnings of anxiety and anxiety disorders

To fully understand the formation of anxiety disorders, knowledge of the underlying genetic and environmental factors is crucial. In recent years, several genes involved in the regulation of anxiety were identified (Hovatta and Barlow, 2008). Although anxiety and other psychiatric disorders are most likely triggered by the combination of a large number of common and rare variants with only small effect size, several risk factors are standing out (Sokolowska and Hovatta, 2013). Just to mention few of them, variants of the glutamic acid decarboxylase 2 have been associated with panic and phobic anxiety (Lydiard, 2003; Smoller et al., 2001), regulator of G protein signaling is related to anxiety, introversion personality traits, and panic disorder (Okimoto et al., 2012; Sokolowska and Hovatta, 2013 and references therein), and peroxisome proliferator-activated receptor gamma coactivator 1 alpha emerged as a novel candidate gene for anxiety disorders (Hettema et al., 2011). Studies in mice revealed that glyoxalase 1 expression was increased in anxious

mouse strains (Hovatta et al., 2005). In addition to these factors, genes encoding for various neuropeptides are involved in the regulation of anxiety, like CRF (Maras and Baram, 2012), neuropeptide Y (Giesbrecht et al., 2010), neuropeptide S (Ionescu et al., 2012), arginine-vasopressin (AVP), and OT (Neumann and Landgraf, 2012). Acute treatment with OT has well studied beneficial effects on anxiety-like behavior (Blume et al., 2008; Jurek et al., 2015; Jurek et al., 2012; Martinetz et al., 2019; Neumann et al., 2000c; Okimoto et al., 2012; Pedersen and Boccia, 2002; Slattery and Neumann, 2010; Sobota et al., 2015; Waldherr and Neumann, 2007). However, profound knowledge on the intracellular signaling downstream of the OT receptor (OTR) induced by chronic OT treatment remains elusive and is the major part of the work presented here.

2. The oxytocin system

The neuropeptide OT and the closely related AVP were first described in 1895 as extracts of the pituitary gland with vasopressor and uterine-contracting properties. Due to these properties, OT was named after the Greek words for “quick birth” (reviewed in Jurek and Neumann, 2018). The nonapeptide OT consists of the amino acids Cys-Tyr-Ile-Gln-Asn-Cys-Pro-Leu-Gly (Fig. 1) and is synthesized in the magno- and parvocellular neurons of the hypothalamic paraventricular nucleus (PVN), the supraoptic nucleus, and the accessory nuclei (Mohr et al., 1988; Sofroniew, 1983). As a secondary structure, OT forms a loop *via* a disulfide bond between the two cysteine amino acids (Busnelli et al., 2016). After storage in large-dense core vesicles (LDCV), distribution and release occur *via* axonal projections (Knobloch et al., 2012) as well as local dendritic release and diffusion (Gimpl and Fahrenholz, 2001; Jurek and Neumann, 2018; Landgraf and Neumann, 2004; Meyer-Lindenberg et al., 2011). Release from axon terminals is mediated by exocytosis, requiring depolymerization of F-actin and the soluble N-ethylmaleimide-sensitive factor attachment receptor (SNARE) complex to open the fusion pore. Exocytosis during axon terminal as well as dendritic release of OT is Ca^{2+} dependent which originates from various sources to trigger dendritic release. Extracellular Ca^{2+} can enter the cell *via* voltage-gated Ca^{2+} channels (VGCCs), ionotropic glutamate receptors including N-methyl-D-aspartate receptors (NMDARs), or intracellular Ca^{2+} levels are directly supplied from intracellular Ca^{2+} stores and Ca^{2+} buffering mechanisms (Ludwig et al., 2016; Ludwig et al., 2002). Additionally, recruitment of intracellular Ca^{2+} also occurs *via* OT-OTR binding and the subsequent activation of transient receptor potential vanilloid type-2 Ca^{2+} channels

(TRPV2, van den Burg et al., 2015). Depending on the stimulus, OT either acts as a rapid neurotransmitter released from axon terminals (Dabrowska et al., 2011) or as a neuromodulator which is released from dendrites, soma, or non-terminal axonal regions (Tobin et al., 2012). In contrast to fast neurotransmission, OT can reach and bind nearby or remote receptors *via* diffusion through the extracellular fluid and thereby exert its effects (Neumann and Landgraf, 2012). However, recent studies support a new model of OT actions *via* focused axonal release (Chini et al., 2017 and references therein).

Despite broad evidence for a coordinated central and peripheral release of OT, plasma levels are only of limited suitability as a global biomarker for the activity of the central OT system, mainly due to the separation by the blood-brain barrier. However, diffusion between extracellular fluid and the ventricular cerebrospinal fluid (CSF) allows conclusions from CSF OT levels to central release (Landgraf and Neumann, 2004; Neumann and Landgraf, 2012).

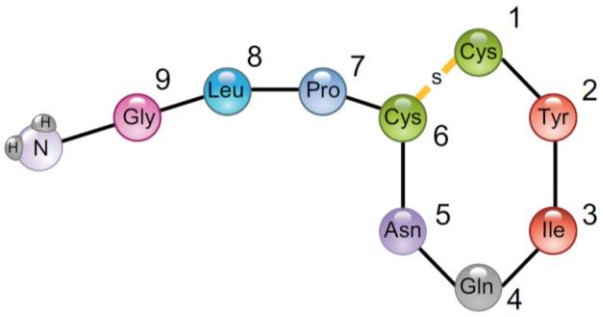

Figure 1. Structure of the nonapeptide OT, consisting of a cyclic part of six amino acids that are being connected with a disulfide bridge between cysteine 1 and cysteine 6. The linear part consisting of a prolin, leucine and glycine is terminated by an amidated COOH terminus (Jurek and Neumann, 2018).

In both rodents and humans, OT plays a key role for the regulation of social behaviors including pair bonding, sexual behavior, maternal care as well as the ability to form normal social attachments (Bosch et al., 2005; Carter et al., 1992; Kosfeld et al., 2005; Waldherr and Neumann, 2007; Young et al., 2001). Moreover, several studies have proven that acute OT applications show anxiolytic and stress-protective effects in rodents and humans (Jurek and Neumann, 2018). In this regard, the pharmacogenetic manipulation of the brain OT system in rats and mice attenuates the response of the hypothalamic-pituitary-adrenal (HPA) axis, reduces anxiety, and improves stress-coping (Amico et al., 2004; Neumann et al., 2000a; Neumann and Landgraf, 2012; Windle et al., 1997). The brain regions involved in mediating those effects are within amygdala and septal regions, the raphe nucleus, and the hypothalamic PVN (Guzman et al., 2013; Jurek et al., 2012; Knobloch et al., 2012;

Neumann et al., 2000a; Yoshida et al., 2009). In summary, OT exerts a plethora of central actions, like anxiolytic and antidepressive effects, and peripheral actions, including milk ejection, uterine contractions, parturition, and lactation (Ludwig et al., 2016; Neumann and Landgraf, 2012). In humans, intranasal application of OT for pharmacological and therapeutic reasons is thought to have effects on *e.g.* fear, anxiety, trust, rejection, empathy, and pro-social effects have been documented as well (Veening and Olivier, 2013). Additionally, cardiovascular effects of OT have been described, resulting in *e.g.* nitric oxide stimulation and therefore cardioprotective effects (Jurek and Neumann, 2018; MacDonald and Feifel, 2014).

2.1. Oxytocin and anxiety

Because of the widespread occurrence of psychosocial stress in modern societies causing somatic diseases, depression, and anxiety-related disorders (reviewed in Jurek and Neumann, 2018) on the one hand, and the missing spectrum of treatment options on the other hand, novel approaches are desperately needed, for which neuropeptides like OT are viable candidates. As already mentioned above, OT is involved in the regulation of anxiety and has been linked to the treatment of anxiety disorders in several studies (reviewed in Neumann and Slattery, 2016). Apart from the effects of the endogenous OT system on anxiety during lactation or sexual activity (Neumann and Slattery, 2016), acute administration of synthetic OT into various brain regions, including PVN exerts a robust anxiolytic phenotype (Blume et al., 2008; Jurek et al., 2012). In the prefrontal cortex, OTR interneurons (OtrIN) expressing the CRF binding protein (CRF-BP) are responsible for sexually dimorphic anxiety-related behavior. Activation of OtrIN in male mice was anxiolytic, whereas in females it had a prosocial effect. Li and coworkers identified the underlying sex-specific molecular mechanism, explaining the behavioral differences between males and females (Li et al., 2016). Not only these brain regions play a critical role in the regulation of anxiety-related behaviors, anxiety cells in the ventral CA1 region of the hippocampus were recently shown to be activated by anxiogenic stimuli. These cells project to the lateral hypothalamic area and thereby control anxiety-related behavior. Learned fear remained unaffected as anxiety cells displayed no projections to the basal amygdala (Jimenez et al., 2018). A recent study in prairie voles illustrated the close relationship between OT and stress, as OT infusions prior to a stressful situation inhibited stress activation of the HPA axis by the activation and release of γ-aminobutyric acid (GABA) in the PVN (Smith et al., 2016).

Chronic treatment with exogenous OT, however, exerts differential effects. The first studies on continuous central infusions of OT *via* osmotic minipumps revealed decreased OTR binding throughout the brain (Insel et al., 1992) as well as enhanced social interactions of male rats treated with chronic OT for 10 days and female stimulus animals (Witt et al., 1992). With regard to anxiety-related behavior, chronic OT for 5 days at 3 different concentrations (1, 10, or 100 ng/h) had no effect on female ovariectomized rats unless a mild stressor was applied on the day of testing on the EPM; the highest dose of OT (100 ng/h) in combination with the mild stressor was then anxiolytic (Windle et al., 1997). Furthermore, chronic OT is also able to attenuate the stress response. 30 min restraint-induced release of adrenocorticotropic hormone (ACTH), corticosterone, and the increase in *Crf*, and *cFos* mRNA was reduced in female rats infused with 1 or 10 ng/h *intracerebroventricularly* (*i.c.v.*) OT for 5 days (Windle et al., 2004). In rats specifically bred for high anxiety, a high dose of chronic OT (10 ng/h over 6 days) attenuated the level of anxiety in female, but not male rats (Slattery and Neumann, 2010). Consequently, these rather neutral to beneficial effects of chronic OT seem to be highly time dependent as short-term (up to 7 days) treatment regimens seem to be less adverse. In detail, 7-day chronic OT treatment (10 ng/h) did not alter anxiety-like behavior in the OFT or EPM in male rats (Havranek et al., 2015), whereas an extended treatment duration of 14 days increased anxiety-like behavior in male mice (Peters et al., 2014). The behavioral and molecular consequences of such long-term treatment have not been assessed in male and female rats so far, and are the main subject of this thesis.

2.2. Oxytocin and stress

Stress and the OT system are very closely linked, as parvocellular OT neurons, projecting towards the brainstem, the spinal cord, or the supraoptic nucleus, belong to neuronal circuits interacting with CRF neurons in the PVN. Stress-induced CRF release and the subsequent activation of the HPA axis are likely to be accompanied by OT release. However, the exact dynamics of stress-induced OT release are less clear (Ebner et al., 2005; Wotjak et al., 1998). As an example, CRF-induced ACTH synthesis is potentiated by OT (Engelmann et al., 2004; Gibbs, 1986; Gibbs et al., 1984; Lang et al., 1983; Suh et al., 1986). Then, ACTH induces the synthesis and release of glucocorticoids (GCs) which are able to cross the blood-brain barrier, where they bind to glucocorticoid receptors (GR) in the PVN or hippocampus. By nuclear translocation, the GC-GR complex binds to its responsive element in the CRF promoter region and thereby reduces CRF gene transcription (Jeanneteau et al., 2012; Winter and Jurek, 2019). In that way, OT dampens the stress

response by amplification of the HPA-axis' inherent negative feedback loop. OT also has a direct impact on CRF gene expression, in more detail it was found to delay *Crf* gene transcription induced by restraint stress. CREB transcriptional co-activator (CRTC3), a cofactor of the cyclic adenosine monophosphate (cAMP) response element-binding protein (CREB) is translocated to the nucleus following stressful stimuli, to stimulate *Crf* transcription. OT was shown to interfere with CRTC3 translocation, whereas CREB and CRTC2 activation remain unaffected by OT (Jurek et al., 2015). A second, indirect regulation of CRF neuronal activity is constituted by GABAergic inhibition that occurs under basal conditions and silences CRF neurons. The synaptic interaction of magnocellular OT neurons with parvocellular CRF neurons enhances this effect, resulting in oxytocinergic inhibition of *Crf* mRNA levels in the PVN (reviewed in Winter and Jurek, 2019). This effect was shown in prairie voles, where the OT-induced anxiolysis is triggered by promoted GABAergic inhibition of CRF neuronal activity (Smith et al., 2016). The reciprocal expression of OTR-CRF and OT-CRFR in distinct neuronal populations of the PVN, and the bed nucleus of the stria terminalis (BNST) underscores the close connection between the OT- and the CRF-system (Dabrowska et al., 2011; Dabrowska et al., 2013). CRF is not the only member of the CRF family interacting with OT. For the CRF-BP a sexually dimorphic mechanism was proposed, as expression of the CRF-BP on OtrIN inhibits the activation of 2/3 pyramidal cells in the prefrontal cortex of male mice only, causing anxiolysis (Li et al., 2016). CRFR1 activation was shown to be anxiogenic in lactating and virgin female rats accompanied by the release of OT in the hypothalamic preoptic area (Klampfl et al., 2018). For the CRFR2, differential effects could be observed depending on the brain region involved, and stress-levels experienced (Bale et al., 2002b). In addition, release of OT in the dorsolateral BNST is modulated by CRFR2 activity (Martinon and Dabrowska, 2018). In this thesis, I provide evidence for the so far unknown impact of OT on PVN CRFR2 expression and activity under mild stress conditions.

2.3. Oxytocin receptor signaling

All effects of OT described in the previous chapters are consequences of interaction of OT with its receptor and further downstream signaling. The OTR is located on chromosome 3 with 4 exons and 3 introns with an overall length of 17 kilobases (kb), encoding for a 388-amino-acid polypeptide (Inoue et al., 1994; Kimura et al., 1992). Two different transcripts were identified in breast tissue (3.6 kb), and in ovary, uterine endometrium, and myometrium (4.4 kb, Kimura et al., 1992). Detailed splicing patterns within the brain remain to be investigated. The precise gene structure has been described for various species

including humans (Inoue et al., 1994), mice (Kubota et al., 1996), and rats (Rozen et al., 1995). The receptor belongs to the G protein-coupled receptor (GPCR) family and ranks among the rhodopsin-type (class I) receptors and consists of seven transmembrane α-helices connected by 3 extracellular and 3 intracellular loops (Fig. 2, Gimpl and Fahrenholz, 2001; Jurek and Neumann, 2018).

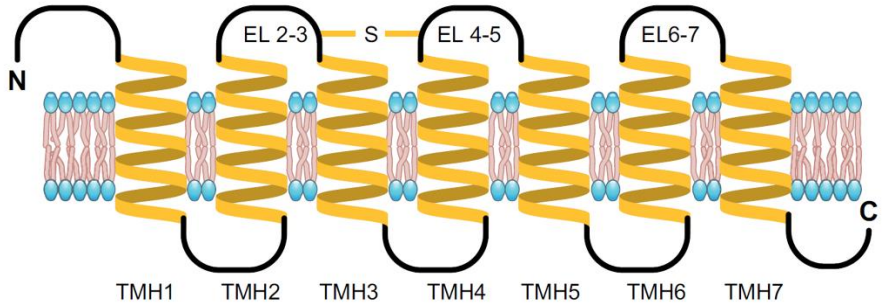

Figure 2. Schematic representation of the OTR structure.

The OTR is a seven-transmembrane helix (TMH1–7) receptor with three extracellular loops (2–7) and three intracellular loops (1–6, adapted from Jurek and Neumann, 2018).

Factors that regulate OTR expression include transcription factors, estrogens, progesterone, OTR promoter methylation, micro RNAs, and, with limited evidence, ligand availability. The OTR is widely distributed in diverse brain areas (reviewed in Jurek and Neumann, 2018).

Multiple pathways have been shown to be linked to OTR signaling. Basis of all OTR-mediated effects is classical G (guanine nucleotide-binding) protein-coupled signaling. OTRs are coupled to 3 G proteins, namely the G_{α} and $G_{\beta/\gamma}$ subunit, whose activation is mediated by the exchange of guanosine diphosphate (GDP) to guanosine triphosphate (GTP). A recent study identified the connection between OT concentrations and the activation of different G protein subunits. The development of a BRET-based biosensor enabled the determination of the EC_{50} values for the different G proteins. Low concentrations of OT (2 nM) activate G_q proteins, whereas high ligand concentrations of 90 nM activate G_{oB} as shown in Figure 4 (Busnelli and Chini, 2018; Busnelli et al., 2012).

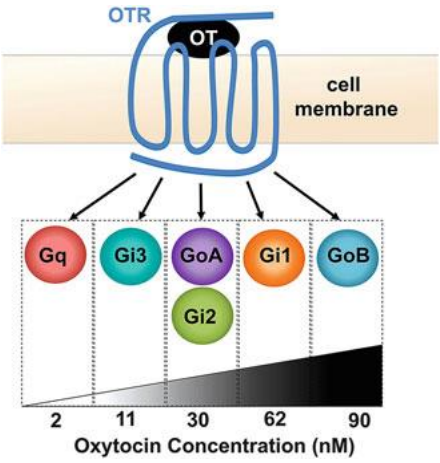

Figure 3. Concentration-dependent G protein-coupling of the OTR.

Depending on ligand availability, the OTR couples to different G-proteins. Those G-proteins induce either activating (G_q, $G_{oA/B}$) or dampening ($G_{i1,2,3}$) signaling cascades, with ligand concentrations ranging from 2 to 90 nM. Higher concentrations likely cross-activate the vasopressin receptor too (Busnelli and Chini, 2018).

Ligand availability but more importantly the duration of stimulation are crucial factors in GPCR-mediated signaling. Upon agonist stimulation, OTRs undergo desensitization and internalization processes, in which almost 85 % of OTR return to the cell surface within 4 h (Conti et al., 2009). The first step in this process is the uncoupling from G proteins after phosphorylation by GPCR kinases (GRK). Binding of β-arrestins mediates the removal from the plasma membrane by endocytosis. In the case of resensitization, the receptors are recycled to the cell surface, whereas degradation leads to downregulation (Conti et al., 2009; Gimpl and Fahrenholz, 2001; Grotegut et al., 2011). For the OTR, a complete internalization was observed within 30 min after agonist application. Longer exposure time up to 18 h leads to a loss of 50 % of high-affinity receptors on the cell surface. Recycling was mediated *via* the “short cycle” involving proteins called Ras-related in brain 4/5 (Rab4/Rab5, Conti et al., 2009). Internalization of OTR occurs mostly *via* a clathrin-dependent pathway. In more detail, phosphorylation by GRK2 protein kinase promotes subsequent binding to β-arrestin and endocytosis *via* clathrin-coated pits (Conti et al., 2009; Gimpl and Fahrenholz, 2001). However, agonist (Carbetocin)-binding can also induce β-arrestin-independent internalization of the OTR (Passoni et al., 2016), which leads to differential downstream cascade activation. Due to the structural similarities between AVP and OT, binding of OT is not limited to the OTR but also occurs at AVP receptors (Akerlund et al., 1999), whereby differences in signaling could be attributed to flexible receptor interactions. Another well-known agonist to study specific receptor-mediated effects is Thr^4, Gly^7-OT (TGOT, Lowbridge et al., 1977).

One pathway includes two G_{α} isoforms $G_{\alpha q}$ and $G_{\alpha 11}$ which are, together with $G_{\beta/\gamma}$, both able to activate phospholipase C-β (PLC) subunits, causing the hydrolysis of phosphatidylinositol 4,5-biphosphate (PIP_2), which results in two products, inositol 1,4,5,-triphosphate (IP3) and 1,2-diacylglycerol (DAG). Finally, protein kinase C (PKC) is stimulated by DAG, whereas IP3 enhances Ca^{2+} release from intracellular stores. Ca^{2+}-dependent signaling includes, among others, downstream cascades like calmodulin-dependent protein kinases (CaMKII, CaMKIV) and Calcineurin (Busnelli and Chini, 2018; Gimpl and Fahrenholz, 2001; Jurek and Neumann, 2018)and references therein). The second pathway involves the G_i/G_o family, consisting of $G_{\alpha i1}$, $G_{\alpha i2}$, $G_{\alpha i3}$, $G_{\alpha oA}$, and $G_{\alpha oB}$. $G_{\alpha i}$ activates phosphatidylinositol-4,5-bisphosphate 3-kinase (PI3K) as well as the mitogen-activated protein kinase (MAPK) pathway *via* the inhibition of adenylyl cyclase and the reduction of cAMP levels (Busnelli and Chini, 2018; Busnelli et al., 2012). In more detail, MAPK activation occurs *via* transactivation of the epidermal growth factor (EGFR, Blume et al., 2008), followed by recruitment of the membrane-associated proto-oncoprotein GTPase Rat sarcoma (Ras). Ras *via* Ras proto-oncogene serine/threonine-protein kinase (Raf-1) triggers a chain reaction to ultimately fully activate the MAPK pathway. The three main kinases are extracellular signal-regulated kinase (ERK1/2), p38, and c-Jun NH2-terminal kinase (JNK1/2/3), the latter not being affected by OTR signaling. ERK1/2 phosphorylation occurs upon mitogen-activated protein kinase kinase (MEK1/2) activation in a cell- and tissue-specific manner, however, evidence also suggests other MEK1/2 targets, independent of the canonical ERK1/2 pathway (Jurek et al., 2012), including PPARγ, MyoD, PI3K, or LIMKinase 1 (Brandt et al., 2010; Burgermeister et al., 2007; Jo et al., 2011). Other ERK substrates include mitogen and stress activated kinases (MSK) and the ribosomal protein S6 kinase (RSK, Jurek and Neumann, 2018).

Well-known downstream targets of MAPK signaling are the transcription factors myocyte enhancer factor 2 (MEF2, for more details see chapter 5.) and CREB with its cofactors CRTC2/3 (Jurek et al., 2015; Tomizawa et al., 2003). However, the pathways mentioned here cannot be considered independently, as inhibition of OT-induced Ca^{2+} influx has deleterious effects on MAPK signaling in hypothalamic cells (van den Burg et al., 2015), indicating an initial role of Ca^{2+} for further second messenger signaling. For an overall summary of OTR signaling, both proven as well as hypothetical see Figure 4.

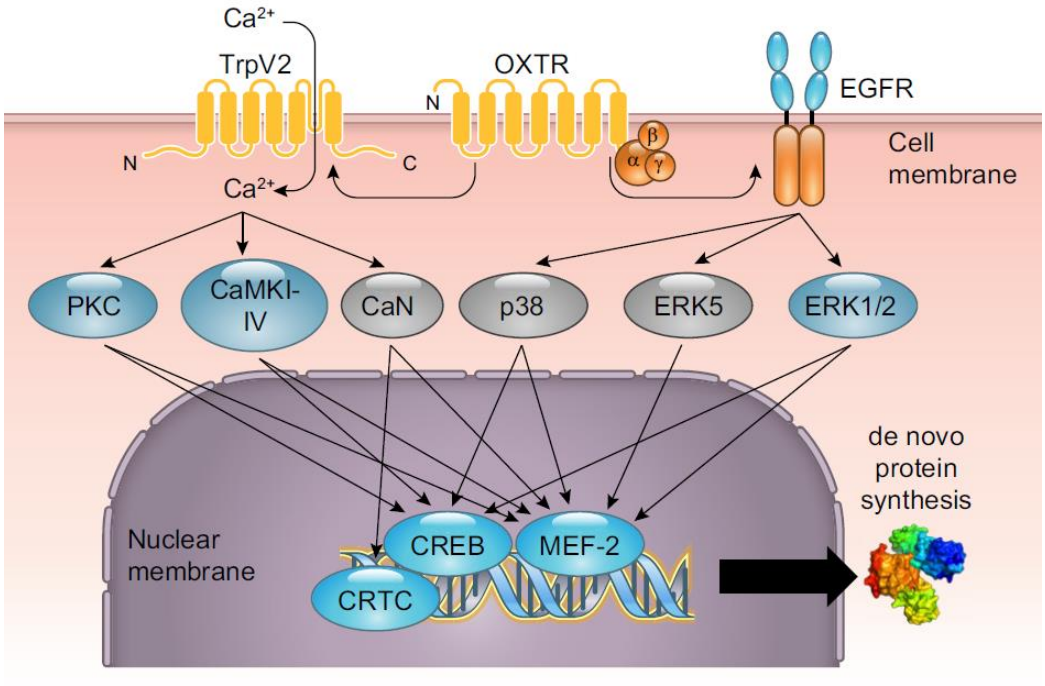

Figure 4. Schematic summary of neuronal OTR signaling.

The 7 transmembrane GPCR OTR (shown here as OXTR) transactivates the TRPV2 cation channel and the EGFR, leading to Ca^{2+}-dependent and -independent signaling. Kinases translocate from the cytoplasm to the nucleus and activate a set of transcription factors, which orchestrate transcription as a complex. Kinases and transcription factors in blue represent cascades that have been proven to be coupled to the neuronal OTR, kinases in gray are hypothetical or shown to be coupled to peripheral OTRs (adapted from Jurek and Neumann, 2018).

In summary, OT concentration, G protein expression, OTR membrane availability, and as a last factor OTR affinity states that are addressed in the next chapter determine the quality and quantity of OTR-mediated signaling.

2.4. Impact of cholesterol on oxytocin receptor activity

OTR receptors occur in two different affinity states, the low-affinity state (K_d > 100 nM) and the high-affinity state (K_d < 1-5 nM, Gimpl et al., 1995). Transitions between those affinity states are reversible and depend on cholesterol content in the plasma membrane (Gimpl et al., 1995; Klein et al., 1995). In general, membranes in cellular systems are known to appear as lipid bilayers. The “fluid mosaic model”, as originally suggested by Singer and Nicholson, has become, with minor modifications, the standard model of membrane structure (Singer and Nicolson, 1972). Specific areas within membranes, so-called “lipid rafts” are dynamic microdomains that are capable of moving within the fluid bilayer. Those rafts are

sphingolipid- and cholesterol-enriched and contain ordered aggregations of membrane-bound signaling proteins. The whole complex represents a membrane-bound anchor, which plays an important role during signal transduction as “transduction platform” (Simons and Ikonen, 1997; Simons and Toomre, 2000). Cholesterol, as one of the most abundant components of membranes (Liscum and Underwood, 1995), is of great significance for the integrity of lipid microdomain structures like caveolae and the already mentioned lipid rafts (Incardona and Eaton, 2000; Simons and Toomre, 2000). OTR agonist binding affinity states s strongly depend on cholesterol contents in the membrane (Gimpl and Fahrenholz, 2000; Reversi et al., 2006; Wiegand and Gimpl, 2012).

On the one hand, OT inhibits cell growth and proliferation in a PI3K-dependent MAPK cascade activation, when the majority of OTRs are excluded from lipid rafts and caveolae. On the other hand, strong PLC-independent mitogenic effects appear when OTRs are located within caveolae, induced by fusion to caveolin-2, a resident raft protein (Reversi et al., 2006; Rimoldi et al., 2003). Upon removal of cholesterol from the membrane *via* methyl-ß-cyclodextrin (MßCD), the OTR was found to be shifted to the low-affinity state, whereas high-affinity binding states could be regained by cholesterol enrichment *via* cholesterol-MßCD. Interestingly, restoring could not be achieved by other steroids, suggesting a specific and direct dependency of the OTR on cholesterol (Klein et al., 1995). Additionally, OTR stability and conformation is strongly influenced by the location in cholesterol-rich domains (Muth et al., 2011).

3. The CRF system

Stress is a major environmental factor contributing to the formation of psychiatric disorders. The 3 physiologists Claude Bernard, Walter B. Cannon, and Hans Selye are considered as the pioneers of stress biology. Their work was the basis for the concept of neuroendocrinology, including the autonomic nervous system and the HPA axis as the key players in the stress response. While the ANS represents the rapid response towards a stressor, the HPA-axis modulates this response in duration and frequency (reviewed in Deussing and Chen, 2018).

3.1. CRF family members

The primary structure of the master regulator of the HPA axis, CRF was first identified in 1981 as a 41 amino acid peptide (Vale et al., 1981), while the evidence for an ACTH releasing mediator already existed since 1955 (Selye, 1955). CRF is synthesized in parvocellular neurons of the hypothalamus and triggers the release of ACTH into the systemic circulation (Rivier and Vale, 1983; Smith and Vale, 2006; Vale et al., 1981). Upon ACTH release, synthesis, and secretion of GCs from the zona fasciculata of the adrenal cortex are promoted. GCs are then responsible for the regulation of a variety of physiological adaptations when binding to their cognate intracellular receptors (Bamberger et al., 1996; Munck et al., 1984; Smith and Vale, 2006). Furthermore, CRF regulates the ANS-mediated stress response and is also able to directly modulate behavioral stress responses (Deussing and Chen, 2018 and references therein). CRF and a group of 3 related proteins called urocortins (UCN), UCN1, UCN2 (also called stresscopin-related peptide), and UCN3 (also called stresscopin) elicit their function *via* binding to two different class B family of G-protein coupled receptor subtypes, the corticotropin releasing factor receptors 1 and 2 (CRFR1, CRFR2, Hillhouse and Grammatopoulos, 2006; Lewis et al., 2001; Reyes et al., 2001; Vaughan et al., 1995). These receptors contain a large extracellular domain at the N-terminus and are able to bind large peptide ligands (Deussing and Chen, 2018). CRF and UCN1 preferentially bind to the CRFR1, while UCN2 and UCN3 bind the CRFR2 with higher affinities (Hillhouse and Grammatopoulos, 2006). CRFRs mainly signal *via* coupling to G_s proteins, followed by the activation of protein kinase A (PKA) and MAPK-ERK pathways and the mobilization of Ca^{2+}. Activation of ERK1/2 *via* PLC and for example $G_{q\alpha}$ is also possible. Internalization and desensitization of CRFR1 and CRFR2 is mostly β–arrestin-mediated. Additionally, receptor activity can be modulated by carboxy-terminal PDZ-domain interactions. Binding to PDZ-domains regulates the cellular location of the receptors and attributes them to larger signaling complexes (Henckens et al., 2016 and references therein). In rodents, there are two isoforms of CRFR2 (α and β) and three in humans (α, β, and γ) arising from separate promoters and 5´ exons which splice to a common set of downstream exons (Chen et al., 2005; Kostich et al., 1998). The CRF-BP regulates the activity of CRF and UCN1 by the binding between both factors. It represents a regulatory capturing function that might partially act in a CRFR2-dependent manner, however, the precise mechanism is unknown (Deussing and Chen, 2018; Eckart et al., 2001; Huising et al., 2008; Karolyi et al., 1999).

Both receptors and ligands are widely distributed throughout the brain (Fig. 5). High levels of CRFR1 are found in the anterior pituitary, olfactory bulb, cerebral cortex, hippocampus, and cerebellum. The mammalian brain variant CRFR2α is located in the lateral septum,

BNST, ventral medial hypothalamus, raphe nuclei, and choroid plexus (Chalmers et al., 1995; Lovenberg et al., 1995; Van Pett et al., 2000).

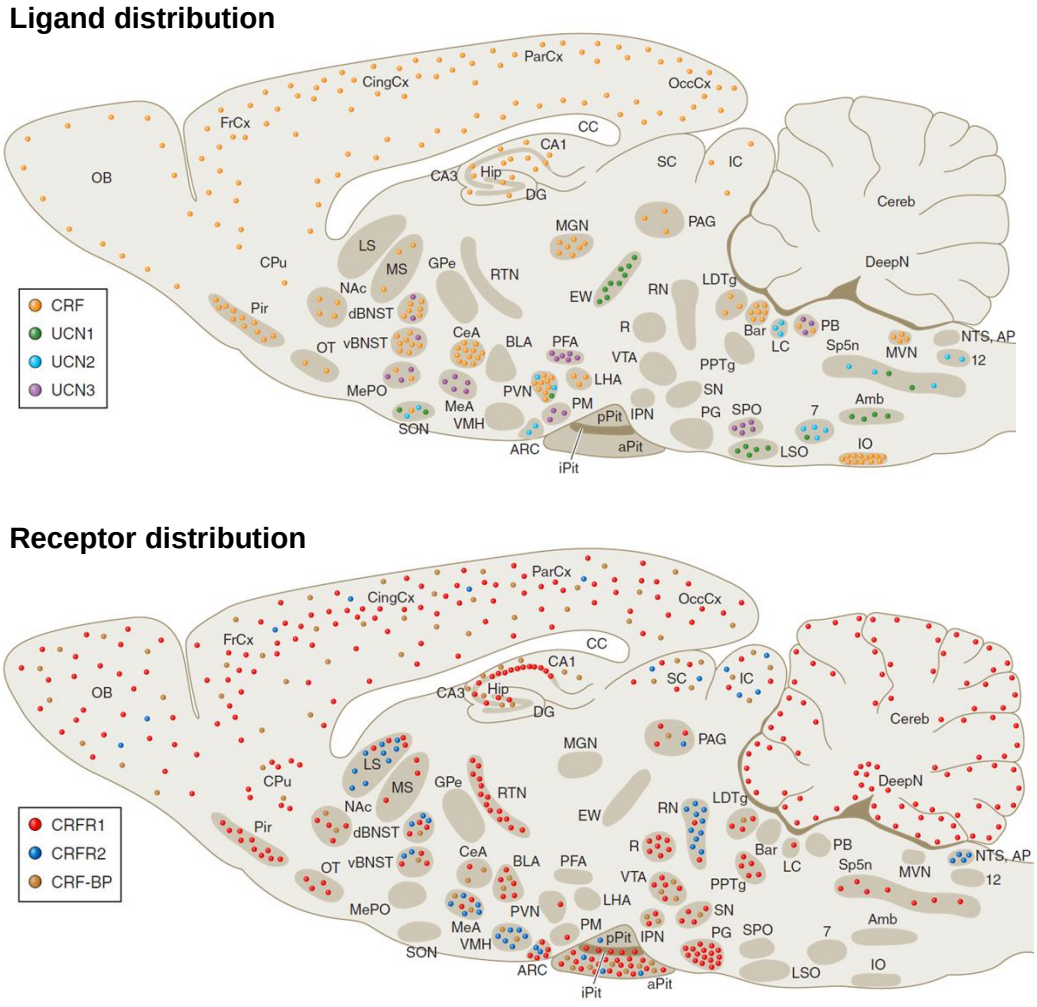

Figure 5. Distribution of CRF, UCN1-3, CRFR1, CRFR2, and CRF-BP mRNA expression in the rodent brain. Scheme taken from Deussing and Chen, 2018. Please note that in the lower scheme, PVN expression of CRFR2 seems to be absent, however, the data presented in this thesis and the according manuscript (Winter et al, in preparation) proves CRFR2 expression in the PVN.

3.2. Ligand-receptor interaction

Binding affinities of the CRFR1 and CRFR2 are different for CRF and the related UCNs (Fig. 6). These differences are mainly determined by the extracellular domain (ECD) of the receptors, but also the extracellular loops (ECL) and the transmembrane domain (TMD) contribute to the specificity of interactions. Within the N-terminus, amino acid residues 43-50 and 76-84 play an important role in ligand binding specificity. The ECD and the TMD are linked by an amino acid segment close to the first TMD that is also essential for ligand

binding. Furthermore, interactions with the ECLs determine ligand binding specificity, as Arg^{189} mediates binding within the first ECL for the CRFR1, whereas His^{189} mediates binding to the CRFR2.

Additionally, glycosylation influences both ligand binding specificity and signal transduction for the CRFR1 as well as the CRFR2. The highly specific interaction between UCN2/UCN3 and the CRFR2 is attributed to several amino acid residues. For example, Pro^{11}, Ala^{35}, and Ala^{39} are uniquely found in those ligands specifically binding to the CRFR2. In general, active ligands consist of 3 main parts. The N-terminal domain, important for receptor binding and activation, the central binding domain, where the CRF-BP interacts, and the C-terminus that mediates ligand affinity and specificity (Deussing and Chen, 2018 and references therein). For both CRFR1 and CRFR2, several splice variants have been identified however, only one functional splice variant of the CRFR1 is expressed in the central nervous system. Alternative splicing of the CRFR2 is further described in Chapter 4. The importance of the CRFR1 for stress-related behavior was supported by several knockout (KO) studies. Loss of CRFR1 causes chronic GC deficiency, accompanied by reduced anxiety-related behavior and impairments in remote fear memory consolidation. Additionally, conditional KO of the CRFR1 in the forebrain lessens stress-induced dendritic remodeling and spine loss (reviewed in Dedic et al., 2018).

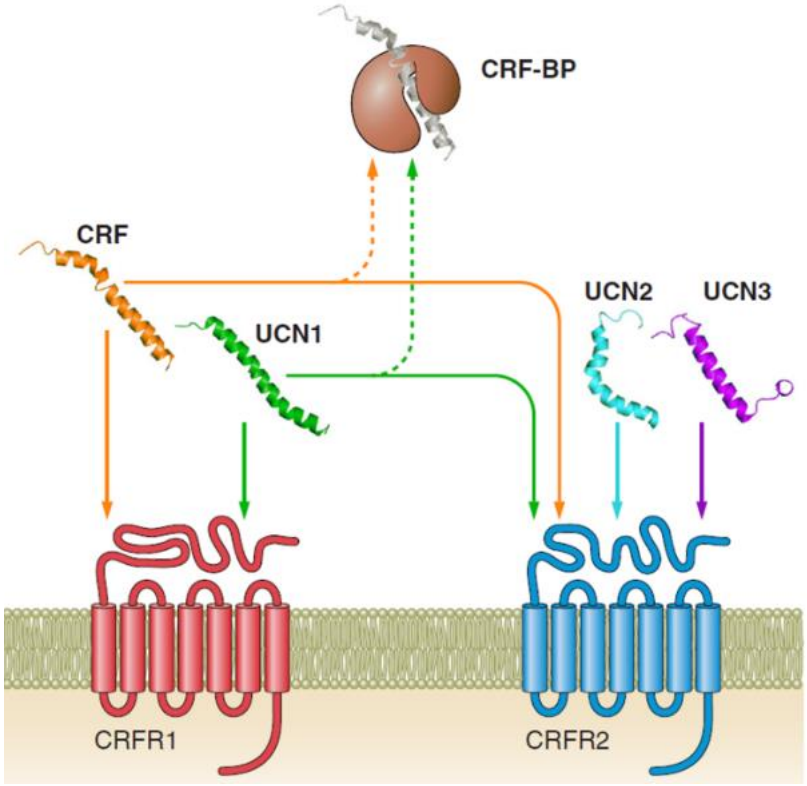

Figure 6. Interactions between CRFR1, CRFR2, and the ligands CRF, UCN1, UCN2, and UCN3.
The potential role of the CRF-BP as a CRF/UCN1-capturing protein is also depicted (adapted from Deussing and Chen, 2018).

3.3. The CRFR2 and its role in anxiety

Studies on the deletion of CRFR2 yield a less clear picture compared to CRFR1. The first 3 conventional CRFR2 KO mouse models revealed normal development of the HPA axis but a hypersensitive response of the HPA axis to stress. Anxiety-like behavior was increased compared to wild-type mice. Both *Ucn* and *Crf* mRNA levels were elevated in the Edinger-Westphal nucleus and central amygdala, respectively (Bale et al., 2000). The effect of CRFR2 deletion or antagonism on baseline anxiety appears the be sex-specific, as the anxiogenic phenotype only occurred in male CRFR2 KO mice but not in females (Kishimoto et al., 2000). Despite the normal development of the HPA axis, CRFR2 is involved in the maintenance of the HPA axis drive and the recovery phase of the HPA response. CRFR2 KO mice display elevated corticosterone levels up to 90 min after stress, in contrast to an early termination of ACTH release (Coste et al., 2000). Impaired stress recovery was also seen in a triple KO mouse, lacking UCN1, UCN2, and UCN3 (Neufeld-Cohen et al., 2010). A more recent study demonstrated that the anxious phenotype of those KOs depends on stress levels. CRFR2 KO mice display increased anxiety-like behavior 24 h after acute restraint stress. However, there were no immediate effects after acute restraint stress as well as after chronic stress in KO compared to wild-type males (Issler et al., 2014). Furthermore, stress-levels, ligand dosage, and brain region are crucial for the impact of CRFR2 activity on anxiety (Bale et al., 2002a; Todorovic et al., 2007). Under low-stress conditions, only a relatively high dose of UCN2 in the septum increased anxiety-like behavior, whereas under high-stress conditions, also lower doses induced anxiety-like behavior (Henry et al., 2006). CRFR2-positive cells in the lateral septum exert GABAergic projections to the anterior hypothalamus. These outputs enhance stress-induced anxiety and promote persistent anxious behaviors, representing a LS circuitry that promotes stress-induced persistent anxiety (Anthony et al., 2014). Antagonism of the CRFR2 with antisauvagine-30 (ASV) also causes differential anxiety-related phenotypes (Hammack et al., 2003; Takahashi et al., 2001). The precise dosage of ASV is essential, as high concentrations might trigger non-CRFR2-mediated effects (Zorrilla et al., 2013).

As already mentioned, UCN2 (Hammack et al., 2003; Valdez et al., 2002) or UCN3 (Valdez et al., 2003) administration and the subsequent activation of the CRFR2 has anxiolytic effects in mice and rats. Moreover, CRFR2 activity is also thought to be related to the serotonergic system (Hammack et al., 2003; Pernar et al., 2004). Application of UCN2 into the dorsal raphe nucleus increased cFOS expression in a subpopulation of serotonergic neurons. However, the precise mechanism behind the effects of UCN and CRFR2 within the serotonergic system remains elusive (Dedic et al., 2018). The serotonergic system is also important for stress-recovery. The CRFR2 mediates the proper functioning of serotonin

(5-HT_{1A}) receptors, as the KO attenuates 5-HT receptor responses in the dorsal raphe nucleus (Issler et al., 2014). In addition to the consequences for anxiety-like behavior, CRFR2 activity also affects social behaviors. KO of either CRFR2 or UCN3 in mice decreases the preference for novel conspecifics and impairs their ability to cope with socially challenging situations (Shemesh et al., 2016). Members of the CRF family, like UCN3, also exhibit in combination with OT, profound effects on long-term potentiation in the rat medial amygdala (Frankiensztajn et al., 2018). Furthermore, blocking of CRFR1 signaling disrupts stress-induced hippocampal tau phosphorylation, a key factor of Alzheimer's disease development. On the contrary, loss of CRFR2 promotes these effects (Rissman et al., 2007).

The generation of different CRFR1 and CRFR2 subforms is mediated by alternative splicing. A mechanism that is found throughout eukaryotes and provides extensive protein diversity.

4. Alternative splicing

Alternative splicing is one of many processes that regulate gene expression, and therefore leads to increased protein diversity. In eukaryotes, genes contain protein-coding sequences (exons) interrupted by non-coding segments (introns, Berget et al., 1977; Chow et al., 1977; Sharp, 1994, 2005). The removal of introns or alternative exons is mediated by a large ribonucleoprotein (RNP) complex, called the spliceosome. The spliceosome mediates RNA cleavage and ligation which are the crucial steps of splicing (Lee and Rio, 2015; Wahl et al., 2009; Will and Luhrmann, 2011). With a number of almost 25.000 genes in the human genome, but around 90.000 proteins being expressed, alternative splicing represents an essential mechanism for diversity in humans, and generally, in mammals (International Human Genome Sequencing, 2004). In fact, around 95 % of human genes undergo alternative splicing. Originally discovered simultaneously with constitutive splicing itself (Gilbert, 1978), there are various types of alternative splicing known today. The most important one for my study is exon skipping, where one so-called cassette exon is either included in the final mRNA or alternatively skipped. This mechanism is based on the formation of the spliceosome, consisting of small nuclear RNAs and small nuclear ribonucleoprotein particles (snRNP). The spliceosome machinery (U1, U2, U4, U5, and U6) assembles on the mRNA, particularly at the 5' splice site (GU), the 3' splice site (AG), and the branch point, upstream of the polypyrimidine tract (PPT). First, U1 forms a base-pairing

interaction with the 5'-splice site, whereas U2 base-pairs with the branch-point. Then, a tri-snRNP complex containing U4, U5, and U6 associates with the forming spliceosome, removing U1 and U4. This leads to two transesterification reactions and joins the exons, excluding the intermediate exon (Fig. 7, La Cognata et al., 2014).

In addition to exon skipping, various other patterns of alternative splicing contribute to the variety of mature mRNA variants. In more detail, alternative 5′ splice sites are additional donor sites and thereby enable different exon lengths at the 3' end. Alternative 3' splice sites function as additional acceptor sites changing the 5' end of the exon. Alternative promoters and alternative 3′ exons lead to different mature mRNA variants by altering the first and last exons, respectively. In the last exon, 3' untranslated regions of different lengths can be created by alternative polyadenylation (Li et al., 2007; Vuong et al., 2016). These mechanisms are the basis for the different transcripts of the OTR gene as well as for the generation of CRFR1 and CRFR2 splice variants. In sheep, alterations in mRNA sequence of the OTR can be observed and are most likely due to alternative use of polyadenylation sites. This represents the first link between alternative splicing and the OTR (Feng et al., 2000).

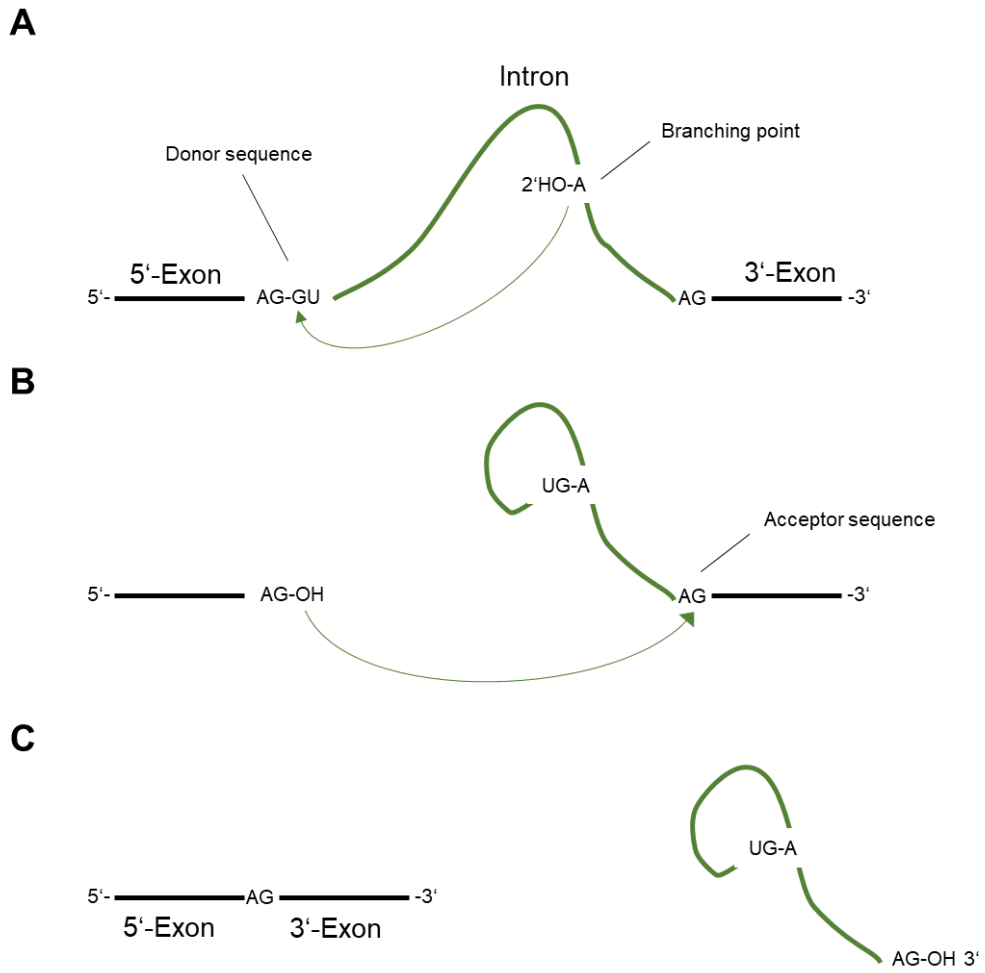

Figure 7. Basic principle of splicing in eukaryotes.

(A) The 5' splice site (donor sequence) is attacked by the 2'OH group of the adenosine at the branching point. **(B)** The released 3'OH group attacks the downstream 3' splice site (acceptor sequence). The intron forms a lariat RNA structure. **(C)** 5' and 3' exons are joined, the intermediate intron is released into degradation (adapted from Seyffert, 2003).

4.1. Alternative splicing of the CRFR2α

The CRFR2 exists as multiple splice variants as described in chapter 3.3. Additional to CRFR2α and CRFR2β (in rodents), and CRFR2γ (humans), another splice variant was discovered recently. It derives from the CRFR2α pre-mRNA, which is translated into a 143-aa soluble protein, consisting of the first ECD of the CRFR2α followed by a unique 38-aa hydrophilic C-terminus. The loss of exon 6 causes a frameshift that leads to a premature termination codon (PTC) in exon 7, ahead of sequences encoding for the transmembrane domain (Fig. 8). Hence, the protein is hypothesized to be released in a soluble form, called sCRFR2α. The sCRFR2α is hypothesized to function as a decoy receptor, however proper

endoplasmic reticulum translocation and trafficking requires expression of the first TMD (Rutz et al., 2006). Evans and Seasholtz confirmed the efficient translation of *sCrfr2α* mRNA. However, the sCRFR2α protein is not trafficked *via* the secretory pathway but rather released by free diffusion through the nucleus pores (Evans and Seasholtz, 2009).
Major sites of cellular expression, as shown by immunohistochemistry, include the olfactory bulb, cortex, midbrain, and the pituitary. Moderate expression of sCRFR2α was found in the PVN of the hypothalamus, while major sites of CRFR2α expression include the lateral septal-, midbrain raphe-, ventromedial hypothalamic-, and medial amygdaloid nuclei (Chen et al., 2005). Due to the intact ECD1, ligand binding activities remained functional. Interaction studies of sCRFR2α with ligands from the CRF family revealed binding of UCN2 and UCN3 with low affinities, whereas binding of CRF and UCN1 occurred with nanomolar affinities, inhibiting the cAMP response to CRF and UCN1 in a dose-dependent manner, and the phosphorylation of ERK1/2 by UCN1 (Chen et al., 2005).

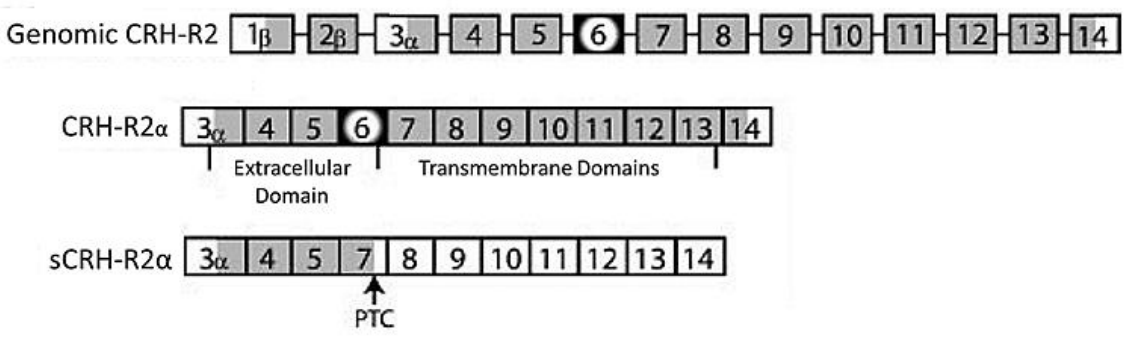

Figure 8. Genomic structure of the *Crfr2* gene.
The Crfr2 consists of 14 exons (upper panel), gray boxes represent translated segments and white boxes indicate untranslated regions. The middle panel depicts the mRNA for the alternative splice variant CRFR2α, including exon 3 to exon 14. *sCrfr2* mRNA consists of exon 3 to exon 7, with a PTC in exon 7, and a unique C-terminal end (figure adapted from Evans and Seasholtz, 2009).

Alternative splicing is not only a mechanism to increase proteomic diversity, but also a potent on- and off switch in gene expression by causing reading frameshifts or the introduction of PTCs. Both events would normally lead to the degradation of the mRNA by nonsense-mediated decay (NMD), as alternative splicing and NMD have shown to be closely linked (da Costa et al., 2017). However, the sCRFR2α mRNA is not targeted for NMD, leading to the synthesis of a functional protein (Evans and Seasholtz, 2009), which has also been shown for other mRNA variants containing a PTC (Denecke et al., 2004;

Dreumont et al., 2005; Ge et al., 2016). This thesis and other studies contribute to the investigation of the function of the sCRFR2α and why its mRNA escapes NMD.

4.2. Neural splicing regulatory networks

Apart from its specific role in sCRFR2 expression, alternative splicing plays an important role in the central nervous system as it is involved in neurogenesis, the regulation of neuronal migration, synaptogenesis, cell survival, the regulation of synaptic function, and has been further linked to neurodegenerative disorders (Vuong et al., 2016). An important splicing factor, nSR100, regulates expression of target genes by inclusion of a neural-specific exon in the transcription factor REST/NRSF. Studies on the knockdown (KD) of nSR100 have revealed impaired neurite outgrowth and neurodevelopmental defects (Raj and Blencowe, 2015; Raj et al., 2011). So far, no studies have assessed the significance of alternative splicing for OTR expression. However, different transcripts found in breast and ovary tissue (Kimura et al., 1992), and alternative polyadenylation patterns (Feng et al., 2000) indicate a link between OTR and alternative splicing.

Other factors linked to splicing/alternative splicing are transcription factors. Interestingly, splicing and alternative splicing can occur co-transcriptionally, meaning all splicing processes are tightly coupled to RNA polymerase II transcription (Kornblihtt et al., 2004). All steps are influenced by each other and coordinated by transcription (Proudfoot et al., 2002). Notably, in neural cells and tissues so-called microexons of 3- to 15 nucleotides length have higher inclusion frequencies compared to standard alternative exons. For example, by the inclusion of microexons, members of the transcription factor family MEF2 are converted into more potent transcriptional activators during neurogenesis (Raj and Blencowe, 2015).

5. MEF2 family of transcription factors

MEF2s are a group of transcription factors (Edmondson and Olson, 1989) belonging to the MADS-box family of transcription factors, whose name is ascribed to the initials of the originally identified members **M**CMI, **A**gamous, **D**eficiens, and **S**erum response factor (Shore and Sharrocks, 1995). Originally discovered in muscle cells, MEF2 occurs in 4 different isoforms, namely MEF2A, B, C, and D, which share high homology in both the amino-terminal MADS domain that mediates DNA binding and the MEF2-specific domain.

This domain affects the affinity of DNA binding and the interaction with cofactors. In contrast to that, C-terminal transcription activation domains of the MEF2 factors exhibit more sequence variation (Fig. 9, Black and Olson, 1998; Brand, 1997). The consensus DNA binding sequence for MEF2 is CTA(A/T)$_4$TAG/A, where MEF2 proteins can bind as homo- or heterodimers (Andres et al., 1995; McKinsey et al., 2002; Molkentin and Olson, 1996; Potthoff and Olson, 2007).

The regulation of MEF2 activity is orchestrated by multiple phosphorylation-, sumoylation-, and acetylation sites. Phosphorylation sites of direct transcriptional activation include MEF2A Threonine 312 (Thr312) and Thr319 as well as MEF2C Serine 387 (S387). In contrast, phosphorylation at MEF2A S408 promotes sumoylation, which prevents acetylation and is ultimately transcriptional inhibitory. Also, phosphorylation of MEF2C at S396 induces sumoylation at Lysine 391 and thereby inhibits transcriptional activity. Phosphorylation at MEF2C S59 enhances DNA binding activity (Molkentin et al., 1996b). Tissue-specific alternative splicing and tissue-specific expression patterns of the 4 different MEF2 isoforms provide highly specific gene activation in different cell types and tissues (reviewed in Brand, 1997). Locations of the highest MEF2 expression include striated muscle and brain tissue (Edmondson et al., 1994).

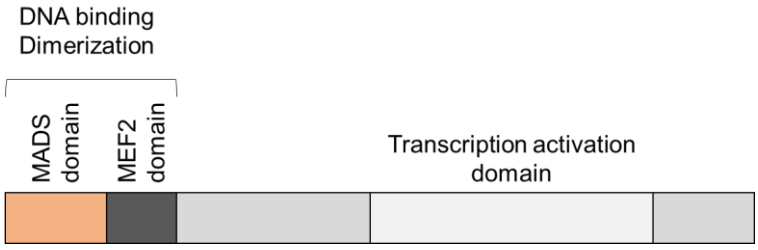

Figure 9. Structure of MEF2 with protein interaction domains indicated (adapted from McKinsey et al., 2002). The MADS domain defines the protein as a member of the MEF2 family and is evolutionary highly conserved. The MEF2 domain defines the MEF2 variant as either A, B, C, or D. The transcription activation domain is highly variable among species (less than 7% similarity between H. sapiens and C. elegans) and MEF2 variants (McKinsey et al., 2002).

5.1. MEF2 signaling cascades

MEF2 is known to be a central regulator of the three major routes of a cell: cell division, differentiation, or death. The activation of diverse genetic programs involved in differentiation, proliferation, morphogenesis, survival, and apoptosis is influenced by MEF2. Signaling towards MEF2 is derived from two main pathways, the MAPK pathway and calcium signaling (Potthoff and Olson, 2007). MEF2 is a well-studied downstream target of

the MAPK pathway, interacting with p38 and ERK pathways (Dodou and Treisman, 1997; Kato et al., 2000; McKinsey et al., 2002). Most prominently, MEF2C is presumed to be a p38-binding protein (Han et al., 1997), but there are also known interactions between MEF2 proteins and the extracellular signal-regulated kinase 5 (ERK5 Devost et al., 2008; Kato et al., 2000; Yang et al., 1998) as well as ERK1/2 (Meyer et al., 2018). One mechanism that mediates calcium signaling is the phosphorylation of class II histone deacetylases (HDACs) by several calcium-regulated protein kinases, including CAMKs. In turn, phosphorylation of class II HDACs regulates MEF2 activity (Lu et al., 2000; McKinsey et al., 2002; Potthoff and Olson, 2007). Another calcium-dependent effector is calcineurin, which activates MEF2 *via* recruitment of NFAT proteins (Blaeser et al., 2000). In neurons, calcineurin was shown to dephosphorylate MEF2A at S408, which causes a switch from sumoylation to acetylation at Lysine 403 (Flavell et al., 2006; Mao and Wiedmann, 1999) and is also involved in OT-induced neurite retraction (Meyer et al., in preparation). Furthermore, expression of MEF2A (Ramachandran et al., 2008) and MEF2C (Wang et al., 2001) itself is controlled by autoregulation.

MEF2 signals then act on a variety of tissues and cell types, like smooth muscle, skeletal muscle, cardiac muscle, neural crest cells, endothelial cells, chondrocytes, lymphocytes, and neurons (Fig. 10).

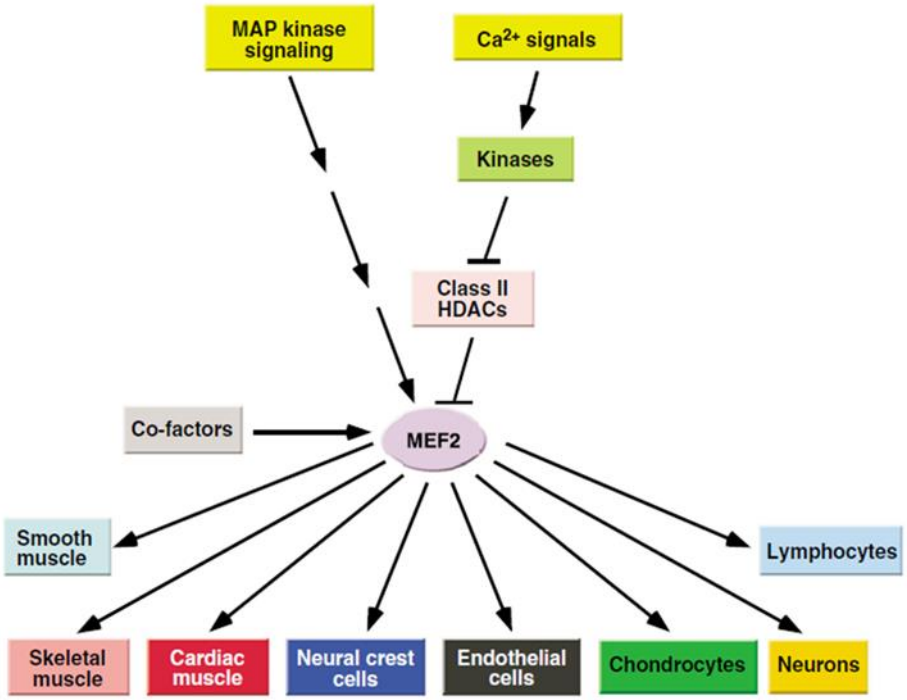

Figure 10. MEF2 signal inputs and downstream effects in various tissues and cell types (Potthoff and Olson, 2007).

5.2. MEF2 functions in the brain

Regions of highest MEF2 expression in the brain are the cerebellum, the cerebral cortex, and the hippocampus (Potthoff and Olson, 2007). MEF2 is involved in synapse regulation and neuronal survival (Mao et al., 1999), dendrite morphogenesis, controlling excitatory synapse formation in hippocampal neurons during development (Flavell et al., 2006; Flavell et al., 2008), and in memory formation and learning-induced spine formation (Barbosa et al., 2008; Cole et al., 2012; Vetere et al., 2011). Furthermore, it was identified as a risk-gene for autism spectrum disorder (ASD Li et al., 2008; Morrow et al., 2008), but not anxiety. The loss of MEF2 proteins exhibits severe effects on synapse number. This was shown for MEF2C, where deletion of MEF2C during postnatal development of mice significantly increased the number of spines in the hippocampus. Learning and memory, however, were not affected (Adachi et al., 2016). The balance between excitatory and inhibitory neurons during development also relies on MEF2C. Conditional deletion of MEF2C during embryogenesis promotes inhibitory synaptic transmission, causing a severe reduction in cortical network activity (Harrington et al., 2016). A brain-specific triple knock out mouse for MEF2A, C, and D led to decreased brain size, impaired synaptic plasticity and increased neuronal apoptosis causing an early death (Akhtar et al., 2012; Akhtar et al., 2009). However, double KO of MEF2A and D neither affected neuronal survival nor altered anxiety-related behavior in the OFT, indicating a partially complementary role of MEF2A and C (Li et al., 2008; Molkentin et al., 1996a).

5.3. Interplay between MEF2 and oxytocin

All MEF2 isoforms are subjected to controlled phosphorylation by MAPK signaling (Han et al., 1997; Kato et al., 2000; Zhao et al., 1999), which is activated by OT (Jurek and Neumann, 2018). OTR activation and MEF2 were linked by the dependency of MEF2 activation by ERK5 (Devost et al., 2008). Furthermore, MEF2 is downstream of MEK1/2 as mentioned above and is phosphorylated by OT *in vitro* (Meyer et al., 2018). Having established that MEF2 is involved in synapse regulation and neuronal survival, in the regulation of excitatory synapses, in memory formation and learning as well as a risk-gene for ASD (for references see chapter 5.2.), it is interesting to note that each of these phenomena have also been linked to OT activity. For example ASD (Parker et al., 2014), spatial memory formation during motherhood (Tomizawa et al., 2003), anti-apoptotic functions, proliferation, and neural differentiation (Jafarzadeh et al., 2014; Leuner et al., 2012; Raymond et al., 2006) or control over GABA synapse development during delivery (Tyzio et al., 2006) are closely connected with the OT system. OT-induced neurite retraction

is mediated by the dephosphorylation of MEF2A at S408 *via* MEK1/2 activity as well as calcineurin signals, bridging the gap between OTR signaling, MEF2 activity, and neuronal morphology (Meyer et al., 2018; Meyer et al., in preparation). The behavioral impact of OT-activated MEF2 signaling and a more detailed analysis of downstream signaling of MEF2 was the main focus of this thesis.

6. Neuronal morphology and its regulation

To understand the function and structure of the nervous system, knowledge of neuronal morphology and functional connectivity is essential (Luo, 2002). Changes in neuronal morphology exert their impact from intracellular signaling to complex emotional behavior.

6.1. Definition of neuronal morphology

Neurons possess two different types of neurites: axons and dendrites, which are morphologically and functionally distinct. Axons extend over long distances and form presynaptic terminals originating from their growth cones. Dendrites extend over shorter distances and often undergo extensive branching, generating so-called dendritic trees. Dendrites interact with axons at their presynaptic terminals and thereby create functional synapses. Small protrusions on dendrites are called spines, forming mostly excitatory synapses in the mammalian brain. Changes in the cytoskeleton are the basis for changes in neuronal morphology. Navigation of neuronal processes is mediated by actin microfilaments, whereas microtubules are responsible for neurite growth. Dynamics of microtubules responsible for neurite growth are regulated by the microtubule-associated proteins (MAPs), in the mammalian brain mostly MAP2 (Goldberg, 2003; Luo, 2002; Mandelkow and Mandelkow, 1995). Intermediate filaments support proliferation and differentiation (Lin and Szaro, 1995), one important factor here is nestin (Hendrickson et al., 2011; Lestanova et al., 2016b).

6.2. Neuropeptides and the regulation of neuronal morphology

Growing evidence suggests the involvement of neuropeptides in the regulation of neuronal growth, neurite extension, and retraction. Neuropeptide signaling *via* GPCRs acts on the organization of the neuronal cytoskeleton by activating PKC pathways as well as by Ca^{2+}-

mediated signaling (reviewed in Lestanova et al., 2016a). GPCR activity, mediated by all G proteins is involved in the regulation of neurite extension and retraction (Karunarathne et al., 2013). OT has emerged as an outstanding effector for neuronal morphology. OT leads to neurite retraction in the rat hypothalamic cell line H32 in a time- and dose-dependent manner. Neurite retraction is under the control of MAPK signaling, as a MEK1/2 inhibitor abolished the OT-induced effect. Further downstream, the transcription factor MEF2A and reduced phosphorylation at S408 account for the morphological effects (Meyer et al., 2018). Interestingly, sex differences in OT effects can be traced back to cellular levels. In human cells derived from a female donor, OT causes neurite elongation in comparison to male Be(2)M17 cells. SH-SY5Y cells have significantly longer neurites after long-term treatment with OT and higher nestin expression levels, whereas MAP2 expression remained unchanged (Lestanova et al., 2016b). OT and OTR ligand exposure have regulatory effects on both MAP2 and nestin expression, indicating a potential role for OT as growth factor for neuronal cells (Bakos et al., 2013). However, these effects appear to be not only sex- but also cell-type specific (Meyer et al., 2018; Zatkova et al., 2018b). In SH-SY5Y cells, the impact of intracellular Ca^{2+} on neuronal morphology was confirmed. OT increases Ca^{2+} levels, whereas antagonism of Ca^{2+} channels reduces neurite length OT-independently. Other proteins involved are SHANK1 and the autism-associated SHANK3 (Zatkova et al., 2018a; Zatkova et al., 2018b). Not only the morphology of single neurons is affected by OT, but also connections between neuronal cells are reinforced by OT stimulations, as the expression of synaptic cell adhesion molecules including neurexins and neuroligins was enhanced (Zatkova et al., 2019).

OT also exhibits profound effects on neuronal morphology *in vivo*. Repeated OT treatment promotes cell proliferation, differentiation, and dendritic complexity of newborn hippocampal neurons (Sanchez-Vidana et al., 2016). Additionally, chronic *i.c.v.* infusions of OT enhances MAP2 levels in the hippocampus of adult male rats, whereas nestin remains unaffected, suggesting a regulatory role for OT in brain plasticity (Havranek et al., 2015). More *in vitro* and *in vivo* OT-mediated effects in the hippocampus were discovered by Ripamonti and colleagues. OT contributes to the development of hippocampal excitatory neurons and thereby supports the balance between excitation and inhibition in the hippocampus. Dysregulations in the connectome of neurons have been linked to several psychiatric disorders including autism (Ripamonti et al., 2017).

Another prominent neuropeptide involved in the regulation of neuronal morphology is CRF. Apart from being a regulator of stress responses, CRF also functions as a differentiating factor. It has been linked to neurite extension and the promotion of growth cones in a cAMP and MAPK-dependent manner (Cibelli et al., 2001). Furthermore, CRF and UCN execute

differential effects on Purkinje cell dendritic outgrowth and differentiation of Purkinje cells. Short-term treatment promotes dendritic outgrowth, whereas long-term exposure had inhibitory effects (Swinny et al., 2004).
As shown for MEF2A in H32 cells (Meyer et al., 2018), transcription factors fundamentally influence neurite outgrowth but it remains a challenge to characterize the interplay between DNA binding factors and cell-surface and cytoskeletal proteins responsible for the morphological shape of neurons (reviewed in Santiago and Bashaw, 2014).

7. The CRISPR-Cas system: a toolbox for investigating the oxytocin system

A comparative analysis of OTR signaling cascades requires the generation of receptor KO cell lines. The CRISPR-Cas system provides the perfect tool and has clear advantages over other techniques, like transient small interfering RNA (siRNA)-mediated KD. The creation of a human OTR KO cell line was an important part of this thesis and therefore, I established the *in vitro* use of the CRISPR-Cas system in our laboratory.

7.1. CRISPR-Cas – the immune system of bacteria

Clustered regularly interspaced short palindromic repeats (CRISPR) and the CRISPR associated (Cas) proteins are encoded in the genome of bacteria and archaea as direct repeats with a length of ~28–40 base pairs (bp), separated by a unique sequence of ~25–40 bp. These so called CRISPR arrays occur as tandems with up to 100 elements (Jansen et al., 2002).
Already discovered in 1987 in *Escherichia coli* (Ishino et al., 1987) and since then identified in various other species of bacteria and archaea (Ishino et al., 2018; Makarova et al., 2015), it took until the early 2000s to unravel the actual function of CRISPR structures: CRISPR-Cas systems represent the acquired immune system of bacteria and archaea against invading nucleic acids, occurring during horizontal gene transfer or conjugation as well as attacking viruses and phages (Bolotin et al., 2005; Mojica et al., 2005; Pourcel et al., 2005). Cas proteins containing functional domains characteristic for nucleases, helicases, polymerases and nucleotide-binding proteins are the mechanistical basis for CRISPR-Cas systems (Haft et al., 2005; Makarova et al., 2006). In type II systems including the Cas9 system, transcription of the precursor CRISPR RNAs (crRNAs) from the CRISPR locus occurs with the support of a *trans*-activating RNA (tracrRNA, Deltcheva et al., 2011).

tracrRNA and crRNA form a complex together with Cas9 and ultimately, the pre-crRNA is cleaved by the endogenous RNase III (Wright et al., 2016). In the last step, interference, a similar complex of mature crRNA, tracrRNA and Cas9 is formed to cleave the target DNA (Jinek et al., 2012). In detail, cleavage of the target strand of the DNA is mediated by the HNH nuclease domain of the nuclease lobe, the RuvC-like nuclease domain mediates cleavage of the non-target strand and contains an intervening α-helical lobe, a HNH domain, and a C-terminal protospacer adjacent motif (PAM)-interacting domain (Anders et al., 2014; Jinek et al., 2012; Wright et al., 2016). PAM-recognition is the important initial step before the helicase subunit starts unwinding the DNA in the seed region, in direct proximity to the PAM sequence (Sternberg et al., 2014). After unwinding, cleavage of both strands of the target DNA starts.

7.2. Genome engineering with CRISPR-Cas9 and more

Programmable nucleases have been employed as efficient tools in genome editing since 1996 (Kim et al., 1996). However, techniques like the zink finger nucleases (ZFNs) and the transcription activator-like effector nucleases (TALENs) have several disadvantages including the expenditure of time, costliness and difficulties in protein design and synthesis. With the discovery of the CRISPR-Cas system, many drawbacks of these techniques could be circumvented. The technology that is used to date in genome editing is the CRISPR-Cas9 system deriving from the class 2 type II system of bacteria, more precisely *Streptococcus pyogenes*, due to its simple mechanism with only one effector protein required. The system only involves the Cas9 protein and a target-specific guide RNA, either as one single-guide RNA molecule or as a complex of crRNA and tracrRNA. Multiplexing with the use of several guide RNAs is facilitated compared to ZFNs or TALENs (Doudna and Charpentier, 2014). Manipulation of the genome is achieved by the response of the cellular DNA repair mechanism to DNA double-strand breaks (DSB) with non-homologous end joining (NHEJ) or microhomology-mediated end joining (MMEJ) which are highly error-prone, frequently resulting in insertion/deletion (In/Del) and frameshift mutations and represent an efficient tool for the generation of KOs (Cubbon et al., 2018; Heidenreich et al., 2003). NHEJ has recently been utilized for the integration of fluorescent tags in a technique called CRISPaint (CRISPR-assisted insertion tagging, Schmid-Burgk et al., 2016). Furthermore, NHEJ is the basis for the so-called VIKING-system, where manipulation of the repair mechanism aims to increase incorporation of the donor DNA into the cut site (Sawatsubashi et al., 2018). Targeted insertions are classically enabled by the

delivery of donor sequences containing homology arms and subsequent homology-directed repair (HDR, Fig. 11, Cubbon et al., 2018).

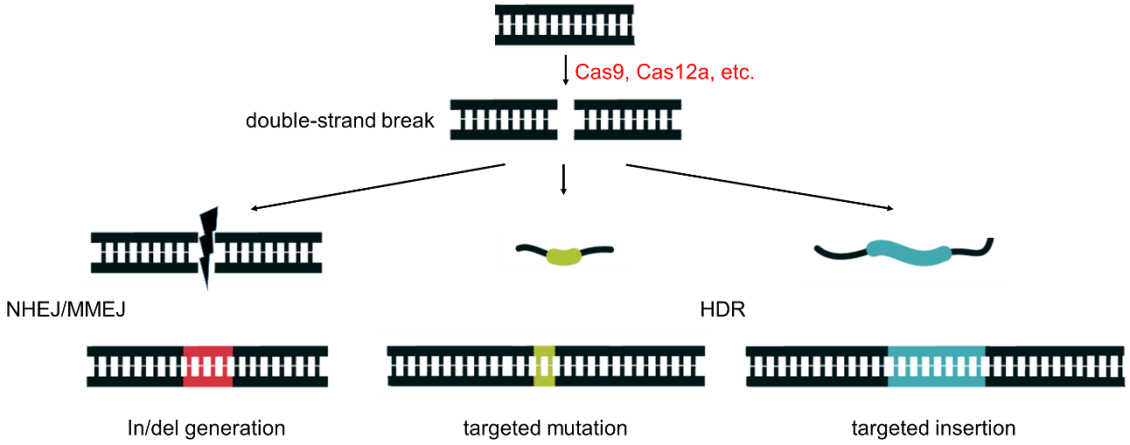

Figure 11. Mechanism of genome editing with CRISPR-Cas.
A site-specific double-strand break is introduced by a nuclease (Cas9, Cas12a, etc.) guided by either sgRNA or crRNA/tracrRNA complex. The cellular DNA repair mechanism reacts with NHEJ or MMEJ, causing a KO, or in the presence of a donor sequence, with HDR leading to a targeted mutation or insertion (adapted from Doudna and Charpentier, 2014).

Cas9 is far from being the only CRISPR-associated protein playing an important role in genome editing approaches. Cas12a, formerly known as Cpf1, has recently been discovered to not only cut double-stranded DNA but also single-stranded DNA (ssDNA) molecules (Chen et al., 2018). Cas proteins targeting RNA include for example proteins from the Cas13 family (Abudayyeh et al., 2016). Difficulties in delivery of Cas9, especially *via* viral transduction, can be now addressed with smaller RNA-guided DNA endonucleases like CasX (Liu et al., 2019) or saCas9 from *Staphylococcus aureus* (Ran et al., 2015). Furthermore, engineered Cas proteins like catalytically deactivated Cas9 (dCas9) to mediate transcriptional activation or down-regulation, or Cas9 D10A nickases to introduce single-strand DNA nicks opened further possibilities for genome engineering with CRISPR-Cas9.

Genome editing without double-strand breaks is enabled by base editing, where a C-G bp is converted into a T-A bp without breaking the DNA double-strand and can be employed for the introduction or correction of point mutations (Komor et al., 2016). The system, called base editor, consists of a cytidine deaminase enzyme coupled to a catalytically inactive Cas9 protein. So far, base editors of the fourth generation have been engineered yielding

up to 50 % editing efficiency (Komor et al., 2016; Komor et al., 2017) and are even further developed *via* phage-assisted continuous evolution, short BE-PACE (Thuronyi et al., 2019). Despite the great advances in the technique since the start of the CRISPR era, especially in molecular and behavioral neuroscience, there are still obstacles that need to be overcome, like brain region-specific delivery of CRISPR components (Heidenreich and Zhang, 2016). In a study from 2017, Staahl and colleagues developed a system for efficient editing in post-mitotic neurons *in vivo* using an engineered version of Cas9 fused to multiple SV40 nuclear localization sequences (NLS). Cas9 with four N-terminal and two C-terminal NLS (4xNLS-Cas9-2xNLS) reached the highest cell penetration and editing efficiencies, making it a promising approach for virus- and chemical carrier molecule-free delivery of CRISPR RNPs into the brain (Staahl et al., 2017). Another step forward was the development of a CRISPR-dCas9 activation system optimized for neurons. Here, dCas9 was fused to a robust transcriptional activator, protein and guide RNA were successfully delivered using a dual lentiviral approach and led to specific activation of the target gene (Savell et al., 2019). Taken together, the CRISPR-Cas system enables fundamental research on cellular function, animal behavior and human neurological disorders. Despite the great efficiency and on-target specificity, off-target editing has to be considered. In addition to easy-to-use off-target detection platforms like DISCOVER-Seq and GUIDE-Seq (Wienert et al., 2019), the development of engineered Cas proteins with minimal off-target cleavage activity has progressed substantially (Ribeiro et al., 2018).

In addition to classical DNA cleavage activity, on-target mRNA dysregulations have been discovered upon CRISPR-Cas9-based introduction of In/Dels. Aberrant mRNA production caused by In/Del mutation can lead to the promotion of internal ribosomal entry, alternatively spliced mRNAs and the induction of exon skipping when exon splicing enhancers are disrupted (Tuladhar et al., 2019).

Taken together, the CRISPR-Cas system harbors the potential for targeted manipulation of alternative splicing and the capability of a directed shift of the ratio between behaviorally relevant splice variants and the corresponding full-length protein, such as the CRFR2α and its soluble variant sCRFR2α. Furthermore, comparative studies on OTR signaling cascades are enabled by the relatively simple generation of KO cell lines.

8. Aim of the thesis

Treatment of psychiatric disorders, including anxiety-related disorders remains rather difficult. With a lifetime prevalence of 30 %, anxiety disorders rank among the most common psychiatric disorders which demonstrates the urgent need for effective treatment but also anamnesis options. The neuropeptide OT as an efficient anxiolytic and antistress factor is a viable candidate and has already been applied in several clinical trials (Neumann and Slattery, 2016). In animal models, the impact of an acute OT bolus on anxiety-related behavior has been assessed and revealed stable anxiolytic effects (Blume et al., 2008; Jurek et al., 2012). However, fundamental knowledge on the molecular background of OT's mode of action is required, especially with regard to repeated and long-term treatment as it would be prescribed to anxiety patients.

The overall aim of this thesis was to identify the signaling cascades involved both in acute and chronic OTR activation, as well as the systemic consequences of such treatment. To achieve this goal, I conducted comparative *in vivo* studies in male and female rats, whose OT system was manipulated by either acute, local OT administration, or the central long-term administration of OT *via* osmotic minipumps, and assessed possible behavioral changes in several behavioral tests, such as EPM, LDB, OFT, and social preference test. As already shown in mice (Peters et al., 2014), chronic treatment with OT for 14 days increases anxiety-related behavior. Based on the previous studies mentioned above, I aimed to reveal the involvement of MAPK signaling in chronic OTR activation. Upon successfully doing so, my next aim was to elucidate the further downstream signaling cascade by which chronic OT exerts its anxiogenic effects. I was able to identify the transcription factor MEF2 as a downstream target of OTR-MAPK signaling and furthermore, I identified a link to alternative splicing of the CRFR2α. The behavioral role of OT-induced alternative splicing *via* a newly identified MAPK-MEF2 signaling pathway will be described in the first part of the thesis presented here.

In the second part of my thesis, I will present my efforts to establish the CRISPR-Cas9 system for differential analyses of OTR-mediated signaling. I was able to create two different KO cell lines, including deletion of the OTR and MEF2A. Cell culture studies of signaling cascades are a viable tool for the reduction of experimental animals needed. My goal was to develop a neuronal *in vitro* system that mimics chronic OT treatment. Stimulations with OT for 12 to 24 h delivered reproducible and reliable results with regard to signaling, alternative splicing, as well as changes in neuronal morphology (Meyer et al., 2018).

Overall, the data presented here contribute to a better understanding of the molecular effects of OTR activation with the focus on clinically relevant chronic administration. They demonstrate an approach for the investigation of treatment duration and dosage and can be potentially applied also for other neuropeptides studied in the context of psychiatric disorders.

Material and Methods

Parts of Materials and Methods have been taken and adapted from the following publication: **Chronic oxytocin signaling reveals alternative splice variant of CRFR2 as biomarker for anxiety** (in preparation).

Julia Winter[1], Magdalena Meyer[1], Ilona Berger[2], Sebastian Peters[3], Melanie Royer[1], Julia Kunze[4], Stefan O. Reber[4], Kerstin Kuffner[5], Anna K. Schmidtner[1], Anna Bludau[1], Marta Bianchi[1], Simone Stang[1], Oliver J. Bosch[1], Erwin van den Burg[6, #] Inga D. Neumann[1, 7, *, #], and Benjamin Jurek[1, #, *]

[1]Department of Behavioural and Molecular Neurobiology, Institute of Zoology, University of Regensburg, Regensburg, Germany; [2]Technische Universität Dresden, University Hospital, Department of Internal Medicine III, Dresden, Germany; [3]Department of Neurology, University Hospital Regensburg, Regensburg, Germany; [4]Laboratory for Molecular Psychosomatics, Clinic for Psychosomatic Medicine and Psychotherapy, University Ulm, Ulm, Germany; [5]Department of Psychiatry and Psychotherapy, University of Regensburg, Regensburg; [6]Centre de neurosciences psychiatriques, Lausanne, Switzerland; [7]lead contact, *corresponding author, [#]these authors contributed equally

Contributions as following:

Conceptualization, B.J., S.P., E.H.vdB., and I.D.N.; Methodology, J.W., M.M., I.B., B.J.; Validation, J.W., M.M., I.B., K.K., M.B., M.R., A.B., Investigation, J.W., M.M., I.B., S.P., M.R., J.K., K.K., O.J.B, A.B., M.B., A.K.S.; Writing – Original Draft, J.W. and B.J.; Writing – Review & Editing, S.P., S.R., O.J.B., E.H.vdB., I.D.N., B.J.; Funding Acquisition, I.D.N. and B.J.; Resources, I.D.N; Supervision, B.J., S.P., E.H.vdB., and I.D.N.

Material and Methods

1. In vivo experiments

1.1. Animals and husbandry

Adult female and male Wistar rats (200-300 g body weight at the beginning of the experiments) were housed under standard laboratory conditions in groups of four (12h light-dark cycle, 22 – 24 °C, lights on at 07.00 h, food and water *ad libitum*). All animal experiments were performed between 08:00 – 11:00 h and were approved by the Government of Unterfranken, Germany. Furthermore, experiments were performed according to the Guide for the Care and Use of Laboratory Animals of the Government of Oberpfalz, the ARRIVE guidelines (Kilkenny et al., 2010), and recommendations from the National Institutes of Health. Group sizes were estimated upon power analysis, based on results from previous publications (Jurek et al., 2012; Peters et al., 2014). Animals were randomly assigned to experimental groups, complying with equal mean body weight between groups. Additionally, blindness of the experimenter to the treatments in all *in vivo* experiments was ensured (Blume et al., 2009). All male rats were obtained from Charles River, Sulzfeld, Germany. Female rats originated from our own breeding at the University of Regensburg.

1.2. Surgical procedures

For the delivery of substances of interest, animals either underwent stereotaxic surgeries for cannula placement, microinfusions, or osmotic minipumps implantation. Prior to surgical procedures, all animals received a subcutaneous injection of Buprenovet as analgesic (Bayer, 0.05 mg/kg Buprenorphine). Surgeries were conducted under isoflurane anesthesia and sterile conditions (Neumann et al., 2000a). Following surgery, the animals received a subcutaneous injection of antibiotics, Baytril, (Bayer, 10 mg/kg Enrofloxacin) and were single-housed in observation cages (38 cm x 22 cm 35 x cm) and monitored daily.

Osmotic minipumps (Alzet, model 1002, flow rate of 0.25 µl/h for 14 days) filled with 40 µM or 4 µM OT (equals 10 ng/h or 1 ng/h OT) were implanted subcutaneously in the abdominal region *via* a 1 cm long incision from the head to the neck of the rat. The pumps were connected to *i.c.v.* cannulas with a silicone tubing (0.5 x 0.9 mm, Reichelt Chemietechnik GmbH + Co., Heidelberg, Germany). After the implantation, kallocryl (Spree-Dental, Groß Köris, Germany) was used for fixation of the cannula and to close the skin. Rats were

monitored daily and weighed on days 1, 8, and 13 of infusion, as well as 4 days after the infusion ended in the respective experiment.

I.c.v. cannulae (21-G, 12 mm) were stereotaxically placed 2 mm above the lateral ventricle (+1.0 mm bregma, +1.6 mm lateral, 2.0 mm below the surface of the skull). For acute local injections into both the left and right PVN of the hypothalamus, 23-G guide cannulae (12 mm) were implanted stereotaxically 2 mm above the PVN (-1.4 mm bregma, -1.8 or +2.1 mm lateral, 6.0 mm below surface of the skull; angle 10°, Paxinos, 1998). In both cases, cannulae were closed using stylets, animals recovered for 1 week with daily handling and cleaning of the stylet to reduce a non-specific stress response by substance injections on the day of experiment.

For OT treatments, oxytocin acetate salt (Bachem, Bubendorf, Switzerland) dissolved in Ringer (B. Braun Melsungen AG) was used at a concentration of 0.01 nmol/0.5 µl per side for local intra-PVN infusions and at a concentration of 0.1 nmol/5µl for lateral *i.c.v.* infusions. Anxiety-related behavior was assessed 10 min after injections (Blume et al., 2008; Jurek et al., 2012). To study the effects of CRFR2α activity on anxiety in the PVN, the antagonist ASV (Tocris Bioscience, Bristol, UK) was dissolved in Ringer (0.28 nmol/µl equals 280 µM per side and animal) was injected 10 min prior to behavioral testings. The CRFR2 agonist stresscopin (SCP, Phoenix Pharmaceuticals, Inc., Burlingame, USA) was applied at a concentration of 3 µg/0.5 µl in Ringer per side and animal, the behavior was assessed 25 min after injections. Ringer solution in corresponding quantity was used as control substance (VEH) in all experiments.

Locked nucleic acid target site blockers (TSB) and GapmeRs (0.5 nmol/0.5 µl per side and animal dissolved in 0.01 M phosphate-buffered saline (1 x PBS; pH 7.4, *in vivo* ready with a 5'-FAM labeling for transfection control; Exiqon/Qiagen, sequences in table 1) were applied by intra-PVN microinfusions using the following coordinates: -1.7 mm bregma, -0.3 mm lateral, 8.2 mm below surface of the skull (Paxinos, 1998). Glass capillaries (VWR, Radnor, USA) for microinfusions with an inner diameter of 0.3 mm, delivering 70 nl per mm, were pulled to create a long narrow shank. The infusion site was closed with sutures and rats were allowed to recover for 7 days.

Table 1. Sequences of TSB, GapmeR and scrambled (scr) control antisense oligonucleotides (ASOs).

TSB/GapmeR	Sequence (5' – 3')
CRFR2-SA6-2	56-FAM-TTCCTCTGCTGGACA
CRFR2-SD7-1	56-FAM-TGGACTCACCGCAGCAC
CRFR2_RAT_SJ5,6_1	56-FAM-TACTTCCTCTGCTTG
NEGATIVE CONTROL A (scr)	56-FAM-ACGTCTATACGCCCA

1.3. Behavioral testings

Anxiety-related behavior was assessed *via* EPM, LDB, and OFT according to the design depicted in figure 12. These tests are based on the natural conflict between the explorative drive and the innate fear of open, bright and exposed areas of rodents. Animals are considered more anxious the more time they spend in dark and unexposed areas of the test setting, e. g. dark box (DB), closed arm (CA) or outer zone (reviewed in Lezak et al., 2017).

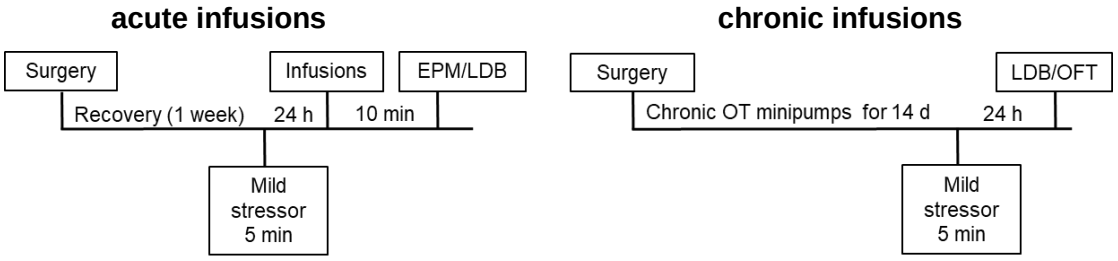

Figure 12. Experimental setup for acute and chronic infusions of OT.

1.3.1. Elevated plus maze

To assess the behavioral impact of acute OT infusions (*i.c.v.* and intra-PVN) animals were tested for 5 min on the EPM as described previously (Pellow et al., 1985; Pellow and File, 1986; Waldherr and Neumann, 2007). Briefly, testing occurred on a plus-shaped maze elevated 70 cm above the floor. Rats were placed in the central neutral zone (10x 10 cm) facing a closed arm and were free to enter both closed (50 x 10 x 40 cm, 10 lux) and open arms (OA, 50 x 10 cm, 100 lux). Behavior was recorded with an overhead camera and analyzed by an observer blind to the treatment by NOLDUS (EthoVision XT 12 version 12, NOLDUS information technology, Wageningen, Netherlands). The percentage of time spent on the OA relative to the time spent on all arms was considered an indicator of anxiety-related behavior. The number of entries into the closed arms reflected locomotor activity.

1.3.2. Light-dark box

The LDB test was performed on day 14 of chronic OT or 10 min after acute infusions as previously described (Peters et al., 2014; Slattery and Neumann, 2010; Waldherr and Neumann, 2007). Only SCP-treated animals underwent LDB testing 25 min after substance application (Klampfl et al., 2014). For LDB testing, the rats were initially placed in the light box (40 cm x 50 cm, 100 lux, LB) facing the DB (40 cm x 30 cm, 0 lux) and allowed to move freely for 5 min. Transitions between the boxes were enabled by a small connection (7.5

cm x 7.5 cm). Distance moved and percentage of time spent in LB and DB were recorded from a top view and analyzed by NOLDUS (EthoVision XT 12 version 12, NOLDUS information technology, Wageningen, Netherlands) by an observer blind to the treatment. The percentage of time spent in the LB relative to the entire test duration was considered an indicator of anxiety-related behavior. Distance moved and velocity reflected locomotor activity.

1.3.3. Open field test

For the third test of anxiety-like behavior, rats were placed in the center of the open field box and allowed to move freely for 5 min. The floor of the box (80 cm x 80 cm, 130 lux in the inner zone (IZ): 40 cm x 40 cm) was divided in squares (10 cm x 10 cm). In a separate cohort of animals social preference was assessed as described previously with modifications (Lukas et al., 2011). First, rats were placed in an open field box and allowed to move freely for 5 min. After this phase of habituation, an empty cage (non-social stimulus) was placed into the inner zone of the box for 5 min. The empty cage was then replaced by a cage with a conspecific (social stimulus) for another 5 min. Duration of direct contact (sniffing) was measured and compared to the investigation time of the non-social stimulus. Distance moved and percentage of time spent in the zones were recorded from a top view and analyzed by NOLDUS (EthoVision XT 12 version 12, NOLDUS information technology, Wageningen, Netherlands) by an observer blind to the treatment.

1.3.4. Acute mild stress paradigm

24 h prior to substance infusion (for chronic OT d13) and the main behavioral testing (EPM, LDB, OFT), all animals underwent a 5 min period of mild stress (novel environment). Stressing occurred either on the OA of the EPM, without access to the CA, or on a circular elevated platform (12 cm diameter, 100 cm height, Blume et al., 2008; Neumann et al., 2000b).

1.4. Collection of trunk blood, brains, tissue, and CSF

Immediately after behavioral testing conscious rats were decapitated, trunk blood was collected in EDTA-coated microtubes (Sarstedt, Nümbrecht, Germany), and centrifuged at 4 °C (5000 g, 10 min). The plasma supernatant was removed and stored for later RIA analysis of plasma OT levels (RIAgnosis, Regensburg). For RNA and protein analysis, PVN

and control regions were directly punched from freshly removed brain tissue and stored at -80 °C in RNAlater (Invitrogen by Thermo Fisher Scientific, Waltham, USA). In selected experiments, CSF was collected before decapitation. For this purpose, rats underwent urethan anesthesia (1.2 g/kg, 25 %, Sigma Aldrich, Darmstadt, Germany). CSF was then recovered *via* the *cisterna magna* using a 25-G cannula and directly frozen on solid CO_2.

1.5. Perfusion and brain slicing

Animals used for the verification of microinfusions of 5' FAM-labelled ASOs were anesthetized with ketamine (10 %, 1 ml/kg, WDT, Wertingen, Germany) and xylazine (2 %, 0.5 ml/kg, Bernburg) and transcardially perfused with 150 ml 1 x PBS and 500 ml 4 % paraformaldehyde (PFA, Sigma Aldrich, Darmstadt, Germany; pH 7.4) in 1 x PBS on ice. Perfusion occurred immediately after the last behavioral test and was performed at a speed of 20 ml/min. After perfusion, removed brains were post-fixed for 24 h in 4 % PFA solution and incubated in 30 % sucrose in 1 x PBS at 4 °C for 3 days for cryoprotection. Processed brains were frozen in ice-cold 2-methylbutane (Sigma Aldrich, Darmstadt, Germany) on dry ice and stored at -80 °C until cryosectioning.

Cannula placement was verified with 40 µm thick Nissl-stained coronal cryosections with the aid of the rat brain atlas (Paxinos, 1998). For verification of correct microinfusions as well as for subsequent immunohistochemical stainings, 40 µm unstained coronal cryosections were used.

2. Cell culture

2.1. Cell lines and cultivation

All cell lines were cultured in 75 cm² cell culture flasks with Dulbecco's Modified Eagle's Medium/Nutrient Mixture F-12 Ham (DMEM/F-12, Sigma Aldrich, Darmstadt, Germany). The medium was supplemented with 10 % heat-inactivated fetal bovine serum (FBS, Capricorn, Germany), and either 1 % Penicillin-Streptomycin (Gibco™, Thermo Fisher Scientific, Waltham, USA) for the rat hypothalamic cell line H32 (Mugele et al., 1993) and the murine N2a cell line (ATCC® CCL-131™), or 1 % MEM non-essential amino acid solution and 0.2 % gentamycin (both Invitrogen, Germany) for human Be(2)-M17 cells (European Collection of Cell Cultures, #95011816). The cells were incubated in humidified atmosphere containing 5 % CO_2 at 37 °C. Passaging was performed weekly by gentle trypsinization

(Trypsin-EDTA solution, 0.25 %, Sigma, Darmstadt, Germany). Primary hypothalamic neurons were obtained as described previously (Jurek et al., 2015), isolation and cultivation of primary cells were performed by Dr. Benjamin Jurek. Briefly, fetal rats were rapidly removed from 18 days pregnant rats after CO_2 sedation and decapitation. Then, fetal hypothalamic tissue was dissected and collected in ice-cold buffer (pH 7.4, containing 137mM NaCl, 5mM KCl, 0.7 mM Na_2HPO_4, 25 mM HEPES buffer, and 100 µg/ml gentamycin). Collagenase type 2 (1 mg/ml; Worthington Biochemical Corporation, Lakewood, USA) was dissolved in the buffer mentioned above, supplemented with 1 mg/ml glucose, 4 mg/ml bovine serum albumin (BSA, Sigma Aldrich, Darmstadt, Germany), 0.2 mg/ml deoxyribonuclease, and used for digestion for 1.5 h. The cell suspension was filtered through a 40-µm cell strainer (BD Falcon, Heidelberg, Germany) and centrifuged at 200 g for 10 min. Cells were washed twice in dispersion buffer and once in plating medium (DMEM/F-12, 100 µg/ml gentamycin and 10 % heat-inactivated FBS) before seeding them in six-well plates coated with poly-L-lysine (1 x 10^6 cells/well). Cells were allowed to grow in the presence of serum for 24 h. Afterward, culture maintenance was performed for eight additional days in neurobasal medium containing B27 supplement (Life Technologies, Inc., Invitrogen). Glial cell proliferation was prevented by using cytosine arabinoside (Sigma Aldrich, Darmstadt, Germany) at a final concentration of 5 µM from day 4 on. After another 6 days, cells were maintained in supplement-free neurobasal medium containing 0.1% BSA (Sigma Aldrich, Darmstadt, Germany; protocol adapted from Liu et al., 2008).

2.2. Stimulations

To investigate signaling pathways activated by OT, several stimulation protocols were performed for subsequent RNA, protein and morphological analyses (for details see chapters below). For protein analysis, H32 cells were seeded at a density of 3 x 10^6 cells in 100 mm culture dishes 24 h prior to experiments and Be(2)-M17 cells were seeded at a density of 6 x 10^6 cells per dish. Stimulations were performed in normal growth medium using OT concentrations of 10 nM and 100 nM. Both acute (10 min to 2 h) and chronic effects (12 h to 24 h) on protein expression and phosphorylation were assessed. Both the OTR specific agonist TGOT as well as AVP were used at a concentration of 100 nM. RNA isolation and morphological analyses required lower cell densities, in detail, 1 x 10^6 H32 and N2a cells, and 2 x 10^6 Be(2)-M17 cells were plated on 50 mm culture dishes. For immunocytochemical analyses, between 1 x 10^4 and 5 x 10^4 cells were plated on chamber slides (BD Falcon, Heidelberg, Germany) 24 h prior to experiments. For methodological details, see chapter 3.4. Immunohistochemistry and immunocytochemistry.

2.3. Differentiation and morphological analysis

Neuronal morphology was assessed according to previous studies (Meyer et al., 2018). As mentioned above, cells were grown in 50 mm culture dishes and cultured in normal growth medium that was complemented with 10 nM or 100 nM OT for 24 h. Afterward, the cellular membrane was stained with Green CellMask (Thermo Fisher Scientific, Waltham, USA) and nuclei were stained with Hoechst 33342 (2 µg/ml, Thermo Fisher Scientific, Waltham, USA). In short, Hoechst 33342 was applied to the cells and incubated for 30 min at 37 °C. After 20 min a dilution of 1 x CellMask was subjoined to the medium and incubated for at least further 10 min at 37 °C. After two 1 x PBS washing steps, the cells were fixed with 4 % PFA and images were taken at the ZOE Fluorescent Microscope (Bio-Rad).

As Be(2)-M17 cells are undifferentiated neurons, a preceding differentiation protocol was required to enable neurite length measurements. Therefore, either 10 mM dibutyryl-cAMP (dbcAMP, Tocris, Cat. No. 1141) for 48 h or neurobasal medium (10% FBS and 0.2% gentamycin) supplied with forskolin (Tocris, Bristol, UK) and retinoic acid (Tocris, Bristol, UK) were applied for 5 consecutive days. After differentiation, cells were recovered in growth medium for 24 h and corresponding stimulations were performed.

2.4. Manipulation of cholesterol content in cellular membranes

The cholesterol content of membranes is a crucial factor for the stability of OTRs (Gimpl and Fahrenholz, 2000, 2002). Low affinity-state receptors in cholesterol-poor membranes can be converted to high-affinity state by the addition of cholesterol and *vice versa* (Gimpl et al., 1995). Thereby, signal transduction and functional activity of the receptor can be manipulated. Cholesterol enrichment and depletion were performed according to the protocol of Prof. Dr. Gerald Gimpl, Mainz. After cholesterol enrichment and depletion, corresponding stimulations were performed as represented in the results section.

2.4.1. Cholesterol enrichment

For the *in vitro* enrichment of cellular membranes with cholesterol, a cholesterol-MßCD solution was prepared. For that, a cholesterol stock (Sigma Aldrich, Darmstadt, Germany) was pre-dissolved in 2-Propanol (3 mM final concentration) and MßCD (Sigma Aldrich, Darmstadt, Germany) was dissolved in double-distilled water (*dd*H_2O) to 40mg/ml. As cholesterol is not soluble in polar solvents, incubation at 80 °C overnight was necessary, whereby MßCD forms a complex with cholesterol and resulted in a clear solution.

Cellular membranes were then enriched for 30 min at 37 °C using a 0.3 mM cholesterol-MßCD solution diluted in DMEM/F-12 with 0.1 % BSA (Sigma Aldrich, Darmstadt, Germany).

2.4.2. Cholesterol depletion

To deplete cellular membranes from cholesterol, a 200mM MßCD stock solution was prepared (2.67g/10ml *dd*H_2O). Cells received DMEM/F-12 with 0.1 % BSA (Sigma Aldrich, Darmstadt, Germany) containing MßCD in a final concentration of 10 mM for 30 min at 37 °C.

2.4.3. Filipin staining

Filipin III (Sigma Aldrich, Darmstadt, Germany) is a polyene macrolide antibiotic, isolated from *Streptomyces filipinensis* and is widely used to visualize cholesterol in plasma membranes due to its ability to bind to sterols (Beknke et al., 1984). Either cholesterol-enriched, -depleted, or VEH treated Be(2)-M17 cells were stained with filipin (100µg/ml in 1 x PBS) under light protected conditions for 2 hours at room temperature (RT). For mounting, p-phenylenediamine (Sigma Aldrich, Darmstadt, Germany) was dissolved in ProLong® Gold Antifade Reagent (Cell Signaling Technologies) to a final concentration of 1 mg/ml. Images were acquired using the SP8 Leica confocal microscope with an x20 objective at an excitation of 415-500 nm and subsequently analyzed with ImageJ Fiji software (Rueden et al., 2017; Schindelin et al., 2012).

2.5. Plasmid-mediated oxytocin receptor overexpression

Transient overexpression of the OTR was achieved by the transfection of a plasmid, containing the human OTR coding sequence. The RC211797 OTR plasmid from Origene was delivered into cells *via* cationic lipid delivery using Lipofectamine™ 3000 and P3000 Reagent (Invitrogen, Carlsbad, USA) according to the manufacturer's protocol. Plasmid construction was based on a pCMV6-Entry vector and contained a myc-DDK tag for target antibody-independent confirmation of expression. Stimulations with OT were performed 3 days after transfection.

2.6. CRISPR-Cas9

Genome editing using the CRISPR-Cas9 system was applied to generate KO cell lines as well as to enable tag-mediated detection of endogenous protein expression.

2.6.1. Otr knockout

For KO of the *Otr* gene in human Be(2)-M17 cells, Oxytocin-R Double Nickase Plasmids (h, Santa Cruz Biotechnology, Dallas, USA) were transfected. Cationic lipid delivery with Lipofectamine™ 3000 and P3000 Reagent (both Invitrogen, Carlsbad, USA) was applied to deliver the plasmids to the cells. Expression of a green fluorescent protein (GFP) on the CRISPR plasmids enabled immediate visual confirmation of transfection efficiency. To obtain single-cell colonies, pre-selection of transfected cells, expressing the antibiotic resistance gene, with a puromycine antibiotic treatment (Puromycin dihydrochloride, Santa Cruz Biotechnology, Dallas, USA) was performed for 5 days at a concentration of 5µg/ml. Afterward, cells were diluted and seeded in 96-well plates at a density of 1 cell per well and re-cultured for several weeks. The genotype of the cell lines acquired was assessed by means of western blot, qPCR, and sequencing.

2.6.2. Mef2a knockout

The Alt-R® CRISPR-Cas9 system (IDT, Coralville, USA) was used to create a *Mef2a* KO H32 cell line. RNP complexes were transfected by cationic lipid delivery using Lipofectamine™ RNAiMAX Transfection Reagent (Invitrogen, Carlsbad, USA) and Opti-MEM (Gibco). Transfected complexes consisted of the functional gRNA duplex, containing the sequence-specific crRNA (sequences in table 2) and the ATTO 550-labeled tracrRNA in nuclease-free duplex buffer, and the S. p. Cas9 Nuclease 3NLS. Transfected single-cells were acquired 2 h after transfection by cell sorting (see chapter 2.6.5.) and re-cultured for several weeks. The genotype was assessed by means of western blot, qPCR, and sequencing.

Table 2. Sequences of crRNA for *Mef2a* KO.

Name	**Sequence (5' - 3')**
Rn.Cas9.MEF2A.1.AA	CAGGACGAACTCGGATATTG
Rn.Cas9.MEF2A.1.AB	GCTTTGTCGTACACTAACCC
Rn.Cas9.MEF2A.1.AC	ACAGACCTCACGGTACCAAA

2.6.3. HiBiT

Membrane-bound CRFR2α was visualized using the Nano-Glo® HiBiT Extracellular Detection System (Promega, Mannheim, Germany). Therefore, a HiBiT-containing Ultramer® ssDNA donor sequence was introduced directly upstream of exon 6 of the CRFR2α gene. H32 cells were transfected with Alt-R® CRISPR-Cas9 complexes as described above; the HiBiT donor sequence was applied together with the RNP complex transfection mixture. Sequences of crRNAs and HiBiT donors are listed in table 3. Single-cell isolation occurred again *via* fluorescence-activated cell sorting (FACS, see chapter 2.6.5.). After re-culturing for several weeks, the genotype was assessed by means of western blot, qPCR, and sequencing.

Table 3. Sequences of crRNA and donor ssDNA for HiBiT-tagging of the CRFR2α.

Name	**Sequence (5' - 3')**
Sequence 1	GCAGGTCATACTTCCTCTGC
Sequence 2	ACTTCCTCTGCTGGACAGAC
Sequence 3	TGCTGGACAGACAGGCAGAC
Linker sequence	Ggatcatcaggaggatcatcagga
HiBiT-encoding sequence	GTGAGCGGCTGGCGGCTGTTCAAGAAGATTAGC

For the detection of membrane-bound CRFR2α, cells were seeded in 96-well plates at a density of 1 x 10^4 cells per well and stimulated with 100 nM OT for 24 h. During incubation with 1:2 LgBiT Protein/HiBiT Extracellular Substrate in Nano-Glo® HiBiT Extracellular Buffer and serum-free (0.1 % BSA Sigma Aldrich, Darmstadt, Germany) DMEM/F-12 (Sigma Aldrich, Germany), the complementary polypeptide LgBiT binds to the HiBiT tag and reconstitutes the luminescent NanoBiT enzyme (Schwinn et al., 2018). Luminescence was measured at the GloMax Explorer (Promega, Mannheim, Germany).

2.6.4. Sequencing

Successful genome editing was confirmed *via* Sanger sequencing performed by Macrogen (Seoul, South Korea). Sequencing results were analyzed and compared to Be(2)-M17 genome using Serial Cloner 2.6.1 software (serialbasics.free.fr/Serial_Cloner.html). For sequencing, corresponding DNA segments containing the CRISPR cutting sites were amplified *via* PCR and purified using the DNeasy Blood & Tissue Kit (Qiagen, Hilden, Germany).

2.6.5. Cell sorting

Single-cell sorting of cells transfected with CRISPR components mentioned above (2.6.2. and 2.6.3.) was performed at the 'Central FACS Facility' (CFF) at the Regensburger Centrum für Interventionelle Immunologie (RCI, PD Dr. Petra Hoffmann). The FACS Aria IIu cell sorter (BD Biosciences, San Jose, USA) at the Institute of Immunology of the University Hospital Regensburg was used, sorting was performed by Irina Fink.

3. Molecular techniques

3.1. Protein isolation

Standard western blot analysis was performed with RIPA buffer-isolated whole-cell protein samples. Briefly, tissue or cells were harvested, resuspended in ice-cold RIPA buffer (Sigma Aldrich, Darmstadt, Germany) supplemented with 1 x Halt™ Protease & Phosphatase Inhibitor Cocktail (Thermo Fisher Scientific, Waltham, USA), and incubated for 1 h at 4 °C with vortexing every 10 min. After centrifugation for 15 min at 13.000 revolutions per min (rpm) and 4 °C, the supernatant containing the proteins was recovered. All samples from *in vitro* stimulations were purified with RIPA buffer. For simultaneous retrieval of *in vivo* protein and RNA samples, the NucleoSpin® RNA/Protein Kit (Macherey-Nagel, Düren, Germany) was used and samples were processed according to the manufacturer's protocol. The Nuclear Extract Kit (Active Motif, Rixensart, Belgium) was used for both whole-cell protein extraction and preparation of nuclear and cytoplasmic fractions from cells and freshly punched tissue. Analysis of OTR protein expression required gentle cell lysis with EDTA lysis buffer, containing 0.5 mM EDTA (0.02 % Sigma Aldrich, Darmstadt, Germany), 250 mM NaCl, 50 mM HEPES (Sigma Aldrich, Darmstadt, Germany), 0.05 % Igepal (Sigma Aldrich, Darmstadt, Germany and 1 x Halt™ Protease & Phosphatase Inhibitor Cocktail (Thermo Fisher Scientific, Waltham, USA). Resuspended cells (Be(2)-M17 and H32) were incubated for 1 h at 4 °C with vortexing every 10 min. After centrifugation at 13.000 rpm and 4 °C for 15 min, the protein supernatant was transferred to a fresh 1.5 ml cup.

Protein concentrations in all samples were determined using the Pierce™ BCA Protein Assay Kit (Thermo Fisher Scientific, Waltham, USA) and compared to the BSA standard curve provided with the kit.

3.2. SDS PAGE, western blot, and dot blot

Protein expression and phosphorylation levels, basal as well as after stimulations or after *in vivo* treatment, were assessed by means of western blot. For all experiments, between 15 and 30 µg protein were loaded onto Mini-PROTEAN® TGX Stain-Free™ Precast Gels or Criterion™ TGX Stain-Free™ Precast Gels (Bio-Rad, Munich, Germany) and separated by their molecular weight at 140 V for 1 h. As band size marker, the prestained protein ladder from Fermentas, Inc. (Glen Burnie, USA) was used. After electrophoretic separation, the gels were placed in Trans-Blot® Turbo™ Mini or Midi Nitrocellulose Transfer Packs and blotted in the Trans-Blot® Turbo™ Transfer System for 7 min. To block all non-specific binding sites, membranes were preincubated in either 5 % BSA (Sigma Aldrich, Darmstadt, Germany) in Tris-buffered saline with Tween20 (1 x TBST; pH 7.4) or in 5 % milk powder (Roth, Karlsruhe, Germany) in 1 x TBST buffer. Antibody solutions were prepared according to table 4 and incubated overnight at 4 °C. The next day, membranes were washed with 1 x TBST and incubated with HRP-labeled secondary antibodies at RT for 1 h. Following three washing steps with 1 x TBST, the membrane was incubated for 5 min with Clarity Western ECL (Bio-Rad, Munich, Germany), or Super Signal West Dura Extended Duration Substrate (Thermo Fisher Scientific, Waltham, USA), and the protein/antibody complexes were visualized *via* a chemiluminescent reaction captured by the ChemiDoc XRS+ Imager (Bio-Rad, Munich, Germany). All images were analyzed with Image Lab software (Bio-Rad, Munich, Germany). To consecutively visualize multiple proteins on one membrane, membranes were stripped following visualization to remove bound antibody complexes using Restore™ Western Blot Stripping Solution (Thermo Fisher Scientific, Waltham, USA). Afterward, membranes were blocked for 5 to 30 min with the respective blocking solution, a primary antibody was applied and the protocol was performed as mentioned above.

To assess non-denatured sCRFR2α content in CSF (undiluted) and plasma samples (1:10 dilution), 10 µl each were spotted onto a nitrocellulose membrane (0.45 µm, Bio-Rad, Munich, Germany). After complete drying of the dots, unspecific binding was avoided by incubation in 5 % BSA (Sigma Aldrich, Darmstadt, Germany) blocking solution for 1 h. Following this, the membrane was incubated with primary sCRFR2 antibody (gift from Prof. Dr. Alon Chen) for 30 min at RT and washed three times for 1 min in 1 x TBST. Afterward, the secondary HRP-labeled anti-rabbit antibody (1:1000 in 1 x TBST, #7074, Cell Signaling Technology, Danvers, USA) was applied for 30 min. Prior to development in Clarity Western ECL (BioRad, Munich, Germany), membranes were washed again three times for 1 min in 1 x TBST. Images were acquired using the ChemiDoc XRS+ Imager (Bio-Rad, Munich, Germany) and analyzed with ImageJ Fiji software (Rueden et al., 2017; Schindelin et al., 2012).

Table 4. List of antibodies used in western blot and dot blot with according dilutions and approximate band size.

Antibody	Cat # and Company	Dilution	Band size
sCRFR2 rabbit polyclonal	Gift from A. Chen	1:10000	30 kDa
MEF2A S408 rabbit polyclonal	CusAb PA000728	1:2000	50 kDa
pMEF2A Thr312 rabbit polyclonal	Abcam ab30644	1:2000	55 kDa
pMEF2A Thr319 rabbit polyclonal	OriGene TA325686	1:2000	55 kDa
pMEF2C S396 rabbit polyclonal	OriGene TA326044	1:1000	55 kDa
pMEF2C S59 rabbit polyclonal	Santa Cruz sc-13919-R	1:1000	50 kDa
pMEF2 (B-11) mouse monoclonal	Santa Cruz sc-377535	1:1000	70 kDa
MEF2A total rabbit polyclonal	Acris AP06372PU-N	1:2000	55 kDa
MEF2C total rabbit polyclonal	OriGene TA326189	1:2000	55 kDa
CRFR2 rabbit polyclonal	Millipore ABN 433	1:1000	50 kDa
pMEK1/2 (41G9) rabbit monoclonal	Cell Signaling 9154	1:1000	45 kDa
MEK1/2 rabbit polyclonal	Cell Signaling 9122	1:1000	45 kDa
pERK1/2 rabbit polyclonal	Cell Signaling 9101	1:5000	42,44 kDa
ERK1/2 rabbit polyclonal	Cell Signaling 9102	1:2000	42,44 kDa
CREB rabbit monoclonal	Millipore 04-218	1:2000	43 kDa
pCREB rabbit polyclonal	Millipore 06-519	1:5000	43 kDa
p90RSK1	Santa Cruz sc-231	1:1000	90 kDa
pp90RSK1 rabbit polyclonal	Cell Signaling 9344	1:2000	90 kDa
pELK-1 rabbit polyclonal	Cell Signaling 9181	1:1000	47 kDa
pMSK1 rabbit monoclonal	Abcam ab81294	1:2000	90 kDa
pp38 rabbit polyclonal	Abcam ab32557	1:1000	42 kDa
OTR rabbit monoclonal	Abcam EPR12789	1:2000	55 kDa

3.3. TransAM® MEF2 transcription factor activation assay

Whole-cell protein extraction from chronic OT treated rats was performed using the Nuclear Extract Kit (Active Motif, Rixensart, Belgium). After protein concentration determination *via* BCA assay (Thermo Fisher Scientific, Waltham, USA), 20 µg protein were applied to the oligo-coated 96-well plate and either incubated with a MEF2A or MEF2C subform specific antibody (OriGene, Rockville, USA) according to the manufacturer's instructions. Developing solution was incubated for 10 – 15 min and fluorescence was determined at 450 nm in a plate reader (FluoStar Optima, BMG LABTECH, Ortenberg, Germany).

3.4 Immunohistochemistry and immunocytochemistry

For the verification of ASO (TSB and GapmeR) infusions, 40 µm thick cryosections containing the PVN were generated and stained according to the following protocol. In addition to 5'-FAM-labeled ASOs, OT-neurons in the PVN were stained using the OT-Neurophysin I antibody (PS38, 1:400, gift from H. Gainer). 40 µm thick cryo cut sections containing the PVN were permeabilized, blocked (1 x PBS supplemented with 2 % BSA, 1 % glycine and 0.3 % TritonX-100 (Sigma Aldrich, Darmstadt, Germany), 1 h at RT). After the staining with PS38, the sections were gently transferred to SUPERFROST® glass slides (Thermo Fisher Scientific, Waltham, USA) and mounted with Surgipath Premier cover slips using ProLong Glass Anti-Fade Reagent with DAPI (Thermo Fisher Scientific, Waltham, USA).

Immunocytochemical stainings were performed in primary cells. 0.05 x 10^6 primary hypothalamic cells were seeded in BD Falcon Chamber slides (Poly-D-Lysine coated), fixed in 3 % glyoxal, rinsed in 1 x PBST (0.1% Triton X-100), and blocked with blocking solution (1 x PBS, 2% BSA, and 0.5 % Triton X-100, 1 % glycine, 0.5 % cold water fish gelatin, all chemicals were obtained from Sigma Aldrich, Darmstadt, Germany) for 1 h followed by primary antibody (see table 5) incubations in 1 x PBST. Cells were mounted with ProLong Glass Anti-Fade (Thermo Fisher Scientific, Waltham, USA) and High Precision cover glass (24, 50, #1.5; CG15KH Thor Labs, Newton, USA). Image acquisition was performed at the Leica TCS SP8 confocal microscope and the Leica DM5000B.

Table 5. List of antibodies used in immunocytochemistry with according secondary antibody and dilution used.

Antibody	**Cat # and Company**	**Secondary antibody**	**Dilution**
sCRFR2 rabbit polyclonal	provided by Salk Institute	Alexa Fluor 594 donkey anti-rabbit	1:2000
GFAP mouse monoclonal	Sigma G3893	Cy3 AffiniPure goat anti-mouse IgG Jackson Labs	1:400
OT mouse monoclonal	Gift from H. Gainer	Cy3 AffiniPure goat anti-mouse IgG Jackson Labs	1:400

3.5. RNA and DNA isolation

For analysis of messenger RNA (mRNA) expression of target genes in specific brain regions, freshly punched tissue from PVN, hippocampus and prefrontal cortex was taken and kept in RNAlater at -80 °C for before further processing according to the instruction manual of the NucleoSpin® RNA/Protein Kit (Macherey-Nagel, Düren, Germany). In a second approach, punched rat brain tissue was frozen in 1 ml peqGold TriFast Gold (VWR Life Science, Radnor, USA), carefully thawed on ice, homogenized by pipetting, and RNA was isolated according to the protocol provided by the manufacturer with some modifications as described previously (Jurek et al., 2015; Meyer et al., 2018).

To isolate RNA from the stimulated cells, the medium was aspirated off, cells were washed with warm 1 x PBS, and RNA was isolated using both methods described above. RNA content was measured at a spectrophotometer (ND-100, NanoDrop, Thermo Fisher Scientific, Waltham, USA).

Sanger sequencing of BeJ(1) and Be(2)-M17 required high amounts of genomic DNA. Isolation from cultured cells was performed using the DNeasy Blood & Tissue Kit (Qiagen, Hilden, Germany). Subsequent extraction of amplified gene fragments from agarose gels required purification using the QIAquick Gel Extraction Kit (Qiagen, Hilden, Germany).

3.6. mRNA analysis

Prior to polymerase chain reaction (PCR) and quantitative PCR analysis, 300 ng of total RNA per sample were reverse transcribed into complementary DNA (cDNA) using the SuperScript IV first-strand synthesis system for reverse transcription PCR (RT-PCR, Invitrogen, Carlsbad, USA) according to the manufacturer's protocol. A total amount of 100 ng cDNA was used for PCR analysis.

3.6.1. Polymerase chain reaction

The amplification of the *Otr* gene gene (primer sequences in table 6) was carried out using the Fermentas Dream Taq™ Green PCR Master Mix (Thermo Fisher Scientific, Waltham, USA). The PCR protocol started with an initial 3 min denaturation step at 95 °C. The amplification cycle consisted of a 30 sec denaturation step at 95 °C followed by 45 sec of primer annealing at 58 °C and an extension step at 72 °C for 1 min. The reaction was concluded with an elongation step at 72 °C for 10 min. Analysis of the PCR products was performed by agarose gel electrophoresis in 1 x tris acetate EDTA buffer at 140 V for 1 h.

Table 6. Primers for OTR sequencing.

Target	Sequence 5' – 3'
Oxtr_hum_seq_for#3	ATGTTCGCCTCCACCTAC
Oxtr_hum_seq_rev#3	GAAGAAGAAAGGCGTCCAG

3.6.2. Quantitative polymerase chain reaction

Relative quantification of MEF2A, sCRFR2α, and CRFR2α mRNA levels was performed using the QuantiFast SYBR® Green PCR Kit (Qiagen, Hilden, Germany), using ribosomal protein L13A (Rpl13A) as housekeeping gene (Bonefeld et al., 2008). Primer efficiency for each primer pair was calculated by serial dilution of test cDNA using the Pfaffl method (Bustin et al., 2009; Pfaffl, 2001). Specificity of the qPCR was assured by omitting reverse transcription and by using *dd*H_2O as template. Cycling conditions consisted of an initial denaturation step of 5 min at 95° C, followed by 50 cycles of denaturation at 95° C for 10 s, and annealing/extension at 60° C for 45 s. At the end of the protocol, a melting curve was generated, and PCR products were analyzed by agarose gel electrophoresis to confirm the specificity of the primers (see table 7 for primer sequences). All samples were run in triplicate.

Table 7. Rat primer sequences for the detection and quantification of target genes *via* qPCR.

Target	Sequence 5' – 3'
MEF2A (NM_001014035.1)	Fwd: AAT GGG GCG AAA GAA AAT AC Rev: GCT GGC GTA CTG AAA CAA CT
CRFR2α (NM_022714.1)	Fwd: ACA TCC GAG ACC ATC CAG TA Rev: GGA CTG CAG GAA AGA GTT GA
sCRFR2α	Fwd: CCC ATT TTG GAT GAC AAG GAG TA Rev: GGA TGA AGG TGG TGA TGA GGT T
Rpl13A (NR_073024)	Fwd: ACA AGA AAA AGC GGA TGG TG Rev: TTC CGG TAA TGG ATC TTT GC

3.6.3. Polymerase chain reaction array

RNA samples for PCR array analysis were processed using the NucleoSpin® RNA/Protein Kit (Macherey-Nagel, Düren, Germany). Reverse transcription into cDNA was performed with the RT^2 First Strand Kit (Qiagen, Hilden, Germany). The custom RT2 PCR array (330171 CLAR25389) was purchased from Qiagen and pipetted according to the

manufacturer's protocol. Calculations are based on the $\Delta\Delta C^T$ method, ACTB, B2M, HPRT1 and LDHA were used as housekeepers.

4. Statistical analyses

Data were analyzed using SigmaPlot (version 11.0.0.75, Systat Software). Behavioral and molecular experiments were statistically analyzed performing parametric one-way (factor treatment) or two-way (factors treatment x time) analysis of variance (ANOVA), followed by Holm-Sidak post hoc correction if appropriate (other post hoc corrections are indicated in the corresponding figure legend). For non-parametric data, the Kruskal-Wallis ANOVA on ranks and the Tukey test were applied (other post hoc corrections are indicated in the corresponding figure legend). To compare two groups, separate parametric t-tests or non-parametric Mann-Whitney U tests were performed. Statistical significance was accepted at $p < 0.05$. For behavior, n represents number of animals, for cell culture experiments, n represents number of wells or dishes. In morphology experiments n represents the number of single-cells. As indicated in the figure legend, data are represented as mean ± or + standard error of the mean (SEM). Statistical analysis for normal distribution and equal variance was performed; However, due to consistency, all data are represented as mean.

Results

Parts of the Results have been taken and adapted from the following publication:

Chronic oxytocin signaling reveals alternative splice variant of CRFR2 as biomarker for anxiety (in preparation).

Julia Winter[1], Magdalena Meyer[1], Ilona Berger[2], Sebastian Peters[3], Melanie Royer[1], Julia Kunze[4], Stefan O. Reber[4], Kerstin Kuffner[5], Anna K. Schmidtner[1], Anna Bludau[1], Marta Bianchi[1], Simone Stang[1], Oliver J. Bosch[1], Erwin van den Burg[6, #], Inga D. Neumann[1, 7, *, #], and Benjamin Jurek[1, #, *]

[1]Department of Behavioural and Molecular Neurobiology, Institute of Zoology, University of Regensburg, Regensburg, Germany; [2]Technische Universität Dresden, University Hospital, Department of Internal Medicine III, Dresden, Germany; [3]Department of Neurology, University Hospital Regensburg, Regensburg, Germany; [4]Laboratory for Molecular Psychosomatics, Clinic for Psychosomatic Medicine and Psychotherapy, University Ulm, Ulm, Germany; [5]Department of Psychiatry and Psychotherapy, University of Regensburg, Regensburg; [6]Centre de neurosciences psychiatriques, Lausanne, Switzerland; [7]lead contact, *corresponding author, [#]these authors contributed equally

Contributions as following:

Conceptualization, B.J., S.P., E.H.vdB., and I.D.N.; Methodology, J.W., M.M., I.B., B.J.; Validation, J.W., M.M., I.B., K.K., M.B., M.R., A.B., Investigation, J.W., M.M., I.B., S.P., M.R., J.K., K.K., O.J.B, A.B., M.B., A.K.S.; Writing – Original Draft, J.W. and B.J.; Writing – Review & Editing, S.P., S.R., O.J.B., E.H.vdB., I.D.N., B.J.; Funding Acquisition, I.D.N. and B.J.; Resources, I.D.N; Supervision, B.J., S.P., E.H.vdB., and I.D.N.

Results

1. Differential effects of acute and chronic oxytocin on anxiety-like behavior in rats

Previous studies (Blume et al., 2008; Jurek et al., 2012; van den Burg et al., 2015) demonstrated that acute local intra-PVN infusions of OT reduce anxiety in male rats on the EPM 10 min after substance application. I was able to reproduce the anxiolytic effect of acute OT, validating my experimental setup.

Male rats injected with 0.1 nmol/0.5 µl OT bilaterally into the PVN spent significantly more time investigating the OA (39.3 % ± 5.1 % time on the OA) compared to VEH treated animals (18.6 % ± 3.9 % time on the OA), indicating decreased anxiety-like behavior (Fig. 13A). This effect occurred only when OT was injected directly into the PVN, *i.c.v.* infusions did not alter anxiety-related behavior tested on the EPM (66.5 % ± 14.5 % time on the OA for VEH, 58.04 ± 13.6 % time on the OA for OT treatment, Fig. 13B). However, the anxiolytic effect of OT converted, when OT was administered over a longer period of time. In detail, chronic *i.c.v.* OT infusions for 14 days at a high dose of 10 ng/h reduced the time the rats spent in the light compartment to about 20% (18.7 % ± 2.6 %, Fig 13C). Notably, the anxiogenic phenotype depended on a mild stressor (elevated platform stress, Neumann et al., 2000a) 24 h prior to LDB testing. Omission of exposure to this stressor but treatment with chronic OT (39.73 % ± 2.8 % time spent in LB) was not capable of altering anxiety levels compared to VEH treatment (37.52 % ± 2.2 % spent in LB, Fig. 13C). While the low dose of 1 ng/h of chronic OT had no impact on anxiety-related behavior in male rats, it significantly reduced the time female rats spent in the LB from 57.3 % ± 4.0 to 42.8 % ± 4.1 %. Females treated with the high dose also spent less time in the LB (48.7 % ± 2.7 %), however, this effect did not reach statistical significance (Fig. 13D).

Despite the profound impact on anxiety, both acute and chronic OT-induced effects were transient. I assessed the permanence of acute OT 3 h after intra-PVN infusion and for chronic OT after additional 5 days. In both cases, animals did not display altered anxiety-related behavior (Fig. 13E and F). 3 h after acute treatment animals spent between 76.8 % ± 14.2 % and 48.7 ± 18.2 % time in the LB (Fig. 13E). After the recovery phase for 5 days after chronic OT, the time spent in the LB ranked between 26.7 % ± 4.2 % and 31.4 % ± 11.0 % (Fig. 13F). Locomotion was not affected in any of the behavioral tests performed in this thesis (data not shown).

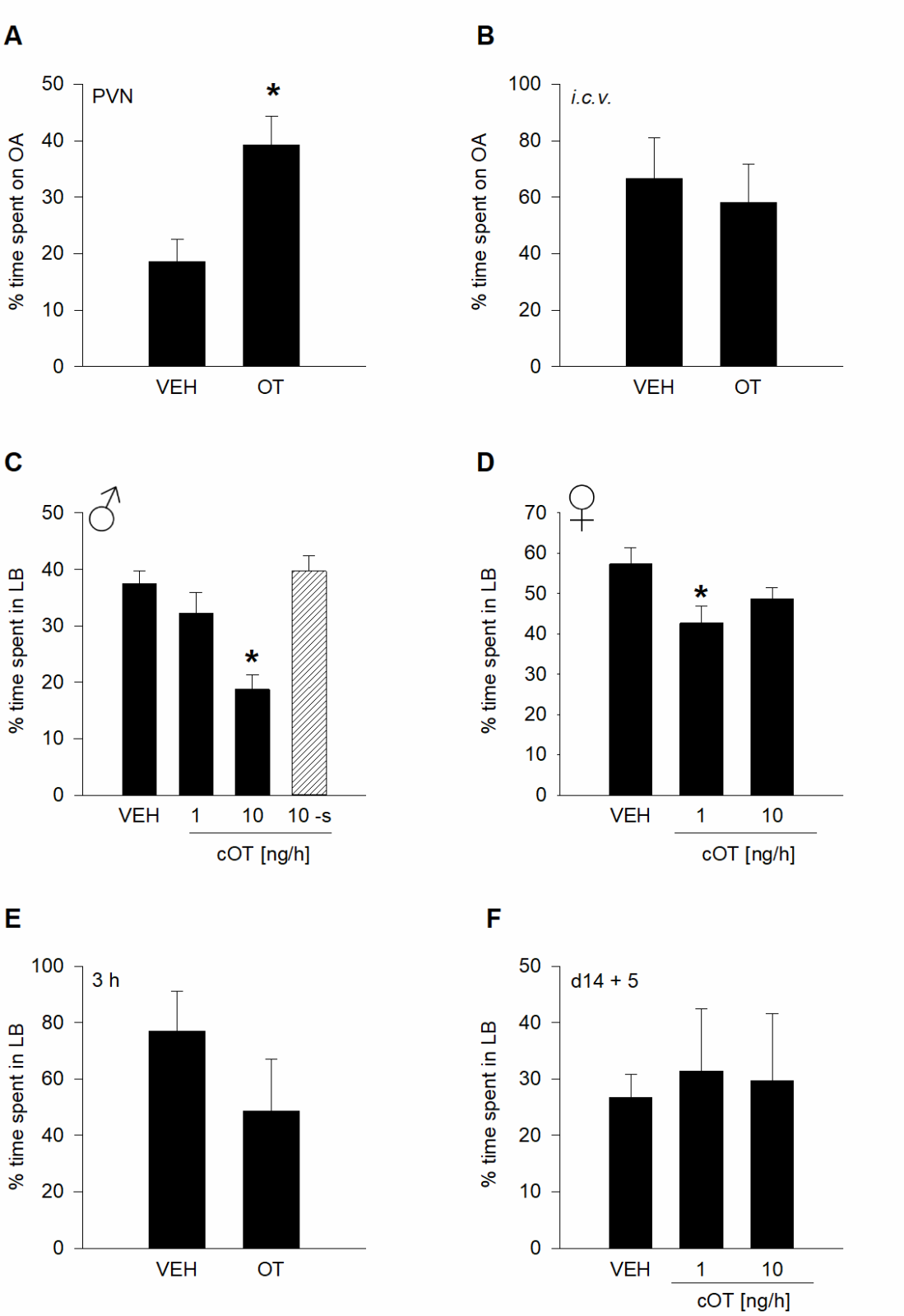

Figure 13. Effects of acute (acOT) and chronic (cOT) OT treatment on anxiety. Due to shortage of space, the abbreviations acOT and cOT are exclusively used in the figures and corresponding legends.

(A) Mean percentage of time male rats spent on the OA of the EPM 10 min after intra-PVN infusions of either VEH (Ringer) or acOT (20µM, corresponding to 0.1nmol/0.5µl per side), representing anxiety-like behavior. Male

rats treated with acOT spent significantly more time on the OA, indicating an anxiolytic effect of OT. Mann-Whitney rank-sum test, * p = 0.006; number of animals: VEH = 8; acOT = 9. **(B)** Anxiety-like behavior represented as mean percentage of time male rats spent on the OA of the EPM 10 min after *i.c.v.* VEH or acOT (20 µM, corresponding to 0.1 nmol/5µl) infusions. No statistically significant differences in anxiety-like behavior were observable, Mann-Whitney U statistic = 17.000, p = 0.937; number of animals: VEH/acOT= 6. **(C)** Anxiety-like behavior represented as mean percentage of time male rats spent in the LB of the LDB after 14 days of *i.c.v.* infusions of VEH (Ringer) or cOT (1 ng/h or 10 ng/h, corresponding to 4 or 40 µM OT dissolved in Ringer, 0.25 µl/h). Animals treated with 10 ng/h cOT spent significantly less time in the LB. One way ANOVA, $F_{(3;59)}$ = 9.577; p < 0.001, Holm-Sidak post hoc test, * p < 0.001 vs VEH; number of animals: VEH = 15, treatment groups = 18, 10 ng/h cOT –s = 9. **(D)** Anxiety-like behavior represented as mean percentage of time female rats spent in the LB of the LDB after 14 days of *i.c.v.* infusions of VEH (Ringer) or cOT (1 ng/h or 10 ng/h, corresponding to 4 or 40 µM OT dissolved in Ringer, 0.25 µl/h). Rats treated with 1 ng/h cOT spent significantly less time in the LB, indicating increased anxiety-like behavior. One way ANOVA on Ranks, H = 7.525 with 2 degrees of freedom, p = 0.023. All Pairwise Multiple Comparison Procedures (Dunn's Method), * p < 0.05 vs VEH; number of animals: VEH = 6, treatment groups = 7. **(E)** Anxiety-like behavior represented as mean percentage of time male rats spent in the LB of the LDB 3 h after intra-PVN infusions of either VEH or OT (20µM, corresponding to 0.1nmol/0.5µl per side). No statistical significant differences, Mann-Whitney U Statistic= 17,000, p = 0.383; number of animals: VEH/treatment group = 7. **(F)** Anxiety-like behavior represented as mean percentage of time male rats spent in the LB of the LDB after 14+5 days of *i.c.v.* infusions of VEH (Ringer) or cOT (1 ng/h or 10 ng/h, corresponding to 4 or 40 µM OT dissolved in Ringer, 0.25 µl/h). The anxiogenic effect of cOT was transient and vanished 5 days after end of infusions. One way ANOVA, $F_{(2;14)}$ = 0.0621, p = 0.940; number of animals: VEH/treatment groups = 5.

2. Downstream signaling of chronic and acute oxytocin

Due to the profound differential behavioral effects of OT, I investigated downstream signaling of OTR with respect to MAPK signaling, the related transcription factor family MEF2 as well as synaptic-plasticity and anxiety-related factors like the CRFR2α and its soluble splice variant sCRFR2α.

2.1. Effects on MAPK and MEF2 signaling

First, I assessed the activity of MEK1/2 in the PVN affected by chronic OT. Phosphorylation levels were increased in both treatment groups compared to VEH. Treatment with 1 ng/h chronic OT increased pMEK1/2 by 4.9-fold (± 1.5), MEK1/2 phosphorylation levels increased 3.8-fold (± 1.0) induced by 10 ng/h chronic OT (Fig. 14A). Also, phosphorylation of ERK1/2 was upregulated but notably only in the high dose of chronic OT (pERK1: 2.5 ± 0.2, pERK2: 2.2 ± 0.2). ERK1/2 activity remained unchanged in the 1 ng/h group (pERK:

1.0 ± 0.2, pERK2: 1.0 ± 0.2, Fig. 14B). This suggests an involvement of the MAPK pathway in the molecular effects of chronic OT similar to its activation seen in pregnancy and lactation or acute OT (Jurek et al., 2012; van den Burg et al., 2015). Total protein levels of MEK1/2 and ERK1/2 remained unchanged (Fig. 14C) Another MAPK signaling kinase ERK5 was phosphorylated in the 1 ng/h group but dephosphorylated in the 10 ng/h group (Fig. 14C). Furthermore, the MAPK-activated transcription factor CREB was significantly increased and activated in both treatment groups whereas MAPK-activated transcription factor ELK-1 remained unchanged (Fig. 14C). Although activated by chronic OT, the involvement of the alternative MAPK pathways p90RSK1 and MSK1/2 in the anxiogenic effect of chronic OT is unlikely, due to unspecific activation in both treatment groups (Fig. 14C). p38 MAP kinase activity remained unchanged in both treatment groups (Fig. 14C).

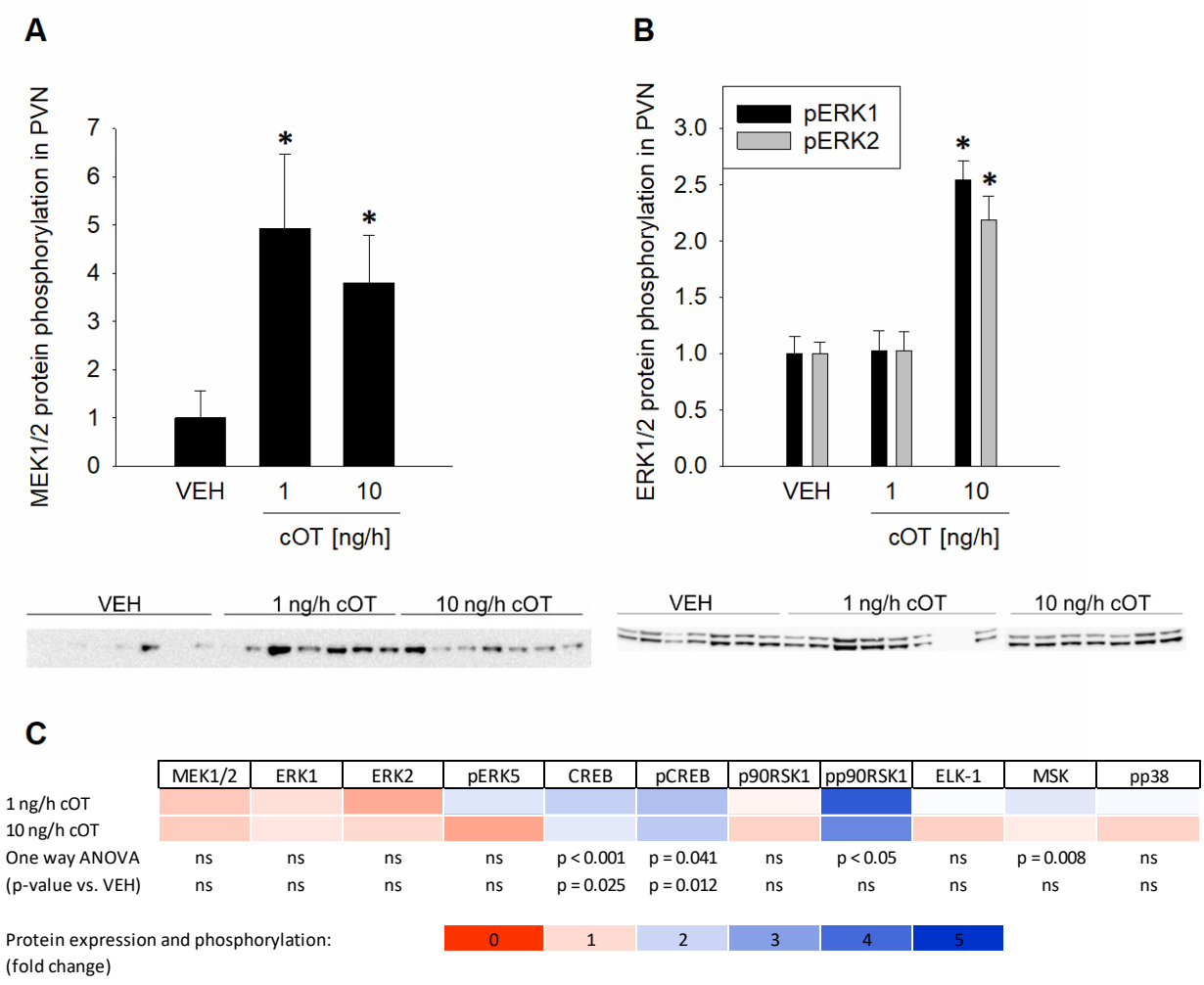

Figure 14. cOT-induced MAPK signaling.

Western blot data is represented as mean fold changes (+SEM) relative to VEH groups.

(A) MEK1/2 protein phosphorylation levels in PVN samples taken from male rats treated with VEH or cOT (1 ng/h or 10 ng/h); number of animals: VEH/treatment groups = 7. One Way ANOVA on Ranks H = 8.396 with 2

degrees of freedom p = 0.015, multiple comparisons versus control group (Dunn's Method), * p < 0.05 1 ng/h and 10 ng/h vs VEH. **(B)** ERK1/2 protein phosphorylation levels in PVN samples taken from male rats treated with VEH or cOT (1 ng/h or 10 ng/h); number of animals: VEH/treatment groups = 7; pERK1: One way ANOVA $F_{(2;20)}$ = 9.672, p = 0.001, Holm-Sidak post hoc test, * p = 0.001 10 ng/h vs VEH and 1 ng/h; pERK2: One Way ANOVA on Ranks H = 10.293 with 2 degrees of freedom p = 0.006. All Pairwise Multiple Comparison Procedures (Tukey Test) * p < 0.05 10 ng/h vs VEH, * p < 0.05 10 ng/h vs 1 ng/h. **(C)** Heat map representing expression and phosphorylation levels of MAPK signaling related kinases.

Focusing on the anxiogenic 10 ng/h chronic OT group, the next question was whether the activation of MAPK pathways culminates in the activation of transcription factors such as MEF2. DNA binding capacity, *i.e.* transcriptional activity of two isoforms, MEF2A and MEF2C was assessed in both male and female rats treated with chronic OT. In the PVN of male rats, MEF2A was activated in all treatment groups, independent of stress levels. The increase ranked between a fold change of 1.6 ± 0.1 (1 ng/h), and 1.5 ± 0.1 (10 ng/h and 10 ng/h – stress, indicated as -s). Significant activation of MEF2C was only detectable in the 1 ng/h (1.1 ± 0.03) group, shifting the focus of research towards MEF2A (Fig. 15A). Chronic OT seems to activate alternative pathways in females, as they displayed no significant changes in MEF2A and MEF2C activity (Fig.15B).

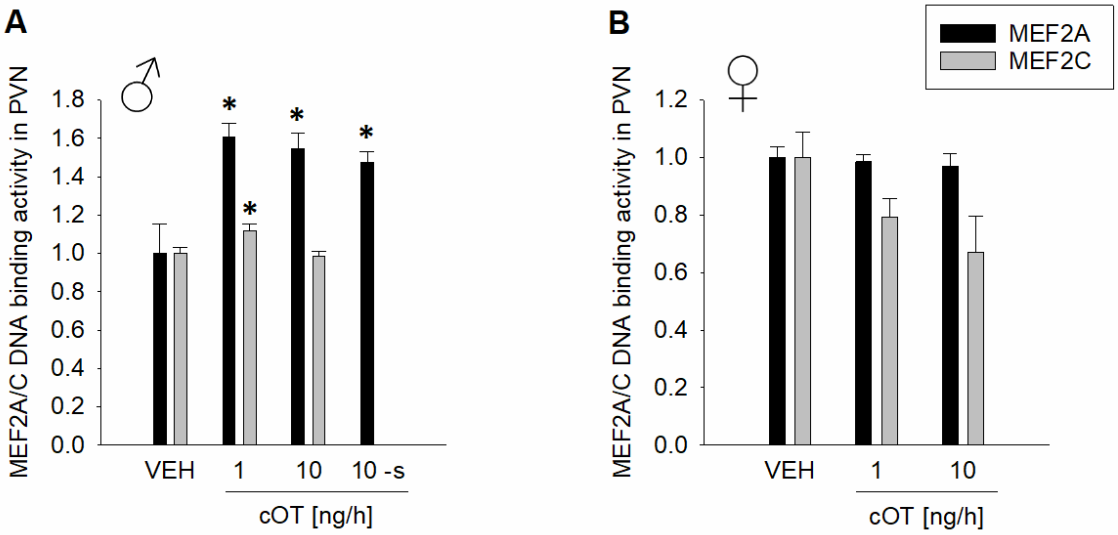

Figure 15. cOT-dependent MEF2A/C activity in PVN of male and female rats.

Analysis of cOT-dependent MEF2A and C activity in PVN samples from both male and female rats treated with VEH or cOT (1 ng/h and 10 ng/h) for 14 d. DNA binding was assesed using the TransAM® MEF2 transcription factor activation assay (Active Motif, Rixensart, Belgium). Results are shown as fold changes (+SEM) in binding activity compared to VEH. **(A)** Binding of MEF2A in males was significantly increased in all treatment groups: One way ANOVA, $F_{(3;39)}$ = 6.732, p = 0.001, Holm-Sidak post hoc test * p < 0.05 vs VEH; number of animals:

VEH = 7; 1 ng/h cOT = 7, 10 ng/h cOT = 16, 10 ng/h cOT –s = 10. Binding of MEF2C in males was only increased in the 1 ng/h group: One way ANOVA $F_{(2;17)}$ = 5.633, p=0.015, Holm-Sidak post hoc test * p=0.015 vs VEH; number of animals: VEH/treatment groups = 6. **(B)** No significant changes in MEF2A and MEF2C DNA binding could be detected in females. Binding MEF2A females: One way ANOVA $F_{(2;22)}$ = 0.177; p = 0.839; number of animals: VEH/1 ng/h cOT = 8, 10 ng/h cOT = 7. Binding MEF2C females: One way ANOVA $F_{(2;22)}$ = 3.186; p = 0.063; number of animals: VEH/ 1 ng/h cOT = 8, 10 ng/h cOT = 7.

Next, I investigated whether the effect of chronic OT-induced MEF2 activation was region-specific for the PVN. In hippocampal tissue of rats treated with chronic OT no changes in MEF2A or MEF2C activity were detectable (Fig 16A). Consistent with the behavioral observations, activation of MEF2A and MEF2C by chronic OT was of transient nature. Chronic OT affected MEF2A/C activity only during ongoing infusion, whereas 5 days after the infusion ended, both MEF2A and MEF2C activity in the PVN returned to basal (Fig. 16B).

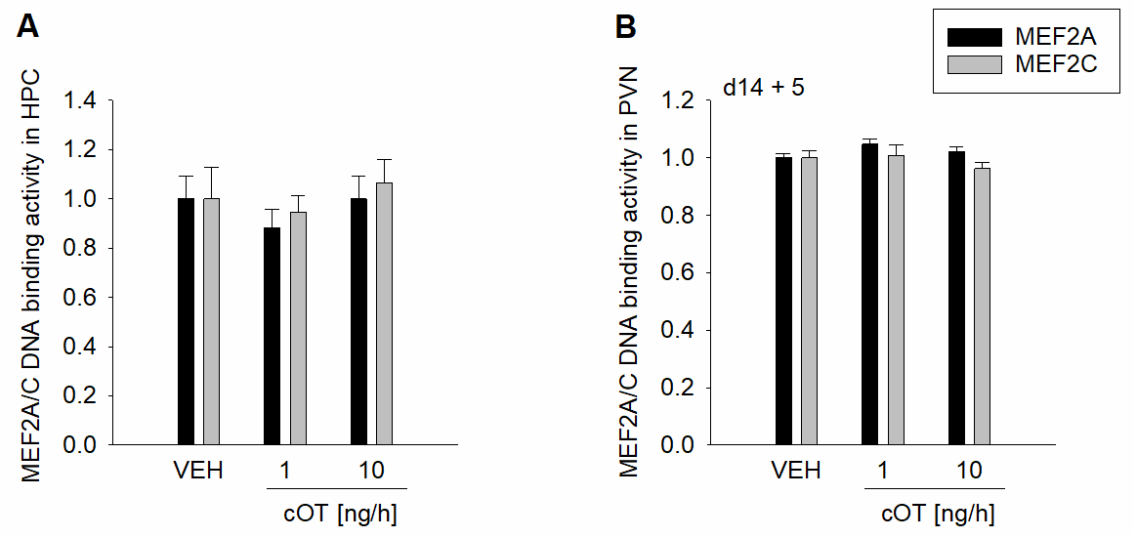

Figure 16. cOT-dependent MEF2A/C activity in hippocampus (HPC) and after recovery.
(A) MEF2A and MEF2C binding activity in HPC tissue of male rats after VEH or cOT (1 ng/h and 10 ng/h) treatment. Shown are fold changes in binding activity compared to VEH. MEF2A: One way ANOVA $F_{(2,20)}$ = 0.632, p = 0.543; number of animals: VEH/treatment groups = 7. MEF2C: One way ANOVA $F_{(2,20)}$ = 0.347, p = 0.712; number of animals: VEH/treatment groups = 7. **(B)** After a 5-days recovery period after cOT, binding of the two MEF2 isoforms was assessed again. No changes could be detected, indicating a transient effect also on a molecular level. MEF2A: One way ANOVA $F_{(2,14)}$ = 2.316, p = 0.141; number of animals: VEH/treatment groups = 5. MEF2C: One way ANOVA $F_{(2;14)}$ = 0.803, p = 0.471; number of animals: VEH/treatment groups = 5.

Having proven that both MEF2A and MEF2C are activated by chronic OT (Fig. 17A), I was focused on a detailed analysis of the different phosphorylation sites. Parallel to the rise in activity, total MEF2 protein levels increased in PVN tissue lysates. In detail, MEF2A total protein levels increased 1.8-fold (± 0.3, 1 ng/h) and 1.6-fold (± 0.1, 10 ng/h) in the OT treatment groups compared to VEH. However, the effect in the 1 ng/h failed to reach significance (Fig. 17A). For MEF2C total protein levels, a significant increase (2.1 fold change ± 0.2) in the 10 ng/h chronic OT group was detected, whereas in the 1 ng/h group (1.6 fold change ± 0.1) significance was not reached (Fig. 17A).

MEF2A activity appeared to be orchestrated by three different phosphorylation sites as shown by further analysis of MEF2 phosphorylation patterns. The phosphorylation of the transcription activating site Thr312 increased 2.2-fold (± 0.4) in the PVN by 1 ng/h chronic OT, whilst 10 ng/h chronic OT increased phosphorylation by 1.7-fold (±0.1, Fig. 17B). A second transcription activating site, Thr319 was significantly activated in both treatment groups (4.1 fold change ± 0.3 for 1 ng/h and 3.3 fold change ± 0.2 for 10 ng/h). Analysis of the transcription inhibitory site S408 revealed a significant 0.5-fold (± 0.1) dephosphorylation exclusively in the PVN of rats treated with the high dose of chronic OT (Fig. 17B). As this phosphorylation pattern corresponded to the increased anxiety-like behavior in the 10 ng/h chronic OT group, the S408 phosphorylation is likely to be the main driver of the chronic OT-induced molecular effects leading to the anxiogenic effect.

Despite the analysis of several phosphorylation sites on MEF2C, its activity could not be linked to the observed behavioral changes induced by the high dose of chronic OT. Phosphorylation at S58 was only increased in the 1 ng/h group (1.8 fold change ± 0.2), whereas phosphorylation at S396 was increased in both treatment groups, 4.1-fold (± 0.3) induced by 1 ng/h and 2.0-fold (± 0.2) by 10 ng/h chronic OT (Fig. 17C). Phosphorylation levels at S387 remained unaffected in both treatment groups compared to VEH (1 ng/h: 1.3 ± 0.2; 10 ng/h: 1.7 ± 0.1, Fig. 17C).

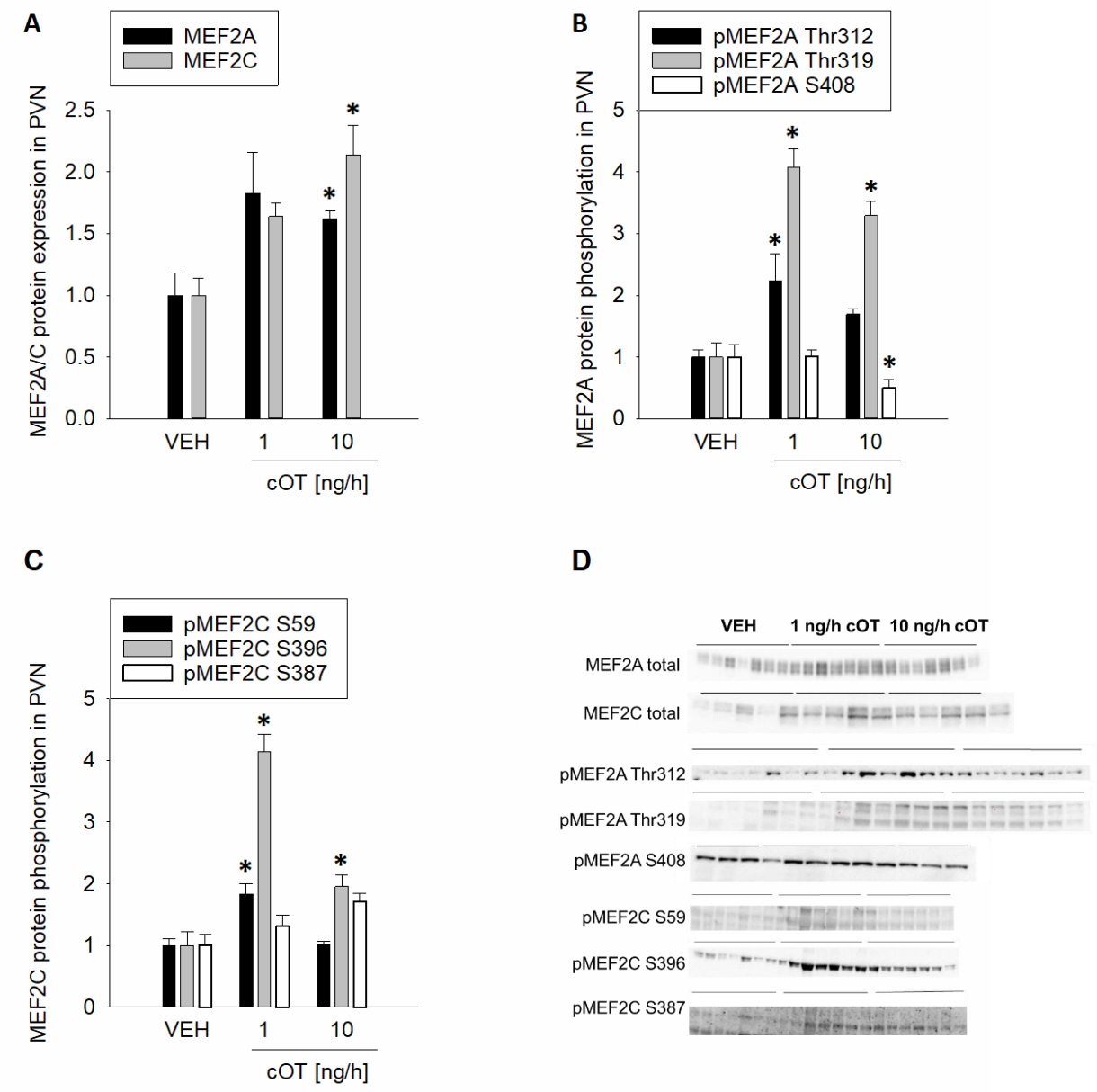

Figure 17. PVN MEF2A and C signaling after cOT in males.

Western blot data is represented as mean fold changes (+SEM) relative to VEH groups.

(A) Both MEF2A and MEF2C total protein expression in PVN were significantly increased after 10 ng/h cOT treatment in male rats. MEF2A: One Way ANOVA on Ranks; H = 7.156 with 2 degrees of freedom, p = 0.028, All Pairwise Multiple Comparison Procedures (Dunn's Method): * p < 0.05 10 ng/h vs VEH; number of animals: VEH/1 ng/h = 6, 10 ng/h = 7. MEF2C: One way ANOVA $F_{(2;19)}$ = 10.189 p < 0.001, Holm-Sidak post hoc test *p < 0.001 10 ng/h vs VEH, VEH = 6, treatment groups = 7. **(B)** Fold changes in phosphorylation levels of MEF2A at several amino acid residues in PVN after VEH or cOT (1 ng/h and 10 ng/h) treatment in male rats. pMEF2A Thr312: One Way ANOVA on Ranks, H = 9.106 with 2 degrees of freedom, p = 0.011. All Pairwise Multiple Comparison Procedures (Tukey Test): * p < 0.05 1 ng/h vs VEH; number of animals: VEH/treatment groups = 7. pMEF2A Thr319: One way ANOVA $F_{(2,17)}$ = 41.139 p < 0.001, Holm-Sidak post hoc test overall significance level p = 0.05; * p < 0.001 1 ng/h vs VEH, * p < 0.001 10 ng/h vs VEH, p = 0.041 1 ng/h vs 10 ng/h; number of animals: VEH/treatment groups = 6. pMEF2A S408: One way ANOVA $F_{(2;23)}$ = 4.614, p = 0.022, Student-

Newman-Keuls post hoc test * p = 0.022 10 ng/h vs 1 ng/h, * p = 0.033 10 ng/h vs VEH; number of animals: VEH/1 ng/h = 7, 10 ng/h = 10. **(C)** Fold changes in phosphorylation levels of MEF2C in PVN after cOT (1 ng/h and 10 ng/h) in male rats compared to VEH treatment. pMEF2C S59: One way ANOVA $F_{(2,20)}$ = 14.718, p < 0.001, Holm-Sidak post hoc test, * p < 0.001 1 ng/h vs VEH, p = 0.988 10 ng/h vs VEH, p < 0.001 1 ng/h vs 10 ng/h; number of animals: VEH/treatment groups = 7. pMEF2C S396: One way ANOVA $F_{(2,17)}$ = 48.277, p < 0.001, Holm-Sidak post hoc test, * p < 0.001 1 ng/h vs VEH, * p = 0.011 10 ng/h vs VEH, p < 0.001 1 ng/h vs 10 ng/h; number of animals: VEH/1 ng/h = 7, 10 ng/h = 6. pMEF2C S387: One way ANOVA $F_{(2,20)}$ = 1.762, p = 0.200; VEH/treatment groups = 7, cOT treatment did not induce statistically significant differences. **(D)** Representative western blots of MEF2A and C protein expression as well as the corresponding phosphorylation sites.

Despite the effect of the low dose of chronic OT on anxiety in female rats, MEF2A and MEF2C DNA binding activity remained unchanged (Fig. 15B), indicating sexually dimorphic downstream signaling. Further analysis of MEF2A and C phosphorylation sites substantiated these observations. The corresponding phosphorylation sites Thr319 and S408 of MEF2A were both not affected by chronic OT treatment in female rats (Fig. 18A). Also, no activation of MEF2C, represented by phosphorylation at the amino acid residue S396 was detectable (Fig. 18A).

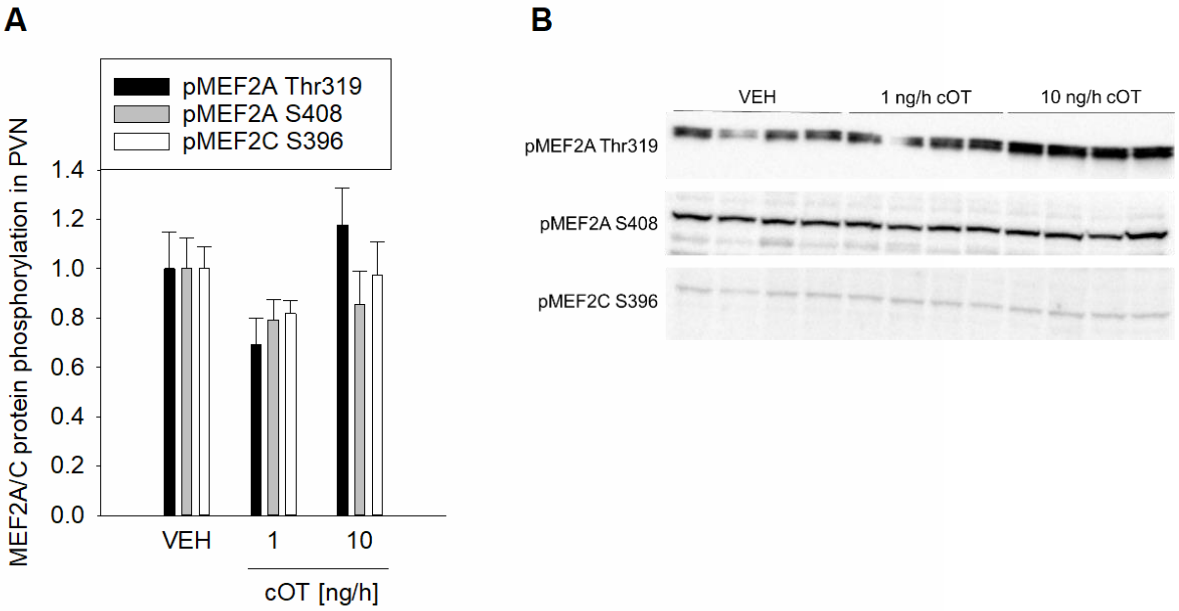

Figure 18. PVN MEF2A and C signaling after cOT in females.

(A) Mean fold changes in protein phosphorylation induced by cOT (1 ng/h and 10 ng/h) treatment compared to VEH. Treatment did not lead to significant differences in female rats. pMEF2A Thr312: One way ANOVA $F_{(2;11)}$ = 3.287, p = 0.085; number of animals: VEH/treatment groups = 4. pMEF2A S408: One way ANOVA $F_{(2;11)}$ = 0.8637, p = 0.454; number of animals: VEH/treatment groups = 4. pMEF2C S396: One way ANOVA $F_{(2;11)}$ = 0.995, p = 0.407; number of animals: VEH/treatment groups = 4. **(B)** Representative western blots of MEF2A and C protein phosphorylation.

To exclude the ability of an acute bolus of OT to increase the transcriptional activity of MEF2A or MEF2C, both total protein expression and DNA binding activity were assessed. Neither an infusion directly into the PVN (Fig. 19A and B), nor an *i.c.v.* infusion (Fig. 19C) had effects on these parameters. This indicated again the transient and late-onset nature of the effect of chronic OT with regard to MEF2A and MEF2C activation.

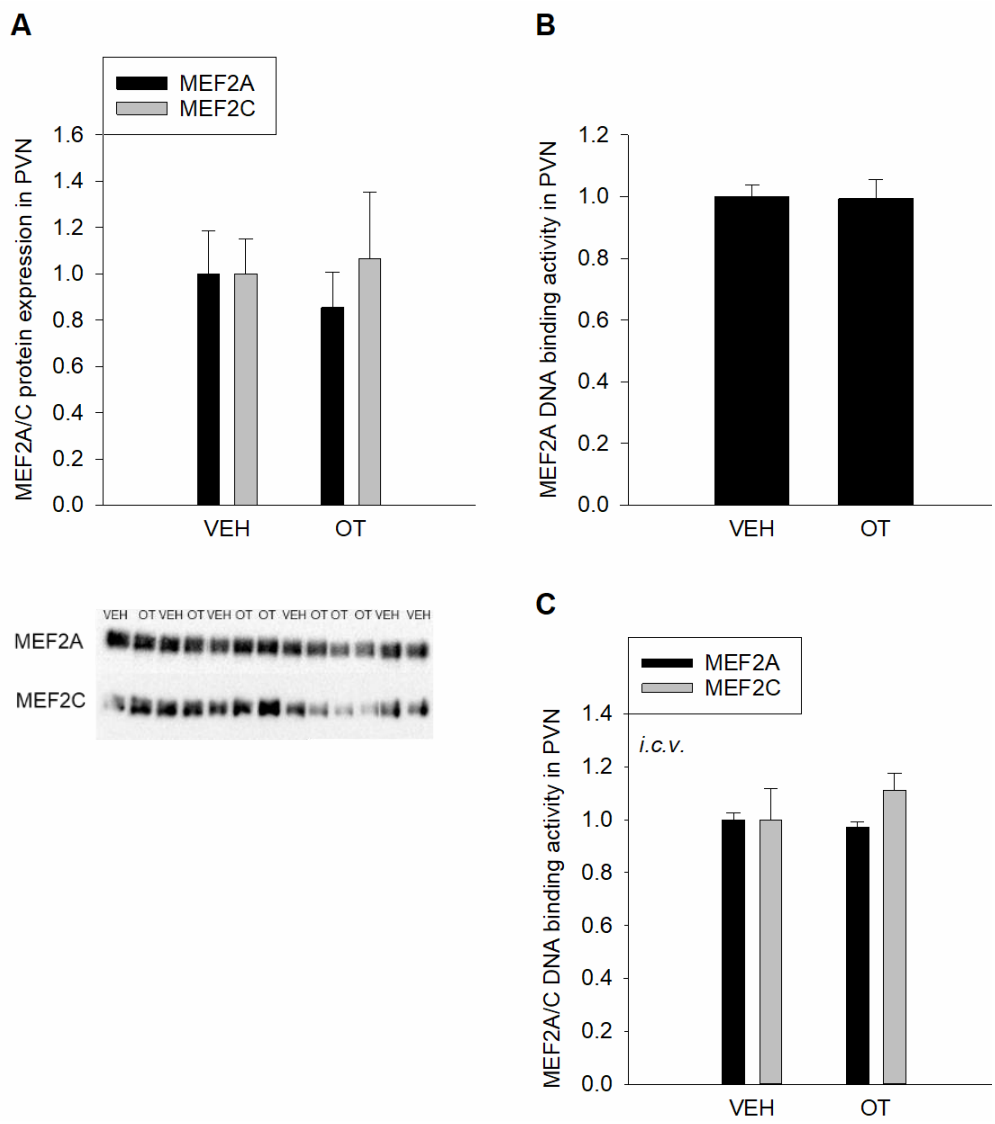

Figure 19. MEF2A/C signaling after acOT treatment.

(A) MEF2A and C total protein levels were assessed after acute treatment with either VEH or OT. For both MEF2A and C, acOT did not lead to altered total protein levels. Data are represented as mean fold changes (+SEM) relative to VEH groups. MEF2A: t = 0.616 with 11 degrees of freedom, one-tailed p-value = 0.275; number of animals: VEH = 6; OT = 7. MEF2C: Rank Sum Test, Mann-Whitney U Statistic= 20.000, p = 0.945; number of animals: VEH = 6; OT = 7. **(B)** acOT-induced MEF2A binding activity in PVN of male rats was analyzed, treatment did not lead to altered MEF2A activity. Data are represented as mean fold changes (+SEM) of DNA binding activity compared to VEH. t = 0.0938 with 11 degrees of freedom, one-tailed p-value = 0.463;

number of animals: VEH = 6, OT = 7. **(C)** MEF2A and MEF2C binding in PVN after *i.c.v.* VEH or acOT treatment. Data are represented as mean fold changes (+SEM) of DNA binding activity compared to VEH. MEF2A: Rank Sum Test; Mann-Whitney U Statistic = 8.000, p = 0.247; number of animals: VEH = 5, OT = 6. MEF2C: Rank Sum Test; Mann-Whitney U Statistic = 11.000, p = 0.537; number of animals: VEH = 5, OT = 6. *i.c.v.* infused acOT has also no effects on MEF2A and MEF2C activity.

In summary, the high dose of chronic OT (10 ng/h) is anxiogenic and, on a molecular level, activates the MAPK pathway *via* phosphorylation of MEK1/2 and ERK1/2. This causes the subsequent dephosphorylation of the transcriptional inhibitory residue S408 at MEF2A. These effects are transient and of late-onset, as after recovery of 5 days as well as after acute OT treatment none of the effects were detectable.

2.2. MEF2A activity induced by chronic oxytocin shifts the expression of mCRFR2α to sCRFR2α

The specific activation of the MAPK pathway and MEF2A signaling in the PVN led to the hypothesis that the hypothalamic PVN is the main target brain region where chronic OT treatment might act. To assess further downstream targets of chronic OT signaling, a PCR array for several stress-, anxiety-, and neuroplasticity-related genes associated with MEF2 was conducted.

PCR array analysis with PVN tissue samples revealed increased *sCrfr2α* (1.3 fold change) and decreased *mCrfr2α* (0.7 fold change) mRNA levels in rats treated with the high dose of OT compared to VEH (Fig. 20A). Furthermore, the transcription factor paired box 3 (*Pax3*) was 0.2-fold downregulated, whereas the closely related *Pax2* was 2-fold upregulated. Despite the behavioral differences, a similar pattern could be observed in the low dose of OT. *Pax2* was 1.5-fold upregulated as well as *sCrfr2α* (1.9 fold change). Additionally, a significant increase in tyrosine hydroxylase (*Th*, 1.7 fold change) mRNA levels and a decrease in *Ucn* (0.4 fold change) mRNA levels appeared. Similar to the 10 ng/h group, *Pax3* (0.3 fold change) and *mCrfr2α* (0.7 fold change) mRNA expression was reduced (Fig. 20B).

Figure 20. cOT-induced effects on stress-, anxiety-, and neuroplasticity-related genes.

(A) PCR array analysis of PVN samples after 10 ng/h cOT compared to VEH. The $\Delta\Delta C^T$ method was used for calculations; number of animals: VEH = 5, 10 ng/h = 6. The following p-values were acquired for statistical significant differences: *Pax3* * p = 0.021, *mCrfr2α* * p = 0.02, *sCrfr2α* # p = 0.09, *Pax2* * p = 0.05. **(B)** PCR array analysis of PVN samples after 1 ng/h cOT compared to VEH. The $\Delta\Delta C^T$ method was used for calculations; number of animals: VEH = 5, 1 ng/h = 6. The following p-values were acquired for statistical significant differences: *Pax3* * p = 0.043, *Ucn* * p = 0.029, *mCrfr2α* * p = 0.022, *sCrfr2α* # p = 0.09, *Th* # p = 0.080.

Data in **(A)** and **(B)** being shown as mean fold changes compared to VEH, values > 1 represent upregulation, values < 1 represent downregulation in mRNA expression.

With the *in silico* detection of a MEF2A responsive element within Exon 6 of the *Crfr2* gene (Winter et al., in preparation) and the data obtained from the PCR array, the CRFR2 was a promising target for chronic OT-mediated MEF2A signaling.

The differential regulation in *mCrfr2α*/*sCrfr2α* mRNA expression was also reflected on protein levels. The behaviorally relevant 10 ng/h group expressed significantly more sCRFR2α protein in the PVN (fold change 4.2 ± 0.6), mCRFR2 levels remained unchanged (fold change 2.4 ± 0.5, Fig. 21A and B). In the 1 ng/h group, OT had no significant impact on mCRFR2α (fold change 2.0 ± 0.3) and sCRFR2α (fold change 2.3 ± 0.3) protein expression (Fig. 21A and B). Despite the regulation of *mCrfr2α*/*sCrfr2α* mRNA in both groups as seen in the PCR array (Fig.20A and B), and the trend to an overall increase in mCRFR2α/sCRFR2α protein levels (Fig. 21A and B), only the high dose of OT caused a significant shift in mCRFR2α/sCRFR2α protein ratio (Fig. 21C lower panel and 21D). The ratio shifted from 79.0 % mCRFR2α in the VEH to 88.3 % in the 10 ng/h OT group, respectively, the sCRFR2α portion halved from 21.1 % (VEH) to 11.8 % (10 ng/h, Fig. 21D). As this shift occurred exclusively in the 10 ng/h chronic OT group, the ration between membrane-bound and soluble receptors appears to be a crucial factor in the regulation of anxiety-related behavior by chronic OT. In line with the absence of MEF2 activation in the PVN of female rats after chronic OT infusions as well as after an acute bolus of OT in males, neither treatment had an impact on mCRFR2α/sCRFR2α protein ratio (Fig. 21E and F). In females, the ratio of mCRFR2α and sCRFR2α ranked between 30.2 % to 69.8 % and 48.0 % to 52.0 % (Fig. 21E). In males treated with acute OT, the percentage of both splice variants was around 50 % and remained unaffected by treatment (Fig. 21F).

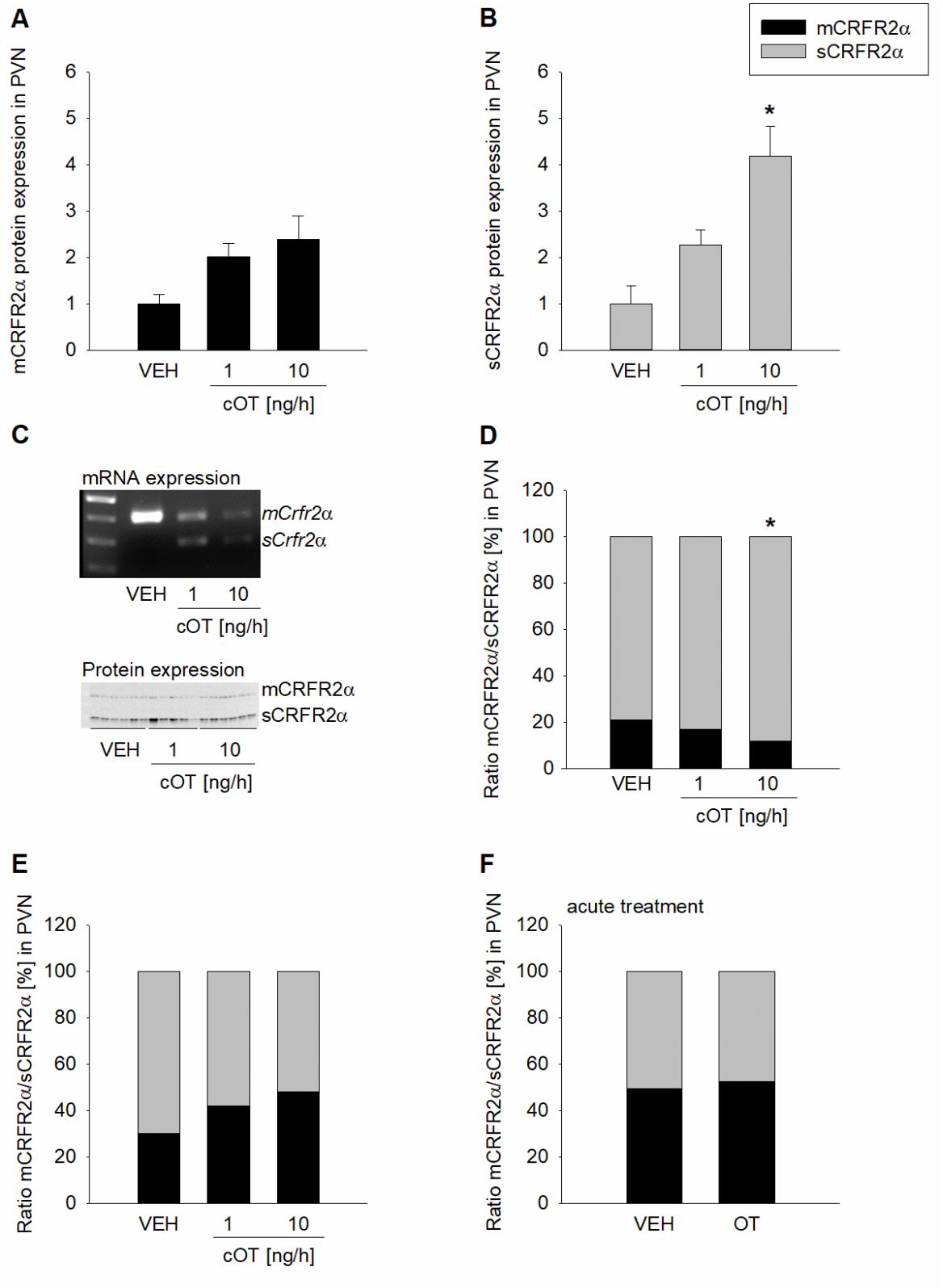

Figure 21. mCRFR2α and sCRFR2α protein expression.

Changes in protein expression levels of mCRFR2α **(A)** and sCRFR2α **(B)** induced by cOT (1 ng/h and 10 ng/h) treatment. Data are shown as mean fold changes (+SEM) compared to VEH. mCRFR2α: One way ANOVA $F_{(2,16)}$ = 3.416, p = 0.062; number of animals: VEH = 5, treatment groups = 6. sCRFR2α: One way ANOVA $F_{(2,16)}$

= 10.630, p = 0.002, Holm-Sidak post hoc test, * p = 0.001 10 ng/h vs VEH, p = 0.025 1 ng/h vs 10 ng/h; number of animals: VEH = 5, treatment groups = 6. **(C)** Upper panel: Representative bands of *mCrfr2α* (400bp)/*sCrfr2α* (300bp) mRNA after VEH and cOT (1 ng/h and 10 ng/h) treatment. Lower panel: Representative western blot image of mCRFR2α (~ 50kDa) and sCRFR2α (~ 30kDa) levels after chronic treatment with either VEH or cOT (1 ng/h and 10 ng/h). The antibody used recognizes both mCRFR2α and sCRFR2α (EMD Millipore, ABN433). **(D)** 10 ng/h cOT led to an increased level of sCRFR2α in relation to mCRFR2α. Data are shown as ratio of mCRFR2α and sCRFR2α protein expression in % after chronic treatment with VEH or cOT (1 ng/h and 10 ng/h) in male rats. One way ANOVA $F_{(2;15)}$ = 5.311, p = 0.021, Holm-Sidak post hoc test * p = 0.019 10 ng/h vs VEH; number of animals: VEH = 6, 1 ng/h = 5, 10 ng/h = 6. **(E)** Analysis of the ratio of mCRFR2α/sCRFR2α protein expression in % revealed no changes induced by cOT (1 ng/h and 10 ng/h) in female rats. One way ANOVA $F_{(2;16)}$ = 1.801, p = 0.201; number of animals: VEH/10 ng/h cOT = 5, 1 ng/h cOT = 7. **(F)** Treatment with acOT had also no effects on the ratio of mCRFR2α/sCRFR2α protein expression in %; t = 0.784 with 11 degrees of freedom, two-tailed p-value = 0.450; number of animals: VEH = 6, OT = 7.

After the importance of the ratio between mCRFR2α and sCRFR2α was proven, the impact of CRFR2 expression but also activity in the PVN on anxiety-like behavior was assessed. Therefore, the highly CRFR2-selective antagonist ASV or the agonist SCP were infused locally into the PVN. Infusion of ASV increased anxiety-like behavior in the LDB from 29.1 % (± 2.4 %) time spent in the LB to 20.9 % (± 1.9 %), whereas SCP acted anxiolytic and increased the time treated animals spent in the LB to 46.2 % (± 7.4 %, Fig 22A). This data provides evidence for the anxiolytic role of CRFR2 activity in the PVN of male rats. To further specify the role of CRFR2α and the soluble splice variant, ASOs targeting either the sCRFR2α (GapmeRs) or the mCRFR2α (TSB) were injected locally into the PVN. Diffusion of locally injected ASOs was representatively analyzed by confocal microscopy of the 5'-FAM label (Fig. 22B; green) in the corresponding brain areas (OT neurons in magenta); ASOs were mostly found in hypothalamic areas with particularly prominent labeling in the PVN target region (Fig. 22B).

Specific KD of the sCRFR2α splice variant in the hypothalamus using GapmeRs, led to decreased anxiety-related behavior both in the LDB (increased time spent in LB from 36.3 % ± 10.8 % to 55.1 % ± 8.6 %; Fig. 22C; left panel) and the OFT (increased time spent in inner zone from 3.9 % ± 1.2 % to 8.0 % ± 2.1 %; Fig. 22C; right panel). On the other hand, blocking of the splice sites flanking exon 6 which are responsible for the inclusion of exon 6 in the mature mRNA by TSBs increased anxiety in the LDB from 53.8 % (± 9.3 %) time spent in the LB to 28.0 % (± 10.5 %) time spent in the LB after TSB treatment (Fig. 22D).

Knocking down the alternative splice variant, thereby leaving the regular form unaltered, yielded in the formerly unknown anxiogenic effect of the splice variant for anxiety-related

behavior. This is supported by increased anxiety levels due to enhanced alternative splicing induced by TSB treatment.

Anxiety and social behaviors are closely linked (Menon et al., 2018), therefore, social preference was assessed after both GapmeR and TSB applications. All animals displayed social preference as they spent 2 to 3 times more time investigating a conspecific compared to a non-social stimulus (empty cage, Fig. 22E), excluding a social component of the sCRFR2α.

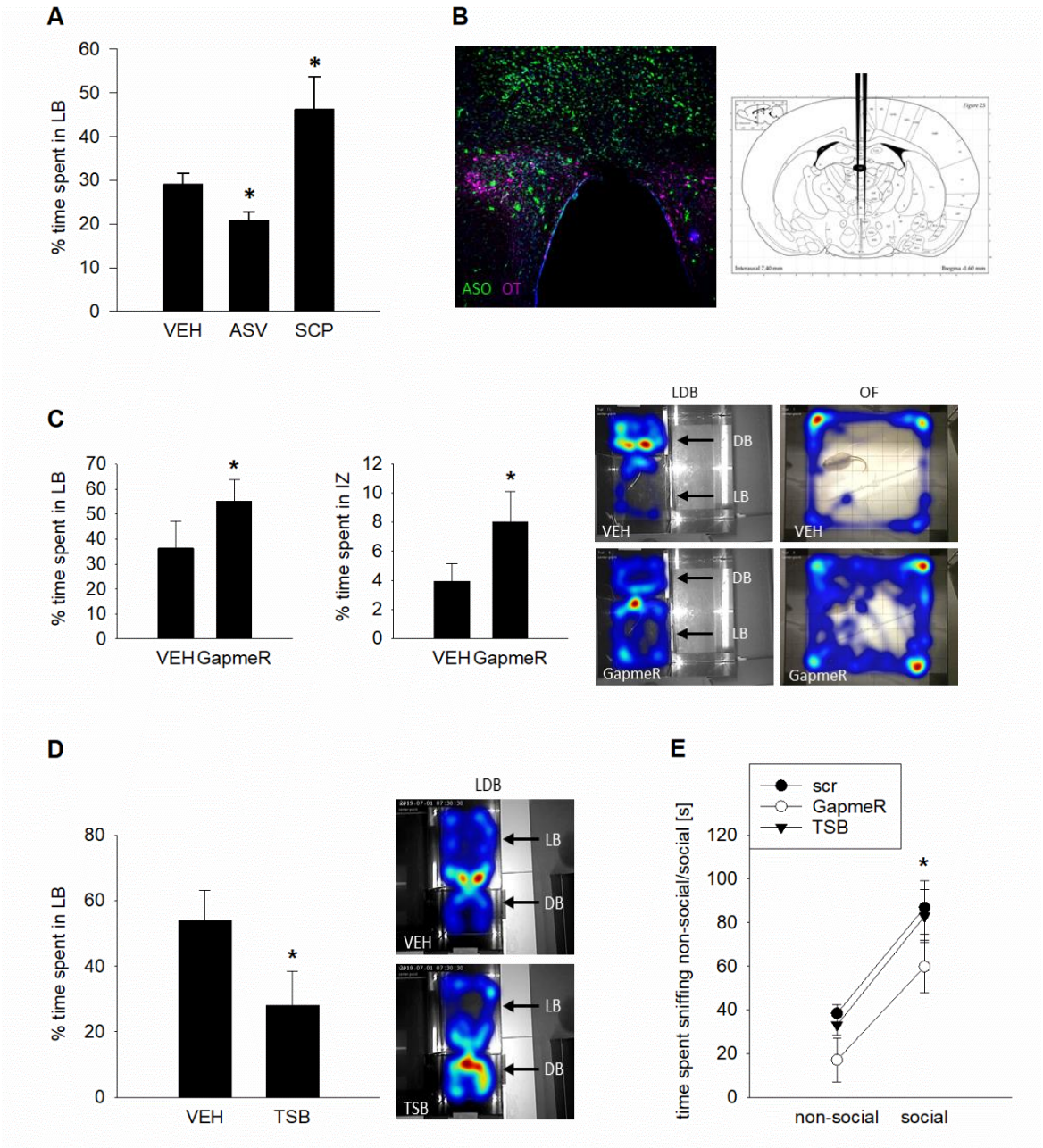

Figure 22. Manipulation of mCRFR2α and sCRFR2α expression in the PVN alters anxiety-related behavior.

(A) Effects of agonism and antagonism of the CRFR2 in the PVN on anxiety-like behavior in male rats. Intra-PVN administration of the CRFR2 antagonist ASV (280 µM, corresponding to 0.14nmol/0.5µl per side) increased anxiety in the LDB 10 min after infusions. On the other hand, administration of CRFR2 agonist SCP (1.4 mM, corresponding to 3µg/0.5 µl per side) led to decreased anxiety-like behavior. Data shown as mean percentage of time spent in the LB. One way ANOVA, $F_{(2;51)} = 12.099$; $p < 0.001$, Holm-Sidak post hoc test * $p = 0.03$ ASV vs VEH, * $p = 0.003$ SCP vs VEH, $p < 0.001$ ASV vs SCP; number of animals: VEH = 23, ASV = 21, SCP = 8. **(B)** Representative distribution of 5'-FAM-labelled ASOs in the hypothalamic area after microinfusions (1nmol/0.5µl per animal). Direct infusions into the PVN resulted in mostly PVN, but also dorsal hypothalamus staining. Magenta: OT-Neurophysin positive neurons, green: ASOs. **(C)** Left panel: The anxiolytic effect of sCRFR2α KD on anxiety-like behavior was assessed in the LDB (7 days after GapmeR infusion) and the OFT (8 days after GapmeR infusion). Data are shown as mean percentage of time spent in the LB ($t = -1.762$ with 16 degrees of freedom, one-tailed t-test * $p = 0.0486$), and the mean percentage of time in the inner zone (IZ) of the OFT (Rank Sum Test, Mann-Whitney U Statistic = 16.000, * $p = 0.037$); animal numbers for both tests: VEH = 10, GapmeR = 8. Right panel: Representative heat maps showing the location of a VEH and GapmeR treated rat in LB and DB of the LDB or the inner and outer zone of the OFT over the testing period. **(D)** Increasing the availability of the splice variant with TSBs had contrary effects on anxiety-like behavior compared to GapmeR treatment. Rats showed increased anxiety-like behavior in the LDB 7 days after TSB administration. $t = 1.843$ with 18 degrees of freedom, one-tailed p-value * $p = 0.0409$; number of animals: VEH/TSB = 10. Right panel: Representative heat maps showing the location of a VEH and TSB treated rat in LB and DB of the LDB over the testing period. **(E)** The impact of sCRFR2α expression on social preference was measured by the percentage of time an animal spent investigating (sniffing) a non-social stimulus (empty cage) versus a social stimulus (cage with a conspecific) for 5 min each. All rats displayed social preference (VEH/scr, * $p = 0.001$ non-social vs social, GapmeR, * $p = 0.033$ non-social vs social, TSB, * $p < 0.01$ non-social vs social; Bonferroni's post hoc analysis; number of animals: VEH/treatment groups = 10) with no significant effect of treatment, indicating an exclusive anxiety-related effect of the splice variant and excludes a social component of the sCRFR2α.

2.3. Chronic oxytocin promotes the release of sCRFR2α and leads to increased anxiety

Release of the sCRFR2α from cells into the culture medium has already been shown, although no secretory properties could be proven (Chen et al., 2005; Evans and Seasholtz, 2009). CSF taken from urethan-anesthetized rats contained detectable amounts of sCRFR2α. Dot blot analysis after GapmeR treatment confirmed the decrease in sCRFR2α levels (Fig. 23A). GapmeR-treated rats had a significantly lower load (fold change 0.5 ± 0.1) of the splice variant in the CSF compared to VEH treated rats. To ensure the specificity of the antibody, several control samples were analyzed (Fig. 23B). Cerebellum tissue served as negative control, with minimal sCRFR2α expression, whereas PVN tissue expressed higher levels of the splice variant (Fig. 23B). A correlation between anxiety levels and sCRFR2α abundance in CSF shed further light on the impact of sCRFR2α on anxiety-like behavior. High sCRFR2α levels significantly correlated with high anxiety levels. The more splice variant was found in the CSF, the less time the animals spent in the LB, indicating

higher anxiety levels (Fig. 23C). Due to the observed interplay between the anxiogenic effect of chronic OT and a previous mild stressor, the impact of stress and OT, respectively, on CSF-sCRFR2α levels was assessed. Unstressed rats had a lower abundance of sCRFR2α in the CSF compared to stressed rats (Fig. 23D). Additional treatment with the high dose of chronic OT even caused doubling of sCRFR2α levels compared to unstressed rats (Fig. 23D), indicating a combinatorial effect of stress and chronic OT on anxiety as well as on sCRFR2α release.

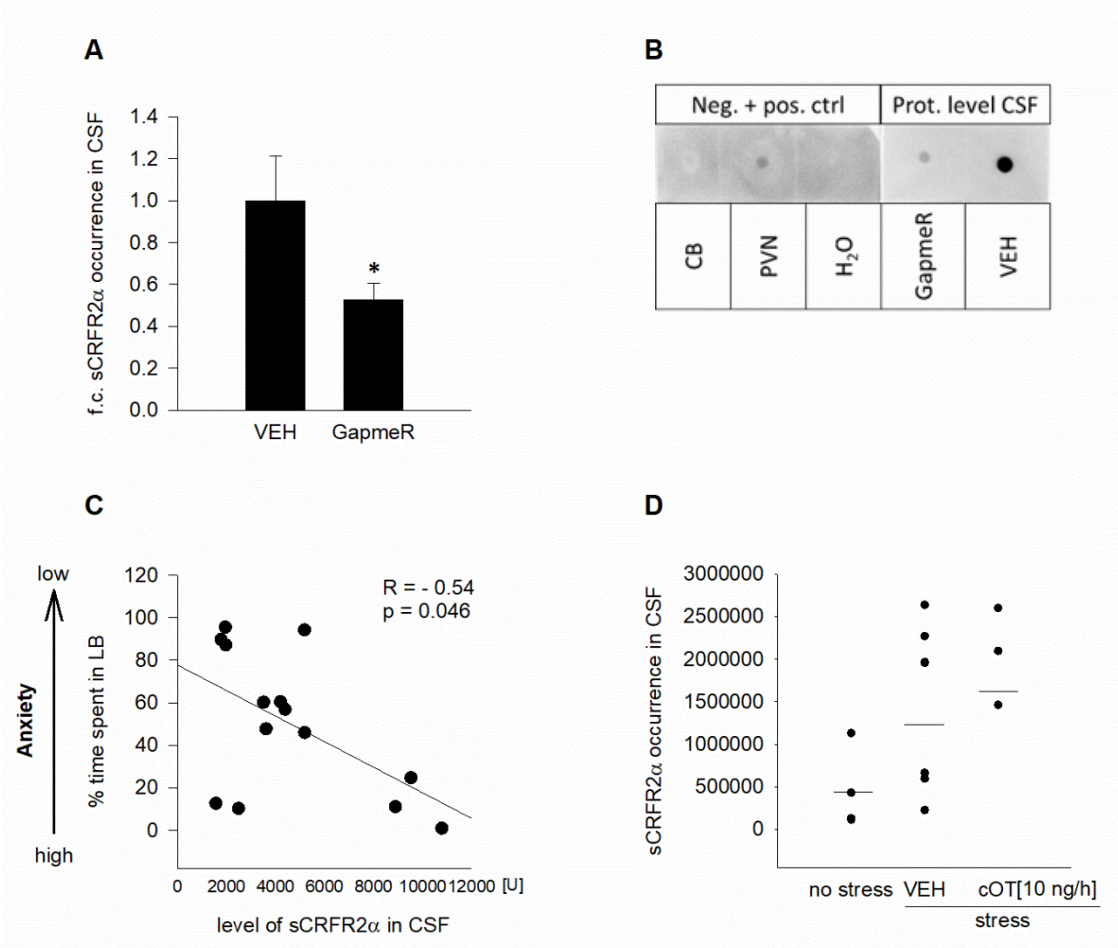

Figure 23. sCRFR2α release into CSF and anxiety.

(A) sCRFR2α levels in the CSF of GapmeR-infused rats were quantified by dot blot analysis. Reduced signal intensity represents reduced release of sCRFR2α, indicating an efficient KD and overall reduced sCRFR2α expression in the brain. Data are shown as fold changes in protein occurrence compared to VEH, t = 1.828 with 12 degrees of freedom, one-tailed t-test, * p = 0.046; number of animals: VEH =8, GapmeR = 6. **(B)** Representative picture of dot blot analysis of CSF (VEH and GapmeR) and control tissue protein lysates (cerebellum = CB as negative control, PVN as positive control, H_2O). **(C)** Significant correlation between CSF levels of sCRFR2α and anxiety-like behavior (% time spent in LB) as shown by linear regression (R = -0.54, one way ANOVA $F_{(1;13)}$ = 4.946, p = 0.046). **(D)** The effect of stress on sCRFR2α release into CSF of rats treated with VEH and 10ng/h cOT and an unstressed control was analyzed by dot blot. Both stress and cOT treatment increased sCRFR2α release compared to unstressed animals. However, the effect did not reach significance,

one way ANOVA $F_{(2,13)}$ = 3.849, p = 0.053; number of animals: no stress = 4, VEH (stress) = 7, 10 ng/h (stress) = 3.

As the mild stress had profound effects on anxiety-related behavior and also influenced release of the sCRFR2α, both mCRFR2α and sCRFR2α protein levels as well as MEF2A activation were determined in animals that underwent LDB with and without prior stress exposure. This experiment aimed to separate the effects of the mild stress from the chronic OT infusion on the CRFR2α and MEF2A. Therefore, it is important to note, that in the graphs shown in Fig. 24, all animals received 10ng/h chronic OT, the difference between the groups being the exposure to stress (+s) or no stress. sCRFR2α protein levels remained unaffected by stress exposure (Fig. 24A). However, there was a slight yet significant increase of 1.4-fold (± 0.2) in mCRFR2α expression after elevated platform stress 24 h before LDB testing. The high dose of chronic OT had no differing effects on MEF2A phosphorylation levels at S408 (Fig. 24B), which suggests stress-independent activation of MEF2A signaling.

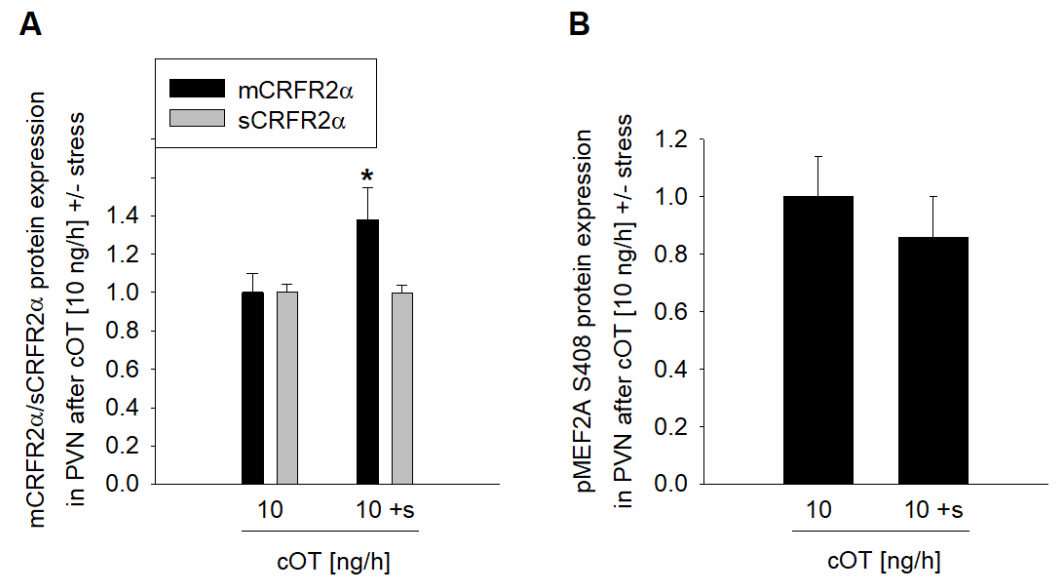

Figure 24. Stress has no effects on protein expression of sCRFR2α and the phosphorylation of MEF2A. A separate group of animals treated with 10 ng/h cOT was analyzed with and without the mild elevated platform stress on day 13. **(A)** No effects on sCRFR2α expression were detected, but a slight yet significant upregulation of the mCRFR2α was caused by the stressor. Data shown as mean fold change compared to VEH treatment. sCRFR2α: t = -0.0214 with 18 degrees of freedom, one-tailed p-value = 0.492; number of animals: all treatment groups = 10. mCRFR2α: Rank Sum Test, Mann-Whitney U Statistic = 23.000, * p = 0.045 10 ng/h +s vs 10 ng/h; number of animals: all treatment groups = 10. **(B)** The mild stressor had no effect on the previously observed decrease in protein phosphorylation of MEF2A S408, t = -0.717 with 18 degrees of freedom, one-tailed p-value = 0.241; number of animals: all treatment groups = 10.

The lateral septum and the hypothalamus are closely related in the regulation of anxiety, *e.g. via* outputs from the lateral septum to the hypothalamus. CRFR2 activity in the lateral septum differentially affects anxiety, depending on cell type and severity of stress, as antagonism of the CRFR2 was shown to be anxiolytic under high-stress conditions (Bale et al., 2002a). As shown in the results above, the hypothalamic PVN was the main brain region where chronic OT exhibited its effects. Several control regions including the hippocampus remained unaffected by chronic OT. The lateral septum as a region of high CRFR2 expression displayed increased *mCrfr2α* mRNA levels upon chronic OT administration. The low dose of chronic OT caused a 13.3-fold (± 0.7) significant increase in mCRFR2α expression, the high dose led to an increase of 5.0-fold (± 0.4, Fig. 25A). sCRFR2α mRNA levels were increased in both treatment groups, 5.4-fold (± 0.4) by 1 ng/h and 8.9-fold (± 0.4) by 10 ng/h, despite the profound elevation, only an overall statistical effect of p = 0.062 could be reached (Fig. 25A). Analysis of the upstream signaling pathway excluded an involvement of MEF2A, no changes in MEF2A mRNA levels could be detected (Fig. 25A). To deepen the understanding of an involvement of the lateral septum in the anxiogenic phenotype of chronic OT, more analysis will be necessary, regarding protein expression and ratio as well as activation of transcription factors. Due to the impact of intra-PVN infusions of TSB and GapmeRs, the lateral septum was not investigated in more depth, however, it will be subject of further studies.

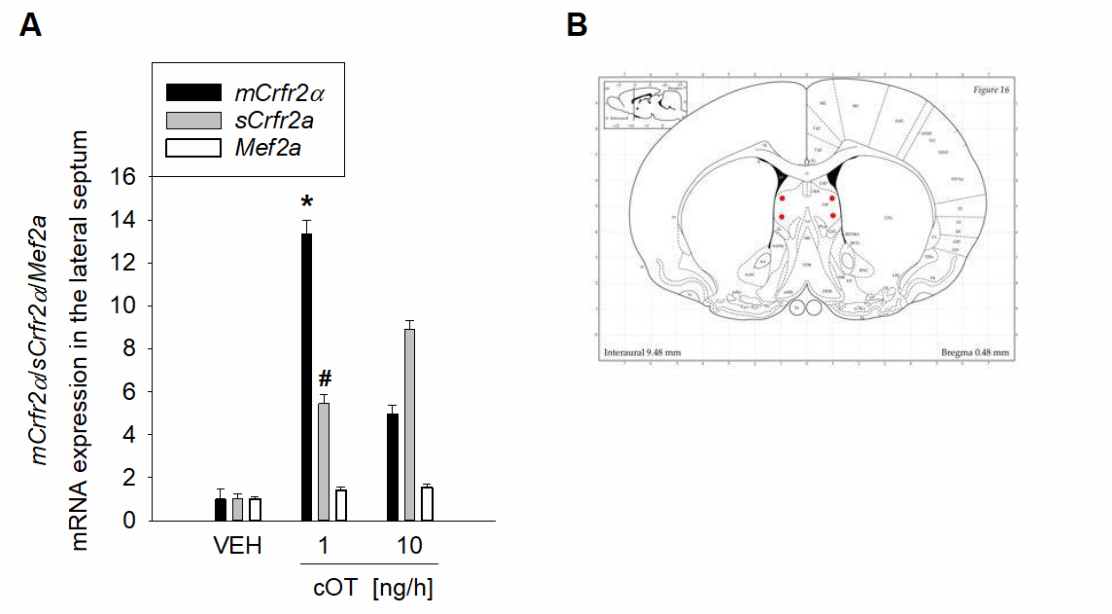

Figure 25. Effects of cOT treatment on *mCrfr2α*, *sCrfr2α*, and *Mef2a* mRNA expression in the lateral septum.

(A) mRNA levels of *mCrfr2α*, *sCrfr2α* and *Mef2a* were analyzed in the lateral septum, as cOT led to a slight reduction of OT binding there (Winter et al., in preparation). Both *Crfr2α* variants were upregulated in the septum

by the low dose of chronic OT, whereas *Mef2a* levels remained unchanged. *mCrfr2α*: One way ANOVA on Ranks, H = 9.773 with 2 degrees of freedom. All pairwise multiple comparison procedure (Tukey test), * p = 0.006 1 ng/h cOT vs VEH; number of animals: VEH = 5, treatment groups = 6. *sCrfr2α*: One way ANOVA on Ranks, H = 5.577 with 2 degrees of freedom, # p = 0.062; VEH = 5, treatment groups = 6. *Mef2a* one way ANOVA on Ranks, H = 3.228 with 2 degrees of freedom, p = 0.199. VEH = 5, treatment groups = 6. **(B)** Localization of the septum within the rodent brain marked with red dots (Paxinos, 1998).

To determine the intracellular reallocation of mCRFR2α and sCRFR2α, the intact transmembrane receptor was labeled using CRISPR-mediated HiBiT tagging. This technique consists of the genomic insertion of a tag-sequence into the target gene, which, once expressed as protein, labels the membrane-bound target protein on the cell surface. In this case, I inserted the HiBiT donor sequence into the Exon 6 of the CRFR2 gene, which resulted in the expression of the HiBiT in an extracellular domain of the CRFR2. By application of the corresponding LgBiT protein (spoken as “large BiT”), the mCRFR2α was made visible in live cells by the fluorescent reaction of the HiBiT-LgBiT-complex (Fig. 26A). As this is no “end-point” assay, in theory, multiple cycles of membrane incorporation and internalization of the receptor can be visualized. However, to prove my point it was sufficient to assess just on time point after OT stimulation. Luminescence measurements revealed a decrease in membrane-bound CRFR2α after long-term stimulation (24 h) using a concentration of 100nM OT, corresponding to the high dose chronic OT treatment *in vivo* (Fig. 26B). Mean luminescence decreased from 1521 (± 79) to 1186 (± 28, Fig. 26B). However, the HiBiT system only allowed the detection and analysis of the intact membrane-bound mCRFR2α. Assessment of sCRFR2α release into the extracellular space was determined by dot blot analysis of sCRFR2-content in the cell culture medium. In line with previous publications, I detected sCRFR2α release into the extracellular medium under basal conditions, however, OT stimulation significantly increased sCRFR2 release into the medium, supporting our *in vivo* data (Fig. 26C and Fig. 23D). In untreated cells the mean gray intensity, reflecting sCRFR2α in the medium, averaged 5811 (± 798), whereas the release increased to 62499 (± 20380) after chronic OT treatment (Fig. 26C).

In addition, the distribution of the sCRFR2α was also detectable in immunocytochemical stainings of rat hypothalamic primary cells (Fig. 26D). The sCRFR2α signal (Fig. 26D; green) was diffuse and detectable within the entire cytoplasm (Fig. 26D, upper panel). Co-stainings with GFAP (Fig. 26D; magenta) demonstrated both neuronal and glial expression of the sCRFR2α, and its distributed expression in the cell soma, neurites, and especially the end-boutons of the neurites (Fig. 26D, lower panel).

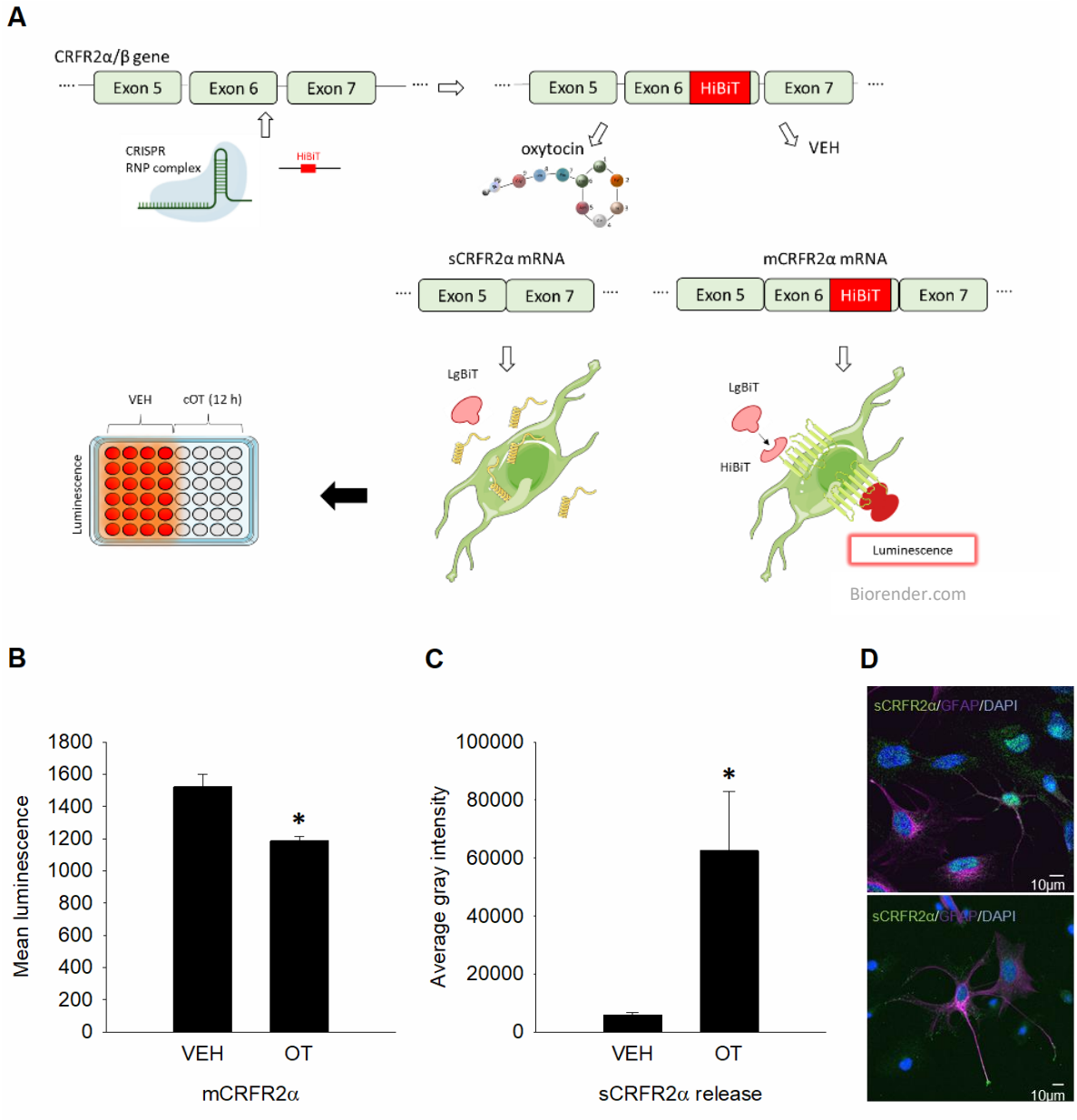

Figure 26. *in vitro* sCRFR2α release and membrane expression of the mCFRFR2α.

(A) Schematic representation of HiBiT-mediated signaling in H32 cells stimulated with either VEH or OT for 24 h. **(B)** mCRFR2α membrane expression was assessed by luminescence caused by the interaction of the extracellular HiBiT-tag and the corresponding substrate (LgBiT) that was applied to the cells before measurements. Treatment with 100 nM OT for 24 h decreased the luminescent signal, indicative of alternative splicing of Exon 6 and the subsequent reduction in membrane expression of mCRFR2α. Data are shown as absolute values of mean luminescence. Rank Sum Test, Mann-Whitney U Statistic = 32.000, * $p \leq 0.001$; n-number: VEH = 20, OT = 12. **(C)** In HiBiT-expressing cells, OT treatment (100 nM for 24 h) also led to a 10-fold increased release of sCRFR2a into the medium. Data are shown as average gray intensity relative to area; Rank Sum Test, Mann-Whitney U Statistic < 0.001, * $p = 0.029$; n-number: VEH/OT = 4. **(D)** Rat hypothalamic mixed primary cultures were stained for DAPI (blue), anti-sCRFR2α (green), and GFAP (magenta), illustrating cytoplasmic distribution of sCRFR2α in neuronal cells (GFAP negative) and astrocytes (GFAP positive).

To specify the role of the transcription factor MEF2A on mCRFR2α expression and alternative splicing, RNA interference was used to generate a transient KD of MEF2A (*Mef2a*_KD). To exclude an effect of siRNA treatment per se, control cells were also treated with a non-targeting scrambled control RNA (scrRNA) and compared to mCRFR2α and sCRFR2α levels of *Mef2a*_KD cells. First, the efficiency of the KD was verified *via* western blot, revealing a decrease to 0.1-fold (± 0.03) of MEF2A protein levels by siRNA treatment for 72 h (Fig. 27A). Both mCRFR2α (0.2 fold change ± 0.02) and sCRFR2α (0.5 fold change ± 0.05) protein levels were significantly decreased by the KD of *Mef2a*, supporting the hypothesis of a direct link between MEF2A and CRFR2α (Fig. 27B). Furthermore, *in silico* analysis revealed a MEF2A responsive element within Exon 6 of the CRFR2 gene. A mechanistic proof for MEF2A binding to the CRFR2 gene has been provided by a Chromatin-Immunoprecipitation experiment (data not shown), as described in my manuscript (Winter et al., in preparation).

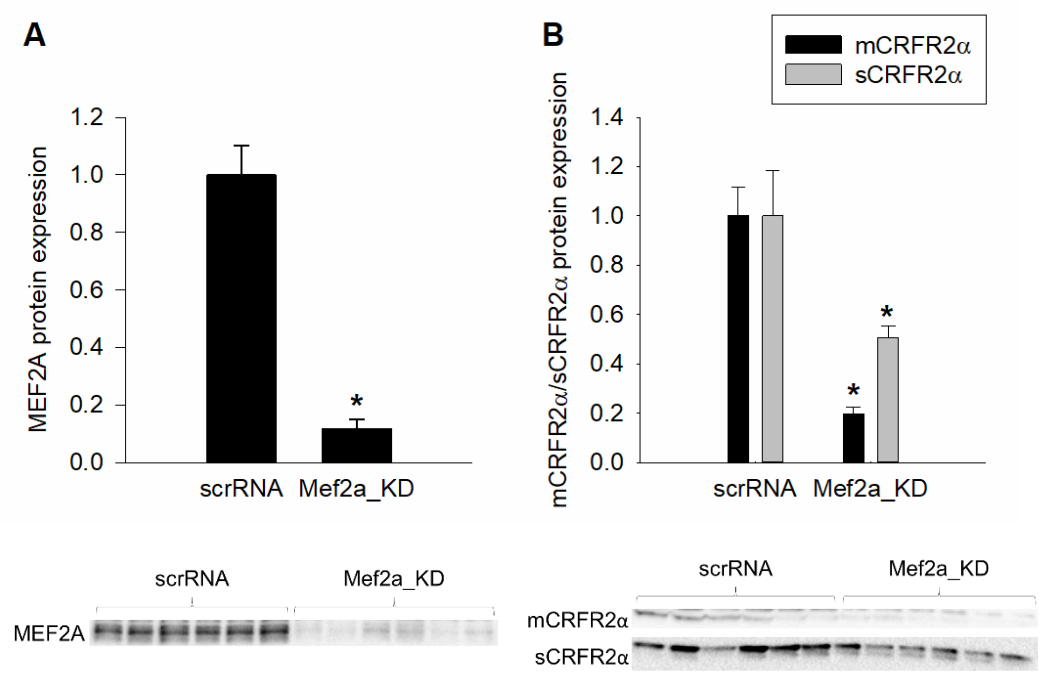

Figure 27. mCRFR2α and sCRFR2α expression are MEF2A-dependent.

mCRFR2α and sCRFR2α expression depend on MEF2A, as revealed by siRNA-mediated KD of MEF2A. Reduced MEF2A availability decreased both mCRFR2α and sCRFR2α protein expression levels in otherwise untreated H32 cells. **(A)** Treatment with siRNA (5µg) targeting *Mef2a* mRNA for 72 h led to a significant reduction in MEF2A protein levels, t = 8.301 with 10 degrees of freedom, two-tailed p-value = 0,00000851, * p < 0.01. **(B)** mCRFR2α and sCRFR2α protein levels were significantly downregulated after siRNA treatment. mCRFR2α: Rank Sum Test, Mann-Whitney U Statistic < 0.001, * p = 0.002. sCRFR2α: t = 2.574 with 10 degrees of freedom; one-tailed p-value = 0.0138; n-number: scrRNA/Mef2a_KD = 6 for all targets.

So far only expression patterns in whole-cell protein lysates, containing membrane-, cytoplasmic-, and nuclear proteins, were assessed. As a next step, to determine internalized receptor proteins, cytoplasmic proteins were separately isolated and analyzed for OT-induced changes in mCRFR2α and sCRFR2α protein expression levels. 24 h of stimulation with 100nM OT caused a significant increase in cytoplasmic sCRFR2α levels (1.5 fold change ± 0.1). The mCRFR2 levels in the cytoplasm, which represent vesicular stored receptors, ready for membrane incorporation, remained constant (Fig. 28A). This result confirms *in vivo* data and the hypothesis of an increase in the soluble, cytoplasmic splice variant sCRFR2α upon OT stimulation.

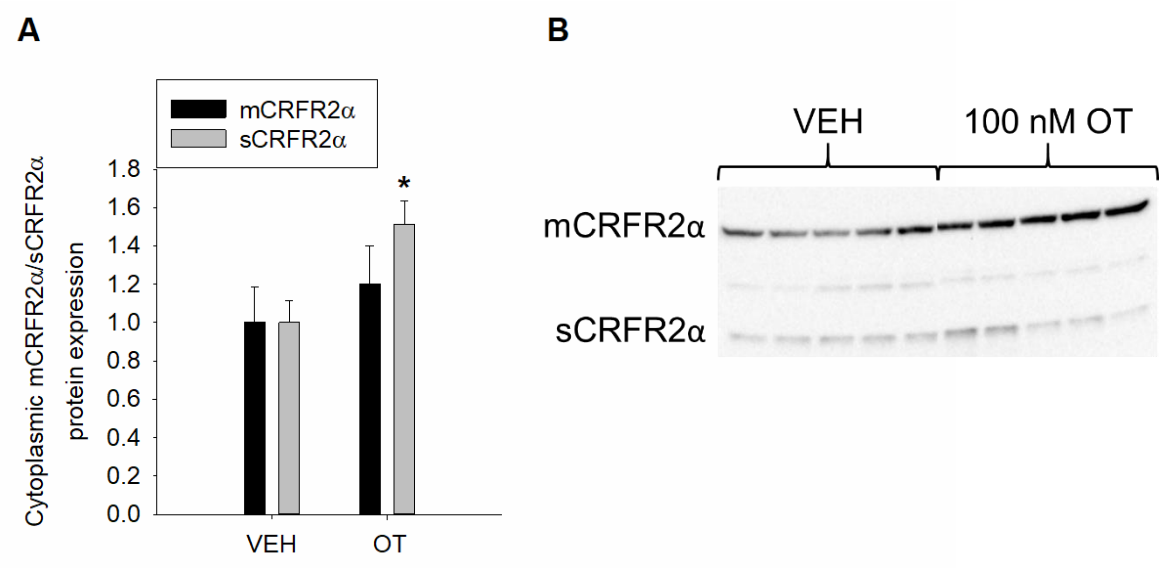

Figure 28. mCRFR2α and sCRFR2α expression in cytoplasm.

(A) Specific isolation of cytoplasmic proteins revealed an increase of sCRFR2α protein levels induced by OT treatment (100 nM OT, 24 h) in H32 cells. Data are shown as mean fold changes of protein expression compared to VEH. mCRFR2α: t = -0.742 with 18 degrees of freedom; one-tailed p-value = 0.234. sCRFR2α: t = -3.071 with 18 degrees of freedom, one-tailed p-value = 0.00329; n-number: VEH/OT = 10. **(B)** Representative western blot images of mCRFR2α and sCRFR2α antibody staining.

Next, as also shown *in vivo*, the *in vitro* effects of a 100 nM acute OT stimulation (10 and 30 min) on CRFR2α expression and alternative splicing in H32 cells were investigated. No statistically significant changes were induced by acute OT treatment, confirming my hypothesis of a CRFR2-system that is only responsive to a chronic OT stimulus. However, the mCRFR2α was slightly reduced by 30 min of OT stimulation (0.3 fold change ± 0.2), whereas sCRFR2α levels remained constant (Fig. 29A). As only a very weak signal of mCRFR2α could be detected in western blot analysis, results should be interpreted carefully

(Fig. 29B). Preliminary analysis of phosphorylation levels of MEF2A S408 revealed a 0.4-fold reduction (± 0.1) after 30 min (data not shown).

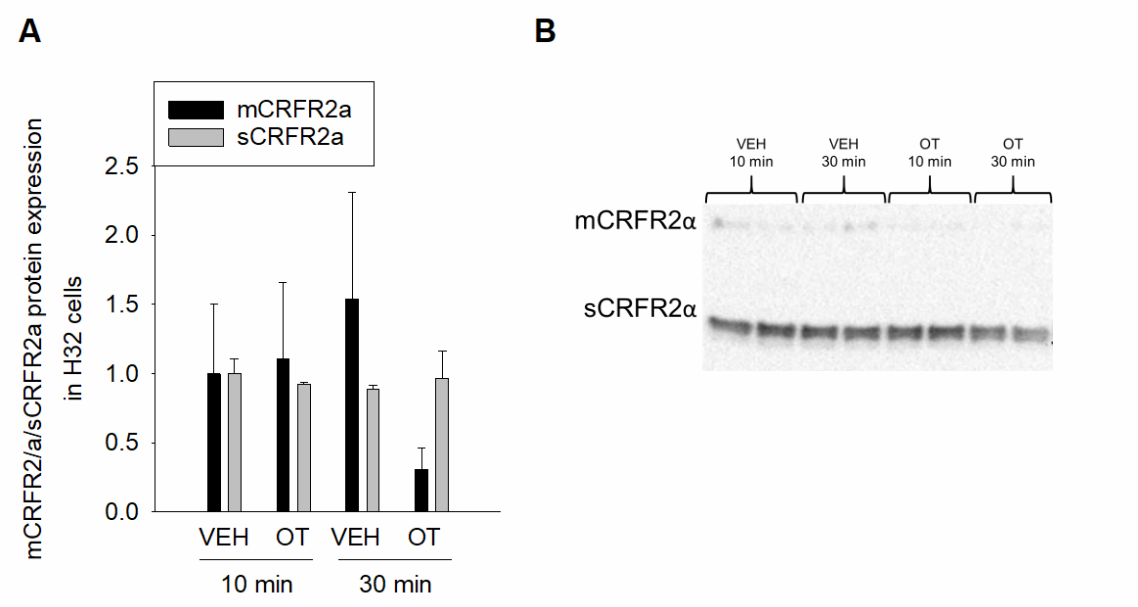

Figure 29. mCRFR2α and sCRFR2α expression induced by acute OT in H32 cells.

(A) Acute treatment with OT (100 nM, 10 and 30 min) had differential effects on mCRFR2α and sCRFR2α expression. mCRFR2α: Two way ANOVA main effect of treatment $F_{(1,15)}$ = 5.384, p = 0.039, there is no main effect of time $F_{(1,15)}$ = 0.284, p = 0.604. There is a statistically significant interaction between treatment and time point $F_{(1,15)}$ = 7.631, p = 0.017; n-number: VEH/OT 10/30 min = 4. sCRFR2α: Two way ANOVA revealed no main effect of treatment $F_{(1,15)}$ = 0.000545, p = 0.982, also treatment had no statistically significant effect $F_{(1,15)}$ = 0.0853, p = 0.775. There is also no statistically significant interaction between treatment and time point $F_{(1,15)}$ = 0.499, p = 0.493; n-number: VEH/OT 10/30 min = 4. **(B)** Representative western blot images of mCRFR2α and sCRFR2α antibody staining.

3. Effects of chronic oxytocin on neuronal morphology and signaling in vitro

Further analysis of OT effects on downstream signaling and neuronal morphology was transferred from *in vivo* experiments to *in vitro* studies in several neuronal cell lines. Cell lines are a powerful tool in studying molecular signaling cascades, furthermore, changes in neuronal morphology become easily accessible. Morphological analysis assesses parameters like the size and shape of a cell (Delarue et al., 2017; Meyer et al., 2018), neurite length (Lestanova et al., 2016b; Lestanova et al., 2017; Meyer et al., 2018; Zatkova et al., 2018a) and nucleus size (Hara and Merten, 2015; Kim et al., 2015), providing important information about cellular function, activity and health of a cell. Also, the use of cell culture contributes to the reduction of experimental animals needed.

3.1. Characterization of Be(2)-M17, H32, and N2a cells

As a first step, the expression profile of several factors of interest was assessed in Be(2)-M17, H32 and N2a cells (see table 8) by means of qPCR analysis. The expression of both the OTR and the CRFR2 was essential for the reproducibility of the data obtained from the *in vivo* experiments described above. All cell lines express the OTR and the CRFR2, whereas only Be(2)-M17 cells express the CRF-BP, the CRFR1 was expressed by neither of the cell lines. The expression of a ligand of the CRFR2, UCN has only be determined in Be(2)M17 cells. The transcription factors MEF2A and MEF2B are present in all cell lines, N2a cells lack the MEF2C isoform. H32 cells express the AVP receptor 1a and lack the AVP receptor 1b, Be(2)-M17 and N2a express the 1b, but not 1a subform. The MAPK signaling kinase ERK5, which is one potential upstream kinase of MEF2, is expressed by all cell lines used here.

Table 8. Characterization of the expression profile in Be(2)-M17, H32 and N2a cells *via* qPCR analysis.
+, ++, +++ indicates expression intensity, n.d. = not determined.

	H32	**Be(2)-M17**	**N2a**
CRFR1	**-**	**-**	**n.d.**
CRFR2	**+**	**+**	**+++**
CRF	**n.d.**	**+**	**+**
CRF-BP	**-**	**+**	**-**
UCN	**n.d.**	**+**	**n.d.**
OTR	**+**	**+**	**+++**

AVPR1a	+	-	-
AVPR1b	-	+	+
MEF2A	+	+	+++
MEF2B	+	++	+
MEF2C	(+)	(+)?	-
MEF2D	++	++	n.d.
ERK5	++	++	++

3.2. Chronic oxytocin induces neurite retraction

Previous studies have shed light on OT-induced morphological changes in neurites. However, the effect is not only time-, dose- and treatment dependent but also varies in different cell types (Lestanova et al., 2016b; Lestanova et al., 2017; Meyer et al., 2018; Zatkova et al., 2018a). In the murine N2a cell line, chronic treatment with OT for 10 h at a concentration of 100 nM induced neurite retraction. The mean neurite length decreased from 85.7 µm in VEH treated cells to 70.0 µm (Fig. 30A and B). Unlike in rat H32 cells (Meyer et al., 2018), this effect was exclusively mediated by OT, no effect of TGOT (88.5 µm) or AVP (87.0 µm) appeared. This indicates that a combined effect of the OTR and AVP receptor results in morphological alterations, which is achieved by the promiscuous binding of OT to both receptor types.

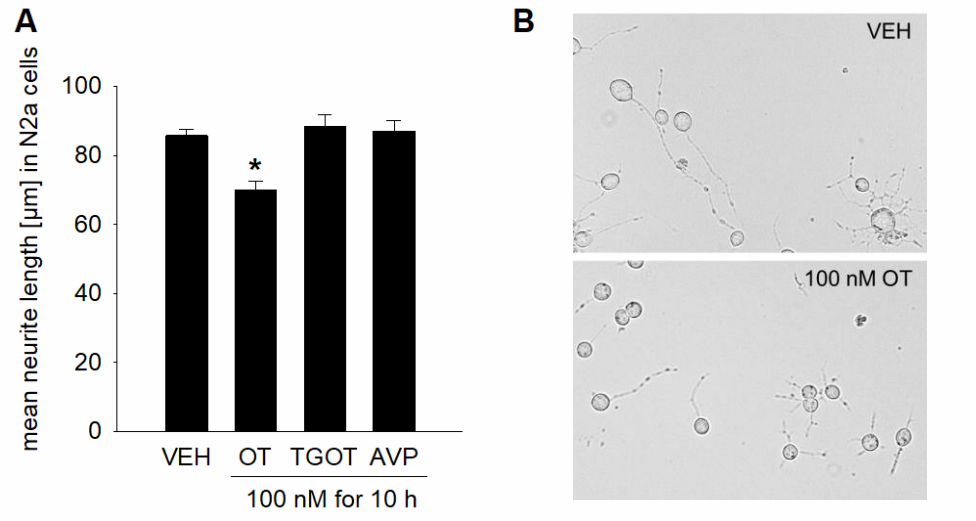

Figure 30. OT-induced morphological changes in murine N2a cells.

(A) Mean neurite length in murine N2a cells decreased after 10 h of OT treatment. TGOT and AVP stimulations had no effect on mean neurite length. One way ANOVA on Ranks, H = 33.809 with 3 degrees of freedom. Dunn's Method * $p < 0.001$ 100 nM OT vs VEH; n-number: VEH = 585, OT = 199, TGOT = 200, AVP = 200.

(B) Representative images of VEH and OT treated cells (unstained). Pictures were taken with a fluorescent cell imager (ZOE™, Bio-Rad, Munich, Germany).

3.3. CRISPR-mediated knockout of the oxytocin receptor impairs MAPK signaling and affects neuronal morphology

The establishment of the CRISPR-Cas9 system *in vitro* was another important part of the thesis presented here. For the generation of OTR KO cells, a plasmid-mediated approach was conducted. After transfection with Oxytocin-R Double Nickase Plasmids (h, sc-400641-NIC, Santa Cruz Biotechnology, USA) and antibiotic pre-selection with puromycin, Be(2)-M17 cells were isolated at a single-cell level and grown back to full confluence. Expression of a GFP control gene on the plasmid allowed immediate visual confirmation of transfection (Fig. 31A). After single-cell isolation, cells were monitored daily for several weeks for cell division and shape/size of the cells, which indicates their health status (Fig. 31B).

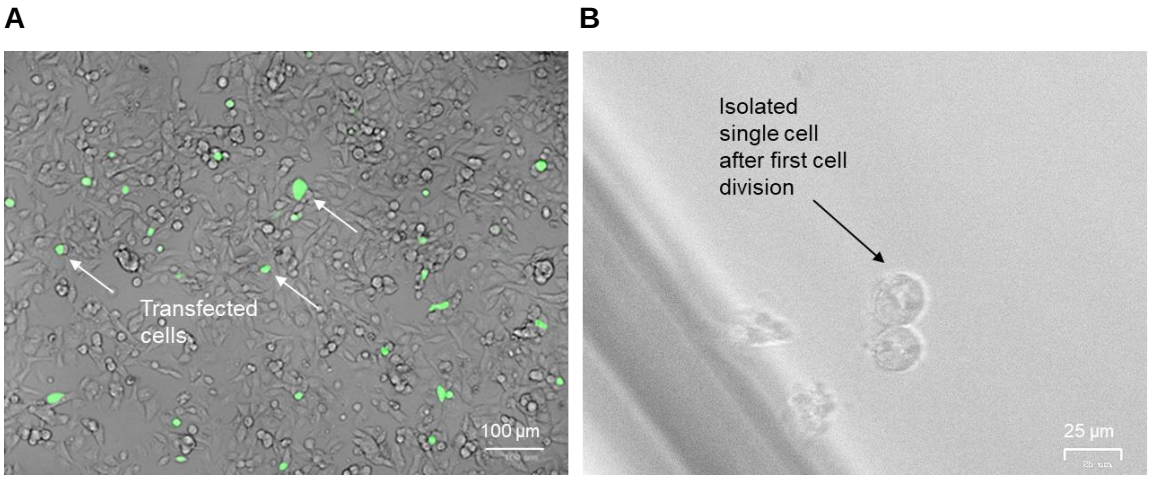

Figure 31. CRISPR transfection.

(A) Representative image of Be(2)-M17 cells after transfection with Oxytocin-R Double Nickase Plasmids (h, sc-400641-NIC, Santa Cruz Biotechnology, Dallas, USA). Visual confirmation of transfection efficiency was enabled by the expression of a GFP control protein (green). **(B)** Successfully isolated BeJ(1) cell after single-cell isolation and first cell division.

Approximately 10 single-cells were re-cultured after single-cell isolation and analyzed by means of western blot, qPCR, PCR and Sanger Sequencing. In figure 32, the representative analysis of one newly obtained OTR KO cell line is depicted. This cell line was named BeJ(1), all further experiments were performed using this cell line.

PCR analysis with primers flanking the CRISPR cutting sites revealed a disruption of the *Otr* gene in BeJ(1) cells, as the expected PCR product with ~ 550 bp could not be amplified

(*Otr*$^{-/-}$). In contrast, amplification of the *Otr* product in wildtype Be(2)-M17 (*Otr*$^{+/+}$) cells carrying the intact *Otr* was possible (Fig. 32A). On the protein level, western blot analysis using the anti-OTR antibody provided by Abcam substantiated the previous PCR results (Fig. 32B). No OTR protein band was detectable in the KO cell line compared to wildtype cells (expected band height ~ 45 kDa). For the final confirmation of the *Otr*$^{-/-}$ genotype, Sanger Sequencing was performed at Macrogen with both bands obtained from PCR amplification (Fig. 32A). Sequence alignment using Serial Cloner software revealed 100 % conformity between the *Otr* whole gene sequence obtained from whole-genome sequencing (StarSEQ, Mainz, Germany) and the *Otr*$^{+/+}$ band (Fig. 32C). Alignment with the lower band from both cell types (Fig. 32A) showed no conformity with the *Otr* whole gene sequence, indicating an unspecific PCR product (data not shown).

For the generation of a second KO cell line, the Alt-R® CRISPR-Cas9 system (IDT, Germany) was used. The transcription factor MEF2A was knocked out in H32 cells, in order to gain more insight into the functional relevance of MEF2A for cellular signaling and morphology. Here, single-cell isolation was performed using FACS. Transfected cells containing the fluorescently labeled tracrRNA ATTO 550 were sorted individually into single wells of a 96-well plate. Untransfected cells served as negative control for gating during FACS analysis. After re-culturing, all single-cells were so far analyzed by means of western blot using the Acris MEF2A antibody (see method section table 10). Figure 32D represents protein levels of a successful KO (Mef2a$^{-/-}$) compared to wildtype H32 cells (Mef2a$^{+/+}$). No protein expression was detectable in Mef2a$^{-/-}$ cells, however further analysis on mRNA level as well as Sanger Sequencing are necessary. Once validated, the newly created cell line will serve as cellular model to study MEF2A-related effects in future studies.

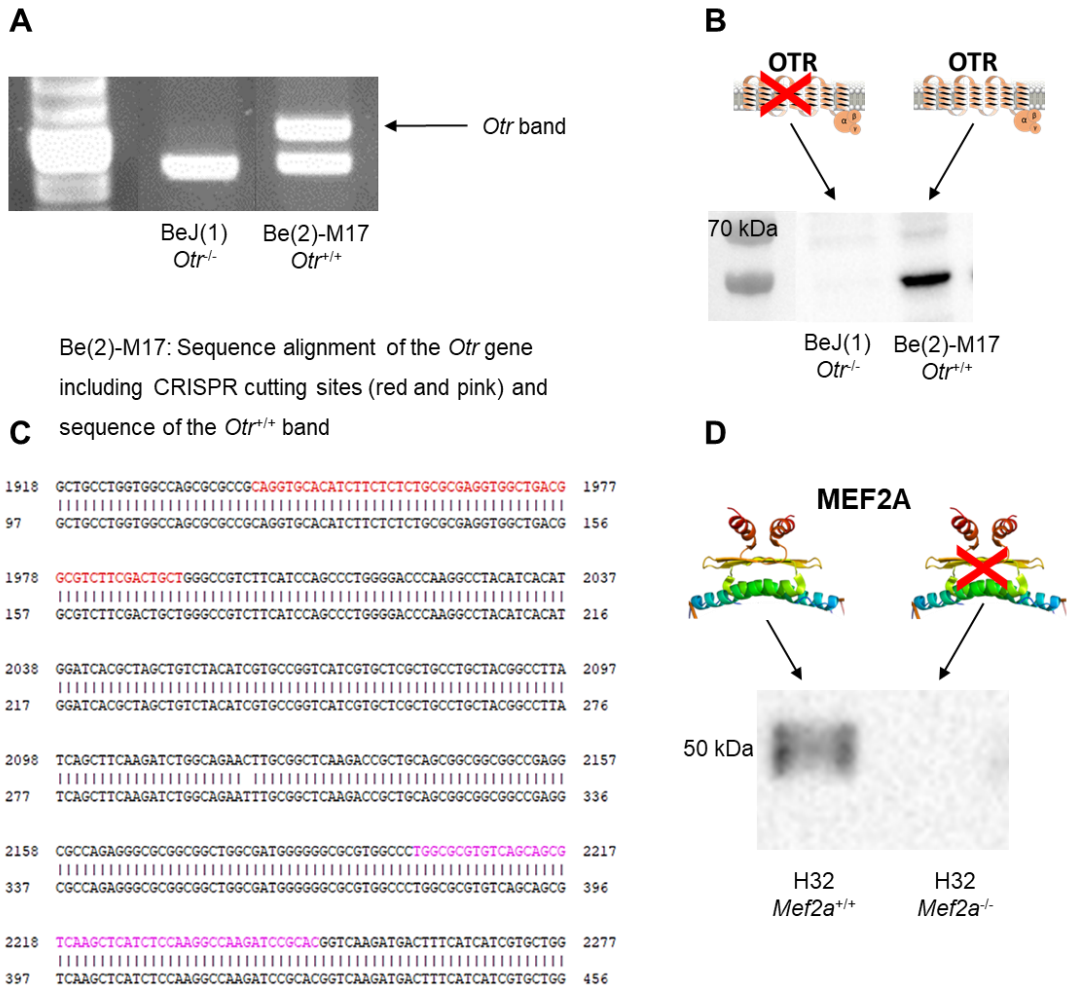

Figure 32. Sequencing and western blot analysis of BeJ(1) cells and H32 Mef2a$^{-/-}$ cells compared to respective wildtype cells.

(A) Representative image of PCR analysis of the *Otr* gene. CRISPR-mediated KO of the *Otr* gene leads to the loss of the respective band in BeJ(1) cells compared to Be(2) cells. **(B)** Representative image of western blot analysis of OTR expression in wildtype and KO cells. BeJ(1) KO cells lack the OTR band at 55 kDa compared to Be(2)-M17 wildtype cells. The OTR [EPR12789] rabbit antibody provided by Abcam (Cambridge, UK) was used. **(C)** Sanger Sequencing analysis of the purified *Otr*$^{+/+}$ band, obtained by PCR, confirmed the loss of the corresponding gene fragment containing the CRISPR cutting sites in BeJ(1) cells. These data confirmed the successful KO. **(D)** Representative image of western blot analysis of MEF2A protein expression in H32 wildtype and KO cells. MEF2A KO cells lack the MEF2A band at 50 kDa compared to H32 wildtype cells. The anti-MEF2A rabbit (AP06372PU-N) antibody provided from Acris (Distributor Germany: Acris; Manufacturer: OriGene Technologies, Rockville, USA) was used.

Unlike N2a cells, the human Be(2)-M17 cell line and consequently also the BeJ(1) cells are undifferentiated neurons. To enable an analysis of morphology in Be(2)-M17 and BeJ(1) cells, a differentiation protocol of 5 days with either forskolin and retinoic acid, or dbcAMP

was performed, resulting in the formation of distinct, measurable neurites (Fig. 33). Differentiation protocols significantly increased neurite length in these cells.

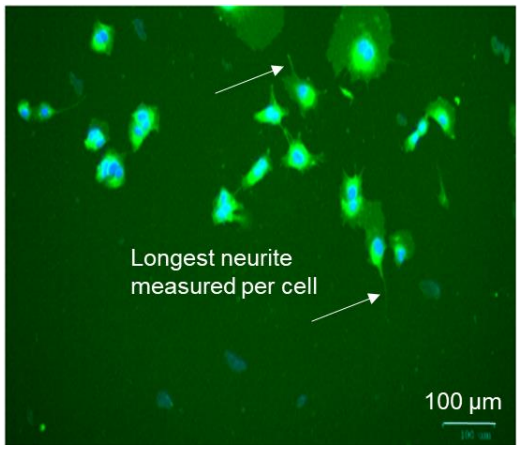

Figure 33. Differentiation of Be(2)-M17 cells.
Representative image of differentiated Be(2)-M17 cells. Differentiation was induced by treatment with forskolin and retinoic acid. Cellular membranes were stained with Green CellMask (Thermo Fisher Scientific, Waltham, USA) and nuclei were stained with Hoechst 33342 (Thermo Fisher Scientific, Waltham, USA).

Comparative signaling studies in Be(2)-M17 and BeJ(1) cells revealed the impact of the loss of the OTR. Firstly, the impact of OT treatment on neuronal morphology was diminished (Fig. 34A) and MAPK and MEF2 signaling were impaired (Fig. 34B). OT caused neurite retraction in Be(2)-M17 cells from 57.9 µm (± 1.9) to 49.5 µm (± 1.4), whereas BeJ(1) cells retained a length between 52.5 µm (± 2.2) and 56.3 µm (± 2.5, Fig. 34A). In the same passage of BeJ(1) cells, OT-induced MAPK signaling, represented by ERK1/2 phosphorylation, remained unchanged (fold change of 1.1 ± 0.2 and 1.1 ± 0.3 compared to VEH). Plasmid-driven OTR overexpression in BeJ(1) cells restored OT-induced ERK1 phosphorylation (fold change of 1.3 ± 0.3 compared to VEH), however, ERK2 phosphorylation levels were still unaltered (fold change 1.1 ± 0.1, Fig. 34B). This lack of ERK2 phosphorylation is likely to be caused by suboptimal transfection efficiency, and would reach significance once ~100% cells express the OTR construct. Due to the minor, but significant, impact on ERK1 phosphorylation, MEF2A S408 phosphorylation levels were assessed. BeJ(1) cells transfected with the empty vector displayed no changes in MEF2A phosphorylation at S408, OTR overexpression and the subsequent activation of ERK1 led to an increase in MEF2A S408 protein phosphorylation (fold change 1.3 ± 0.1, Fig. 34C). However, as expected, overall phosphorylation levels of pMEF2A S408 were relatively low in BeJ(1) cells (Fig. 34D).

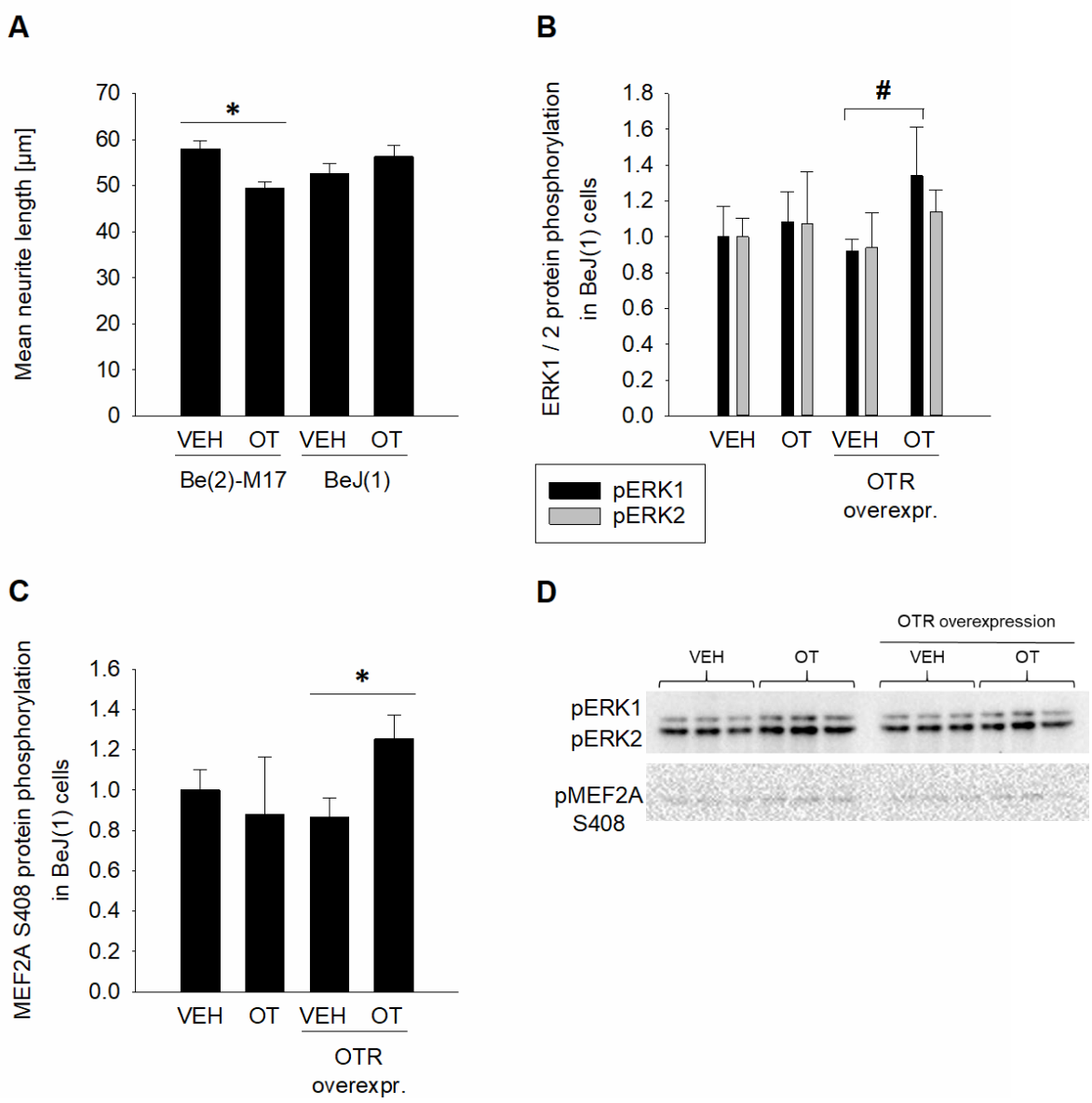

Figure 34. Effects of OT treatment on morphology and MAPK signaling in BeJ(1) cells.

(A) Mean neurite length in human Be(2)-M17 decreased after 24 h of OT treatment (100 nM). Rank Sum Test, Mann-Whitney U Statistic = 9243.500, * p = 0.002; n-number: VEH = 135, OT = 173. OT had no effect on neuronal morphology in BeJ(1) cells. Rank Sum Test, Mann-Whitney U Statistic = 8498.500; n-number: VEH = 134, OT = 136. Data shown as mean +SEM. **(B)** Analysis of ERK1/2 protein phosphorylation after VEH and OT treatment in BeJ(1) cells. Cells were either pretreated with an empty control vector or an OTR overexpression vector. Data shown as mean fold change compared to VEH +SEM. pERK1 (empty vector): t = -0.307 with 4 degrees of freedom, one-tailed p-value = 0.387; n-number: VEH = 3, OT = 3. pERK1 (OTR vector): t = -1.772 with 4 degrees of freedom, # one-tailed p-value = 0.0756; n-number: VEH = 3, OT = 3. pERK2 (empty vector): t = -0.233 with 4 degrees of freedom, one-tailed p-value = 0.414; n-number: VEH = 3, OT = 3. pERK2 (OTR vector): t = -0.884 with 4 degrees of freedom, one-tailed p-value = 0.213; n-number: VEH = 3, OT = 3. **(C)** Analysis of MEF2A S408 protein phosphorylation after VEH and OT treatment in BeJ(1) cells. Cells were either pretreated with an empty control vector or an OTR overexpression vector. Data shown as mean fold change compared to VEH +SEM. Empty vector: t = 0.397 with 4 degrees of freedom, one-tailed p-value = 0.356; n-

number: VEH = 3, OT = 3. OTR vector: t = -2.557 with 4 degrees of freedom, * one-tailed p-value = 0.0314; n-number: VEH = 3, OT = 3. **(D)** Representative western blot images of pERK1/2 and pMEF2A S408 antibody staining.

3.4. Optimizing the in vitro model for oxytocin receptor signaling with cholesterol

The cholesterol content of cell membranes has profound effects on signal transduction and functional activity of the OTR (for detailed references see Introduction part 2.4.). In order to create a solid cellular model of the intracellular OTR pathway with reproducible outcomes my aim was to optimize the cellular machinery by cholesterol enrichment. Cholesterol is typically not a supplement in cell culture medium, so all cell line based models suffer from those artificial conditions. Therefore, Be(2)-M17 cells were enriched with cholesterol as described in the methods section and MAPK signaling, represented by ERK1/2 phosphorylation levels, was assessed. To exclude a basal impact of higher cholesterol contents in the membrane on signaling, pERK1/2 levels were measured in untreated (0 or VEH) and cholesterol enriched (+ or +chol) cells. Without prior OT stimulation, ERK1/2 phosphorylation levels remained unchanged in both untreated and enriched cells (fold change pERK1: cytoplasm 0.7 ± 0.1, nucleus 0.7 ± 0.2; pERK2: cytoplasm 0.7 ± 0.1, nucleus 0.8 ± 0.2, Fig. 35A and B). Cytoplasmic and nuclear proteins were analyzed separately, in order to detect nuclear translocation of either pERK1 or pERK2. However, nuclear translocation was also unaffected by cholesterol enrichment (Fig. 35A and B).

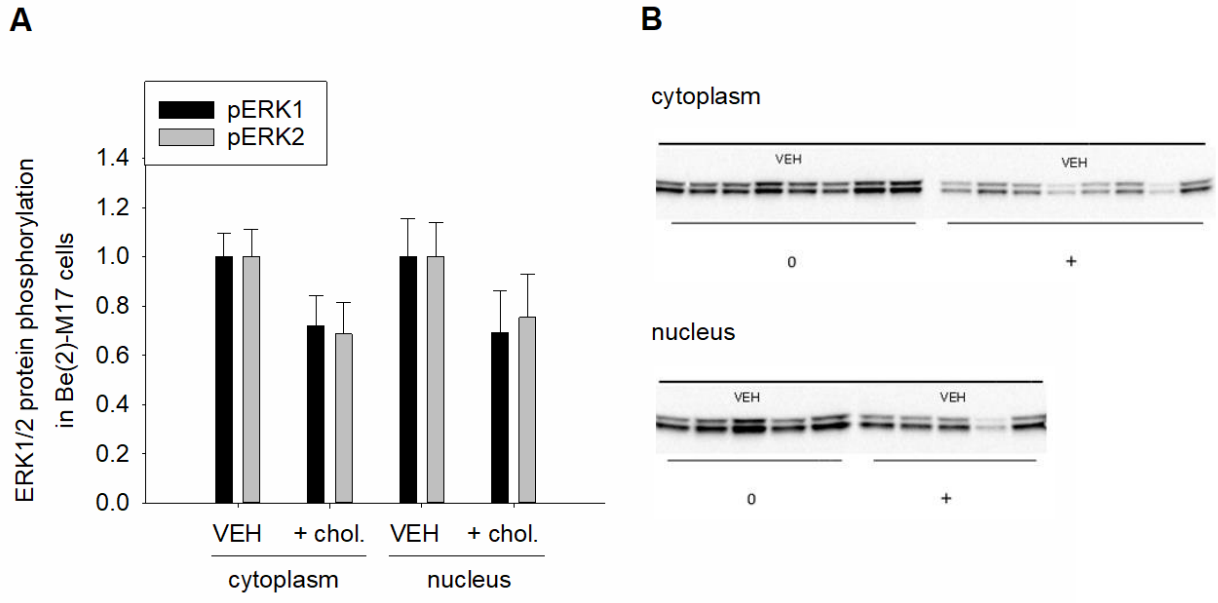

Figure 35. Western blot analysis of cholesterol effects on ERK1/2 phosphorylation in Be(2)-M17 cells. To study the effects of OT treatment on MAPK signaling of cells enriched with cholesterol, the basal effect of cholesterol enrichment was assessed. Cholesterol enrichment had no statistically significant effects on ERK1/2 phosphorylation in Be(2)-M17 cells. Both protein samples from cytoplasmic and nuclear fractions were analyzed.

Data shown as mean fold changes (+SEM) compared to respective VEH groups. **(A)** Cytoplasm: pERK1 vs pERK1 + chol. t = 1.865 with 13 degrees of freedom, two-tailed p-value = 0.0849; n-number: VEH = 8, + chol. = 7. pERK2 vs pERK2 + chol. t = 1.855 with 14 degrees of freedom, two-tailed p-value = 0.0848; n-number: VEH/+ chol. = 8. Nucleus: pERK1 vs pERK1 + chol. t = 1.335 with 8 degrees of freedom, two-tailed p-value = 0.218; n-number: VEH/+ chol. = 5. pERK2 vs pERK2 + chol. t = 1.111 with 8 degrees of freedom, two-tailed p-value = 0.299; n-number: VEH/+ chol. = 5. **(B)** Representative image of pERK1/2 western blot analysis. 0 represents in blot pictures no cholesterol treatment, + represents cholesterol treatment.

As the increased membrane content of cholesterol had no significant effects on ERK1/2 protein phosphorylation, the next step was to assess the effect of OT treatment on ERK1/2 phosphorylation. Two concentrations of OT were used (10 nM and 100 nM) for 5, 10 and 20 min after enrichment with a cholesterol-MßCD solution. Cytoplasmic and nuclear proteins were assessed separately, as activated (phosphorylated) ERK translocates to the nucleus. As a control, all OT stimulations were also conducted without cholesterol enrichment. The lower concentration of OT (10 nM) had no time-dependent impact on ERK1/2 phosphorylation, neither in the cytoplasmic nor in the nuclear fraction (Fig. 36A and B, Table 9). However, there was a significant effect of cholesterol enrichment on pERK2 expression in the cytoplasm (Fig. 36A, table 9). In the nucleus, both pERK1 and pERK2 were altered by cholesterol pre-treatment (Fig. 36B, table 9). Despite some exceptions, the overall impact of cholesterol points towards a reduction in ERK1/2 phosphorylation induced by cholesterol treatment. Stimulations with a higher dose of OT (100 nM) had no significant time-dependent effects (Fig. 36C and D, table 9). Also, the stabilization of the OTR with cholesterol pre-treatment was not able to increase ERK1/2 phosphorylation levels significantly in a two way ANOVA analysis (Fig. 36C and D, table 9). However, the expression patterns of pERK1/2 after cholesterol enrichment displayed an increase in phosphorylation compared to non-enriched cells, pointing towards positive effects of cholesterol enrichment on MAPK signaling (Fig. 36C and D).

Table 9. Summary of effects of cholesterol enrichment and OT stimulation on pERK1/2 in Be(2)-M17 cells.

Statistical significant differences are indicated with check marks. For statistical details see legend (Fig. 36).

		pERK1	pERK2	Effect of:
10 nM	Cytoplasma	-	-	Time
		-	✓	Cholesterol treatment
	Nucleus	-	-	Time
		✓	✓	Cholesterol treatment
100 nM	Cytoplasma	-	-	Time
		-	-	Cholesterol treatment
	Nucleus	-	-	Time
		-	-	Cholesterol treatment

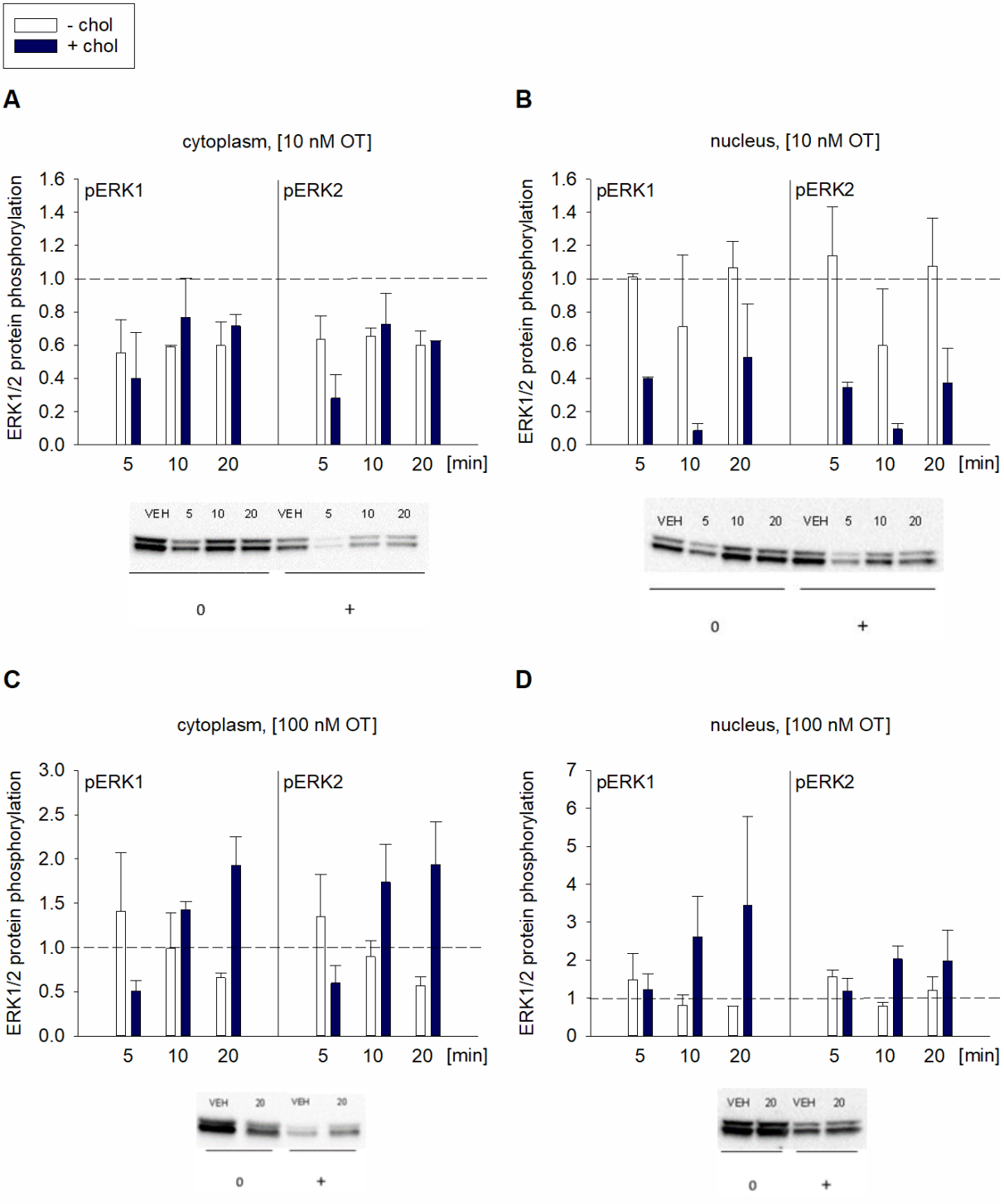

Figure 36. Western blot analysis of cholesterol effects on OT-induced pERK1/2 expression in Be(2)-M17 cells.

Effects of cholesterol on the impact of OT treatment on ERK1/2 phosphorylation over a time course of 20 min. Data are shown as fold change (+SEM) compared to respective VEH set to 1. 0 represents in blot pictures no cholesterol treatment, + represents cholesterol treatment. n-number per time point was 2, overall n-number per + chol and- chol was 6.

(A) Cytoplasm [10 nM OT]: pERK1, no time dependent effect, two way ANOVA $F_{(2,11)} = 0.509$, $p = 0.625$. No effect of cholesterol treatment, two way ANOVA $F_{(1,11)} = 5.253$, $p = 0.062$. pERK2, No time dependent effect,

two way ANOVA $F_{(2,11)}$ = 1.251, p = 0.351. Effect of cholesterol treatment, two way ANOVA $F_{(1,11)}$ = 18.081, p = 0.005, Holm-Sidak post hoc test, * p < 0.05 - chol vs + chol. **(B)** Nucleus [10 nM]: pERK1, no time dependent effect, two way ANOVA $F_{(2,11)}$ = 1.225, p = 0.358. Effect of cholesterol treatment, two way ANOVA $F_{(1,11)}$ = 20.794, p = 0.004, Holm-Sidak post hoc test, * p < 0.05 - chol vs + chol. pERK2, no time dependent effect, two way ANOVA $F_{(2,11)}$ = 1.452, p = 0.306. Effect of cholesterol treatment, two way ANOVA $F_{(3,13)}$ = 17.919, p = 0.005, Holm-Sidak post hoc test, * p < 0.05 - chol vs + chol. **(C)** Cytoplasm [100 nM]: pERK1, no time dependent effect, two way ANOVA $F_{(2,11)}$ = 0.00828, p = 0.992. No effect of cholesterol treatment, two way ANOVA $F_{(1,11)}$ = 1.413, p = 0.279. pERK2, no time dependent effect, two way ANOVA $F_{(2,11)}$ = 0.108, p = 0.899. No effect of cholesterol treatment, two way ANOVA $F_{(1,11)}$ = 0.209, p = 0.663. **(D)** Nucleus [100 nM]: pERK1, no time dependent effect, two way ANOVA $F_{(2,11)}$ = 0.0836, p = 0.921. No effect of cholesterol treatment, two way ANOVA $F_{(1,11)}$ = 0.293, p = 0.608. pERK2, no time dependent effect, two way ANOVA $F_{(2,11)}$ = 0.244, p = 0.791. No effect of cholesterol treatment, two way ANOVA $F_{(1,11)}$ = 0.643, p = 0.453.

Evidence for the success and efficiency of cholesterol enrichment was provided by Filipin III staining. Filipin III specifically binds to cholesterol in membranes and can be visualized *via* blue fluorescence. VEH treated cells displayed moderate intensities (Fig. 37A) in comparison to cells after 30 min of cholesterol depletion (Fig. 37B). Both 15 min and 30 min of enrichment clearly enhanced the cholesterol content in the treated cells as shown by increased fluorescence (Fig. 37C and D), confirming the efficiency of the protocol used for enrichment.

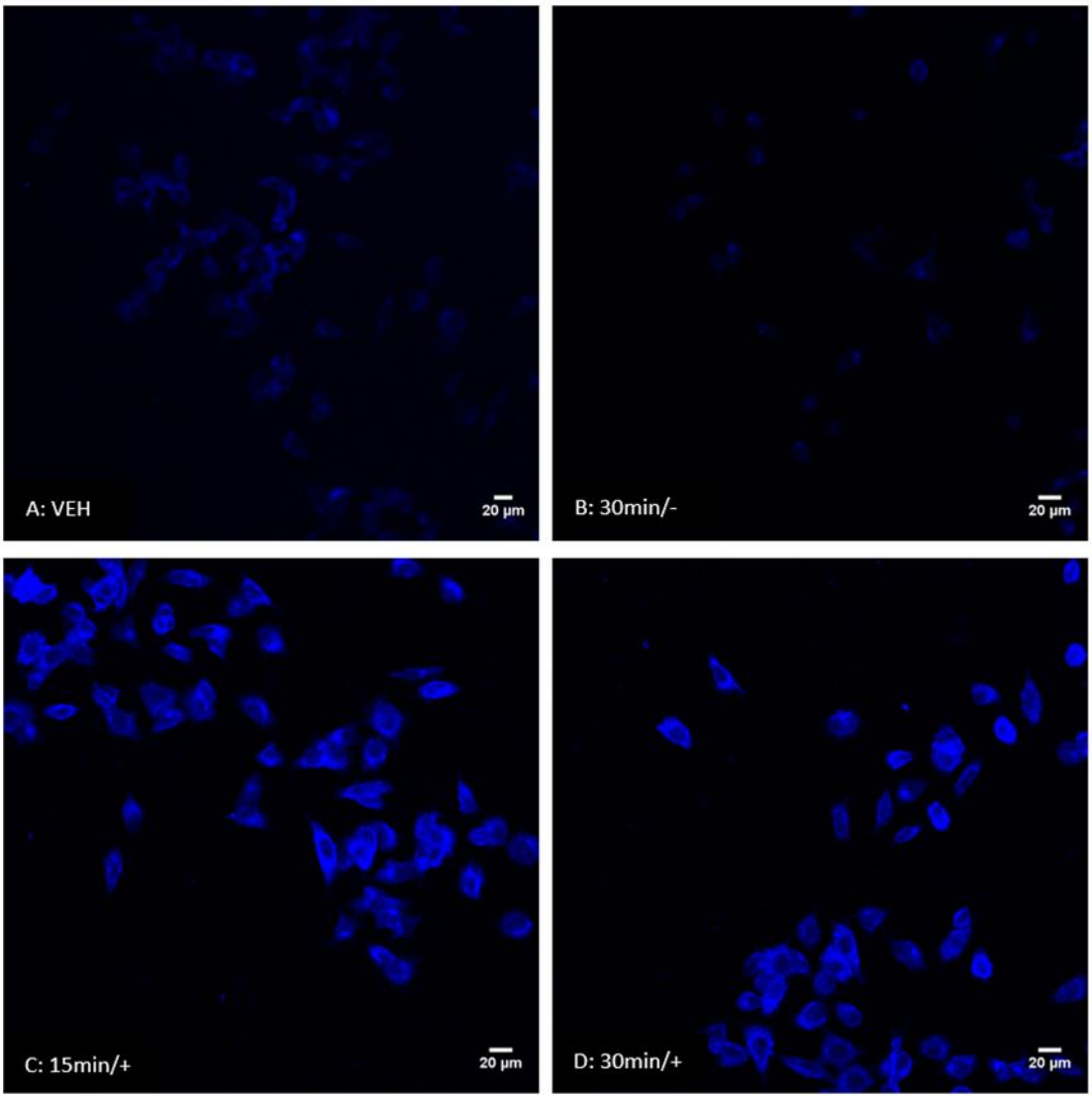

Figure 37. Representative fluorescent microscopic images of Be(2)-M17 cells with Filipin III staining. **(A)** Cells after 30 min of incubation with MßCD. **(B)** Cells after 15 min of incubation with cholesterol-MßCD. **(C)** Cells after 30 min of incubation with cholesterol-MßCD **(D)**. Images were taken at the SP8 Leica confocal microscope with a x20 objective, Filipin III was visualized under DAPI filter.

Discussion

Parts of the Discussion have been taken and adapted from the following publication:

Chronic oxytocin signaling reveals alternative splice variant of CRFR2 as biomarker for anxiety (in preparation).

Julia Winter[1], Magdalena Meyer[1], Ilona Berger[2], Sebastian Peters[3], Melanie Royer[1], Julia Kunze[4], Stefan O. Reber[4], Kerstin Kuffner[5], Anna K. Schmidtner[1], Anna Bludau[1], Marta Bianchi[1], Simone Stang[1], Oliver J. Bosch[1], Erwin van den Burg[6, #], Inga D. Neumann[1, 7, *, #], and Benjamin Jurek[1, #, *]

[1]Department of Behavioural and Molecular Neurobiology, Institute of Zoology, University of Regensburg, Regensburg, Germany; [2]Technische Universität Dresden, University Hospital, Department of Internal Medicine III, Dresden, Germany; [3]Department of Neurology, University Hospital Regensburg, Regensburg, Germany; [4]Laboratory for Molecular Psychosomatics, Clinic for Psychosomatic Medicine and Psychotherapy, University Ulm, Ulm, Germany; [5]Department of Psychiatry and Psychotherapy, University of Regensburg, Regensburg; [6]Centre de neurosciences psychiatriques, Lausanne, Switzerland; [7]lead contact, *corresponding author, [#]these authors contributed equally

Contributions as following:

Conceptualization, B.J., S.P., E.H.vdB., and I.D.N.; Methodology, J.W., M.M., I.B., B.J.; Validation, J.W., M.M., I.B., K.K., M.B., M.R., A.B., Investigation, J.W., M.M., I.B., S.P., M.R., J.K., K.K., O.J.B, A.B., M.B., A.K.S.; Writing – Original Draft, J.W. and B.J.; Writing – Review & Editing, S.P., S.R., O.J.B., E.H.vdB., I.D.N., B.J.; Funding Acquisition, I.D.N. and B.J.; Resources, I.D.N; Supervision, B.J., S.P., E.H.vdB., and I.D.N.

Data from this publication will be discussed in this thesis, however, as some of the experiments conducted have not been performed by myself, they are not part of the Results section of this thesis, indicated as Winter et al, in preparation.

Discussion

In this thesis, the molecular mechanism underlying the anxiogenic phenotype resulting from chronic OT delivery was assessed. With numerous clinical and preclinical studies on OT as a potential treatment option for psychiatric disorders like ASD (Guastella and Hickie, 2016; Parker et al., 2017), schizophrenia (Feifel et al., 2010; Macdonald and Feifel, 2012), depression (Domes et al., 2016), and anxiety disorders (Neumann and Slattery, 2016), fundamental knowledge on OT's mode of action and in particular on long-term effects remains relatively sparse (reviewed in Jurek and Neumann, 2018). Here, chronic OT treatment for 14 days increased anxiety in male and female rats in a dose-dependent manner. When compared to an anxiolytic bolus of acute OT, substantial differences were discovered with regard to activation of intracellular signaling cascades and target gene expression, specifically the transcription factor MEF2 and alternative splicing of the CRFR2α. MEF2A-mediated alternative splicing increased the cytoplasmic, soluble sCRFR2α variant shifting the ratio between mCRFR2α and sCRFR2α towards sCRFR2α in the PVN and even led to a release into the CSF, ultimately increasing anxiety-like behavior.

1. The two faces of oxytocin in anxiety – effects of chronic vs acute oxytocin

Acute and short term applications of OT have well-known positive effects in rodents and humans. Infusions of synthetic OT into the lateral ventricle, PVN, hippocampus, septum, amygdala, as well as intranasal delivery revealed improved anxiety, sociability, or stress coping (Jurek and Neumann, 2018; Neumann and Landgraf, 2012 and references therein). The PVN was confirmed as the region of action of OT-mediated anxiolysis (this thesis, Blume et al., 2008; Jurek et al., 2012), as only local-intra PVN infusions were able to alter anxiety-like behavior in contrast to *i.c.v.* infusions. To date, only very few studies have addressed the behavioral and molecular effects of chronic OT (Calcagnoli et al., 2014; Du et al., 2017; Havranek et al., 2015; Peters et al., 2014; Slattery and Neumann, 2010; Windle et al., 2004; Windle et al., 1997). In the present thesis, I found a transient, dose-dependent anxiogenic effect of *i.c.v.* chronic OT treatment in male and female rats and investigated the underlying molecular mechanism. Interestingly, the anxiogenic effect depended on a mild stressor 24 h before the LDB test, corroborating previous findings that OT requires a second stimulus like stress to be effective (Blume et al., 2008; Jurek and Neumann, 2018; Jurek et al., 2015). This accounts not only for rats but was also recently

shown in mandarin voles, where a dose of *i.c.v.* chronic OT (10 ng/h) had no effect on anxiety-like behavior. Yet, a mechanism in mandarin voles that is distinct from rats has to be considered (Du et al., 2017). Chronic OT caused a sexual dimorphic phenotype, as female rats display increased anxiety already after the low dose of OT (1 ng/h) and appear to be more sensitive to chronic treatment than males. Although the effect in the high dose ceased to reach significance, this lack of effect has to be taken with caution since the experiment was statistically underpowered. As the level of anxiety also tended to increase in the high dose group, it is possible that it might reach significance when the experiment is repeated. Sex differences with regard to OT treatment have been reported previously. OT has anxiolytic properties in males and more prosocial effects in females (Li et al., 2016). Therefore, the underlying molecular mechanism of chronic OT-induced behavioral changes in females represents a fundamental research question worth investigating in further studies.

In males, an intrinsic brain mechanism, rather than a peripheral stress response seems to be responsible for the anxious phenotype, as plasma corticosterone and ACTH levels were not changed (Winter et al., in preparation). Chronic activation of the HPA axis can lead to increased anxiety-like behavior in rats (Reber and Neumann, 2008), however, I found no evidence for this mechanism in my study. In fact, there was no peripheral parameter altered after 14 days of chronic *i.c.v.* OT, although the exogenous OT we infused could be detected in the plasma (described in Master thesis Serena Gusmerini 2015).

OT has a half-life of 3 to 6 min in plasma (Rydén and Sjöholm, 1969) and is degraded 20 min after *i.c.v.* application in CSF (Mens et al., 1983), the activated OTR is recycled to the cell surface within about 4 hours (Conti et al., 2009). Nevertheless, the anxiolytic effect of intra-PVN infusions vanished after 3 hours after local infusions. A recovery or wash-out period of 5 days after chronic infusions also restored anxiety levels back to basal, confirming a reversible and slow onset molecular mechanism within the brain. The mechanism behind does not consist of altered OTR expression or binding in the PVN, as both parameters were not affected by chronic OT treatment (Winter et al., in preparation). In addition to the PVN, the septum potentially contributes to the observed phenotype, as both *mCrfr2α* and *sCrfr2α* mRNA levels were affected by chronic OT. No effects on any parameter measured were detected in other stress/OT-related brain regions, such as the hippocampus or prefrontal cortex, though, highlighting the important role of the hypothalamic PVN as a central regulator of the OT system and anxiety-like behavior.

2. MAPK and MEF2 signaling induced by chronic oxytocin

Parallel to intracellular signaling induced by acute OT administration (this study and Blume et al., 2008; Jurek et al., 2015; Jurek et al., 2012), chronic OT also activated the MAPK pathway, represented by phosphorylation of MEK1/2, ERK1/2, and further downstream the transcription factors MEF2A, MEF2C and CREB. As CREB was equally activated by the low and the high dose of chronic OT, an exclusive involvement in the differential anxiogenic effect of the high dose can be excluded. However, MEF2A and MEF2C are known to be part of a larger transcriptional complex, including CREB and its cofactors CRTC, and each factor is related to OT signaling (Devost et al., 2008; Jurek et al., 2015; Meyer et al., 2018; Tomizawa et al., 2003). Here, the low and the high dose of chronic OT caused a differential activation of MEF2A and MEF2C, as MEF2C DNA binding activity was only increased by the low dose of chronic OT. Since no behavioral parameters were changed in the low dose OT group, MEF2C activity seems to be irrelevant for the anxiogenic effect of OT.

DNA binding is a feasible parameter to assess activity of a target transcription factor, but, more importantly, the downstream inhibitory or activating nature has to be determined. The three phosphorylation sites in MEF2A (S408, Thr312, Thr319) directed the factor towards transcriptional activation, especially in the high dose OT group, where S408 dephosphorylation drives gene transcription. Phosphorylation of MEF2A at S408 is known to inhibit transcription, potentially influenced by cyclin-dependent kinase 5 (Gong et al., 2003; Shalizi et al., 2006). MEF2A-induced gene transcription *via* S408 was exclusive for the high dose OT group, providing a solid link between the phosphorylation status of MEF2A and anxiety-like behavior. Upstream factors regulating the phosphorylation status, in addition to MEK1/2-ERK1/2, might include ERK5 (kinase activity, Devost et al., 2008) and calcineurin (phosphatase activity, Lynch et al., 2005; Mao and Wiedmann, 1999). ERK1/2 and ERK5 contain several similarities with regard to signaling, however, ERK5 might exhibit differential effects on MEF2 activation by the phosphorylation of distinct amino acid residues of different isoforms (Nishimoto and Nishida, 2006). Also, previous *in vitro* experiments revealed the prominent activation of MEF2C by ERK5 (Kato et al., 1997). However, providing definitive evidence for an OT-induced physical binding of those factors was beyond the scope of this thesis. To assess the molecular underpinnings of the anxiogenic effect of chronic OT it is important to identify the downstream targets of activated MEF2A. Among the many possible target genes, the CRFR2 represents a central factor that might mediate observed changes in anxiety-like behavior, which I will discuss in more detail below. The pathway described, starting from the activated OTR to nuclear MEF2A *via* the MAPK pathway and the transcription of target genes like the CRFR2 might underlie the

anxiogenic effect of chronic OT. Yet, the question remains why this only occurs in chronically treated rats. What is the difference between an acute bolus of OT, directly infused into a brain region like the PVN or *i.c.v.*, and the chronic treatment paradigm that I applied over the course of 14 days? One major factor is the availability and activity of MEF2A. Only after 14 days of treatment, I could detect an increase in MEF2A total protein levels, and this higher amount of MEF2A in the brain showed greater activity. Acute OT infusions failed to reach a certain threshold that initiates the transcription, translation, and post-translational modification of MEF2A within a certain time frame. If the high level and activity of this central factor is missing, OT acts *via* the TRPV2-Ca^{2+}- PKC- MAPK-, CREB/CRTC pathway (Jurek and Neumann, 2018), to orchestrate a relatively rapid anxiolytic response.

In addition to the differences between chronic and acute OT in male rats, the behavioral response of female rats that received chronic OT treatment differed slightly from that of males, which raises the interesting question whether the underlying molecular pathway is also sex-specific. Indeed, DNA binding activity of MEF2A and MEF2C remained at basal levels after 14 days of the chronic OT treatment. Consistent with the missing effect on MEF2A and MEF2C DNA binding activity, phosphorylation levels at activating or inhibitory residues remained unchanged. Although it is beyond the scope of this thesis to investigate the alternative pathway responsible for the anxiogenic effect of the low dose of chronic OT in female rats, I can exclude the MAPK-MEF2A-centered pathway in the PVN that is responsible in male rats. Sex-specific activation of MAPK or equivalent pathways has been shown previously in related contexts, *e.g.* learning and memory formation (Mizuno and Giese, 2010), neurite outgrowth (Kumar et al., 2018), as well as anxiety (Jurek et al., 2012) and could be involved here as well. Whatever the nature of the alternative pathway in female rats is, it is likely to be located within the PVN, as this region is close to the ventricular system, expresses OT, OTR, MEF2A/C and CRF receptors, and, when manipulated is known to influence anxiety-like behavior (Jurek and Neumann, 2018; Neumann et al., 2000c; Smith et al., 2016). In fact, other brain regions that have been associated with anxiety and fear, like the hippocampus with its high levels of OTR expression (Grinevich et al., 2014) displayed no chronic OT-induced alterations of MEF2A or C expression or activity, and no changes in CRFR2 expression are therefore to be expected.

By means of an additional experimental design, I was able to test the permanence of the chronic OT-induced effects in males. The osmotic minipumps I implanted have a defined pumping rate and reservoir volume, resulting in a clear-cut pumping time, after which the pumps stop delivering their content. I utilized this effect to leave the pumps implanted after the flow stopped for a “wash-out-period” of 5 days. This resulted in a 14+5 days-time frame

from surgery to final behavioral test and tissue collection. Intriguingly, all effects seen on day 14, *i.e.* anxiogenesis, MEF2A activation, or CRFR2α transcription, recovered to basal levels, suggesting only transient effects of the neuromodulator OT.

Taken together, this data obtained from rats treated with chronic OT might explain the transient and slow onset characteristics of the anxiogenic effect of chronic OT. Acute OT is not enough to alter protein levels and activity of MEF2A, and the downstream transcriptional activity of MEF2A, as discussed in the following paragraph, requires additional time to take effect.

3. CRFR2α alternative splicing increases anxiety induced by chronic oxytocin

To shed further light on the molecular pathway behind increased anxiety caused by chronic OTR activation, potential MEF2A downstream targets were analyzed. In order to do so in the most efficient way possible, I pre-selected genes that have been associated with anxiety, stress, neuronal morphology, synaptic plasticity, and carry a MEF2 binding sequence within their promoters or gene. While the MEF2 binding sequence is non-selective between the A and C subform of MEF2, I already have proven that MEF2A is the main driving force of the anxiogenic effect in the high dose OT group, and so all regulatory effects on those genes can be attributed to MEF2A activity.

A central factor for this thesis is the CRFR2α, that carries multiple MEF2 binding sequences in its promoter and throughout the gene, and has been associated with anxiety and stress in a multitude of publications (Deussing and Chen, 2018 and references therein).

The CRFR2α is almost exclusively expressed in the brain (Lovenberg et al., 1995; Van Pett et al., 2000), and an alternative splice variant lacking the trans-membrane domain has been identified. This shorter sCRFR2α form is unable to incorporate into the cellular membrane; instead, it diffuses randomly into the cytoplasm and is released into the extracellular space (Chen et al., 2005; Evans and Seasholtz, 2009). With an antibody that detects both the full-length mCRFR2α and the splice variant sCRFR2α, protein levels in the PVN of rats after chronic OT treatment were analyzed. Chronic OT promoted sCRFR2α expression, whereas mCRFR2α levels remained unchanged, which resulted in a shift of the sCRFR2 to mCRFR2 ratio. On mRNA level, even a decrease in *mCrfr2α* mRNA could be detected, as both the full-length receptor and the splice variant derive from the same mRNA. Regulation of full-length mRNA availability is thought to be one of the functions of alternative splicing of the

CRFR2α (Evans and Seasholtz, 2009; Markovic and Grammatopoulos, 2009). Also, mRNA processing and alternative splicing are common ways to regulate class B GPCR availability and function (Deussing and Chen, 2018; Furness et al., 2012). This might account for the effects of chronic OT on alternative splicing as well, as a shifted protein ratio towards sCRFR2α promotes the anxious phenotype that was exclusively observed in male rats that received the high dose of chronic OT.

The question how OT induces the process of alternative splicing might conveniently be answered already, *i.e.* by the activity of MEF2A. MEF2A as a transcription factor is not intuitively linked to the process of alternative splicing. However, recent findings support the hypothesis that transcription and alternative splicing are two processes closely working in conjunction and depend on each other. MEF2A is part of a large complex of transcription and splicing-regulating factors, such as Brg1/Brm, BAF47, BAF170, BAF155, MyoD, and a histone acetyl transferase. These factors contribute to the correct transcription and immediate splicing of the transcript (Proudfoot et al., 2002; Zhang et al., 2016). It is therefore perfectly feasible to infer a parallel role for MEF2A in the transcription and alternative splicing of the CRFR2α gene. This might also explain how the sexual dimorphic anxiety-like behavior of chronically treated male rats persists on a molecular level. No changes in the mCRFR2α/sCRFR2α ratio could be detected in females and in males treated with acute OT, as in both circumstances substantial MEF2A activity was missing.

To elucidate the so far unknown effects of CRFR2α activity in the PVN on anxiety, I conducted behavioral experiments to assess both agonism (SCP) and antagonism (ASV) of the CRFR2, and confirmed the anxiolytic properties of the mCRFR2α in the PVN. The dosage of ASV was chosen at a concentration that mostly excludes CRFR1 activation (Tebbe et al., 2005; Zorrilla et al., 2013) and considered carefully, as contradictory effects of ASV in other brain regions that have been reported in literature are mainly due to the use of supra-maximal doses (Zorrilla et al., 2013). On the contrary, stimulation of PVN-CRFR2α with the specific CRFR2 agonist SCP acted anxiolytic, in favor of my hypothesis.

I have so far in this discussion assumed that the ratio between the regular mCRFR2α and the intra- or extracellular sCRFR2α was the main cause of the chronic OT-induced anxiogenesis. However, a second scenario is equally possible, that involves the short splice variant as an independent behavioral effector either by intracellular actions or by acting as a decoy receptor in the extracellular space.

The second scenario is supported by the use of locked nucleic ASOs, in more detail GapmeRs or TSBs to either increase mCRFR2α or sCRFR2α expression. The elegance of this experiment lies in the mechanism to manipulate either variant. While the GapmeRs are designed to target the Exon 5-7 boundary, which only exists in the sCRFR2α splice variant,

and therefore eliminates all sCRFR2α without alterations of the mCRFR2α expression, the TSBs, in turn, prevent the formation of the regular *mCrfr2α* mRNA, which results in the exclusive translation of sCRFR2α. This design allowed me to study the behavioral effects of each variant independently. Low levels of sCRFR2α protein expression led to low anxiety levels, whereas increased expression of sCRFR2α, in consequence, enhanced anxiety-related behaviors. This data led me to conclude, with all the scientific rigor and carefulness, that the above described scenario of an independent anxiogenic effect of the sCRFR2α variant is the most likely hypothesis.

In addition, high CSF-sCRFR2α levels negatively correlated with anxiety, supporting the anxiogenic effect as well as the supposed release into the extracellular space (Chen et al., 2005; Evans and Seasholtz, 2009). Here, the sCRFR2α is supposedly cleared from the parenchyma into the ventricular system and the peripheral circulation to be either degraded or taken up. The exact fate, however, is so far subject to speculation.

Taken these results into account, the extracellular sCRFR2α might serve as a biomarker that is easily detectable in various tissues and body fluids (CSF, plasma, urine, saliva; personal communication with Dr. Benjamin Jurek) and represents a potential treatment target for anxiety disorders.

A potential treatment option for human anxiety patients includes the use of the above-described GapmeRs. *In vivo* application of ASOs is a viable approach for the manipulation of mRNA translation, due to their efficacy, stability, and cell penetrating properties , *i.e.* no need for any transfection reagent (Aartsma-Rus and van Ommen, 2007). Additionally, changes in mCRFR2α and sCRFR2α expression had no effect on social behavior or general arousal, suggesting that the effects might be specific for anxiety-related behaviors.

The great impact of stress on CRFR2 activity and behavioral outcomes has been addressed in the Introduction section of this thesis (also see Anthony et al., 2014; Issler et al., 2014). In addition, stress also induces synthesis of CRFR2 and membrane integration (Reyes et al., 2008). The high dose of chronic OT in combination with a mild stressor caused a moderate increase in mCRFR2α expression compared to unstressed animals. The induction of mCRFR2α expression under chronic OT-stress-conditions could be interpreted as a stress-coping and compensatory mechanism of the animal in order to dampen the stress experienced. This should not be confused with the overall effect of the chronic OT treatment compared to stressed VEH treated animals, which led to increased sCRFR2α expression and stable mCRFR2α levels, ultimately resulting in a shifted sCRFR2α/mCRFR2α ratio and anxiogenesis.

When summarized, my data reveal the paramount importance of the cellular localization of the CRFR2α, *i.e.* either membrane-bound (mCRFR2α) or intra/extracellularly (sCRFR2α).

Specific detection of the splice variant is enabled by an antibody against the sCRFR2α, whose specificity has been tested and published previously (Chen et al., 2005). However, antibody specificity and their use in semi-quantitative methods like western blotting or dot blots is a recurrent topic in the scientific literature, and has been proposed as one of many reasons for the “reproducibility-crisis” in science (Baker, 2015; Bradbury and Pluckthun, 2015; Simpson and Browning, 2017). In consequence, a detection system that only relies on antibody detection can be risky and prone to bias. To test my hypothesis with scrutiny and scientific rigor, I developed an antibody-independent method to clearly distinguish between membrane-bound mCRFR2α and intracellular sCRFR2α in a live-cell setting.

I established a CRISPR-based detection system, where I inserted a tag (HiBiT) into the extracellular domain of the CRFR2α by means of genome editing. The extracellular domain is the part of the protein that is removed by alternative splicing, thereby removing the tag from the final protein. The HiBiT-tag itself is visualized by its cognate substrate, the so-called “LgBiT”, which is simply added to the cell culture medium. Once bound, the HiBiT-LgBiT-complex produces a fluorescent signal, whose intensity can be recorded from living cells. This allows to clearly distinguish between the two receptor variants, independent of antibodies. To detect changes in membrane expression of CRFR2α, I mimicked *in vivo* chronic OT treatment in cell culture experiments by stimulating H32 cells for 24 h with 100 nM OT. Analysis of the HiBiT-labelled membrane-bound receptor confirmed my hypothesis, as OT reduced membrane expression of the CRFR2α.

Furthermore, extracellular release of the splice variant was not only detectable under basal conditions, as described by Chen et al., 2005 in CosM6 cells, but was stimulated by OT in cell culture, which supports H32 cells as an ideal model for the analysis of signaling cascades activated by chronic OT. Additionally, the cytoplasmic content of sCRFR2α in OT stimulated H32 cells was analyzed and revealed an intracellular accumulation of the sCRFR2α. In primary hypothalamic neurons a mainly perinuclear distribution along the neurites of neurons and glial cells with an accumulation at the end-boutons of neurites became visible. Those accumulations at the end-boutons of neurites could facilitate the secretion of the sCRFR2α into the extracellular space and CSF. The *in vitro* effects were again limited to chronic OT treatment, acute applications between 10 and 30 min had no effect on either mCRFR2α or sCRFR2α protein expression. However, 30 min after the onset of OT stimulation, phosphorylation of MEF2A at S408 was decreased. MEF2A as a transcription factor undergoes rapid activation, whereas detectable levels of alternative splicing apparently require more time. This indicates 30 min as the starting point of chronic OT effects *in vitro*.

Once secreted, the sCRFR2α is able to bind its ligand with nanomolar affinity (Chen et al., 2005) and could act as a ligand decoy receptor to prevent the activation of the anxiolytic (PVN)-membrane-bound CRFR2α. A possible future experiment to test this hypothesis could involve a co-immunoprecipitation pulldown experiment, to prove physical coupling of the sCRFR2α with its ligand, and a reporter-protein being coupled to the mCRFR2α to reveal reduced activation by the trapped ligand.

However, the origin of ligand inputs into the PVN involved in chronic OT-induced anxiety remains an open question. Regions of high UCN2 and UCN3 expression include the supraoptic nucleus, arcuate nucleus, locus coeruleus, the brain stem, median preoptic area, medial amygdala, and the BNST (Deussing and Chen, 2018). Retrograde tracing studies would reveal whether it is a rather intrinsic circuit within the PVN or whether innervation from distinct brain regions like the amygdala or the BNST plays a role (Bale et al., 2002a).

In the discussion above I focused on MEF2A and its target CRFR2α as the main factors regulating chronic OT-induced anxiogenesis. However, the complexity of the human brain is unrivaled in biology, and to assume that only one transcription factor (MEF2A), regulating one downstream target (CRFR2α) is sufficient to orchestrate a complex emotional behavior such as anxiety would be naïve. However, the complexity of the system only allows to investigate a finite set of factors in great detail. Consequently, especially within the time frame of a PhD thesis, other factors that might be equally involved can only be discussed superficially.

Two of those candidate factors that are MEF2-dependently regulated within the PVN are the transcription factors Pax2 and Pax3. In PVN tissue-lysates of male rats treated with the high dose of OT, *Pax2* mRNA was increased, whereas *Pax3* was decreased. Pax2 is one of the earliest Pax genes to be expressed during development and is critically involved in the formation of the midbrain-hindbrain boundary, which controls midbrain and cerebellar development. Also, it was shown to recruit histone methyltransferase complexes to the promoter regions of target genes (Blake and Ziman, 2014). Pax3 mostly acts as a transcriptional activator, only rare cases of transcriptional repression have been reported. The most common downstream targets of Pax3 include factors like NCAM, MyoD or cMET which are involved in cell adhesion, differentiation, proliferation and cell survival (Mayanil et al., 2001; Stuart and Gruss, 1996). In summary, additive to the morphological effects of chronic OT *in vitro* that will be discussed in the next chapter, changes in neuronal morphology in the brain of rats treated with chronic OT are very likely and are potentially mediated *via* OTR-MEF2-Pax signaling. However, the exact interplay and the role of Pax in the OT pathway has to be determined in future studies.

Another gene affected by chronic OT was the tyrosine hydroxylase (*Th*), which suggests a potential involvement of chronic OT in depression-like symptoms. As *Th* is involved in dopamine synthesis (Molinoff and Axelrod, 1971) and dysregulations have been shown to be associated with depression in humans (Zhu et al., 1999) or depressive-like symptoms in rats (Nestler et al., 1990), there might be a yet undetermined effect of chronic OT on the dopamine system and subsequently a depression-like phenotype.

Overall, from the *in vivo* and *in vitro* results I obtained regarding mCRFR2α and sCRFR2α expression, the following conclusions can be drawn: a permanent “overdose” of OT causes a switch in intracellular signaling by the activation of MEF2A and the subsequent alternative splicing of the CRFR2α. The alternative splice variant sCRFR2α is anxiogenic and can be released into the periphery due to its soluble properties (Fig. 38).
The evolutionary background of such alterations in both intracellular signaling and behavior remains an open question. A shifted equilibrium between activation and degradation that was also shown in other cases of chronic receptor activation (Zhou et al., 2018) could be responsible for the activation of the MEF2A-CRFR2α-pathway by chronic OT treatment. However, an escalation of the OT system by the extremely high doses of exogenous OT could also be responsible for the negative behavioral effects and the changes in signaling. Based on these speculations, the final answer to this question has to be subjected to further studies.

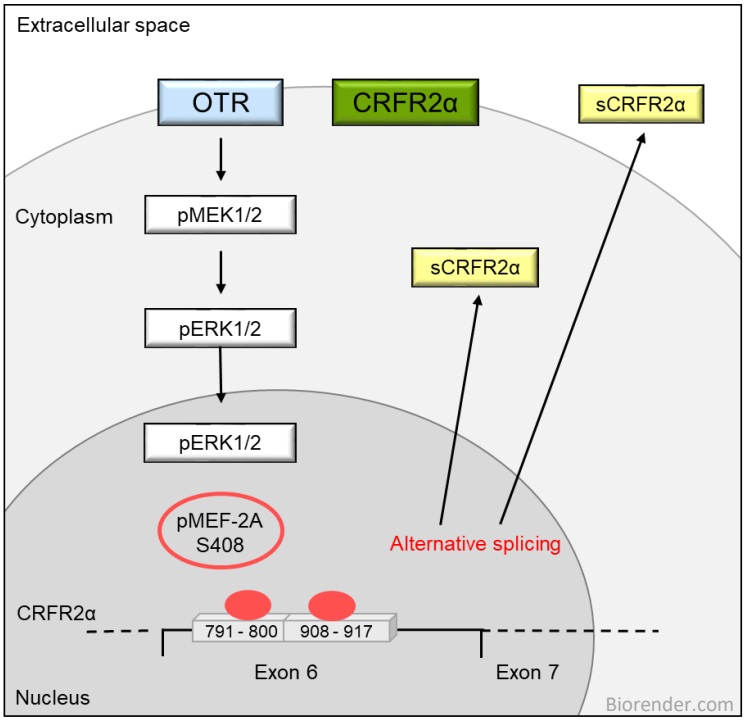

Figure. 38. Signaling scheme of chronic OT *via* MEF2A and alternative splicing of the CRFR2α.

4. Bridging the gap between intracellular genomic effects and behavior: oxytocin-induced morphological alterations

Having established the intracellular pathway leading from the activated OTR to nuclear MEF2A and stimulated gene transcription/alternative splicing, the question remains how those molecular changes translate into subtle shifts in the emotional behavior of an animal. In other words, which mechanism transports the OT message from a single neuron to the level of conscious behavior? The answer might again lie in the function of MEF2A: MEF2A has previously been described as a regulator of excitatory synapse number, neuronal plasticity and cellular morphology (Fiore et al., 2009; Flavell et al., 2006; Flavell and Greenberg, 2008; Flavell et al., 2008). Dysregulations in connectivity between neurons, such as hyperconnectivity cause severe psychiatric disorders like ASD (Tang et al., 2014; Zaslavsky et al., 2019). The neuronal connectome depends on the regulation of cellular morphology, *i.e.* neurite retraction and outgrowth, to form new-, or prune redundant synaptic connections (Tang et al., 2014). Intriguingly, various studies have shown that OT is involved in neurogenesis and neural differentiation both *in vivo* and *in vitro* (Jafarzadeh et al., 2014; Lestanova et al., 2016b; Leuner et al., 2012; Meyer et al., 2018). Not only neuronal morphology, but also glial coverage of neuronal circuits is modulated by OT (Theodosis, 2002).

4.1. Chronic oxytocin induces neurite retraction in vitro in various cell lines

In our group we have focused on the morphological alterations of neuronal cells that follow exposure to OT. OT-induced neurite retraction is not only observable in rat H32 or human SH-SY5Y cells but also in murine N2a cells. Using the protocol that was recently established in our laboratory (Meyer et al., 2018), I could show that N2a cells displayed similar OT-induced neurite retraction as H32 cells. OT treated cells had significantly shorter neurites compared to cells after VEH, TGOT or AVP treatment. The OTR-specific agonist TGOT as well as AVP were used to investigate receptor specificity of the observed phenotype. Neurite retraction in N2a cells appears to be not exclusively mediated by the OTR, as TGOT failed to induce neurite retraction. A combinatorial effect of OTR and the AVP receptor 1a is likely, also due to the missing impact of AVP alone. In H32 cells, not only OT but also TGOT and AVP impaired neurite outgrowth, indicating a strong involvement of the OTR and a slow onset of AVP-mediated morphological effects (Meyer et al., 2018).This supports a differential signaling pathway of neuronal morphology in N2a cells, however, an involvement of MEF2 is likely as previous studies confirmed MAPK-MEF2-mediated morphological

changes. In more detail, stimulation with β-hydroxy-β-methylbutyrate induces MAPK/ERK-dependent neurite outgrowth in N2a cells (Salto et al., 2015). Also, KD of the long non-coding RNA Malat1 promotes neurite outgrowth in N2a cells ERK/MAPK-dependently (Chen et al., 2016). However, more detailed analysis of OT-induced signaling in N2a cells is required.

With regard to the *in vivo* data presented in this thesis, the parallel activation of OTR and AVP receptors by chronic OT is very likely. As both receptors exert similar downstream effects (Jurek and Neumann, 2018) this is not an issue for the interpretation of the behavioral results.

4.2. CRISPR-Cas9-mediated gene knockout

Alongside with extensive knowledge *in vivo*, the intracellular effects of OTR activation are well studied in cell culture (Jurek and Neumann, 2018). The CRISPR-Cas9 system provides the perfect tool for the generation of specific KO cell lines. The human neuroblastoma cell line Be(2)-M17 which expresses the OTR was used to create a neuronal OTR KO cell line, named BeJ(1). In a second approach, the transcription factor MEF2A was knocked out in the rat hypothalamic cell line H32. Both cell lines can be employed in a variety of further studies, like signaling and morphological studies, as well as for the generation of spheroids to assess cellular interactions. During the creation of genetically modified cell lines with CRISPR-Cas9, several issues had to be addressed that I will discuss briefly in the following. First, the transfection protocol for either vector-based constructs or RNP complexes had to be optimized for the corresponding cell line. For Be(2)-M17 and H32 cells, cationic lipid-mediated delivery yielded the highest transfection rates with great cell survival. Cationic lipid delivery also displays a viable method for *in vivo* delivery of CRISPR-Cas components (Zuris et al., 2015) and is equally suitable for vector and RNP-based gene editing (Ewert et al., 2010). After the generation of monoclonal cell lines by single-cell isolation, the phenotype of the newly created BeJ(1) and H32 MEF2A KO cells was assessed by means of western blot. In both cases a clear reduction in antibody signal could be detected in the KO cells compared to WT cells. For MEF2A KO cells further analysis is missing and will be addressed in a separate project. Positive results for BeJ(1) cells had to be interpreted carefully due to the assumed lack of specificity of OTR antibodies (Yoshida et al., 2009). However, these results were confirmed with PCR and Sanger sequencing. As the gene fragment flanked by the CRISPR cutting sites could not be amplified *via* PCR for Sanger Sequencing, deletion of this part of the OTR gene is granted. The sequencing of the WT fragment revealed an intact *Otr* gene. The second band obtained by PCR was likely due to

unspecific primer annealing, as there was no corresponding sequence within the *Otr*. So far no off-target analysis was performed *via* whole-genome sequencing. Taken together, KO cell lines created by means of CRISPR-Cas9 are the perfect control for comparative signaling and morphological studies, and further analysis of OT-induced neuronal connectivity.

4.3. Oxytocin receptor-mediated signaling and neuronal morphology

Wildtype Be(2)-M17 cell and BeJ(1) KO cells were now used to investigate the link between OTR signaling cascades, alternative splicing, morphology and behavior.

First, loss of the OTR caused impaired MAPK signaling and subsequent MEF2A S408 phosphorylation. This defect could be restored with transient plasmid-mediated OTR expression in BeJ(1) cells, excluding an impact of potential off-target effects. Furthermore, BeJ(1) cells lacked the characteristic retraction of neurites upon long-term OT treatment, indicating a mainly OTR-mediated morphological effect. These data qualify the Be(2)-M17 cell line and the corresponding OTR KO line, BeJ(1), for further investigation of the link between alternative splicing and morphology. This approach is supported by the known importance of splicing factors for the regulation of neuronal morphology (Raj and Blencowe, 2015). Moreover, *in vitro* studies on the interaction of OT-induced MEF2 activity, splicing factors, alternative splicing, and potential morphological alterations could be improved by the use of fluorescently-tagged human induced pluripotent stem cells (hiPSCs), which simplify morphological analyses. These cell lines are available in the Allen Cell Catalogue (allencell.org) and contain the potential for various applications including CRISPR-Ca9-mediated genomic manipulations.

Additionally, BeJ(1) cells can be employed for advanced receptor studies by the introduction of modified receptors. The impact of single nucleotide polymorphisms, alternative internalization patterns, like β-arrestin independent internalization (Passoni et al., 2016) or constitutive receptor activity (Holliday et al., 2007) can be addressed. Especially the investigation of internalization could provide more detailed insights into receptor recycling dynamics upon chronic OTR stimulation.

In contrast to the KO of the *Otr* gene, receptor stability was increased using a model of manipulation of cholesterol content in the cell membrane. As already mentioned, cholesterol content and receptor location within the membrane play a crucial role in OTR-mediated signaling (Gimpl and Fahrenholz, 2000; Klein et al., 1995). Also, membrane cholesterol contents are involved in the functional activity of several other GPCRs as shown for the galanin receptor (Pang et al., 1999), the μ-opioid receptor (Lagane et al., 2000), and the

somatostatin receptor (Pucadyil and Chattopadhyay, 2004). Formation and stabilization of lipid rafts and caveolae in the membrane require high levels of cholesterol hence, around 80-90 % of total cellular cholesterol can be found in the plasma membrane (Prinz, 2002). Consequently, depletion of cholesterol destabilizes these structures and impairs receptor-mediated signal transduction (Simons and Toomre, 2000). The human Be(2)-M17 cell line expresses the OTR and MAPK signaling occurs upon OT stimulation (this thesis and Jurek et al., 2015). Here, cholesterol enrichment itself had no effect on MAPK signaling, excluding constitutive activity of the OTR (Reversi et al., 2006; Seifert and Wenzel-Seifert, 2002) in Be(2)-M17 cells and confirming an exclusive OT effect in the following experiments. However, to completely rule out overall cellular effects of cholesterol enrichment, cell viability should be addressed in further studies. Stimulations with 100 nM OT caused increasingly higher phosphorylation levels for both ERK1 and ERK2 in cholesterol-enriched cells. This effect failed to reach significance and requires potentially longer stimulation with OT, also at higher concentrations. Possibly, 30 min enrichment with 0.3 mM cholesterol-MßCD were not sufficient to force enough OTRs into lipid rafts and caveolae (Reversi et al., 2006) and extended enrichment is required. However, cholesterol was successfully introduced into membranes of Be(2)-M17 cells using the described protocol as Filipin III staining revealed increased fluorescence in cholesterol treated cells and a reduced signal due to cholesterol depletion (Beknke et al., 1984). Furthermore, manipulation of cholesterol in membranes with the MßCD method is very well established and has produced reliable results in several previous studies (Gimpl et al., 1997; Klein et al., 1995; Reversi et al., 2006). Due to the changes in membrane fluidity by cholesterol, higher cholesterol levels increase the stiffness of the membrane, extension of the enrichment has to be performed carefully, as cholesterol concentrations over a threshold value of 60 % has no beneficial effects on OTR binding anymore (Gimpl et al., 1997; Gimpl and Fahrenholz, 2000). As cholesterol extraction and analysis have been described previously (Bligh and Dyer, 1959; Borroni et al., 2007; Gimpl and Fahrenholz, 2000), more profound knowledge on the possible impact of cholesterol enrichment and depletion on OTR signaling Be(2)-M17 cells could be achieved by analysis of exact cholesterol contents in untreated cells.

In summary, cell culture systems like the ones presented here, are reliable tools for the investigation of OTR-mediated effects on signaling cascades, alternative splicing and neuronal morphology. I established an approach for the manipulation of OTR expression using CRISPR-Cas9, accompanied by increased receptor stability due to cholesterol enrichment. This is the basis for the investigation of the definite connection between chronic OT-induced changes in signaling, as well as morphological changes. Future steps might include the investigation of OT-induced changes in neuronal morphology *in vivo*.

7. Conclusion

The present study provides insight into the molecular mechanism that causes increased anxiety-like behavior following chronic OT treatment. I showed that chronic OT promoted alternative splicing of the CRFR2α *via* activated MAPK pathway and MEF2A signaling, which led to a proportional increase of the soluble splice variant sCRFR2α. This shift from membrane-associated CRFR2α towards cytoplasmic distribution and extracellular release of sCRFR2α underlies the anxiogenic effect of chronic OT, as activity of the regular mCRFR2α acted anxiolytic in the PVN. Elevation or reduction of sCRFR2α mRNA levels revealed a direct correlation between high sCRFR2α levels in the PVN and increased anxiety-like behavior. However, this mechanism seems to be sexually dimorphic as the anxiogenic effect of chronic OT in female rats was not mediated by MEF2A activity and the subsequent shift in mCRFR2α/sCRFR2α ratio. Unmasking the anxiogenic properties of chronic OT required an additional mild stressor that activated the *Crfr2* gene. This reflects the situation in real life with human patients where stressors are omnipresent, so adverse side effects of an otherwise helpful OT treatment have to be considered. However, any molecular and behavioral alterations seem to be reversible after termination of the treatment, and long-term consequences are not be expected in adult brains and periphery. The impact on developing brains in children and juveniles, however, is an important aspect requiring further investigation. Furthermore, mechanistic details could be reproduced in the hypothalamic rat cell line H32, proving cell culture as a suitable model to study the intracellular, molecular mechanism of chronic OTR activation.

In addition to detrimental behavioral effects and the activation of the alternative splicing machinery, chronic OT also induced changes in neuronal morphology. Neurite retraction was confirmed in the murine cell line N2a as well as in human Be(2)-M17 cells. The impact on the morphology of Be(2)-M17 cells was exclusively OTR-dependent as a CRISPR-mediated KO abolished neurite retraction. Also, OT-induced MAPK signaling in the OTR KO cells BeJ(1) was impaired, whereas enrichment with cholesterol in the membrane had beneficial effects on ERK1/2 phosphorylation. I was able to establish the *in vitro* use of the CRISPR-Cas9 system in our laboratory, paving the way for further extensive cellular studies including the use of hiPSCs and potentially the cultivation of 3D-organoids.

The presented results extend the understanding of OT's molecular downstream signaling (Fig. 39) and challenge its status as a treatment option for psychiatric disorders, potentially representing a prerequisite for a translation into clinical application. Treatment with chronic or repetitive OT requires careful consideration of dosage, treatment duration and sex of the

patients. Additionally, the discovery of the anxiogenic splice variant sCRFR2α in this context bears promising potential as an alternative marker that might serve as a viable target for the anamnesis and treatment of anxiety disorders.

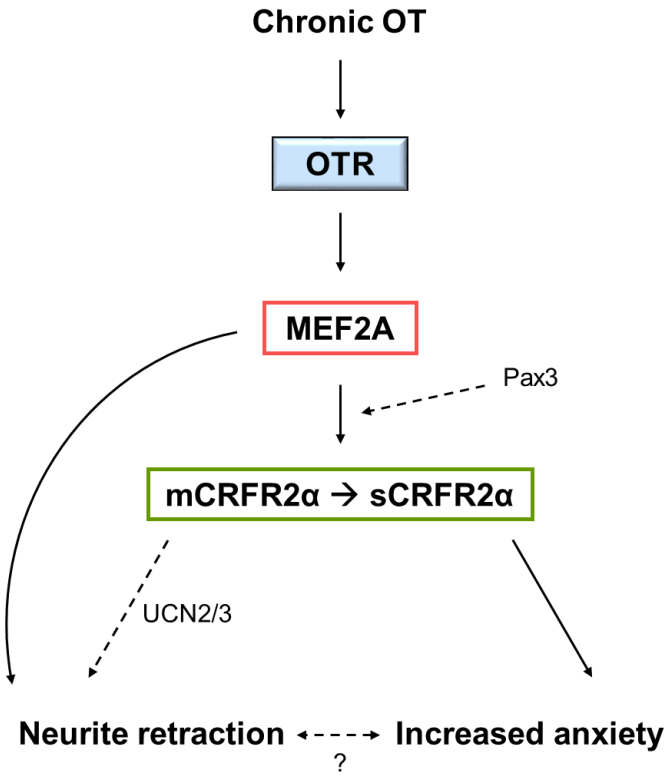

Figure 39. Signaling scheme of known (bold arrows) and hypothetical (dashed arrows) interactions of OTR signaling upon chronic stimulation.

Perspectives

The identification of sCRFR2α as a key player in anxiety and its detectability in CSF and serum provides a powerful new approach to the diagnosis of psychiatric disorders and could be combined with simple detection platforms like CRISPR-based diagnostic. This technique is based on the rapid detection of RNA and DNA with attomolar sensitivity and provides a portable detection platform (Gootenberg et al., 2017). In addition, to get a more translational insight into the brain mechanisms after chronic OT treatment, the use of programmable minipumps should be considered, as treatment in humans rather occurs in a repeated than a chronic fashion. These data can be compared to the extensive data I obtained with regard to the chronic administration of OT. For the medication of human patients suffering from anxiety disorders or ASD, knowledge on uncritical dosage and treatment duration is indispensable. This knowledge will also help to assess the underlying mechanism in animals that are unresponsive to OT, as treatment resilience complicates the successful medication of psychiatric disorders. Moreover, as a clear sexual dimorphic effect of prolonged OT application became apparent, extended studies on downstream signaling cascades in females are required. With regard to ASD, the inclusion of juveniles in the paradigm should be considered. Taken together, these approaches will contribute to provide more personalized and effective treatment options.

On a molecular level, the development of an additional CRISPR-based HiBiT system to directly detect and trace the splice variant will provide more detailed knowledge on the release and expression dynamics of the sCRFR2α. Manipulation of the splice variant within OTR Cre mice enables the assessment of further behavioral paradigms, including social fear conditioning, and allows the investigation of spatial interactions between the OTR and sCRFR2α-positive neurons or astrocytes.

To fully understand the effects of chronic OT it is crucial to further investigate the interplay of the PVN system described here, with other brain regions like the septum. Techniques including optogenetic stimulation and retrograde tracing could help to elucidate interactions of brain regions involved in the anxiogenic phenotype and determine ligand origin. Furthermore, with the great advances in the use of viral approaches *in vivo*, direct GapmeR-based manipulation of sCRFR2α expression could be achieved by OTR-cell specific, optogenetic activation of GapmeR expression.

The identification of several factors involved in the anxiogenic phenotype (MEF2A, CRFR2α) is the basis for the creation of new disease models, exploiting state-of-the-art techniques like CRISPR-Cas9. The establishment of the CRISPR-Cas9 system for the

manipulation of the OTR and MEF2A *in vitro* paved the way for the application *in vivo*, enabling targeted modification in one or more brain regions to finally answer the question of the interaction between morphological changes and anxiety-related behavior.

In summary, the data presented here provide an outline or tentative general strategy on how to address temporal and dosage-related issues when studying neuropeptides with regard to potential medical use. Addressing these open questions will broaden the understanding of how prolonged administration of high doses of OT and in more general neuropeptides take effects.

References

Aartsma-Rus, A., and van Ommen, G.J. (2007). Antisense-mediated exon skipping: a versatile tool with therapeutic and research applications. RNA *13*, 1609-1624.

Abudayyeh, O.O., Gootenberg, J.S., Konermann, S., Joung, J., Slaymaker, I.M., Cox, D.B., Shmakov, S., Makarova, K.S., Semenova, E., Minakhin, L.*, et al.* (2016). C2c2 is a single-component programmable RNA-guided RNA-targeting CRISPR effector. Science (New York, NY *353*, aaf5573.

Adachi, M., Lin, P.Y., Pranav, H., and Monteggia, L.M. (2016). Postnatal Loss of Mef2c Results in Dissociation of Effects on Synapse Number and Learning and Memory. Biological psychiatry *80*, 140-148.

Akerlund, M., Bossmar, T., Brouard, R., Kostrzewska, A., Laudanski, T., Lemancewicz, A., Serradeil-Le Gal, C., and Steinwall, M. (1999). Receptor binding of oxytocin and vasopressin antagonists and inhibitory effects on isolated myometrium from preterm and term pregnant women. Br J Obstet Gynaecol *106*, 1047-1053.

Akhtar, M.W., Kim, M.S., Adachi, M., Morris, M.J., Qi, X., Richardson, J.A., Bassel-Duby, R., Olson, E.N., Kavalali, E.T., and Monteggia, L.M. (2012). In vivo analysis of MEF2 transcription factors in synapse regulation and neuronal survival. PloS one *7*, e34863.

Akhtar, M.W., Raingo, J., Nelson, E.D., Montgomery, R.L., Olson, E.N., Kavalali, E.T., and Monteggia, L.M. (2009). Histone deacetylases 1 and 2 form a developmental switch that controls excitatory synapse maturation and function. J Neurosci *29*, 8288-8297.

Ambrogi Lorenzini, C., Bucherelli, C., and Giachetti, A. (1984). Passive and active avoidance behavior in the light-dark box test. Physiology & behavior *32*, 687-689.

Amico, J.A., Mantella, R.C., Vollmer, R.R., and Li, X. (2004). Anxiety and stress responses in female oxytocin deficient mice. Journal of neuroendocrinology *16*, 319-324.

Anders, C., Niewoehner, O., Duerst, A., and Jinek, M. (2014). Structural basis of PAM-dependent target DNA recognition by the Cas9 endonuclease. Nature *513*, 569-573.

Andres, V., Cervera, M., and Mahdavi, V. (1995). Determination of the consensus binding site for MEF2 expressed in muscle and brain reveals tissue-specific sequence constraints. The Journal of biological chemistry *270*, 23246-23249.

Anthony, T.E., Dee, N., Bernard, A., Lerchner, W., Heintz, N., and Anderson, D.J. (2014). Control of stress-induced persistent anxiety by an extra-amygdala septohypothalamic circuit. Cell *156*, 522-536.

Association, A.P. (2013). Diagnostic and Statistical Manual of Mental Disorders, 5 edn (Arlington, VA: American Psychiatric Publishing).

Baker, M. (2015). Reproducibility crisis: Blame it on the antibodies. Nature *521*, 274-276.

Bakos, J., Strbak, V., Paulikova, H., Krajnakova, L., Lestanova, Z., and Bacova, Z. (2013). Oxytocin receptor ligands induce changes in cytoskeleton in neuroblastoma cells. J Mol Neurosci *50*, 462-468.

Baldwin, H.A., Rassnick, S., Rivier, J., Koob, G.F., and Britton, K.T. (1991). CRF antagonist reverses the "anxiogenic" response to ethanol withdrawal in the rat. Psychopharmacology *103*, 227-232.

Bale, T.L., Contarino, A., Smith, G.W., Chan, R., Gold, L.H., Sawchenko, P.E., Koob, G.F., Vale, W.W., and Lee, K.F. (2000). Mice deficient for corticotropin-releasing hormone receptor-2 display anxiety-like behaviour and are hypersensitive to stress. Nature genetics *24*, 410-414.

Bale, T.L., Lee, K.F., and Vale, W.W. (2002a). The role of corticotropin-releasing factor receptors in stress and anxiety. Integr Comp Biol *42*, 552-555.

Bale, T.L., Picetti, R., Contarino, A., Koob, G.F., Vale, W.W., and Lee, K.F. (2002b). Mice deficient for both corticotropin-releasing factor receptor 1 (CRFR1) and CRFR2 have an impaired stress response and display sexually dichotomous anxiety-like behavior. The Journal of neuroscience : the official journal of the Society for Neuroscience *22*, 193-199.

Bamberger, C.M., Schulte, H.M., and Chrousos, G.P. (1996). Molecular determinants of glucocorticoid receptor function and tissue sensitivity to glucocorticoids. Endocr Rev *17*, 245-261.

Barbosa, A.C., Kim, M.S., Ertunc, M., Adachi, M., Nelson, E.D., McAnally, J., Richardson, J.A., Kavalali, E.T., Monteggia, L.M., Bassel-Duby, R.*, et al.* (2008). MEF2C, a transcription factor that facilitates learning and memory by negative regulation of synapse numbers and function. Proceedings of the National Academy of Sciences of the United States of America *105*, 9391-9396.

Beknke, O., Tranum-Jensen, J., and van Deurs, B. (1984). Filipin as a cholesterol probe. I. Morphology of filipin-cholesterol interaction in lipid model systems. Eur J Cell Biol *35*, 189-199.

Berget, S.M., Moore, C., and Sharp, P.A. (1977). Spliced segments at the 5' terminus of adenovirus 2 late mRNA. Proceedings of the National Academy of Sciences of the United States of America *74*, 3171-3175.

Black, B.L., and Olson, E.N. (1998). Transcriptional control of muscle development by myocyte enhancer factor-2 (MEF2) proteins. Annual review of cell and developmental biology *14*, 167-196.

Blaeser, F., Ho, N., Prywes, R., and Chatila, T.A. (2000). Ca(2+)-dependent gene expression mediated by MEF2 transcription factors. The Journal of biological chemistry *275*, 197-209.

Blake, J.A., and Ziman, M.R. (2014). Pax genes: regulators of lineage specification and progenitor cell maintenance. Development (Cambridge, England) *141*, 737-751.

Blanchard, R.J., Blanchard, D.C., Griebel, G., and Nutt, D.J. (2008). Handbook of Anxiety and Fear, Vol 17, First edition edn (Elsevier).

Bligh, E.G., and Dyer, W.J. (1959). A rapid method of total lipid extraction and purification. Can J Biochem Physiol *37*, 911-917.

Blume, A., Bosch, O.J., Miklos, S., Torner, L., Wales, L., Waldherr, M., and Neumann, I.D. (2008). Oxytocin reduces anxiety via ERK1/2 activation: local effect within the rat hypothalamic paraventricular nucleus. The European journal of neuroscience *27*, 1947-1956.

Blume, A., Torner, L., Liu, Y., Subburaju, S., Aguilera, G., and Neumann, I.D. (2009). Prolactin induces Egr-1 gene expression in cultured hypothalamic cells and in the rat hypothalamus. Brain research *1302*, 34-41.

Bolotin, A., Quinquis, B., Sorokin, A., and Ehrlich, S.D. (2005). Clustered regularly interspaced short palindrome repeats (CRISPRs) have spacers of extrachromosomal origin. Microbiology *151*, 2551-2561.

Borroni, V., Baier, C.J., Lang, T., Bonini, I., White, M.M., Garbus, I., and Barrantes, F.J. (2007). Cholesterol depletion activates rapid internalization of submicron-sized acetylcholine receptor domains at the cell membrane. Mol Membr Biol *24*, 1-15.

Bosch, O.J., Meddle, S.L., Beiderbeck, D.I., Douglas, A.J., and Neumann, I.D. (2005). Brain oxytocin correlates with maternal aggression: link to anxiety. The Journal of neuroscience : the official journal of the Society for Neuroscience *25*, 6807-6815.

Bradbury, A., and Pluckthun, A. (2015). Reproducibility: Standardize antibodies used in research. Nature *518*, 27-29.

Brand, N.J. (1997). Myocyte enhancer factor 2 (MEF2). The international journal of biochemistry & cell biology *29*, 1467-1470.

Brandt, K.J., Carpintero, R., Gruaz, L., Molnarfi, N., and Burger, D. (2010). A novel MEK2/PI3Kdelta pathway controls the expression of IL-1 receptor antagonist in IFN-beta-activated human monocytes. Journal of leukocyte biology *88*, 1191-1200.

Burgermeister, E., Chuderland, D., Hanoch, T., Meyer, M., Liscovitch, M., and Seger, R. (2007). Interaction with MEK causes nuclear export and downregulation of peroxisome proliferator-activated receptor gamma. Molecular and cellular biology *27*, 803-817.

Busnelli, M., and Chini, B. (2018). Molecular Basis of Oxytocin Receptor Signalling in the Brain: What We Know and What We Need to Know. Curr Top Behav Neurosci *35*, 3-29.

Busnelli, M., Kleinau, G., Muttenthaler, M., Stoev, S., Manning, M., Bibic, L., Howell, L.A., McCormick, P.J., Di Lascio, S., Braida, D.*, et al.* (2016). Design and Characterization of Superpotent Bivalent Ligands Targeting Oxytocin Receptor Dimers via a Channel-Like Structure. Journal of medicinal chemistry *59*, 7152-7166.

Busnelli, M., Sauliere, A., Manning, M., Bouvier, M., Gales, C., and Chini, B. (2012). Functional selective oxytocin-derived agonists discriminate between individual G protein family subtypes. The Journal of biological chemistry *287*, 3617-3629.

Calcagnoli, F., Meyer, N., de Boer, S.F., Althaus, M., and Koolhaas, J.M. (2014). Chronic enhancement of brain oxytocin levels causes enduring anti-aggressive and pro-social explorative behavioral effects in male rats. Hormones and behavior *65*, 427-433.

Calhoon, G.G., and Tye, K.M. (2015). Resolving the neural circuits of anxiety. Nat Neurosci *18*, 1394-1404.

Carter, C.S., Williams, J.R., Witt, D.M., and Insel, T.R. (1992). Oxytocin and social bonding. Annals of the New York Academy of Sciences *652*, 204-211.

Chalmers, D.T., Lovenberg, T.W., and De Souza, E.B. (1995). Localization of novel corticotropin-releasing factor receptor (CRF2) mRNA expression to specific subcortical nuclei in rat brain: comparison with CRF1 receptor mRNA expression. The Journal of neuroscience : the official journal of the Society for Neuroscience *15*, 6340-6350.

Chen, A.M., Perrin, M.H., Digruccio, M.R., Vaughan, J.M., Brar, B.K., Arias, C.M., Lewis, K.A., Rivier, J.E., Sawchenko, P.E., and Vale, W.W. (2005). A soluble mouse brain splice variant of type 2alpha corticotropin-releasing factor (CRF) receptor binds ligands and modulates their activity. Proceedings of the National Academy of Sciences of the United States of America *102*, 2620-2625.

Chen, J.S., Ma, E., Harrington, L.B., Da Costa, M., Tian, X., Palefsky, J.M., and Doudna, J.A. (2018). CRISPR-Cas12a target binding unleashes indiscriminate single-stranded DNase activity. Science (New York, NY *360*, 436-439.

Chen, L., Feng, P., Zhu, X., He, S., Duan, J., and Zhou, D. (2016). Long non-coding RNA Malat1 promotes neurite outgrowth through activation of ERK/MAPK signalling pathway in N2a cells. Journal of cellular and molecular medicine *20*, 2102-2110.

Chini, B., Verhage, M., and Grinevich, V. (2017). The Action Radius of Oxytocin Release in the Mammalian CNS: From Single Vesicles to Behavior. Trends in pharmacological sciences *1463*, 10.

Chow, L.T., Gelinas, R.E., Broker, T.R., and Roberts, R.J. (1977). An amazing sequence arrangement at the 5' ends of adenovirus 2 messenger RNA. Cell *12*, 1-8.

Cibelli, G., Corsi, P., Diana, G., Vitiello, F., and Thiel, G. (2001). Corticotropin-releasing factor triggers neurite outgrowth of a catecholaminergic immortalized neuron via cAMP and MAP kinase signalling pathways. The European journal of neuroscience *13*, 1339-1348.

Cole, C.J., Mercaldo, V., Restivo, L., Yiu, A.P., Sekeres, M.J., Han, J.H., Vetere, G., Pekar, T., Ross, P.J., Neve, R.L.*, et al.* (2012). MEF2 negatively regulates learning-induced structural plasticity and memory formation. Nat Neurosci *15*, 1255-1264.

Conti, F., Sertic, S., Reversi, A., and Chini, B. (2009). Intracellular trafficking of the human oxytocin receptor: evidence of receptor recycling via a Rab4/Rab5 "short cycle". American journal of physiology *296*, E532-542.

Coste, S.C., Kesterson, R.A., Heldwein, K.A., Stevens, S.L., Heard, A.D., Hollis, J.H., Murray, S.E., Hill, J.K., Pantely, G.A., Hohimer, A.R.*, et al.* (2000). Abnormal adaptations to stress and impaired cardiovascular function in mice lacking corticotropin-releasing hormone receptor-2. Nature genetics *24*, 403-409.

Cubbon, A., Ivancic-Bace, I., and Bolt, E.L. (2018). CRISPR-Cas immunity, DNA repair and genome stability. Biosci Rep *38*.

da Costa, P.J., Menezes, J., and Romao, L. (2017). The role of alternative splicing coupled to nonsense-mediated mRNA decay in human disease. The international journal of biochemistry & cell biology *91*, 168-175.

Dabrowska, J., Hazra, R., Ahern, T.H., Guo, J.D., McDonald, A.J., Mascagni, F., Muller, J.F., Young, L.J., and Rainnie, D.G. (2011). Neuroanatomical evidence for reciprocal regulation of the corticotrophin-releasing factor and oxytocin systems in the hypothalamus and the bed nucleus of the stria terminalis of the rat: Implications for balancing stress and affect. Psychoneuroendocrinology *36*, 1312-1326.

Dabrowska, J., Hazra, R., Guo, J.D., Dewitt, S., and Rainnie, D.G. (2013). Central CRF neurons are not created equal: phenotypic differences in CRF-containing neurons of the rat paraventricular hypothalamus and the bed nucleus of the stria terminalis. Frontiers in neuroscience *7*, 156.

Deacon, R.M. (2011). Hyponeophagia: a measure of anxiety in the mouse. Journal of visualized experiments : JoVE.

Dedic, N., Chen, A., and Deussing, J.M. (2018). The CRF Family of Neuropeptides and their Receptors - Mediators of the Central Stress Response. Curr Mol Pharmacol *11*, 4-31.

Delarue, M., Weissman, D., and Hallatschek, O. (2017). A simple molecular mechanism explains multiple patterns of cell-size regulation. PloS one *12*, e0182633.

Deltcheva, E., Chylinski, K., Sharma, C.M., Gonzales, K., Chao, Y., Pirzada, Z.A., Eckert, M.R., Vogel, J., and Charpentier, E. (2011). CRISPR RNA maturation by trans-encoded small RNA and host factor RNase III. Nature *471*, 602-607.

Denecke, J., Kranz, C., Kemming, D., Koch, H.G., and Marquardt, T. (2004). An activated 5' cryptic splice site in the human ALG3 gene generates a premature termination codon insensitive to nonsense-mediated mRNA decay in a new case of congenital disorder of glycosylation type Id (CDG-Id). Hum Mutat *23*, 477-486.

Deussing, J.M., and Chen, A. (2018). The Corticotropin-Releasing Factor Family: Physiology of the Stress Response. Physiological reviews *98*, 2225-2286.

Devost, D., Wrzal, P., and Zingg, H.H. (2008). Oxytocin receptor signalling. Progress in brain research *170*, 167-176.

Dodou, E., and Treisman, R. (1997). The Saccharomyces cerevisiae MADS-box transcription factor Rlm1 is a target for the Mpk1 mitogen-activated protein kinase pathway. Molecular and cellular biology *17*, 1848-1859.

Domes, G., Normann, C., and Heinrichs, M. (2016). The effect of oxytocin on attention to angry and happy faces in chronic depression. BMC psychiatry *16*, 92.

Doudna, J.A., and Charpentier, E. (2014). Genome editing. The new frontier of genome engineering with CRISPR-Cas9. Science (New York, NY *346*, 1258096.

Dreumont, N., Maresca, A., Boisclair-Lachance, J.F., Bergeron, A., and Tanguay, R.M. (2005). A minor alternative transcript of the fumarylacetoacetate hydrolase gene produces a protein despite being likely subjected to nonsense-mediated mRNA decay. BMC Mol Biol *6*, 1.

Du, P., He, Z., Cai, Z., Hao, X., Dong, N., Yuan, W., Hou, W., Yang, J., Jia, R., and Tai, F. (2017). Chronic central oxytocin infusion impairs sociability in mandarin voles. Pharmacology, biochemistry, and behavior *161*, 38-46.

Dunn, A.J., and File, S.E. (1987). Corticotropin-releasing factor has an anxiogenic action in the social interaction test. Hormones and behavior *21*, 193-202.

Ebner, K., Bosch, O.J., Kromer, S.A., Singewald, N., and Neumann, I.D. (2005). Release of oxytocin in the rat central amygdala modulates stress-coping behavior and the release of excitatory amino acids. Neuropsychopharmacology : official publication of the American College of Neuropsychopharmacology *30*, 223-230.

Eckart, K., Jahn, O., Radulovic, J., Tezval, H., van Werven, L., and Spiess, J. (2001). A single amino acid serves as an affinity switch between the receptor and the binding

protein of corticotropin-releasing factor: Implications for the design of agonists and antagonists. Proceedings of the National Academy of Sciences of the United States of America *98*, 11142-11147.

Edmondson, D.G., Lyons, G.E., Martin, J.F., and Olson, E.N. (1994). Mef2 gene expression marks the cardiac and skeletal muscle lineages during mouse embryogenesis. Development (Cambridge, England) *120*, 1251-1263.

Edmondson, D.G., and Olson, E.N. (1989). A gene with homology to the myc similarity region of MyoD1 is expressed during myogenesis and is sufficient to activate the muscle differentiation program. Genes & development *3*, 628-640.

Engelmann, M., Landgraf, R., and Wotjak, C.T. (2004). The hypothalamic-neurohypophysial system regulates the hypothalamic-pituitary-adrenal axis under stress: an old concept revisited. Frontiers in neuroendocrinology *25*, 132-149.

Evans, R.T., and Seasholtz, A.F. (2009). Soluble Corticotropin-Releasing Hormone Receptor 2α Splice Variant Is Efficiently Translated But Not Trafficked for Secretion. Endocrinology *150*, 4191-4202.

Ewert, K.K., Zidovska, A., Ahmad, A., Bouxsein, N.F., Evans, H.M., McAllister, C.S., Samuel, C.E., and Safinya, C.R. (2010). Cationic liposome-nucleic acid complexes for gene delivery and silencing: pathways and mechanisms for plasmid DNA and siRNA. Top Curr Chem *296*, 191-226.

Feifel, D., Macdonald, K., Nguyen, A., Cobb, P., Warlan, H., Galangue, B., Minassian, A., Becker, O., Cooper, J., Perry, W*., et al.* (2010). Adjunctive intranasal oxytocin reduces symptoms in schizophrenia patients. Biological psychiatry *68*, 678-680.

Feng, H.C., Bhave, M., and Fairclough, R.J. (2000). Regulation of oxytocin receptor gene expression in sheep: tissue specificity, multiple transcripts and mRNA editing. Journal of reproduction and fertility *120*, 187-200.

Fiore, R., Khudayberdiev, S., Christensen, M., Siegel, G., Flavell, S.W., Kim, T.K., Greenberg, M.E., and Schratt, G. (2009). Mef2-mediated transcription of the miR379-410 cluster regulates activity-dependent dendritogenesis by fine-tuning Pumilio2 protein levels. The EMBO journal *28*, 697-710.

Flavell, S.W., Cowan, C.W., Kim, T.K., Greer, P.L., Lin, Y., Paradis, S., Griffith, E.C., Hu, L.S., Chen, C., and Greenberg, M.E. (2006). Activity-dependent regulation of MEF2 transcription factors suppresses excitatory synapse number. Science *311*, 1008-1012.

Flavell, S.W., and Greenberg, M.E. (2008). Signaling mechanisms linking neuronal activity to gene expression and plasticity of the nervous system. Annual review of neuroscience *31*, 563-590.

Flavell, S.W., Kim, T.K., Gray, J.M., Harmin, D.A., Hemberg, M., Hong, E.J., Markenscoff-Papadimitriou, E., Bear, D.M., and Greenberg, M.E. (2008). Genome-wide analysis of MEF2 transcriptional program reveals synaptic target genes and neuronal activity-dependent polyadenylation site selection. Neuron *60*, 1022-1038.

Frankiensztajn, L.M., Gur-Pollack, R., and Wagner, S. (2018). A combinatorial modulation of synaptic plasticity in the rat medial amygdala by oxytocin, urocortin3 and estrogen. Psychoneuroendocrinology *92*, 95-102.

Furness, S.G., Wootten, D., Christopoulos, A., and Sexton, P.M. (2012). Consequences of splice variation on Secretin family G protein-coupled receptor function. British journal of pharmacology *166*, 98-109.

Ge, Z., Quek, B.L., Beemon, K.L., and Hogg, J.R. (2016). Polypyrimidine tract binding protein 1 protects mRNAs from recognition by the nonsense-mediated mRNA decay pathway. eLife *5*.

Gibbs, D.M. (1986). Stress-specific modulation of ACTH secretion by oxytocin. Neuroendocrinology *42*, 456-458.

Gibbs, D.M., Vale, W., Rivier, J., and Yen, S.S. (1984). Oxytocin potentiates the ACTH-releasing activity of CRF(41) but not vasopressin. Life sciences *34*, 2245-2249.

Giesbrecht, C.J., Mackay, J.P., Silveira, H.B., Urban, J.H., and Colmers, W.F. (2010). Countervailing modulation of Ih by neuropeptide Y and corticotrophin-releasing factor in basolateral amygdala as a possible mechanism for their effects on stress-related behaviors. J Neurosci *30*, 16970-16982.

Gilbert, W. (1978). Why genes in pieces? Nature *271*, 501.

Gimpl, G., Burger, K., and Fahrenholz, F. (1997). Cholesterol as modulator of receptor function. Biochemistry *36*, 10959-10974.

Gimpl, G., and Fahrenholz, F. (2000). Human oxytocin receptors in cholesterol-rich vs. cholesterol-poor microdomains of the plasma membrane. Eur J Biochem *267*, 2483-2497.

Gimpl, G., and Fahrenholz, F. (2001). The oxytocin receptor system: structure, function, and regulation. Physiological reviews *81*, 629-683.

Gimpl, G., and Fahrenholz, F. (2002). Cholesterol as stabilizer of the oxytocin receptor. Biochimica et biophysica acta *1564*, 384-392.

Gimpl, G., Klein, U., Reilander, H., and Fahrenholz, F. (1995). Expression of the human oxytocin receptor in baculovirus-infected insect cells: high-affinity binding is induced by a cholesterol-cyclodextrin complex. Biochemistry *34*, 13794-13801.

Goldberg, J.L. (2003). How does an axon grow? Genes & development *17*, 941-958.

Gong, X., Tang, X., Wiedmann, M., Wang, X., Peng, J., Zheng, D., Blair, L.A., Marshall, J., and Mao, Z. (2003). Cdk5-mediated inhibition of the protective effects of transcription factor MEF2 in neurotoxicity-induced apoptosis. Neuron *38*, 33-46.

Gootenberg, J.S., Abudayyeh, O.O., Lee, J.W., Essletzbichler, P., Dy, A.J., Joung, J., Verdine, V., Donghia, N., Daringer, N.M., Freije, C.A.*, et al.* (2017). Nucleic acid detection with CRISPR-Cas13a/C2c2. Science (New York, NY *356*, 438-442.

Grinevich, V., Desarmenien, M.G., Chini, B., Tauber, M., and Muscatelli, F. (2014). Ontogenesis of oxytocin pathways in the mammalian brain: late maturation and psychosocial disorders. Frontiers in neuroanatomy *8*, 164.

Grotegut, C.A., Feng, L., Mao, L., Heine, R.P., Murtha, A.P., and Rockman, H.A. (2011). beta-Arrestin mediates oxytocin receptor signaling, which regulates uterine contractility and cellular migration. American journal of physiology *300*, E468-477.

Guastella, A.J., and Hickie, I.B. (2016). Oxytocin Treatment, Circuitry, and Autism: A Critical Review of the Literature Placing Oxytocin Into the Autism Context. Biological psychiatry *79*, 234-242.

Guzman, Y.F., Tronson, N.C., Jovasevic, V., Sato, K., Guedea, A.L., Mizukami, H., Nishimori, K., and Radulovic, J. (2013). Fear-enhancing effects of septal oxytocin receptors. Nat Neurosci *16*, 1185-1187.

Haft, D.H., Selengut, J., Mongodin, E.F., and Nelson, K.E. (2005). A guild of 45 CRISPR-associated (Cas) protein families and multiple CRISPR/Cas subtypes exist in prokaryotic genomes. PLoS Comput Biol *1*, e60.

Hall, C.S., and Ballachey, E.L. (1932). A Study of the Rat's Behavior in a Field: A Contribution to Method in Comparative Psychology, Vol 6 (University of California Publications in Psychology: University of California Press).

Hammack, S.E., Schmid, M.J., LoPresti, M.L., Der-Avakian, A., Pellymounter, M.A., Foster, A.C., Watkins, L.R., and Maier, S.F. (2003). Corticotropin releasing hormone type 2 receptors in the dorsal raphe nucleus mediate the behavioral consequences of uncontrollable stress. J Neurosci *23*, 1019-1025.

Han, J., Jiang, Y., Li, Z., Kravchenko, V.V., and Ulevitch, R.J. (1997). Activation of the transcription factor MEF2C by the MAP kinase p38 in inflammation. Nature *386*, 296-299.

Hara, Y., and Merten, C.A. (2015). Dynein-Based Accumulation of Membranes Regulates Nuclear Expansion in Xenopus laevis Egg Extracts. Developmental cell *33*, 562-575.

Harrington, A.J., Raissi, A., Rajkovich, K., Berto, S., Kumar, J., Molinaro, G., Raduazzo, J., Guo, Y., Loerwald, K., Konopka, G.*, et al.* (2016). MEF2C regulates cortical inhibitory and excitatory synapses and behaviors relevant to neurodevelopmental disorders. Elife *5*.

Havranek, T., Zatkova, M., Lestanova, Z., Bacova, Z., Mravec, B., Hodosy, J., Strbak, V., and Bakos, J. (2015). Intracerebroventricular oxytocin administration in rats enhances object recognition and increases expression of neurotrophins, microtubule-associated protein 2, and synapsin I. Journal of neuroscience research *93*, 893-901.

Heidenreich, E., Novotny, R., Kneidinger, B., Holzmann, V., and Wintersberger, U. (2003). Non-homologous end joining as an important mutagenic process in cell cycle-arrested cells. The EMBO journal *22*, 2274-2283.

Heidenreich, M., and Zhang, F. (2016). Applications of CRISPR-Cas systems in neuroscience. Nature reviews Neuroscience *17*, 36-44.

Heilig, M. (2004). The NPY system in stress, anxiety and depression. Neuropeptides *38*, 213-224.

Henckens, M.J., Deussing, J.M., and Chen, A. (2016). Region-specific roles of the corticotropin-releasing factor-urocortin system in stress. Nature reviews Neuroscience *17*, 636-651.

Hendrickson, M.L., Rao, A.J., Demerdash, O.N., and Kalil, R.E. (2011). Expression of nestin by neural cells in the adult rat and human brain. PloS one *6*, e18535.

Henry, B., Vale, W., and Markou, A. (2006). The effect of lateral septum corticotropin-releasing factor receptor 2 activation on anxiety is modulated by stress. J Neurosci *26*, 9142-9152.

Hettema, J.M., Webb, B.T., Guo, A.Y., Zhao, Z., Maher, B.S., Chen, X., An, S.S., Sun, C., Aggen, S.H., Kendler, K.S.*, et al.* (2011). Prioritization and association analysis of murine-derived candidate genes in anxiety-spectrum disorders. Biological psychiatry *70*, 888-896.

Hillhouse, E.W., and Grammatopoulos, D.K. (2006). The molecular mechanisms underlying the regulation of the biological activity of corticotropin-releasing hormone receptors: implications for physiology and pathophysiology. Endocr Rev *27*, 260-286.

Hoffman, E.J., and Mathew, S.J. (2008). Anxiety disorders: a comprehensive review of pharmacotherapies. Mt Sinai J Med *75*, 248-262.

Holliday, N.D., Holst, B., Rodionova, E.A., Schwartz, T.W., and Cox, H.M. (2007). Importance of constitutive activity and arrestin-independent mechanisms for intracellular trafficking of the ghrelin receptor. Molecular endocrinology (Baltimore, Md *21*, 3100-3112.

Holsboer, F. (1999). The rationale for corticotropin-releasing hormone receptor (CRH-R) antagonists to treat depression and anxiety. Journal of psychiatric research *33*, 181-214.

Holsboer, F., and Ising, M. (2008). Central CRH system in depression and anxiety--evidence from clinical studies with CRH1 receptor antagonists. European journal of pharmacology *583*, 350-357.

Hovatta, I., and Barlow, C. (2008). Molecular genetics of anxiety in mice and men. Annals of medicine *40*, 92-109.

Hovatta, I., Tennant, R.S., Helton, R., Marr, R.A., Singer, O., Redwine, J.M., Ellison, J.A., Schadt, E.E., Verma, I.M., Lockhart, D.J.*, et al.* (2005). Glyoxalase 1 and glutathione reductase 1 regulate anxiety in mice. Nature *438*, 662-666.

Huising, M.O., Vaughan, J.M., Shah, S.H., Grillot, K.L., Donaldson, C.J., Rivier, J., Flik, G., and Vale, W.W. (2008). Residues of Corticotropin Releasing Factor-binding Protein (CRF-BP) That Selectively Abrogate Binding to CRF but Not to Urocortin 1. The Journal of biological chemistry *283*, 8902-8912.

Incardona, J.P., and Eaton, S. (2000). Cholesterol in signal transduction. Curr Opin Cell Biol *12*, 193-203.

Inoue, T., Kimura, T., Azuma, C., Inazawa, J., Takemura, M., Kikuchi, T., Kubota, Y., Ogita, K., and Saji, F. (1994). Structural organization of the human oxytocin receptor gene. The Journal of biological chemistry *269*, 32451-32456.

Insel, T.R., Winslow, J.T., and Witt, D.M. (1992). Homologous regulation of brain oxytocin receptors. Endocrinology *130*, 2602-2608.

International Human Genome Sequencing, C. (2004). Finishing the euchromatic sequence of the human genome. Nature *431*, 931-945.

Ionescu, I.A., Dine, J., Yen, Y.C., Buell, D.R., Herrmann, L., Holsboer, F., Eder, M., Landgraf, R., and Schmidt, U. (2012). Intranasally administered neuropeptide S (NPS) exerts anxiolytic effects following internalization into NPS receptor-expressing neurons. Neuropsychopharmacology *37*, 1323-1337.

Ishino, Y., Krupovic, M., and Forterre, P. (2018). History of CRISPR-Cas from Encounter with a Mysterious Repeated Sequence to Genome Editing Technology. J Bacteriol *200*.

Ishino, Y., Shinagawa, H., Makino, K., Amemura, M., and Nakata, A. (1987). Nucleotide sequence of the iap gene, responsible for alkaline phosphatase isozyme conversion in Escherichia coli, and identification of the gene product. J Bacteriol *169*, 5429-5433.

Issler, O., Carter, R.N., Paul, E.D., Kelly, P.A.T., Olverman, H.J., Neufeld-Cohen, A., Kuperman, Y., Lowry, C.A., Seckl, J.R., Chen, A.*, et al.* (2014). Increased anxiety in corticotropin-releasing factor type 2 receptor-null mice requires recent acute stress exposure and is associated with dysregulated serotonergic activity in limbic brain areas. Biology of mood & anxiety disorders *4*, 1-1.

Jafarzadeh, N., Javeri, A., Khaleghi, M., and Taha, M.F. (2014). Oxytocin improves proliferation and neural differentiation of adipose tissue-derived stem cells. Neuroscience letters *564*, 105-110.

Jansen, R., Embden, J.D., Gaastra, W., and Schouls, L.M. (2002). Identification of genes that are associated with DNA repeats in prokaryotes. Mol Microbiol *43*, 1565-1575.

Jeanneteau, F.D., Lambert, W.M., Ismaili, N., Bath, K.G., Lee, F.S., Garabedian, M.J., and Chao, M.V. (2012). BDNF and glucocorticoids regulate corticotrophin-releasing hormone (CRH) homeostasis in the hypothalamus. Proceedings of the National Academy of Sciences of the United States of America *109*, 1305-1310.

Jimenez, J.C., Su, K., Goldberg, A.R., Luna, V.M., Biane, J.S., Ordek, G., Zhou, P., Ong, S.K., Wright, M.A., Zweifel, L.*, et al.* (2018). Anxiety Cells in a Hippocampal-Hypothalamic Circuit. Neuron *97*, 670-683 e676.

Jinek, M., Chylinski, K., Fonfara, I., Hauer, M., Doudna, J.A., and Charpentier, E. (2012). A programmable dual-RNA-guided DNA endonuclease in adaptive bacterial immunity. Science (New York, NY *337*, 816-821.

Jo, C., Cho, S.J., and Jo, S.A. (2011). Mitogen-activated protein kinase kinase 1 (MEK1) stabilizes MyoD through direct phosphorylation at tyrosine 156 during myogenic differentiation. The Journal of biological chemistry *286*, 18903-18913.

Jurek, B., and Neumann, I.D. (2018). The Oxytocin Receptor: From Intracellular Signaling to Behavior. Physiological reviews *98*, 1805-1908.

Jurek, B., Slattery, D.A., Hiraoka, Y., Liu, Y., Nishimori, K., Aguilera, G., Neumann, I.D., and van den Burg, E.H. (2015). Oxytocin Regulates Stress-Induced Crf Gene Transcription through CREB-Regulated Transcription Coactivator 3. The Journal of neuroscience : the official journal of the Society for Neuroscience *35*, 12248-12260.

Jurek, B., Slattery, D.A., Maloumby, R., Hillerer, K., Koszinowski, S., Neumann, I.D., and van den Burg, E.H. (2012). Differential contribution of hypothalamic MAPK activity to anxiety-like behaviour in virgin and lactating rats. PloS one *7*, e37060.

Karolyi, I.J., Burrows, H.L., Ramesh, T.M., Nakajima, M., Lesh, J.S., Seong, E., Camper, S.A., and Seasholtz, A.F. (1999). Altered anxiety and weight gain in corticotropin-releasing hormone-binding protein-deficient mice. Proceedings of the National Academy of Sciences of the United States of America *96*, 11595-11600.

Karunarathne, W.K., Giri, L., Kalyanaraman, V., and Gautam, N. (2013). Optically triggering spatiotemporally confined GPCR activity in a cell and programming neurite

initiation and extension. Proceedings of the National Academy of Sciences of the United States of America *110*, E1565-1574.

Kato, Y., Kravchenko, V.V., Tapping, R.I., Han, J., Ulevitch, R.J., and Lee, J.D. (1997). BMK1/ERK5 regulates serum-induced early gene expression through transcription factor MEF2C. The EMBO journal *16*, 7054-7066.

Kato, Y., Zhao, M., Morikawa, A., Sugiyama, T., Chakravortty, D., Koide, N., Yoshida, T., Tapping, R.I., Yang, Y., Yokochi, T.*, et al.* (2000). Big mitogen-activated kinase regulates multiple members of the MEF2 protein family. The Journal of biological chemistry *275*, 18534-18540.

Kilkenny, C., Browne, W.J., Cuthill, I.C., Emerson, M., and Altman, D.G. (2010). Improving bioscience research reporting: The ARRIVE guidelines for reporting animal research. J Pharmacol Pharmacother *1*, 94-99.

Kim, D.H., Li, B., Si, F., Phillip, J.M., Wirtz, D., and Sun, S.X. (2015). Volume regulation and shape bifurcation in the cell nucleus. Journal of cell science *128*, 3375-3385.

Kim, Y.G., Cha, J., and Chandrasegaran, S. (1996). Hybrid restriction enzymes: zinc finger fusions to Fok I cleavage domain. Proceedings of the National Academy of Sciences of the United States of America *93*, 1156-1160.

Kimura, T., Tanizawa, O., Mori, K., Brownstein, M.J., and Okayama, H. (1992). Structure and expression of a human oxytocin receptor. Nature *356*, 526-529.

Kishimoto, T., Radulovic, J., Radulovic, M., Lin, C.R., Schrick, C., Hooshmand, F., Hermanson, O., Rosenfeld, M.G., and Spiess, J. (2000). Deletion of crhr2 reveals an anxiolytic role for corticotropin-releasing hormone receptor-2. Nature genetics *24*, 415-419.

Klampfl, S.M., Brunton, P.J., Bayerl, D.S., and Bosch, O.J. (2014). Hypoactivation of CRF receptors, predominantly type 2, in the medial-posterior BNST is vital for adequate maternal behavior in lactating rats. J Neurosci *34*, 9665-9676.

Klampfl, S.M., Schramm, M.M., Gassner, B.M., Hubner, K., Seasholtz, A.F., Brunton, P.J., Bayerl, D.S., and Bosch, O.J. (2018). Maternal stress and the MPOA: Activation of CRF receptor 1 impairs maternal behavior and triggers local oxytocin release in lactating rats. Neuropharmacology *133*, 440-450.

Klein, U., Gimpl, G., and Fahrenholz, F. (1995). Alteration of the myometrial plasma membrane cholesterol content with beta-cyclodextrin modulates the binding affinity of the oxytocin receptor. Biochemistry *34*, 13784-13793.

Knobloch, H.S., Charlet, A., Hoffmann, L.C., Eliava, M., Khrulev, S., Cetin, A.H., Osten, P., Schwarz, M.K., Seeburg, P.H., Stoop, R.*, et al.* (2012). Evoked axonal oxytocin release in the central amygdala attenuates fear response. Neuron *73*, 553-566.

Komor, A.C., Kim, Y.B., Packer, M.S., Zuris, J.A., and Liu, D.R. (2016). Programmable editing of a target base in genomic DNA without double-stranded DNA cleavage. Nature *533*, 420-424.

Komor, A.C., Zhao, K.T., Packer, M.S., Gaudelli, N.M., Waterbury, A.L., Koblan, L.W., Kim, Y.B., Badran, A.H., and Liu, D.R. (2017). Improved base excision repair inhibition and bacteriophage Mu Gam protein yields C:G-to-T:A base editors with higher efficiency and product purity. Sci Adv *3*, eaao4774.

Kornblihtt, A.R., de la Mata, M., Fededa, J.P., Munoz, M.J., and Nogues, G. (2004). Multiple links between transcription and splicing. RNA *10*, 1489-1498.

Kosfeld, M., Heinrichs, M., Zak, P.J., Fischbacher, U., and Fehr, E. (2005). Oxytocin increases trust in humans. Nature *435*, 673-676.

Kostich, W.A., Chen, A., Sperle, K., and Largent, B.L. (1998). Molecular identification and analysis of a novel human corticotropin-releasing factor (CRF) receptor: the CRF2gamma receptor. Molecular endocrinology (Baltimore, Md *12*, 1077-1085.

Kubota, Y., Kimura, T., Hashimoto, K., Tokugawa, Y., Nobunaga, K., Azuma, C., Saji, F., and Murata, Y. (1996). Structure and expression of the mouse oxytocin receptor gene. Molecular and cellular endocrinology *124*, 25-32.

Kumar, V.J., Grissom, N.M., McKee, S.E., Schoch, H., Bowman, N., Havekes, R., Kumar, M., Pickup, S., Poptani, H., Reyes, T.M.*, et al.* (2018). Linking spatial gene expression patterns to sex-specific brain structural changes on a mouse model of 16p11.2 hemideletion. Translational psychiatry *8*, 109.

La Cognata, V., Iemmolo, R., D'Agata, V., Scuderi, S., Drago, F., Zappia, M., and Cavallaro, S. (2014). Increasing the Coding Potential of Genomes Through Alternative Splicing: The Case of PARK2 Gene. Curr Genomics *15*, 203-216.

Lagane, B., Gaibelet, G., Meilhoc, E., Masson, J.M., Cezanne, L., and Lopez, A. (2000). Role of sterols in modulating the human mu-opioid receptor function in Saccharomyces cerevisiae. The Journal of biological chemistry *275*, 33197-33200.

Landgraf, R., and Neumann, I.D. (2004). Vasopressin and oxytocin release within the brain: a dynamic concept of multiple and variable modes of neuropeptide communication. Frontiers in neuroendocrinology *25*, 150-176.

Lang, R.E., Heil, J.W., Ganten, D., Hermann, K., Unger, T., and Rascher, W. (1983). Oxytocin unlike vasopressin is a stress hormone in the rat. Neuroendocrinology *37*, 314-316.

Lee, Y., and Rio, D.C. (2015). Mechanisms and Regulation of Alternative Pre-mRNA Splicing. Annual review of biochemistry *84*, 291-323.

Lestanova, Z., Bacova, Z., and Bakos, J. (2016a). Mechanisms involved in the regulation of neuropeptide-mediated neurite outgrowth: a minireview. Endocr Regul *50*, 72-82.

Lestanova, Z., Bacova, Z., Kiss, A., Havranek, T., Strbak, V., and Bakos, J. (2016b). Oxytocin Increases Neurite Length and Expression of Cytoskeletal Proteins Associated with Neuronal Growth. J Mol Neurosci *59*, 184-192.

Lestanova, Z., Puerta, F., Alanazi, M., Bacova, Z., Kiss, A., Castejon, A.M., and Bakos, J. (2017). Downregulation of Oxytocin Receptor Decreases the Length of Projections Stimulated by Retinoic Acid in the U-87MG Cells. Neurochemical research *42*, 1006-1014.

Leuner, B., Caponiti, J.M., and Gould, E. (2012). Oxytocin stimulates adult neurogenesis even under conditions of stress and elevated glucocorticoids. Hippocampus *22*, 861-868.

Lewis, K., Li, C., Perrin, M.H., Blount, A., Kunitake, K., Donaldson, C., Vaughan, J., Reyes, T.M., Gulyas, J., Fischer, W.*, et al.* (2001). Identification of urocortin III, an additional member of the corticotropin-releasing factor (CRF) family with high affinity for the CRF2 receptor. Proceedings of the National Academy of Sciences of the United States of America *98*, 7570-7575.

Lezak, K.R., Missig, G., and Carlezon, W.A., Jr. (2017). Behavioral methods to study anxiety in rodents. Dialogues in clinical neuroscience *19*, 181-191.

Li, H., Radford, J.C., Ragusa, M.J., Shea, K.L., McKercher, S.R., Zaremba, J.D., Soussou, W., Nie, Z., Kang, Y.J., Nakanishi, N.*, et al.* (2008). Transcription factor MEF2C

influences neural stem/progenitor cell differentiation and maturation in vivo. Proceedings of the National Academy of Sciences of the United States of America *105*, 9397-9402.

Li, K., Nakajima, M., Ibanez-Tallon, I., and Heintz, N. (2016). A Cortical Circuit for Sexually Dimorphic Oxytocin-Dependent Anxiety Behaviors. Cell *167*, 60-72 e11.

Li, Q., Lee, J.A., and Black, D.L. (2007). Neuronal regulation of alternative pre-mRNA splicing. Nature reviews Neuroscience *8*, 819-831.

Lin, W., and Szaro, B.G. (1995). Neurofilaments help maintain normal morphologies and support elongation of neurites in Xenopus laevis cultured embryonic spinal cord neurons. J Neurosci *15*, 8331-8344.

Liscum, L., and Underwood, K.W. (1995). Intracellular cholesterol transport and compartmentation. The Journal of biological chemistry *270*, 15443-15446.

Liu, J.J., Orlova, N., Oakes, B.L., Ma, E., Spinner, H.B., Baney, K.L.M., Chuck, J., Tan, D., Knott, G.J., Harrington, L.B.*, et al.* (2019). CasX enzymes comprise a distinct family of RNA-guided genome editors. Nature *566*, 218-223.

Liu, Y., Kamitakahara, A., Kim, A.J., and Aguilera, G. (2008). Cyclic adenosine 3',5'-monophosphate responsive element binding protein phosphorylation is required but not sufficient for activation of corticotropin-releasing hormone transcription. Endocrinology *149*, 3512-3520.

Lovenberg, T.W., Chalmers, D.T., Liu, C., and De Souza, E.B. (1995). CRF2 alpha and CRF2 beta receptor mRNAs are differentially distributed between the rat central nervous system and peripheral tissues. Endocrinology *136*, 4139-4142.

Lowbridge, J., Manning, M., Haldar, J., and Sawyer, W.H. (1977). Synthesis and some pharmacological properties of [4-threonine, 7-glycine]oxytocin, [1-(L-2-hydroxy-3-mercaptopropanoic acid), 4-threonine, 7-glycine]oxytocin (hydroxy[Thr4, Gly7]oxytocin), and [7-Glycine]oxytocin, peptides with high oxytocic-antidiuretic selectivity. Journal of medicinal chemistry *20*, 120-123.

Lu, J., McKinsey, T.A., Nicol, R.L., and Olson, E.N. (2000). Signal-dependent activation of the MEF2 transcription factor by dissociation from histone deacetylases. Proceedings of the National Academy of Sciences of the United States of America *97*, 4070-4075.

Ludwig, M., Apps, D., Menzies, J., Patel, J.C., and Rice, M.E. (2016). Dendritic Release of Neurotransmitters. Comprehensive Physiology *7*, 235-252.

Ludwig, M., Sabatier, N., Bull, P.M., Landgraf, R., Dayanithi, G., and Leng, G. (2002). Intracellular calcium stores regulate activity-dependent neuropeptide release from dendrites. Nature *418*, 85-89.

Lukas, M., Toth, I., Reber, S.O., Slattery, D.A., Veenema, A.H., and Neumann, I.D. (2011). The neuropeptide oxytocin facilitates pro-social behavior and prevents social avoidance in rats and mice. Neuropsychopharmacology : official publication of the American College of Neuropsychopharmacology *36*, 2159-2168.

Luo, L. (2002). Actin cytoskeleton regulation in neuronal morphogenesis and structural plasticity. Annual review of cell and developmental biology *18*, 601-635.

Lydiard, R.B. (2003). The role of GABA in anxiety disorders. The Journal of clinical psychiatry *64 Suppl 3*, 21-27.

Lynch, J., Guo, L., Gelebart, P., Chilibeck, K., Xu, J., Molkentin, J.D., Agellon, L.B., and Michalak, M. (2005). Calreticulin signals upstream of calcineurin and MEF2C in a critical Ca(2+)-dependent signaling cascade. The Journal of cell biology *170*, 37-47.

Macdonald, K., and Feifel, D. (2012). Oxytocin in schizophrenia: a review of evidence for its therapeutic effects. Acta neuropsychiatrica *24*, 130-146.

MacDonald, K., and Feifel, D. (2014). Oxytocin's role in anxiety: a critical appraisal. Brain Res *1580*, 22-56.

Makarova, K.S., Grishin, N.V., Shabalina, S.A., Wolf, Y.I., and Koonin, E.V. (2006). A putative RNA-interference-based immune system in prokaryotes: computational analysis of the predicted enzymatic machinery, functional analogies with eukaryotic RNAi, and hypothetical mechanisms of action. Biol Direct *1*, 7.

Makarova, K.S., Wolf, Y.I., Alkhnbashi, O.S., Costa, F., Shah, S.A., Saunders, S.J., Barrangou, R., Brouns, S.J., Charpentier, E., Haft, D.H.*, et al.* (2015). An updated evolutionary classification of CRISPR-Cas systems. Nat Rev Microbiol *13*, 722-736.

Mandelkow, E., and Mandelkow, E.M. (1995). Microtubules and microtubule-associated proteins. Current opinion in cell biology *7*, 72-81.

Mao, Z., and Wiedmann, M. (1999). Calcineurin enhances MEF2 DNA binding activity in calcium-dependent survival of cerebellar granule neurons. The Journal of biological chemistry *274*, 31102-31107.

Maras, P.M., and Baram, T.Z. (2012). Sculpting the hippocampus from within: stress, spines, and CRH. Trends in neurosciences *35*, 315-324.

Markovic, D., and Grammatopoulos, D.K. (2009). Focus on the splicing of secretin GPCRs transmembrane-domain 7. Trends in biochemical sciences *34*, 443-452.

Martinetz, S., Meinung, C.P., Jurek, B., von Schack, D., van den Burg, E.H., Slattery, D.A., and Neumann, I.D. (2019). De Novo Protein Synthesis Mediated by the Eukaryotic Elongation Factor 2 Is Required for the Anxiolytic Effect of Oxytocin. Biological psychiatry *85*, 802-811.

Martinon, D., and Dabrowska, J. (2018). Corticotropin-Releasing Factor Receptors Modulate Oxytocin Release in the Dorsolateral Bed Nucleus of the Stria Terminalis (BNST) in Male Rats. Frontiers in neuroscience *12*, 183.

Mayanil, C.S., George, D., Freilich, L., Miljan, E.J., Mania-Farnell, B., McLone, D.G., and Bremer, E.G. (2001). Microarray analysis detects novel Pax3 downstream target genes. The Journal of biological chemistry *276*, 49299-49309.

McKinsey, T.A., Zhang, C.L., and Olson, E.N. (2002). MEF2: a calcium-dependent regulator of cell division, differentiation and death. Trends in biochemical sciences *27*, 40-47.

Menon, R., Grund, T., Zoicas, I., Althammer, F., Fiedler, D., Biermeier, V., Bosch, O.J., Hiraoka, Y., Nishimori, K., Eliava, M.*, et al.* (2018). Oxytocin Signaling in the Lateral Septum Prevents Social Fear during Lactation. Curr Biol *28*, 1066-1078 e1066.

Mens, W.B., Witter, A., and van Wimersma Greidanus, T.B. (1983). Penetration of neurohypophyseal hormones from plasma into cerebrospinal fluid (CSF): half-times of disappearance of these neuropeptides from CSF. Brain Res *262*, 143-149.

Meyer-Lindenberg, A., Domes, G., Kirsch, P., and Heinrichs, M. (2011). Oxytocin and vasopressin in the human brain: social neuropeptides for translational medicine. Nature reviews Neuroscience *12*, 524-538.

Meyer, M., Berger, I., Winter, J., and Jurek, B. (2018). Oxytocin alters the morphology of hypothalamic neurons via the transcription factor myocyte enhancer factor 2A (MEF-2A). Molecular and cellular endocrinology *477*, 156-162.

Meyer, M., Winter, J., and Jurek, B. (in preparation). MEF2A defines morphological effects of OT in neurons.

Mizuno, K., and Giese, K.P. (2010). Towards a molecular understanding of sex differences in memory formation. Trends in neurosciences *33*, 285-291.

Mohr, E., Bahnsen, U., Kiessling, C., and Richter, D. (1988). Expression of the vasopressin and oxytocin genes in rats occurs in mutually exclusive sets of hypothalamic neurons. FEBS letters *242*, 144-148.

Mojica, F.J., Diez-Villasenor, C., Garcia-Martinez, J., and Soria, E. (2005). Intervening sequences of regularly spaced prokaryotic repeats derive from foreign genetic elements. J Mol Evol *60*, 174-182.

Molinoff, P.B., and Axelrod, J. (1971). Biochemistry of catecholamines. Annual review of biochemistry *40*, 465-500.

Molkentin, J.D., Black, B.L., Martin, J.F., and Olson, E.N. (1996a). Mutational analysis of the DNA binding, dimerization, and transcriptional activation domains of MEF2C. Molecular and cellular biology *16*, 2627-2636.

Molkentin, J.D., Li, L., and Olson, E.N. (1996b). Phosphorylation of the MADS-Box transcription factor MEF2C enhances its DNA binding activity. The Journal of biological chemistry *271*, 17199-17204.

Molkentin, J.D., and Olson, E.N. (1996). Combinatorial control of muscle development by basic helix-loop-helix and MADS-box transcription factors. Proceedings of the National Academy of Sciences of the United States of America *93*, 9366-9373.

Morrow, E.M., Yoo, S.Y., Flavell, S.W., Kim, T.K., Lin, Y., Hill, R.S., Mukaddes, N.M., Balkhy, S., Gascon, G., Hashmi, A.*, et al.* (2008). Identifying autism loci and genes by tracing recent shared ancestry. Science *321*, 218-223.

Mugele, K., Kugler, H., and Spiess, J. (1993). Immortalization of a fetal rat brain cell line that expresses corticotropin-releasing factor mRNA. DNA and cell biology *12*, 119-126.

Munck, A., Guyre, P.M., and Holbrook, N.J. (1984). Physiological functions of glucocorticoids in stress and their relation to pharmacological actions. Endocr Rev *5*, 25-44.

Murrough, J.W., Yaqubi, S., Sayed, S., and Charney, D.S. (2015). Emerging drugs for the treatment of anxiety. Expert Opin Emerg Drugs *20*, 393-406.

Muth, S., Fries, A., and Gimpl, G. (2011). Cholesterol-induced conformational changes in the oxytocin receptor. The Biochemical journal *437*, 541-553.

Nestler, E.J., McMahon, A., Sabban, E.L., Tallman, J.F., and Duman, R.S. (1990). Chronic antidepressant administration decreases the expression of tyrosine hydroxylase in the rat locus coeruleus. Proceedings of the National Academy of Sciences of the United States of America *87*, 7522-7526.

Neufeld-Cohen, A., Tsoory, M.M., Evans, A.K., Getselter, D., Gil, S., Lowry, C.A., Vale, W.W., and Chen, A. (2010). A triple urocortin knockout mouse model reveals an essential role for urocortins in stress recovery. Proceedings of the National Academy of Sciences of the United States of America *107*, 19020-19025.

Neumann, I.D., Kromer, S.A., Toschi, N., and Ebner, K. (2000a). Brain oxytocin inhibits the (re)activity of the hypothalamo-pituitary-adrenal axis in male rats: involvement of hypothalamic and limbic brain regions. Regulatory peptides *96*, 31-38.

Neumann, I.D., and Landgraf, R. (2012). Balance of brain oxytocin and vasopressin: implications for anxiety, depression, and social behaviors. Trends in neurosciences *35*, 649-659.

Neumann, I.D., and Slattery, D.A. (2016). Oxytocin in General Anxiety and Social Fear: A Translational Approach. Biological psychiatry *79*, 213-221.

Neumann, I.D., Torner, L., and Wigger, A. (2000b). Brain oxytocin: differential inhibition of neuroendocrine stress responses and anxiety-related behaviour in virgin, pregnant and lactating rats. Neuroscience *95*, 567-575.

Neumann, I.D., Wigger, A., Torner, L., Holsboer, F., and Landgraf, R. (2000c). Brain oxytocin inhibits basal and stress-induced activity of the hypothalamo-pituitary-adrenal axis in male and female rats: partial action within the paraventricular nucleus. Journal of neuroendocrinology *12*, 235-243.

Nishimoto, S., and Nishida, E. (2006). MAPK signalling: ERK5 versus ERK1/2. EMBO Rep *7*, 782-786.

Okimoto, N., Bosch, O.J., Slattery, D.A., Pflaum, K., Matsushita, H., Wei, F.Y., Ohmori, M., Nishiki, T., Ohmori, I., Hiramatsu, Y.*, et al.* (2012). RGS2 mediates the anxiolytic effect of oxytocin. Brain research *1453*, 26-33.

Pang, L., Graziano, M., and Wang, S. (1999). Membrane cholesterol modulates galanin-GalR2 interaction. Biochemistry *38*, 12003-12011.

Parker, K.J., Garner, J.P., Libove, R.A., Hyde, S.A., Hornbeak, K.B., Carson, D.S., Liao, C.P., Phillips, J.M., Hallmayer, J.F., and Hardan, A.Y. (2014). Plasma oxytocin concentrations and OXTR polymorphisms predict social impairments in children with and without autism spectrum disorder. Proceedings of the National Academy of Sciences of the United States of America *111*, 12258-12263.

Parker, K.J., Oztan, O., Libove, R.A., Sumiyoshi, R.D., Jackson, L.P., Karhson, D.S., Summers, J.E., Hinman, K.E., Motonaga, K.S., Phillips, J.M.*, et al.* (2017). Intranasal oxytocin treatment for social deficits and biomarkers of response in children with autism. Proceedings of the National Academy of Sciences of the United States of America *114*, 8119-8124.

Passoni, I., Leonzino, M., Gigliucci, V., Chini, B., and Busnelli, M. (2016). Carbetocin is a Functional Selective Gq Agonist That Does Not Promote Oxytocin Receptor Recycling After Inducing beta-Arrestin-Independent Internalisation. Journal of neuroendocrinology *28*.

Patel, S., Hill, M.N., Cheer, J.F., Wotjak, C.T., and Holmes, A. (2017). The endocannabinoid system as a target for novel anxiolytic drugs. Neuroscience and biobehavioral reviews *76*, 56-66.

Paxinos, G., Watson, CR (1998). The Rat Brain in Stereotaxic Coordinates (4th Edition). New York Academic press.

Pedersen, C.A., and Boccia, M.L. (2002). Oxytocin links mothering received, mothering bestowed and adult stress responses. Stress (Amsterdam, Netherlands) *5*, 259-267.

Pellow, S., Chopin, P., File, S.E., and Briley, M. (1985). Validation of open:closed arm entries in an elevated plus-maze as a measure of anxiety in the rat. Journal of neuroscience methods *14*, 149-167.

Pellow, S., and File, S.E. (1986). Anxiolytic and anxiogenic drug effects on exploratory activity in an elevated plus-maze: a novel test of anxiety in the rat. Pharmacology, biochemistry, and behavior *24*, 525-529.

Pernar, L., Curtis, A.L., Vale, W.W., Rivier, J.E., and Valentino, R.J. (2004). Selective activation of corticotropin-releasing factor-2 receptors on neurochemically identified neurons in the rat dorsal raphe nucleus reveals dual actions. J Neurosci *24*, 1305-1311.

Peters, S., Slattery, D.A., Uschold-Schmidt, N., Reber, S.O., and Neumann, I.D. (2014). Dose-dependent effects of chronic central infusion of oxytocin on anxiety, oxytocin receptor binding and stress-related parameters in mice. Psychoneuroendocrinology *42*, 225-236.

Potthoff, M.J., and Olson, E.N. (2007). MEF2: a central regulator of diverse developmental programs. Development *134*, 4131-4140.

Pourcel, C., Salvignol, G., and Vergnaud, G. (2005). CRISPR elements in Yersinia pestis acquire new repeats by preferential uptake of bacteriophage DNA, and provide additional tools for evolutionary studies. Microbiology *151*, 653-663.

Prinz, W. (2002). Cholesterol trafficking in the secretory and endocytic systems. Seminars in cell & developmental biology *13*, 197-203.

Proudfoot, N.J., Furger, A., and Dye, M.J. (2002). Integrating mRNA processing with transcription. Cell *108*, 501-512.

Pucadyil, T.J., and Chattopadhyay, A. (2004). Cholesterol modulates ligand binding and G-protein coupling to serotonin(1A) receptors from bovine hippocampus. Biochimica et biophysica acta *1663*, 188-200.

Raj, B., and Blencowe, B.J. (2015). Alternative Splicing in the Mammalian Nervous System: Recent Insights into Mechanisms and Functional Roles. Neuron *87*, 14-27.

Raj, B., O'Hanlon, D., Vessey, J.P., Pan, Q., Ray, D., Buckley, N.J., Miller, F.D., and Blencowe, B.J. (2011). Cross-regulation between an alternative splicing activator and a transcription repressor controls neurogenesis. Molecular cell *43*, 843-850.

Ramachandran, B., Yu, G., Li, S., Zhu, B., and Gulick, T. (2008). Myocyte enhancer factor 2A is transcriptionally autoregulated. The Journal of biological chemistry *283*, 10318-10329.

Ran, F.A., Cong, L., Yan, W.X., Scott, D.A., Gootenberg, J.S., Kriz, A.J., Zetsche, B., Shalem, O., Wu, X., Makarova, K.S.*, et al.* (2015). In vivo genome editing using Staphylococcus aureus Cas9. Nature *520*, 186-191.

Raymond, A.D., Kucherepa, N.N., Fisher, K.R., Halina, W.G., and Partlow, G.D. (2006). Neurogenesis of oxytocin-containing neurons in the paraventricular nucleus (PVN) of the female pig in 3 reproductive states: puberty gilts, adult gilts and lactating sows. Brain research *1102*, 44-51.

Reber, S.O., and Neumann, I.D. (2008). Defensive behavioral strategies and enhanced state anxiety during chronic subordinate colony housing are accompanied by reduced hypothalamic vasopressin, but not oxytocin, expression. Annals of the New York Academy of Sciences *1148*, 184-195.

Reversi, A., Rimoldi, V., Brambillasca, S., and Chini, B. (2006). Effects of cholesterol manipulation on the signaling of the human oxytocin receptor. American journal of physiology Regulatory, integrative and comparative physiology *291*, R861-869.

Reyes, B.A., Valentino, R.J., and Van Bockstaele, E.J. (2008). Stress-induced intracellular trafficking of corticotropin-releasing factor receptors in rat locus coeruleus neurons. Endocrinology *149*, 122-130.

Reyes, T.M., Lewis, K., Perrin, M.H., Kunitake, K.S., Vaughan, J., Arias, C.A., Hogenesch, J.B., Gulyas, J., Rivier, J., Vale, W.W.*, et al.* (2001). Urocortin II: a member of the corticotropin-releasing factor (CRF) neuropeptide family that is selectively bound by type 2 CRF receptors. Proceedings of the National Academy of Sciences of the United States of America *98*, 2843-2848.

Ribeiro, L.F., Ribeiro, L.F.C., Barreto, M.Q., and Ward, R.J. (2018). Protein Engineering Strategies to Expand CRISPR-Cas9 Applications. Int J Genomics *2018*, 1652567.

Rimoldi, V., Reversi, A., Taverna, E., Rosa, P., Francolini, M., Cassoni, P., Parenti, M., and Chini, B. (2003). Oxytocin receptor elicits different EGFR/MAPK activation patterns depending on its localization in caveolin-1 enriched domains. Oncogene *22*, 6054-6060.

Ripamonti, S., Ambrozkiewicz, M.C., Guzzi, F., Gravati, M., Biella, G., Bormuth, I., Hammer, M., Tuffy, L.P., Sigler, A., Kawabe, H.*, et al.* (2017). Transient oxytocin signaling primes the development and function of excitatory hippocampal neurons. eLife *6*.

Rissman, R.A., Lee, K.F., Vale, W., and Sawchenko, P.E. (2007). Corticotropin-releasing factor receptors differentially regulate stress-induced tau phosphorylation. J Neurosci *27*, 6552-6562.

Rivier, C., and Vale, W. (1983). Modulation of stress-induced ACTH release by corticotropin-releasing factor, catecholamines and vasopressin. Nature *305*, 325-327.

Rozen, F., Russo, C., Banville, D., and Zingg, H.H. (1995). Structure, characterization, and expression of the rat oxytocin receptor gene. Proceedings of the National Academy of Sciences of the United States of America *92*, 200-204.

Rueden, C.T., Schindelin, J., Hiner, M.C., DeZonia, B.E., Walter, A.E., Arena, E.T., and Eliceiri, K.W. (2017). ImageJ2: ImageJ for the next generation of scientific image data. BMC Bioinformatics *18*, 529.

Rutz, C., Renner, A., Alken, M., Schulz, K., Beyermann, M., Wiesner, B., Rosenthal, W., and Schulein, R. (2006). The corticotropin-releasing factor receptor type 2a contains an N-terminal pseudo signal peptide. The Journal of biological chemistry *281*, 24910-24921.

Rydén, G., and Sjöholm, I. (1969). HALF-LIFE OF OXYTOCIN IN BLOOD OF PREGNANT AND NON-PREGNANT WOMEN. Acta Endocrinologica *61*, 425-431.

Salto, R., Vilchez, J.D., Giron, M.D., Cabrera, E., Campos, N., Manzano, M., Rueda, R., and Lopez-Pedrosa, J.M. (2015). beta-Hydroxy-beta-Methylbutyrate (HMB) Promotes Neurite Outgrowth in Neuro2a Cells. PloS one *10*, e0135614.

Sanchez-Vidana, D.I., Chan, N.M., Chan, A.H., Hui, K.K., Lee, S., Chan, H.Y., Law, Y.S., Sze, M.Y., Tsui, W.C., Fung, T.K.*, et al.* (2016). Repeated treatment with oxytocin promotes hippocampal cell proliferation, dendritic maturation and affects socio-emotional behavior. Neuroscience *333*, 65-77.

Santiago, C., and Bashaw, G.J. (2014). Transcription factors and effectors that regulate neuronal morphology. Development (Cambridge, England) *141*, 4667-4680.

Savell, K.E., Bach, S.V., Zipperly, M.E., Revanna, J.S., Goska, N.A., Tuscher, J.J., Duke, C.G., Sultan, F.A., Burke, J.N., Williams, D.*, et al.* (2019). A Neuron-Optimized CRISPR/dCas9 Activation System for Robust and Specific Gene Regulation. eNeuro *6*.

Sawatsubashi, S., Joko, Y., Fukumoto, S., Matsumoto, T., and Sugano, S.S. (2018). Development of versatile non-homologous end joining-based knock-in module for genome editing. Scientific reports *8*, 593.

Schindelin, J., Arganda-Carreras, I., Frise, E., Kaynig, V., Longair, M., Pietzsch, T., Preibisch, S., Rueden, C., Saalfeld, S., Schmid, B.*, et al.* (2012). Fiji: an open-source platform for biological-image analysis. Nat Methods *9*, 676-682.

Schmid-Burgk, J.L., Honing, K., Ebert, T.S., and Hornung, V. (2016). CRISPaint allows modular base-specific gene tagging using a ligase-4-dependent mechanism. Nat Commun *7*, 12338.

Schwinn, M.K., Machleidt, T., Zimmerman, K., Eggers, C.T., Dixon, A.S., Hurst, R., Hall, M.P., Encell, L.P., Binkowski, B.F., and Wood, K.V. (2018). CRISPR-Mediated Tagging of Endogenous Proteins with a Luminescent Peptide. ACS Chem Biol *13*, 467-474.

Seifert, R., and Wenzel-Seifert, K. (2002). Constitutive activity of G-protein-coupled receptors: cause of disease and common property of wild-type receptors. Naunyn-Schmiedeberg's archives of pharmacology *366*, 381-416.

Selye, H. (1955). Stress and disease. Science (New York, NY *122*, 625-631.

Seyffert, W. (2003). Lehrbuch der Genetik, 2 edn (Spektrum Akademischer Verlag).

Shalizi, A., Gaudilliere, B., Yuan, Z., Stegmuller, J., Shirogane, T., Ge, Q., Tan, Y., Schulman, B., Harper, J.W., and Bonni, A. (2006). A calcium-regulated MEF2 sumoylation switch controls postsynaptic differentiation. Science (New York, NY *311*, 1012-1017.

Sharp, P.A. (1994). Split genes and RNA splicing. Cell *77*, 805-815.

Sharp, P.A. (2005). The discovery of split genes and RNA splicing. Trends in biochemical sciences *30*, 279-281.

Shemesh, Y., Forkosh, O., Mahn, M., Anpilov, S., Sztainberg, Y., Manashirov, S., Shlapobersky, T., Elliott, E., Tabouy, L., Ezra, G.*, et al.* (2016). Ucn3 and CRF-R2 in the medial amygdala regulate complex social dynamics. Nat Neurosci *19*, 1489-1496.

Shore, P., and Sharrocks, A.D. (1995). The MADS-box family of transcription factors. European journal of biochemistry / FEBS *229*, 1-13.

Simons, K., and Ikonen, E. (1997). Functional rafts in cell membranes. Nature *387*, 569-572.

Simons, K., and Toomre, D. (2000). Lipid rafts and signal transduction. Nat Rev Mol Cell Biol *1*, 31-39.

Simpson, K., and Browning, M. (2017). Antibodies That Work Again and Again and Again. Methods Mol Biol *1554*, 41-59.

Singer, S.J., and Nicolson, G.L. (1972). The fluid mosaic model of the structure of cell membranes. Science (New York, NY *175*, 720-731.

Slattery, D.A., and Neumann, I.D. (2010). Chronic icv oxytocin attenuates the pathological high anxiety state of selectively bred Wistar rats. Neuropharmacology *58*, 56-61.

Smith, A.S., Tabbaa, M., Lei, K., Eastham, P., Butler, M.J., Linton, L., Altshuler, R., Liu, Y., and Wang, Z. (2016). Local oxytocin tempers anxiety by activating GABAA receptors in the hypothalamic paraventricular nucleus. Psychoneuroendocrinology *63*, 50-58.

Smith, S.M., and Vale, W.W. (2006). The role of the hypothalamic-pituitary-adrenal axis in neuroendocrine responses to stress. Dialogues in clinical neuroscience *8*, 383-395.

Smoller, J.W., Rosenbaum, J.F., Biederman, J., Susswein, L.S., Kennedy, J., Kagan, J., Snidman, N., Laird, N., Tsuang, M.T., Faraone, S.V.*, et al.* (2001). Genetic association analysis of behavioral inhibition using candidate loci from mouse models. Am J Med Genet *105*, 226-235.

Sobota, R., Mihara, T., Forrest, A., Featherstone, R.E., and Siegel, S.J. (2015). Oxytocin reduces amygdala activity, increases social interactions, and reduces anxiety-like behavior irrespective of NMDAR antagonism. Behavioral neuroscience *129*, 389-398.

Sofroniew, M.V. (1983). Morphology of vasopressin and oxytocin neurones and their central and vascular projections. Progress in brain research *60*, 101-114.

Sokolowska, E., and Hovatta, I. (2013). Anxiety genetics - findings from cross-species genome-wide approaches. Biology of mood & anxiety disorders *3*, 9.

Sorensen, G., Lindberg, C., Wortwein, G., Bolwig, T.G., and Woldbye, D.P. (2004). Differential roles for neuropeptide Y Y1 and Y5 receptors in anxiety and sedation. Journal of neuroscience research *77*, 723-729.

Staahl, B.T., Benekareddy, M., Coulon-Bainier, C., Banfal, A.A., Floor, S.N., Sabo, J.K., Urnes, C., Munares, G.A., Ghosh, A., and Doudna, J.A. (2017). Efficient genome editing in the mouse brain by local delivery of engineered Cas9 ribonucleoprotein complexes. Nat Biotechnol *35*, 431-434.

Sternberg, S.H., Redding, S., Jinek, M., Greene, E.C., and Doudna, J.A. (2014). DNA interrogation by the CRISPR RNA-guided endonuclease Cas9. Nature *507*, 62-67.

Stuart, E.T., and Gruss, P. (1996). PAX: developmental control genes in cell growth and differentiation. Cell Growth Differ *7*, 405-412.

Suh, B.Y., Liu, J.H., Rasmussen, D.D., Gibbs, D.M., Steinberg, J., and Yen, S.S. (1986). Role of oxytocin in the modulation of ACTH release in women. Neuroendocrinology *44*, 309-313.

Swinny, J.D., Metzger, F., J, I.J.-P., Gounko, N.V., Gramsbergen, A., and van der Want, J.J. (2004). Corticotropin-releasing factor and urocortin differentially modulate rat Purkinje cell dendritic outgrowth and differentiation in vitro. The European journal of neuroscience *19*, 1749-1758.

Takahashi, L.K., Ho, S.P., Livanov, V., Graciani, N., and Arneric, S.P. (2001). Antagonism of CRF(2) receptors produces anxiolytic behavior in animal models of anxiety. Brain Res *902*, 135-142.

Tang, G., Gudsnuk, K., Kuo, S.H., Cotrina, M.L., Rosoklija, G., Sosunov, A., Sonders, M.S., Kanter, E., Castagna, C., Yamamoto, A.*, et al.* (2014). Loss of mTOR-dependent macroautophagy causes autistic-like synaptic pruning deficits. Neuron *83*, 1131-1143.

Tebbe, J.J., Mronga, S., Tebbe, C.G., Ortmann, E., Arnold, R., and Schafer, M.K. (2005). Ghrelin-induced stimulation of colonic propulsion is dependent on hypothalamic neuropeptide Y1- and corticotrophin-releasing factor 1 receptor activation. Journal of neuroendocrinology *17*, 570-576.

Theodosis, D.T. (2002). Oxytocin-secreting neurons: A physiological model of morphological neuronal and glial plasticity in the adult hypothalamus. Frontiers in neuroendocrinology *23*, 101-135.

Thuronyi, B.W., Koblan, L.W., Levy, J.M., Yeh, W.H., Zheng, C., Newby, G.A., Wilson, C., Bhaumik, M., Shubina-Oleinik, O., Holt, J.R.*, et al.* (2019). Continuous evolution of base editors with expanded target compatibility and improved activity. Nat Biotechnol.

Tobin, V., Leng, G., and Ludwig, M. (2012). The involvement of actin, calcium channels and exocytosis proteins in somato-dendritic oxytocin and vasopressin release. Frontiers in physiology *3*, 261.

Todorovic, C., Radulovic, J., Jahn, O., Radulovic, M., Sherrin, T., Hippel, C., and Spiess, J. (2007). Differential activation of CRF receptor subtypes removes stress-induced memory deficit and anxiety. The European journal of neuroscience *25*, 3385-3397.

Tomizawa, K., Iga, N., Lu, Y.F., Moriwaki, A., Matsushita, M., Li, S.T., Miyamoto, O., Itano, T., and Matsui, H. (2003). Oxytocin improves long-lasting spatial memory during motherhood through MAP kinase cascade. Nature neuroscience *6*, 384-390.

Tuladhar, R., Yeu, Y., Tyler Piazza, J., Tan, Z., Rene Clemenceau, J., Wu, X., Barrett, Q., Herbert, J., Mathews, D.H., Kim, J.*, et al.* (2019). CRISPR-Cas9-based mutagenesis frequently provokes on-target mRNA misregulation. Nat Commun *10*, 4056.

Tyzio, R., Cossart, R., Khalilov, I., Minlebaev, M., Hubner, C.A., Represa, A., Ben-Ari, Y., and Khazipov, R. (2006). Maternal oxytocin triggers a transient inhibitory switch in GABA signaling in the fetal brain during delivery. Science *314*, 1788-1792.

Valdez, G.R., Inoue, K., Koob, G.F., Rivier, J., Vale, W., and Zorrilla, E.P. (2002). Human urocortin II: mild locomotor suppressive and delayed anxiolytic-like effects of a novel corticotropin-releasing factor related peptide. Brain Res *943*, 142-150.

Valdez, G.R., Zorrilla, E.P., Rivier, J., Vale, W.W., and Koob, G.F. (2003). Locomotor suppressive and anxiolytic-like effects of urocortin 3, a highly selective type 2 corticotropin-releasing factor agonist. Brain Res *980*, 206-212.

Vale, W., Spiess, J., Rivier, C., and Rivier, J. (1981). Characterization of a 41-residue ovine hypothalamic peptide that stimulates secretion of corticotropin and beta-endorphin. Science (New York, NY *213*, 1394-1397.

van den Burg, E.H., Stindl, J., Grund, T., Neumann, I.D., and Strauss, O. (2015). Oxytocin Stimulates Extracellular Ca2+ Influx Through TRPV2 Channels in Hypothalamic Neurons to Exert Its Anxiolytic Effects. Neuropsychopharmacology : official publication of the American College of Neuropsychopharmacology *40*, 2938-2947.

Van Pett, K., Viau, V., Bittencourt, J.C., Chan, R.K., Li, H.Y., Arias, C., Prins, G.S., Perrin, M., Vale, W., and Sawchenko, P.E. (2000). Distribution of mRNAs encoding CRF receptors in brain and pituitary of rat and mouse. J Comp Neurol *428*, 191-212.

Vaughan, J., Donaldson, C., Bittencourt, J., Perrin, M.H., Lewis, K., Sutton, S., Chan, R., Turnbull, A.V., Lovejoy, D., Rivier, C*., et al.* (1995). Urocortin, a mammalian neuropeptide related to fish urotensin I and to corticotropin-releasing factor. Nature *378*, 287-292.

Veening, J.G., and Olivier, B. (2013). Intranasal administration of oxytocin: behavioral and clinical effects, a review. Neuroscience and biobehavioral reviews *37*, 1445-1465.

Vetere, G., Restivo, L., Cole, C.J., Ross, P.J., Ammassari-Teule, M., Josselyn, S.A., and Frankland, P.W. (2011). Spine growth in the anterior cingulate cortex is necessary for the consolidation of contextual fear memory. Proceedings of the National Academy of Sciences of the United States of America *108*, 8456-8460.

Vuong, C.K., Black, D.L., and Zheng, S. (2016). The neurogenetics of alternative splicing. Nature reviews Neuroscience *17*, 265-281.

Wahl, M.C., Will, C.L., and Luhrmann, R. (2009). The spliceosome: design principles of a dynamic RNP machine. Cell *136*, 701-718.

Waldherr, M., and Neumann, I.D. (2007). Centrally released oxytocin mediates mating-induced anxiolysis in male rats. Proceedings of the National Academy of Sciences of the United States of America *104*, 16681-16684.

Wang, D.Z., Valdez, M.R., McAnally, J., Richardson, J., and Olson, E.N. (2001). The Mef2c gene is a direct transcriptional target of myogenic bHLH and MEF2 proteins during skeletal muscle development. Development (Cambridge, England) *128*, 4623-4633.

Wiegand, V., and Gimpl, G. (2012). Specification of the cholesterol interaction with the oxytocin receptor using a chimeric receptor approach. European journal of pharmacology *676*, 12-19.

Wienert, B., Wyman, S.K., Richardson, C.D., Yeh, C.D., Akcakaya, P., Porritt, M.J., Morlock, M., Vu, J.T., Kazane, K.R., Watry, H.L.*, et al.* (2019). Unbiased detection of CRISPR off-targets in vivo using DISCOVER-Seq. Science (New York, NY *364*, 286-289.

Will, C.L., and Luhrmann, R. (2011). Spliceosome structure and function. Cold Spring Harb Perspect Biol *3*.

Windle, R.J., Kershaw, Y.M., Shanks, N., Wood, S.A., Lightman, S.L., and Ingram, C.D. (2004). Oxytocin attenuates stress-induced c-fos mRNA expression in specific forebrain regions associated with modulation of hypothalamo-pituitary-adrenal activity. In J Neurosci, pp. 2974-2982.

Windle, R.J., Shanks, N., Lightman, S.L., and Ingram, C.D. (1997). Central oxytocin administration reduces stress-induced corticosterone release and anxiety behavior in rats. Endocrinology *138*, 2829-2834.

Winter, J., and Jurek, B. (2019). The interplay between oxytocin and the CRF system: regulation of the stress response. Cell and tissue research *375*, 85-91.

Winter, J., Meyer, M., Berger, I., Peters, S., Royer, M., Kunze, J., Reber, S.O., Kuffner, K., Schmidtner, A.K., Bludau, A.*, et al.* (in preparation). Chronic oxytocin signaling reveals alternative splice variant of CRFR2 as biomarker for anxiety.

Witt, D.M., Winslow, J.T., and Insel, T.R. (1992). Enhanced social interactions in rats following chronic, centrally infused oxytocin. Pharmacology, biochemistry, and behavior *43*, 855-861.

Wittchen, H.U., Jacobi, F., Rehm, J., Gustavsson, A., Svensson, M., Jonsson, B., Olesen, J., Allgulander, C., Alonso, J., Faravelli, C.*, et al.* (2011). The size and burden of mental disorders and other disorders of the brain in Europe 2010. European neuropsychopharmacology : the journal of the European College of Neuropsychopharmacology *21*, 655-679.

Wotjak, C.T., Ganster, J., Kohl, G., Holsboer, F., Landgraf, R., and Engelmann, M. (1998). Dissociated central and peripheral release of vasopressin, but not oxytocin, in response to repeated swim stress: new insights into the secretory capacities of peptidergic neurons. Neuroscience *85*, 1209-1222.

Wright, A.V., Nunez, J.K., and Doudna, J.A. (2016). Biology and Applications of CRISPR Systems: Harnessing Nature's Toolbox for Genome Engineering. Cell *164*, 29-44.

Yang, C.C., Ornatsky, O.I., McDermott, J.C., Cruz, T.F., and Prody, C.A. (1998). Interaction of myocyte enhancer factor 2 (MEF2) with a mitogen-activated protein kinase, ERK5/BMK1. Nucleic acids research *26*, 4771-4777.

Yoshida, M., Takayanagi, Y., Inoue, K., Kimura, T., Young, L.J., Onaka, T., and Nishimori, K. (2009). Evidence that oxytocin exerts anxiolytic effects via oxytocin receptor expressed in serotonergic neurons in mice. J Neurosci *29*, 2259-2271.

Young, L.J., Lim, M.M., Gingrich, B., and Insel, T.R. (2001). Cellular mechanisms of social attachment. Hormones and behavior *40*, 133-138.

Zaslavsky, K., Zhang, W.B., McCready, F.P., Rodrigues, D.C., Deneault, E., Loo, C., Zhao, M., Ross, P.J., El Hajjar, J., Romm, A.*, et al.* (2019). SHANK2 mutations associated with autism spectrum disorder cause hyperconnectivity of human neurons. Nat Neurosci *22*, 556-564.

Zatkova, M., Bacova, Z., Puerta, F., Lestanova, Z., Alanazi, M., Kiss, A., Reichova, A., Castejon, A.M., Ostatnikova, D., and Bakos, J. (2018a). Projection length stimulated by oxytocin is modulated by the inhibition of calcium signaling in U-87MG cells. J Neural Transm (Vienna) *125*, 1847-1856.

Zatkova, M., Reichova, A., Bacova, Z., and Bakos, J. (2019). Activation of the Oxytocin Receptor Modulates the Expression of Synaptic Adhesion Molecules in a Cell-Specific Manner. J Mol Neurosci *68*, 171-180.

Zatkova, M., Reichova, A., Bacova, Z., Strbak, V., Kiss, A., and Bakos, J. (2018b). Neurite Outgrowth Stimulated by Oxytocin Is Modulated by Inhibition of the Calcium Voltage-Gated Channels. Cellular and molecular neurobiology *38*, 371-378.

Zhang, Z., Cao, M., Chang, C.W., Wang, C., Shi, X., Zhan, X., Birnbaum, S.G., Bezprozvanny, I., Huber, K.M., and Wu, J.I. (2016). Autism-Associated Chromatin Regulator Brg1/SmarcA4 Is Required for Synapse Development and Myocyte Enhancer Factor 2-Mediated Synapse Remodeling. Molecular and cellular biology *36*, 70-83.

Zhao, M., New, L., Kravchenko, V.V., Kato, Y., Gram, H., di Padova, F., Olson, E.N., Ulevitch, R.J., and Han, J. (1999). Regulation of the MEF2 family of transcription factors by p38. Molecular and cellular biology *19*, 21-30.

Zhou, S., Appleman, V.A., Rose, C.M., Jun, H.J., Yang, J., Zhou, Y., Bronson, R.T., Gygi, S.P., and Charest, A. (2018). Chronic platelet-derived growth factor receptor signaling exerts control over initiation of protein translation in glioma. Life Sci Alliance *1*, e201800029.

Zhu, M.Y., Klimek, V., Dilley, G.E., Haycock, J.W., Stockmeier, C., Overholser, J.C., Meltzer, H.Y., and Ordway, G.A. (1999). Elevated levels of tyrosine hydroxylase in the locus coeruleus in major depression. Biological psychiatry *46*, 1275-1286.

Zorrilla, E.P., Roberts, A.J., Rivier, J.E., and Koob, G.F. (2013). Anxiolytic-like effects of antisauvagine-30 in mice are not mediated by CRF2 receptors. PloS one *8*, e63942.

Zuris, J.A., Thompson, D.B., Shu, Y., Guilinger, J.P., Bessen, J.L., Hu, J.H., Maeder, M.L., Joung, J.K., Chen, Z.Y., and Liu, D.R. (2015). Cationic lipid-mediated delivery of proteins enables efficient protein-based genome editing in vitro and in vivo. Nat Biotechnol *33*, 73-80.

Acknowledgements - Danksagung

Acknowledgements - Danksagung

An erster Stelle möchte ich mich bei Prof. Dr. Inga Neumann für die Möglichkeit bedanken meine Doktorarbeit an ihrem Lehrstuhl durchzuführen. Liebe Inga, vielen Dank, dass du mir dies ermöglicht hast. Danke für deine wissenschaftliche Unterstützung, deine konstruktive Kritik und deine Förderung zu jeder Zeit. Du hast mit deiner Betreuung als meine 1. Mentorin einen großen Beitrag zu meiner wissenschaftlichen und auch persönlichen Entwicklung geleistet. Vielen Dank für die schöne Zeit am Lehrstuhl.

Ben, Sir-blot-a-lot, Dr. MEK, danke für die herausragende Betreuung meiner Doktorarbeit. Ich konnte mich sowohl von fachlicher, als auch von menschlicher Seite immer auf dich verlassen. Selbst in den stressigsten Phasen hattest du immer ein offenes Ohr und hast dir Zeit für mich genommen. Danke für deine Hilfe bei der Vorbereitung auf zahlreiche Konferenzen und Vorträge und deine große Hilfe im Endspurt der Schreibphase. Danke, dass du mir einen offenen, positiven und innovativen Blick auf die Wissenschaft, aber auch Geduld vermittelt hast, wenn im ersten Moment gar nichts zu funktionieren schien.
Du hast nicht nur als Papa von Junior, sondern auch als mein Doktorvater vollen Einsatz gezeigt. Es war mir eine große Ehre deine erste Doktorandin zu sein.

Vielen herzlichen Dank auch an meinen 2. Mentor, Prof. Dr. Christian Wetzel, der mich jederzeit unterstützt hat.

Nicht zu vergessen, danke an die gesamte AG Harn Solo; Ben, Magdalena und Ilona (und zeitweise auch Simone und Caro). Vielen Dank für die tolle Zusammenarbeit, eure Hilfe, grandiose Science Meetings, Brunch Treffen (es ist halb 11, sollen wir jetzt echt Rotwein trinken?!) und mehr oder weniger unfallfreie Balkonabende.

Meine Mädels und Jungs aus dem Office, Marianela, Magdalena, Carl und Tobi (und natürlich auch Vini, Kathi, Meli, Kerstin und Anna). Danke für eure wissenschaftliche Unterstützung, die vielen tollen Gespräche, Feierabende, Oktoberfeste, Partys und Konferenzen, die ich mit euch erleben durfte. Es war und ist mir eine Freude.

Ein großer Dank geht an Anna a.k.a. Schmidti, für viele Weinabende, Motivation, strenge Schreibpläne, Shoppingausflüge und dass du immer ein offenes Ohr für mich hast.

Thanks to ,,The best people ever'', I had an unforgettable time with you.

Ganz herzlich möchte ich mich auch bei allen meinen Kollegen und Freunden an den Lehrstühlen Neumann, Egger und Flor bedanken. Vielen Dank für eure Unterstützung, eine gute Arbeitsatmosphäre, tolle und auch teilweise gefährliche Konferenzen, großartige Feste und Tennisstunden.

Ein weiterer Dank geht an Prof. Dr. Oliver Bosch. Vielen Dank, vor allem für die gute Zusammenarbeit bei der Klausurvorbereitung, aber auch für deine wissenschaftliche Unterstützung.

Ein herzliches Dankeschön geht an alle meine Studenten und Praktikanten, die mir eine große Hilfe waren und viel zu den hier gezeigten Daten beigetragen haben.

Liebe Eva, liebe Tanja, danke, dass ihr alles im Griff habt und durch euch alles Organisatorische so unkompliziert und reibungslos funktioniert.

Vielen Dank an die TAs, allen voran Rodrigue. Ohne deine große Hilfe bei den OPs wäre vieles nicht möglich gewesen und danke für deine Geduld mir immer und immer wieder beim Einspannen zu helfen. Andrea, danke, dass du mir bei meiner allerersten OP überhaupt zur Seite gestanden hast und alles erklärt hast. Danke Martina für die Hilfe am Cryo.

Ein großer Dank geht an meine Familie und meine Freunde, die immer für mich da sind.
Sophitschi, danke, dass ich immer auf dich zählen kann, du dir endlose Laborgeschichten anhörst und mir im richtigen Moment wieder ins Gedächtnis rufst, worauf es wirklich ankommt.

Liebe Mama, lieber Papa, danke für einfach alles. Ohne eure bedingungslose Unterstützung, Motivation und Liebe wäre das alles nicht möglich gewesen. Danke, dass ihr nie den Glauben an mich verloren habt. Hier nun hoffentlich die Antwort auf ,,mei, für was lasst man di studieren?''.

Und natürlich: Danke Theo ☺

Curriculum vitae and publications

Curriculum vitae

Education and Degree

2015 ongoing Ph.D. in Neurobiology (Department of Behavioral and Molecular Neurobiology, Prof. Dr. Inga D. Neumann) 'From intracellular signaling cascades to behavior: towards a better understanding of oxytocin's molecular effects' (Supervisor: Dr. Benjamin Jurek)

2012 - 2015 Master of Science, Biology, University of Regensburg
Master thesis Department of Nephrology, University Medical Center Regensburg

2009 - 2012 Bachelor of Science, Biology, University of Regensburg
Bachelor thesis Department of Microbiology, University of Regensburg

Awards and Stipends

- 2019 - 13th Göttingen Meeting of the German Neuroscience Society – Travel Grant and invitation for Students Talk
- 2018 - FAPESP-BAYLAT Workshop on Neural Basis of Stress, Fear and Anxiety (Talk and Travel Grant)
- 2017 - Travel grant by the Financial Incentive System for Equality Promotion
- 2017 - 12th World Congress on Neurohypophysial Hormones - American Physiological Society Travel Award, talk at the Young Investigator Symposium
- 2016 - Graduation initial funding by the Financial Incentive System for Equality Promotion – University of Regensburg

References

- Dr. Benjamin Jurek, Department of Molecular and Behavioral Neuroscience, University of Regensburg, +49 941 943 3080, Benjamin.Jurek@ur.de (Supervisor)
- Prof. Dr. Inga D Neumann, Department of Molecular and Behavioral Neuroscience, University of Regensburg, +49 941 943 3055, Inga.Neumann@ur.de (Mentor)
- Dr. Simone Reichelt-Wurm, Department of Nephrology, University Medical Center Regensburg, +49 941 944 7388, Simone.Reichelt-Wurm@klinik.uni-regensburg.de

Publications

- **Winter J.** and Jurek B. The interplay between oxytocin and the CRF system: regulation of the stress response. Cell Tissue Res. 2018 Jun 18. doi: 10.1007/s00441-018-2866-2.

- Meyer M., Berger I., **Winter J.**, Jurek B. Oxytocin alters the morphology of hypothalamic neurons via the transcription factor myocyte enhancer factor 2A (MEF-2A). Mol Cell Endocrinol. 2018 Dec 5;477:156-162. doi: 10.1016/j.mce.2018.06.013.

- **Winter J.**, Meyer M., Berger I., Peters S., Royer M., Kunze J., Reber S.O., Kuffner K., Schmidtner A.K., Bludau A., Bianchi M., Stang S., Bosch O.J., van den Burg E. Neumann I.D., and Jurek B. (in preparation). Chronic oxytocin signaling reveals alternative splice variant of CRFR2 as biomarker for anxiety.

- **Winter J.**, Meyer M., Stang S., Salehi S., Rom-Jurek E.M., Meinung C.P., Molthof C., Irlbeck C., Jurek B. (in preparation). Oxytocin receptor stability: implications for cellular morphology and intracellular signaling.

- Meyer M., **Winter J.**, and Jurek B. (in preparation). MEF2A defines morphological effects of OT in neurons.